USC
UNIVERSIDADE
DE SANTIAGO
DE COMPOSTELA

Obestatin/GPR39: an autocrine-paracrine system involved in differentiation, glucose metabolism and regeneration

Uxía Gurriarán Rodríguez

Santiago de Compostela, 2013

Universidade de Santiago de Compostela
Facultade de Medicina
Departamento de Medicina
Laboratorio de Endocrinoloxía Celular

Obestatin/GPR39: an autocrine-paracrine system involved in differentiation, glucose metabolism and regeneration

Uxía Gurriarán Rodríguez

Santiago de Compostela, Setembro 2013

Universidade de Santiago de Compostela
Facultade de Medicina
Departamento de Medicina
Laboratorio de Endocrinoloxía Celular

Obestatin/GPR39: an autocrine-paracrine system involved in differentiation, glucose metabolism and regeneration

Memoria para optar ó Grado de Doutora en Química
pola Universidade de Santiago de Compostela presentada por:

Uxía Gurriarán Rodríguez

Santiago de Compostela, Setembro 2013

A memoria adxunta titulada **"Obestatin/GPR39: an autocrine-paracrine system involved in differentiation, glucose metabolism and regeneration"** que para optar ó Grao de Doutora en Química presenta Dna. Uxía Gurriarán Rodríguez, foi realizada baixo a nosa dirección na Área de Endocrinoloxía Molecular e Celular do Instituto de Investigación Sanitaria de Santiago do Complexo Hospitalario Universitario de Santiago de Compostela.

Considerando que constitúe un traballo de Tesis Doutoral, autorizamos a súa presentación na Universidade de Santiago de Compostela.

E para que así conste, firmamos a presente en Santiago de Compostela a Setembro de 2013.

Dr. Jesús Pérez Camiña
Investigador SERGAS

Prof. Dr. Felipe Casanueva Freijo
Catedrático de Medicina

Santiago de Compostela, Setembro 2013

Á miña nai, por non esgotar forzas en batallas perdidas
e por ter loitado nas que realmente pagan a pena

INDEX

55 MATERIALS & METHODS

ABBREVIATIONS

AB	antibody
ACC	acetyl-CoA-carboxilase
AG	acylated ghrelin
AMPK	adenosine monophosphate-activated protein kinase
AraC	arabinofuranosyl cytidine
Arg	arginin
ATP	adenosine triphosphate
BAT	brown adipose tissue
BDNF	brain-derived neurotrophic factor
BF	blocking buffer
BMP	bone morphogenetic proteins
BSA	bovine serum albumin
C/EBP	CCAT/enhancer-binding protein
cAMP	cyclic adenosine monophosphate
CamkII	calmoduline proteine kinase II
CCAT	cytidine-cytidine-adenosine-thymidine
CDK6	cyclin-dependent kinase-6
CK	creatine kinase
CM	conditioned medium
CPT-1	cholinephosphotransferase 1
CREB	cAMP response element-binding protein
CTX	cardiotoxin
CyB	cytochalasin B
DEX	dexamethasone
DM	differenciated medium
EGFR	epidermal growth factor receptor
eIF2B	eukariotic translational initiation factor
EM	electronic microscopy
eMHC	embrionic myosin heavy chain
ER	endoplasmatic reticulum
ERK1/2	extracellular signal-regulated kinase-1/2
Ex-4	exendin-4
FAS	fatty acid synthetase
FAT/CD36	fatty acid translocase
FATP1	fatty acid transport proteins 1
FATP4	fatty acid transport proteins 4
FBS	fetal calf serum
FC	flow cytometry
FFAs	free fatty acids
FKHR	Forkhead in human rhabdomyosarcoma
FoxO1	forkhead box O1
GAP	GTPase-acting protein
GH	growth hormone
GHSR1a	growth hormone secretagogue receptor type 1a
GLP-1r	glucagon-like peptide-1receptor
GLUT	glucose transporters
GM	growth medium
GOAT	ghrelin O-acyl transferase
GPDH	glycerol-3-phosphate dehydrogenase
GSK3β	glycogen synthase kinase 3 β
HE	hematoxilin and eoxin
HEXIM1	hexamethylene bis-acetamide inducible
HFD	high-fat diet
HGF	hepatocitic growth factor
hRPEs	human retinal pigmented epithelial cells
IBMX	3-isobutyl-1-methylxanthine
ICC	immunocitochemistry
IF	immunofluorescence
IGF-I	insulin growth factor-I
IHC	immunohistochemistry
IL	interleukin
IMAT	intermuscular adiposse tissue

IP	intraperitoneal
IRS	insulin-receptor substrate
IRS-1	insulin receptor substrate-1
LAP	latency-associated peptide
Leu	leucine
LPL	lipoprotein lipase
MAPK	mitogen-activated protein kinase
MBOAT	membrane bound O-acyl transferases
MBOAT4	membrane-bound O-acyltransferase 4
MEF2	myocyte enhancer factor-2
MEFs	mouse embryonic fibroblasts
MHC	myosin heavy chain
MMPs	metalloproteinases
MMTV	mouse mammary tumor virus
MPs	macrophages
MRFs	myogenic regulatory factors
MSCs	mesenchymal stem cells
MTJs	myotendinous junctions
mTOR	mammalian target of rapamycin
mTORC1	mTOR complex 1
MVF	micro vascular fragments
NC	neural crest
NFATC2	nuclear factor of activated T cells
PBS	phosphate buffer saline
PBT	PBS-Triton X-100
PC1/3	prohormone convertase 1/3
PDK1	phosphoinositide-dependent kinase 1
PEDF	plateled endothelial growth factor
PFA	paraformaldehide
PI3K	phosphatidylinositol 3-kinase
PKB/AKT	protein kinase B/AKT
PM	plasma membrane
PPARγ	peroxisome proliferator–activated receptor-γ
RNA	ribonucleic acid
RT	room temperature
RTKs	receptor tyrosine kinases
S	sinthesys phase
sc	subcutaneus
SCs	satellite cells
SD	Standard diet
Ser	serina
siRNA	small interfering RNA
SR	sarcoplasmatic reticulum
SREBPs	sterol regulatory element-binding proteins
SWAT	subcutaneous adipose tissue
TA	tibialis anterior
Thr	triptophan
TIMP-3	tissue inhibitor of metalloproteinase
TNF-α	tumor necrosis factor-α
TSC2	tuberous sclerosis protein 2
Tyr	tyrosin
UCP1	uncoupling protein-1
V1a-R	vasopressin receptor
VEGF	vascular endothelial growth factor
VEGFR	vascular endothelial growth factor receptor
VLA-4	very late antigen-4 integrin
VWAT	visceral adipose tissue
WAT	white adipose tissue
WB	western blot

OBJETIVES

White adipose tissue and skeletal muscle are the largest organs in the body and both are composed of distinct cell types with a common origin, the mesenchymal steam cells. The adipose tissue is composed by the adipocyte while myocyte are the defining cell of skeletal muscle. Both adipocyte and myocyte secrete a range of bioactive molecules that are involved in local autocrine/paracrine interactions as well as in an endocrine cross-talk with other tissues. Based on it, the main aim of the present work was to explore and to validate the role of the obestatin/GPR39 system in the differentiation program that determines adipogenesis and myogenesis. This aim was divided in the following points:

1. To determine the role of the obestatina/GPR39 system, as autocrine/paracrine signal, in the adipogenic program.
2. To determine the role of the obestatina/GPR39 system on adipocyte metabolism.
3. To establish the role of the obestatin/GPR39 system as autocrine/paracrine signal in the myogenesis.
4. To ascertain the role of the obestatina/GPR39 system on muscle metabolism.
5. To validate the use of obestatin as a potential therapeutic peptide for skeletal muscle regeneration.
6. To determine the action of obestatin in the activation and differentiation of satellite stem cells from skeletal muscle.

INTRODUCTION

A COMMON ORIGIN FOR ADIPOCYTES AND MUSCLE

The embryonic development compromises different well orchestred processes that need to be switched on for organulogenesis[1]. Three are the germ layers that are implicated in the development of the different internal organs. The endoderm produces tissue within the lungs, thyroid, and pancreas. The ectoderm produces tissues within the epidermis and aids in the formation of neurons within the brain, and melanocytes. The mesoderm aids in the production of muscle and adipose tissue, tissues within the kidneys, and red blood cells. All of the many different kinds of specialized cells that make up the body are derived from one of these germ layers[2]. The term stem cell is used to describe progenitors that give rise to cells derived from these three embryonic germ layers. Stem cells are capable of self-renewal and multilineage differentiation through a process of asymmetric mitosis that leads to two daughter cells, one identical to the stem cell and one capable of differentiation into more mature cells. Depending on its differentiation capacity, stem cells are classified in:

1. **Totipotent**, i. e. early embryonic cells (1-3 days from oocyte fertilization), which can give rise to all the embryonic tissues and placenta.
2. **Pluripotent**, i. e. embryonic cells from blastocysts (days 4-14 after oocyte fertilization), which can differentiate only into embryonic tissues belonging to the inner cell mass (ectoderm, mesoderm, and endoderm).
3. **Multipotent**, i. e. embryonic cells from the 14th day onwards, fetal stem cells, cord blood stem cells, and adult stem cells, which can give rise only to tissues belonging to one embryonic germ layer (ectoderm or mesoderm or endoderm)[3].

Among the three embryonic germ layers, the mesoderm is a major source of the mesenchymal precursors giving rise to most mesodermal tissues. Consequently, growth and development of fat and muscle tissues have a common embryonic origin, the mesenchymal stem cells (MSCs) from the mesoderm[4]. MSCs are a versatile group of non-hematopoietic stem cells with high potency of proliferation and multipotency of the mesodermal lineage, such as adipocytes, myocytes, osteocytes, as well as other embryonic lineages[5]. MSCs are abundant in the skeletal muscle at early developmental stages, especially during the fetal and neonatal stages. While most of the MSCs develop into myogenic cells, a small portion of these cells differentiates into adipocytes[6] (**SCHEME-1**). The mesoderm is not the only germ-layer source of mesenchymal cells. In the head, for example, the facial bones, jaws and associated connective tissues have been shown to derive from the neural crest (NC). The NC is a vertebrate cell population that arises from the neuroectoderm[7].

MSCs are not only involved in embryonic development and pre-natal stages. In addition, different mammal adult tissues harbour small amounts of MSCs, which have the potential to give a rise to all cell types of the specific tissue in which they reside aiming to repair, replace damaged tissue or to expand in response to chronic energy overload; dividing essentially without limit to replenish other cells as long as the person or animal is still alive. Depending on the type of host tissue, as well as age and state of the donor's health, the plasticity can vary considerably[8]. This process is regulated by means of complex and incompletely understood mechanisms of communication among cells. MSCs were found mostly in human adult bone marrow but they are also found in muscle, fat, brain, cartilage, dental pulp, etc. Numerous publications have demonstrated the broad therapeutic potential of MSCs, due to their ability to differentiate towards multiple adult cell types under appropriate conditions after birth[9]. Therefore, it is necessary further investigations to elucidate the complex mechanisms involved in the differentiation process of the different MSCs derived cells. The study of different signals will amplify the broad of new therapeutic targets in order to improve the knowledge and treatment of different pathologies related with differentiation cell processes abnormalities.

1. Slack, J. M. Origin of stem cells in organogenesis. *Science*. 2008; 322 (5907): 1498-501.
2. Bongso, A. et al. History and perspective of stem cell research. *Best Pract. Res. Clin. Obstet. Gynaecol*. 2004; 18 (6): 827-34.
3. Hochedlinger, K. et al. Epigenetic reprogramming and induced pluripotency. *Development*. 2009; 136: 509-3.
4. Vodyanik, M.A. et al. A mesoderm-derived precursor for mesenchymal stem and endothelial cells. *Cell Stem Cell*. 2010; 7 (6): 718-29.
5. Krampera, M. et al. Mesenchymal stem cells: from biology to clinical use. *Blood Transfus*. 2007; 5: 120-9.
6. Dodson, M. V. et al. Skeletal Muscle Stem Cells from Animals I. Basic Cell Biology. *Int. J. Biol. Sci*. 2010; 6 (5): 465-74.
7. Billon, N. et al. The generation of adipocytes by the neural crest. *Development*. 2007; 134: 2283-92.
8. Xiang, X. et al. mTOR and the differentiation of mesenchymal stem cells. *Acta Biochim. Biophys. Sin*. 2011; 43 (7): 501-10.
9. Malek, A. et al. Human placental stem cells: biomedical potential and clinical relevance. *J. Stem Cells*. 2011; 6 (2): 75-92.

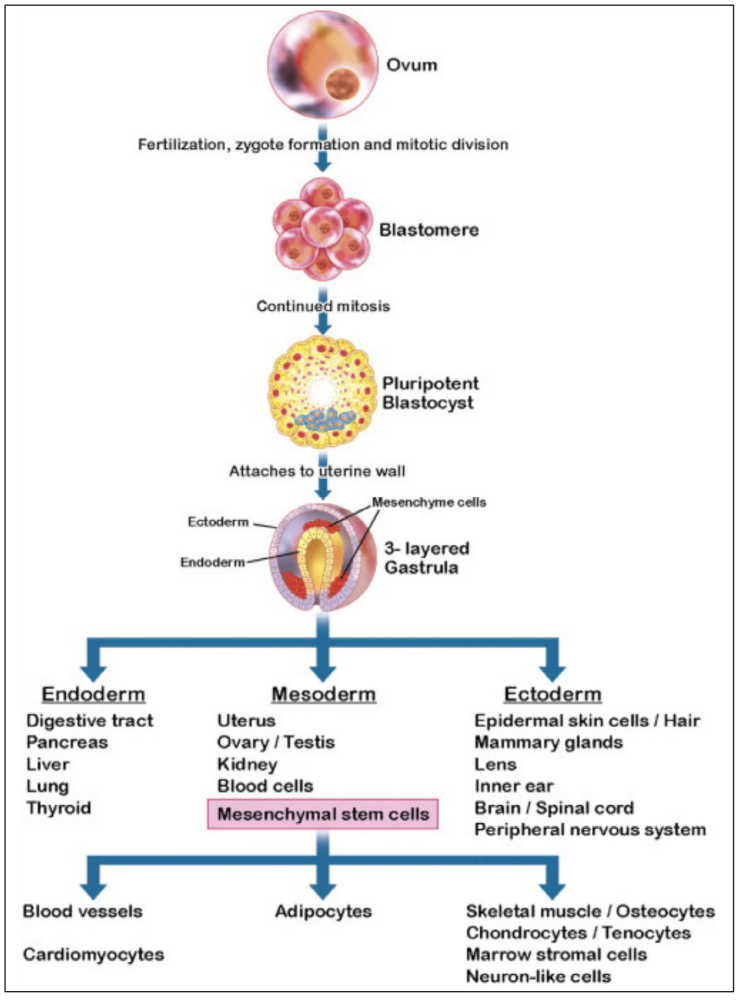

SCHEME-1. Diagram of the common embryonic origin of myocytes and adipocytes. After fertilization of the ovum and mitotic divisions of the zygote, the subsequent pluripotent stem cells give rise to endoderm, ectoderm, and mesoderm. The mesoderm may differentiate into hematopoietic tissue, kidney, and sex organs, as well as mesenchymal stem cells. Mesenchymal stem cells may differentiate into skeletal myoblasts and adipocytes, as well as osteoblasts, chondroblasts, tenoblasts, marrow stromal cells, neuron-like cells, and into cardiomyocytes. Through the formation of mesenchymal stem cells, both myocytes and adipocytes share a common genetic lineage (Figure extracted from *J. Am. Coll. Cardiol.* 2011; 57: 2461-73)

ADIPOGENESIS

Types of tissues, characteristics and different functions

Two functionally different types of adipose tissues are classically described in mammals, which differ in several important properties: brown adipose tissue (BAT) and white adipose tissue (WAT)[10]. Both are involved in energy balance, but assume opposite functions, even if they have a similar genetic content. BAT is specialized in energy dissipation as heat during cold and diet-induced thermogenesis, whereas WAT is mainly involved in energy storage, and mobilization in the form of triacylglycerol. BAT stores less lipid and have more mitochondrias than WAT. BAT expresses almost all the genes that are expressed in WAT, but it also expresses some distinct genes, including uncoupling protein-1 (UCP1), which allows energy to be dissipated as heat without generating adenosine triphosphate (ATP)[11,12] **(SCHEME-2)**. Most BAT in rodents is localized in the interscapular region. Humans have large depots of BAT during infancy, but only small amounts that are dispersed throughout depots of WAT persist in adults. WAT is found in several depots throughout the body, and location varies between species. For mammals and birds, the largest fat tissues are intra-abdominal and subcutaneous, but it can also be found in other areas, such as the face and extremities, and within bone marrow. WAT from different locations have distinct molecular and physiological properties[13]. WAT is distributed throughout the body in the form of two major types: subcutaneous adipose tissue (SWAT) and the intra-abdominal visceral adipose tissue (VWAT). VWAT tissue is associated with insulin resistance, diabetes mellitus, dyslipidemia, hypertension, atherosclerosis, hepatic steatosis, and overall mortality. Subcutaneous and visceral adipocytes derive from different progenitor cells that exhibit a different gene expression pattern. SWAT responds better to the antilipolytic effects of insulin and other hormones, secrets more adiponectin and less inflammatory cytokines, and is differentially affected by molecules involved in signal transduction as well as drugs compared with VWAT. For example, adipocytes in visceral depots are less sensitive to lipolytic stimuli, whereas adipocytes from structural depots, such as around the eyes and in the heel pads, do not release stored lipid easily. Increased visceral adipose tissue is associated with an increased risk of insulin resistance and cardiovascular disease, whereas increased subcutaneous adipose tissue is not. Therefore it is necessary to distinguish properly between subcutaneous and visceral adipose tissue and its different

10. Saely, C. H. Brown versus white adipose tissue: A Mini-Review. *Gerontology*. 2012; 58: 15-23.
11. Christodoulides, C. Adipogenesis and WNT signalling. *Trends Endocrinol. Metab*. 2009; 20 (1): 16-24.
12. Enerbäck, S. The origins of brown adipose tissue. *N. Engl. J. Med*. 2009; 360: 2021-3.
13. Rosen, E. D. et al. Adipocyte differentiation from the inside out. *Nat. Rev. Mol. Cell Biol*. 2006; 7 (12): 885-96.

physiological implications[14,15].

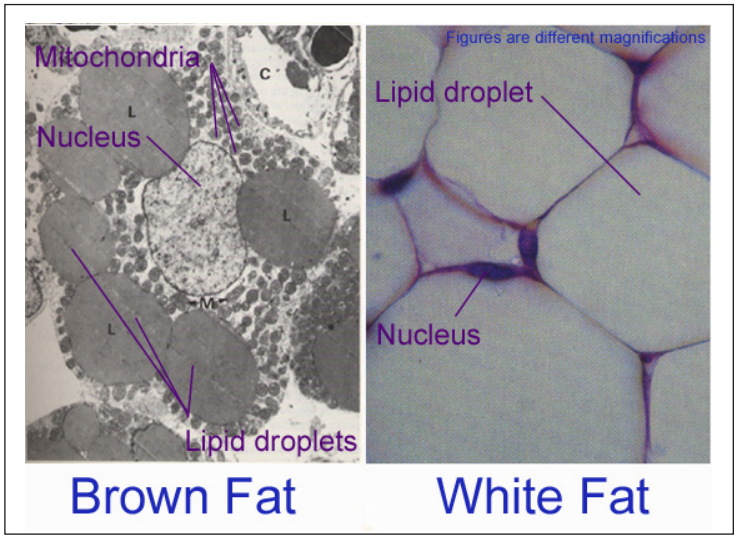

SCHEME-2. Electronic micrograph comparing cross-sections from BAT and WAT adipose tissues. In contrast to WAT, which stores triglycerides in a single lipid droplet, BAT contains numerous smaller droplets and a much higher number of (iron-containing) mitochondria, which make it brown. BAT also contains more capillaries than WAT, since it has a greater need for oxygen than most tissues. (Figure extracted from http://thepsychologyoffitness.com/2012/03/01/the-science-of-fat-loss-part-1-different-types-of-body-fat/)

The adipogenic differentiation process

Whereas the development of BAT takes place mainly during the embryonic/fetal period, the development of WAT can be understood as a continuous process throughout life[16]. In rodents, WAT develops mainly after birth, first in the perigonadal and subcutaneous depots, and only later in the omental depot. In humans, WAT formation begins during the second trimester of gestation and by birth both the visceral and subcutaneous depots are apparent. The fact developing further adipose tissue after birth, reflects the need of the newborn to survive in a new environment and to adapt to new intervals between nutrient intake[17]. Strikingly, the study of the developmental origin of fat tissues has received very little attention until now. Adipocytes, similar to muscle and bone cells, are derived from MSCs, which themselves are thought to arise from mesoderm. However, studies to define MSCs precise lineage origin and development of adipocytes during embryogenesis have not been performed[18,19]. Initially it was thought that we were born with all the fat cells we shall ever have, and that obesity resulted solely from adipocyte hypertrophy. *In vivo* studies showed that Zucker rats display adipocyte hypertrophy until a crucial cell size is reached, after which they further expand fat mass by adipocyte hyperplasia[20]. We also know that pre-adipocytes from elderly humans retain the capacity to differentiate *in vitro*[21]. Even at the adult stage, the potential to generate new fat cells persists[22]. Adipogenesis probably continues throughout life at a low rate until energy-storage demand promotes further differentiation, although crucial data in humans are lacking on this point[23]. Excessive caloric intake without a rise in energy expenditure promotes adipocyte hyperplasia and hypertrophy after birth. As mature adipocytes do not divide, regeneration of adipocytes and the increase in adipocyte number depend on self-renewal of a pool of adipocyte precursors that remains present during adult life and that can be recruited to form new fat cells. The rise in adipocyte number is triggered by signalling factors that induce conversion of MSCs that differentiate into adipocytes. MSCs are recruited from the vascular stroma of adipose tissue as from the bone marrow[24].

The adipogenic process is divided in two main phases: determination and terminal differentiation. Determination results in the conversion of the stem cell to preadipocytes, which cannot be distinguished morphologically from its precursor cell but has lost the potential to differentiate into other cell types. Recruitment to this lineage gives rise to preadipocytes, which, when induced, undergoes multiple rounds of mitosis (mitotic clonal expansion) and then differentiate into adipocytes. Whether 'mitotic clonal expansion' is required for differentiation is controversial[25]; however, it is

14. Gil, A. et al. Is adipose tissue metabolically different at different sites? *Int. J. Pediatr. Obes*. 2011; 6 (1): 13-20.
15. Montague, C. T. et al. The perils of portliness: causes and consequences of visceral adiposity. *Diabetes*. 2009; 49: 883-8.
16. Ailhaud, G. et al. Hormonal regulation of adipose differentiation. *Trends Endocrinol. Metab*. 1994; 5: 132-6.
17. MacDougald, O. A. et al. Transcriptional regulation of gene expression during adipocyte differentiation. *Annu. Rev. of Biochem*. 1995; 64: 345-73.
18. Dani, C. et al. Adipocyte Precursors: Developmental Origins, Self-Renewal, and Plasticity. Adipose Tissue Biology, 1. Ed. M.E. Symonds , Springer. (New York, USA). 2012.
19. Billion, N. et al. Developmental origin of adipocytes-new insights into a pending question. *Biol. Cell*. 2008; 100 (10): 563-75.
20. Cleary, M. P. et al. Developmental changes in thymidine kinase, DNA, and fat cellularity in Zucker rats. *Am. J. Physiol*. 1979; 236: E508-E513.
21. Hauner, H. et al. Promoting effect of glucocorticoids on the differentiation of human adipocyte precursor cells cultured in a chemically defined medium. *J. Clin. Invest*. 1989; 84: 1663-70.
22. Gregoire, F. M. et al. Understanding adipocyte differentiation. *Physiol. Rev*. 1998; 78 (3): 783-809.
23. Rosen, E. D. et al. Adipocyte differentiation from the inside out. *Nat. Rev. Mol. Cell Biol*. 2006; 7 (12): 885-96.
24. Spalding, K. L. et al. Dynamics of fat cell turnover in humans. *Nature*. 2008; 453: 783-7.
25. Otto, T. C. et al. Adipose development: from stem cell to adipocyte. *Crit. Rev. Biochem. Mol. Biol*. 2005; 40: 229-42.

clear that some of the checkpoint proteins for mitosis also regulate aspects of adipogenesis. For instance, expression of cell cycle regulators, like p21 Waf1/Cip1 or p27 Kip1 are reduced during the clonal expansion[26]. Correlating with this, loss of p21 Waf1/Cip1 and/or p27 Kip1produced adipocyte hyperplasia and obesity[27]. In the second phase, terminal differentiation, preadipocytes takes on the characteristics of the mature adipocyte, it acquires the machinery that is necessary for lipid transport and synthesis, insulin sensitivity and the secretion of adipocyte-specific proteins**.** Much progress has been made in defining the transcriptional networks controlling the terminal differentiation of preadipocytes into mature adipocytes; however, the early steps of adipocyte development origin of this lineage remain poorly known[28].

Several factors have been identified that commit the conversion of multipotent stem cells to produce preadipocytes. These include bone morphogenetic proteins (BMP)[29], Wingless-type mouse mammary tumor virus (MMTV) integration site family members (Wnt)[30,31]. BMP proteins, include BMP4, BMP2; the BMP receptors, BMPr2 and BMPr1a; and SMAD-1, -5, -8. Binding of BMP to the BMPr1: BMPr2 complex induces phosphorylation and, thus, activation of the BMPr1 kinase, that phosphorylates SMAD-1, -5, -8, which forms a complex with SMAD4 that translocate into the nucleus and regulates the transcription of target genes[32]. Exposure of dividing C3H10T1/2 stem cells to either BMP4 or BMP2 gives rise to preadipocyte-like cells which, when treated at growth arrest with differentiation inducers, enter the adipose development pathway, express adipocyte markers, and acquire the adipocyte phenotype[33]. The Wnts comprise a family of secreted signalling glycoproteins whose effects are mediated through the Frizzled Receptor and low-density lipoprotein-related protein 5/6 co-receptor[34]. Surprisingly, the Wnts act at two points in the adipose development program, early in the program as an activator of lineage commitment and late in the program as an inhibitor of adipocyte differentiation, perhaps through the actions of different Wnt proteins[35]. Wnts exert their effects by signalling through multiple so-called 'canonical' and 'non-canonical' pathways to control cell proliferation, survival, fate and behavior. Canonical Wnt signalling regulates mesenchymal stem cell fate[36]. Activation of Wnt/β-catenin signalling promotes differentiation of mesenchymal precursor cells into myocytes and osteocytes while suppressing commitment to the adipocytic lineage and terminal differentiation. Late Wnt signalling restrains adipocyte differentiation by inhibiting the expression of nuclear peroxisome proliferator–activated receptor-γ (PPARγ), transcription factors cytidine-cytidine-adenosine-thymidine (CCAT) and the complexes formed by CCAT and different enhancer-binding protein (EBP), CCAT/EBP (C/EBP), the central regulators of adipogenesis. These transcription factors are induced directly by C/EBPβ and C/EBPδ in response to adipogenic stimuli, which also serve to switch off the canonical Wnt pathway. PPARγ and C/EBPα subsequently feed back to induce their own expression, in addition to activating many downstream target genes whose expression defines the adipocyte. Conversely, there are some works that assert, Wnt signalling serves to increase the number of preadipocytes during commitment and mitotic clonal expansion, versus a "non-canonical" pathway[37] **(SCHEME-3)**.

Following commitment, adipocyte precursors re-entry into the cell cycle (mitotic clonal expansion) and undergo approximately two rounds of division, is a prerequisite for differentiation. Early markers of differentiation, such as lipoprotein lipase (LPL), are then expressed, and these cells are known as preadipocytes[38]. In the case of *in vitro* differentiation it is necessary a cocktail of inducers, including an agent to elevate cellular cyclic adenosine monophosphate (cAMP) in

26. Morrison, R. F. et al. Role of PPARγ in regulating a cascade expression of cyclin-dependent kinase inhibitors, p18 (INK4c) and p21 (Waf1/ Cip1), during adipogenesis. *J. Biol. Chem*. 1999; 274: 17088-97.
27. Naaz, A. et al. Loss of cyclin-dependent kinase inhibitors produces adipocyte hyperplasia and obesity. *FASEB J*. 2004; 18: 1925-7.
28. Billion, N. et al. Developmental origin of adipocytes-new insights into a pending question. *Biol. Cell*. 2008; 100 (10): 563-75.
29. Bowers, R. R. et al. Stable stem cell commitment to the adipocyte lineage by inhibition of DNA methylation: role of the BMP-4 gene. *Proc. Natl. Acad. Sci. USA*. 2006; 103: 13022-7.
30. Ross, S. E. et al. Inhibition of adipogenesis by Wnt signalling. *Science*. 2000; 289: 950-3.
31. Bowers, R. R. et al. Wnt signalling and adipocyte lineage commitment. *Cell Cycle*. 2008; 7: 1191-6.
32. Huang, H. Y. et al. BMP signalling pathway is required for commitment of C3H10T1/2 pluripotent stem cells to the adipocyte lineage. *Proc. Natl. Acad. Sci. USA*. 2009; 106: 12670-5.
33. Tang, Q. Q. et al. Commitment of C3H10T1/2 pluripotent stem cells to the adipocyte lineage. *Proc. Natl. Acad. Sci. USA*. 2004; 101: 9607-11.
34. Komiya, Y. et al. Wnt signal transduction pathways. *Organogenesis*. 2008; 4: 68-75.
35. Ross, S. E. et al. Inhibition of adipogenesis by Wnt signalling. *Science*. 2000; 289: 950-3.
36. Kang, S. et al. Wnt signalling stimulates osteoblastogenesis of mesenchymal precursors by suppressing CCAAT/enhancer-binding protein alpha and peroxisome proliferator-activated receptor gamma. *J. Biol. Chem*. 2007; 282(19): 14515-24 .
37. Bowers, R. et al. Wnt signalling and adipocyte lineage commitment. *Cell. Cycle*. 2008; 7: 1191-6.
38. Kokta, T. A. et al. Intercellular signalling between adipose tissue and muscle tissue. *Domest. Anim. Endocrinol*. 2004; 27: 303-31.

fetal bovine serum (FBS) containing medium, like 3-isobutyl-1-methylxanthine (IBMX), dexamethasone (DEX), as well as a high level of insulin or low level of insulin growth factor I (IGF-I)[39], a hormone similar in molecular structure to insulin that has a considerable homology to insulin. Circulating IGF-I is synthesized primarily in the liver but also by adipocytes, suggesting autocrine/paracrine effects[40]. These inducers activate IGF-I, glucocorticoids, and cAMP-signalling pathways, respectively. In the early stages of adipogenesis, insulin functions predominantly through IGF-I receptor signalling, as preadipocytes express many more receptors for IGF-I than for insulin, although this ratio shifts as differentiation proceeds[41]. It has been established that the IGF-I, rather than insulin, is the true inducer ligand. IGF-I binds~100-fold more tightly than insulin to the IGF receptor[42].

Mitotic clonal expansion involves a transcription factor cascade, followed by the expression of adipocyte genes that triggers the differentiation of preadipocytes to adipocytes. Over the past two decades, attention was centered on the role of PPARγ and members of the family C/EBP. Immediately after induction of differentiation, cAMP response element-binding protein (CREB) becomes phosphorylated and activates the expression of C/EBPβ[43,44]. However, at this point, C/EBPβ lacks DNA-binding activity. At 14–16 h after induction, dual phosphorylation on T188 by mitogen-activated protein kinase (MAPK) and on S184 or T179 by glycogen synthase kinase 3β (GSK3β), induced conformational changes in C/EBPβ that promotes dimerization and gives rise to DNA binding activity as the preadipocytes reenter the cell cycle. Beginning 18-24h, C/EBPβ triggers transcription of PPARγ and C/EBPα, which, in turn, coordinately activate genes whose expression produces the adipocyte phenotype. C/EBPα and PPARγ function together as pleiotropic transcriptional activators of the large group of genes that produce the adipocyte phenotype[45,46,47]. Within their proximal promoters, both the C/EBPα and PPARγ genes possess C/EBP regulatory elements at which C/EBPβ binds to coordinately activate transcription[48,49,50,51]. Once expressed, PPARγ and C/EBPα positively cross-activate each other through their respective C/EBP regulatory elements. Presumably, this action perpetuates the adipocyte phenotype in the mature adipocyte[52,53].

After preadipocytes stop proliferating, late markers of differentiation, such as glycerol-3-phosphate dehydrogenase (GPDH) and fatty acid synthetase (FAS) are detected. Cells then begin lipid accumulation in the cytosol at which time cells are called adipocytes. Terminal adipocyte differentiation is seen as the accumulation of lipid so that the nucleus is displaced from the center to the periphery of the cell[54]. Likewise, numerous regulatory proteins, characteristic of adipocytes *in situ*, are coordinately expressed, including insulin receptors, the insulin- responsive glucose transporter, leptin, and others[55,56].

39. MacDougald, O. A. et al. Transcriptional regulation of gene expression during adipocyte differentiation. *Annu. Rev. Biochem*. 1995; 64: 345-73.
40. Peter, M. A. et al. Regulation of insulin-like growth factor-I (IGF-I) and IGF-binding proteins by growth hormone in rate white adipose tissue. *Endocrinology*. 1993; 133: 2624-31.
41. Smith, P. J. et al. Insulin-like growth factor-I is an essential regulator of the differentiation of 3T3-L1 adipocytes. *J. Biol. Chem*. 1988; 263: 9402-8.
42. Otto, T. C. et al. Adipose development: from stem cell to adipocyte. *Crit. Rev. Biochem. Mol. Biol*. 2005; 40: 229-42.
43. Zhang, J. W. et al. Role of CREB in transcriptional regulation of CCAAT/enhancer-binding protein beta gene during adipogenesis. *J. Biol. Chem*. 2004; 279: 4471-8.
44. Zhang, Jm W. et al. Dominant-negative C/EBP disrupts mitotic clonal expansion and differentiation of 3T3-L1 preadipocytes. *Proc. Natl. Acad. Sci. USA*. 2004; 101: 43-7.
45. MacDougald, O. A. et al. Transcriptional regulation of gene expression during adipocyte differentiation. *Annu. Rev. Biochem*. 1995; 64: 345-73.
46. Hwang, C. S. et al. Adipocyte differentiation and leptin expression. *Annu. Rev. Cell Dev. Biol.* 1997; 13: 231-59.
47. Rosen, E. D. et al. Molecular regulation of adipogenesis. *Annu. Rev. Cell Dev. Biol.* 2000, 16: 145-71.
48. Lane, M. D. et al. Role of C/EBPα in adipocyte differentiation. In Nutrition Genetics Obesity: Pennington Center Nutrition Series. Ed. GA Bray, DH Ryan. (Lousiana, USA) 1999.
49. Christy, R. J. et al. CCAAT/enhancer binding protein gene promoter: binding of nuclear factors during differentiation of 3T3-L1 preadipocytes. *Proc. Natl. Acad. Sci. USA*. 1991; 88: 2593-7.
50. Abboud, T. K. et al. Desflurane: a new volatile anesthetic for cesarean section. Maternal and neonatal effects. *Acta Anaesthesiol. Scand*. 1995; 39: 723-6.
51. Clarke, S. L. et al. CAAT/enhancer binding proteins directly modulate transcription from the peroxisome proliferator-activated receptor gamma 2 promoter. *Biochem. Biophys. Res. Commun*. 1997; 240: 99-103.
52. Date, T. et al. Bone morphogenetic protein-2 induces differentiation of multipotent C3H10T1/2 cells into osteoblasts, chondrocytes, and adipocytes in vivo and in vitro. *J. Orthop. Sci*. 2004; 9: 503-8.
53. Elberg, G. et al. Modulation of the murine peroxisome proliferator-activated receptor gamma 2 promoter activity by CCAAT/enhancer-binding proteins. *J. Biol. Chem*. 2000; 275: 27815-22.
54. Giorgino, F. et al. Regional differences of insulin action in adipose tissue: insights from in vivo and in vitro studies. *Acta Physiol. Scand.* 2005: 183: 13-30.
55. Taylor-Jones, J. M. et al. Activation of an adipogenic program in adult myoblasts with age. *Mech. Ageing Dev*. 2002; 123: 649-61.
56. Rosen, E. D. et al. Adipocyte differentiation from the inside out. *Nat. Rev. Mol. Cell Biol*. 2006; 7 (12): 885-96.

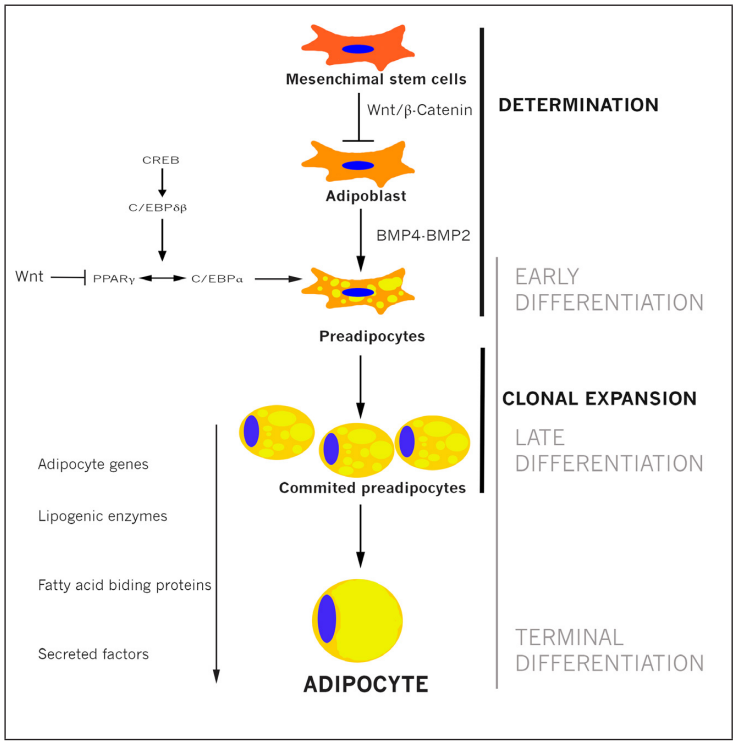

SCHEME-3. Intracellular signalling pathways involved in adipogenesis. Canonical WNT signalling regulates mesenchymal stem cell fate. Activation of WNT/β-catenin signalling promotes differentiation of mesenchymal precursor cells into myocytes and osteocytes while suppressing commitment to the adipocytic lineage and terminal differentiation. WNT signalling restrains adipocyte differentiation by inhibiting the expression of PPARγ and C/EBPα, the central regulators of adipogenesis. These transcription factors are induced directly by C/EBPβ and C/EBPδ in response to adipogenic stimuli, which also serve to switch off the canonical WNT pathway. PPARγ and C/EBPα A subsequently feed back to induce their own expression, in addition to activating many downstream target genes whose expression defines the adipocyte.

Autocrine and paracrine factors regulating adipogenic differentiation

WAT it is not only a site of energy storage providing a massive energy reserve that could be mobilized upon demand, with considerable capacity to expand, making it perhaps the only tissue in the body with the ability to increase in size so drastically without underlying transformation of the cellular phenotype[57]. The discovery of PPARγ and the C/EBPs gave the field a starting point, but it is becoming clear that the participation of these factors do not fully explain the transcriptional basis of adipocyte differentiation. Recent studies have revealed that WAT acts as an autocrine/paracrine organ that releases different hormones, adipokines and new transcription factors, in addition to a complex and interleaving set of cofactors, that act locally or in an endocrine manner, playing key roles in global energy metabolism[58,59]. Adiponectin avoids insulin resistance. Although it circulates in high concentrations, adiponectin levels are lower in obese subjects than in lean subjects, and are also reduced in association with insulin resistance and diabetes type II[60]. Leptin, which is expressed and secreted by adipocytes in proportion to adipose tissue mass, is anorectic and acts to limit energy storage when adipose tissue reserves have been filled. Leptin interacts with specific receptors in the hypothalamus to reduce food intake. In the obese state, however, resistance to leptin occurs, limiting its effectiveness. It also promotes angiogenesis in adipose tissue, to prevent adipocyte hypoxia[61]. Omentin, which is also preferentially expressed and release by visceral adipose tissue, appears to increase adipocyte insulin sensitivity and promote insulin- stimulated glucose uptake, via stimulation of Akt signalling pathway[62]. Chemerin promotes insulin receptor substrate-1 (IRS-1) phosphorylation and concomitantly enhances glucose uptake in 3T3-L1 adipocytes[63]. Pre-adipocytes and adipocytes express and secrete high amounts of IGF-I in humans and several animal models. The production rate increases during adipocyte differentiation, suggesting an autocrine/paracrine action of IGF-I during adipose tissue development[64]. IGF-I increases glucose transport and lipogenesis and inhibits lipolysis[65].

Adipose tissue is also under the control of the central nervous system because it is innervated by neurons of the sympathetic nervous system that secrete adrenergic hormones (epinephrine/

57. Blüher, S. Insulin-like growth factor I, growth hormone and insulin in white adipose tissue. *Best Pract. Res. Clin. Endocrinol. Metab*. 2005; 19 (4): 577-87.

58. Saltiel, A. R. You are what you secrete. *Nature Medicine*. 2001; 7: 887-8.
59. Kratchmarova, I. et al. A proteomic approach for identification of secreted proteins during the differentiation of 3T3-L1 preadipocytes to adipocytes. *Mol. Cell Proteomics*. 2002; 1: 213-22.
60. Lihn, A. S. et al. Adiponectin: action, regulation and association to insulin sensitivity. *Obes. Rev*. 2005; 6 (1): 13-21.
61. Friedman, J. M. Leptin, leptin receptors and the control of body weight. *Eur. J. Med. Res*. 1997; 2: 7-13.
62. Yang, R. Z. et al. Identification of omentin as a novel depot- specific adipokine in human adipose tissue: possible role in modulating insulin action. *Am. J. Physiol. Endocrinol. Metab*. 2006; 290: E1253-E1261.
63. Takahashi, M. et al. Chemerin, a novel adipokine that regulates adipogenesis and adipocyte metabolism. *FEBS Lett*. 2008; 282: 573-8.
64. Gaskin, H. R. et al. Regulation of insulin-like growth factor-Iribonucleicadic expression, polypeptide secretion, and binding protein activity by growth hormone in porcine preadipocyte cultures. *Endocrinology* .1990; 126: 622-30.
65. Wabitsch, M. et al. The role of growth hormone/insulin-like growth factors in adipocyte differentiation. *Metabolism*. 1995; 44: 45-9.

norepinephrine) that promote fat mobilization[66,67]. The cyclin dependent-3/cyclin-dependent kinase-6 (CDK6) complex binds to and phosphorylates PPARγ resulting in increased transcriptional activity of PPARγ, which promotes adipogenesis[68]. Cyclin-dependent kinase-4 (CDK4) also interacts with and activates PPARγ; this interaction requires the kinase domain of CDK4 but does not seem to involve direct phosphorylation of PPARγ[69]. Conversely, cyclin D1 represses PPARγ activity and inhibits adipocyte differentiation[70].

Circulating free fatty acids (FFAs) derived from adipocytes are elevated in obesity states and have been suggested to contribute to the insulin resistance of diabetes and obesity by inhibiting glucose uptake, glycogen synthesis and glucose oxidation, by increasing hepatic glucose output[71].

Molecular mechanisms implicated in adipogenic differentiation

As discussed above, the program of adipogenesis is modeled by the sequential activation of transcription factors. These transcription factors function as a downstream of signalling pathways that transduce information about the suitability of intracellular and extracellular conditions for differentiation[72]. Two kinase systems, mitogen-activated protein kinase (MAPK) and phosphatidylinositol 3-kinase (PI3K)- Akt/protein kinase B (PKB), in 3T3-L1 cells can be activated by insulin, the main adipogenic hormone[73]. Several studies have looked at the effects of MAPK family members on adipogenesis with conflicting results[74]. The weight of evidence favors a role for extracellular signal-regulated kinase-1 (ERK1) and p38 in adipocyte differentiation, with confusion stemming from divergent effects in different phases of differentiation. ERK1, for example, is required in the proliferative phase of differentiation, and blockade of ERK activity in 3T3-L1 cells, or in mice inhibits adipogenesis. By contrast, in the terminal differentiation phase, ERK1 activity leads to phosphorylation of PPARγ, which inhibits differentiation. This implies that ERK1 activity has to be reduced after proliferation so that differentiation can proceed; this reduction is mediated in part by MAPK phosphatase-1 (MAPKP-1)[75]. Data in 3T3-L1 cells indicated that p38 might be required for adipogenesis; however, loss of p38 seems to promote differentiation in primary pre-adipocytes, ES cells and $p38^{-/-}$ MEFs. The answer to this paradox seems to lie within 3T3-L1 cells, in which p38 has a unique pro-adipogenic effect that is not seen in other cell models[76]. Downstream components of the insulin-IGF-I signalling cascade are also crucially important for adipogenesis. The loss of individual insulin-receptor substrate (IRS) proteins inhibits adipogenesis, because it promotes CREB phosphorylation[77].

Moving down the insulin-signalling cascade, PI3K as well as Akt play an essential role in adipogenesis. PI3K/Akt signalling acts as the node for multiple growth factors and their cellular responses[78]. RNAi-mediated decrease in Akt1 was found to block the differentiation of 3T3- L1 cells[79]. Constitutively active Akt can promote the differentiation of 3T3-L1 cells into adipocytes, even in the absence of other inputs[80]. Furthermore, mouse embryonic fibroblasts (MEFs) and 3T3-L1 lacking Akt1 display an inability to differentiate into adipocytes[81], this defect stems from an inability to induce PPARγ expression at the initiation of the adipogenesis program[82, 83]. The PPARγ transcription factor is the master regu-

66. Rodbell, M. The metabolism of isolated fat cells. IV. Regulation of release of protein by lipolytic hormones and insulin. *J. Biol. Chem.* 1966; 241: 3909-17.
67. Karastergiou, K. et al. The autocrine and paracrine roles of adipokines. *Mol. Cell. Endocrinol*. 2010; 318: 69-78.
68. Sarruf, D. A. et al. Cyclin D3 promotes adipogenesis through activation of peroxisome proliferator-activated receptor. *Mol. Cell. Biol*. 2005; 25: 9985-95.
69. Abella, A. et al. Cdk4 promotes adipogenesis through PPARγ activation. *Cell Metab*. 2005; 2: 239-49.
70. Fu, M. et al. Cyclin D1 inhibits peroxisome proliferator-activated receptor γ-mediated adipogenesis through histone deacetylase recruitment. *J. Biol. Chem.* 2005; 280, 16934-41.
71. Bergman, R. N. et al. Free fatty acids and pathogenesis of type 2 diabetes mellitus. *Trends Endocrinol. Metab*. 2000; 11: 351-6.
72. Rosen, E. D. et al. Adipocyte differentiation from the inside out. *Nat. Rev. Mol. Cell Biol*. 2006; 7 (12): 885-96.
73. Jinfei, X. et al. PKB/Akt Plays Pivotal Role in IGF-I Adipocyte Differentiation. *J. Biol. Chem*. 2004; 279 (20): 35914-22.
74. Bost, F. et al. The role of MAPKs in adipocyte differentiation and obesity. *Biochimie*. 2005; 87: 51-6.
75. Sakaue, H. et al. Role of MAPK phosphatase-1 (MKP-1) in adipocyte differentiation. *J. Biol. Chem*. 2004; 279: 39951-7.
76. Aouadi, M. et al. Inhibition of p38MAPK increases adipogenesis from embryonic to adult stages. *Diabetes*. 2006; 55: 281-9.
77. Cypess, A. M. et al. Insulin/IGF-I regulation of Necdin and Brown Adipocyte Differentiation Via CREB- and FoxO1- Associated Pathways. *Endocrinology*. 2011; 152 (10): 3680-9.
78. Jinfei, X. et al. PKB/Akt Plays pivotal role in IGF-I adipocyte differentiation. *J. Biol Chem.* 2004; 279 (20): 35914-22.
79. Xu, J. et al. Protein kinase B/Akt 1 plays a pivotal role in insulin-like growth factor-1 receptor signalling induced 3T3-L1 adipocyte differentiation. *J. Biol. Chem.* 2004; 279: 35914-22.
80. Kohn, A. D. et al. Expression of a constitutively active Akt Ser/Thr kinase in 3T3-L1 adipocytes stimulates glucose uptake and glucose transporter 4 translocation. *J. Biol. Chem.* 1996; 271 (49): 31372-8.
81. Baudry, A. et al. PKBα is required for adipose differentiation of mouse embryonic fibroblasts. *J. Cell Sci.* 2006; 119: 889-97.
82. Peng, X. D. et al. Dwarfism, impaired skin development, skeletal muscle atrophy, delayed bone development, and impeded adipogenesis in mice lacking Akt1 and Akt2. *Genes Dev*. 2003; 17: 1352-65.
83. Yun, S. J. et al. Isoform- specific regulation of adipocyte differentiation by Akt/protein kinase B α. *Biochem. Biophys. Res. Commun.* 2008; 371: 138-43.

lator of adipocyte differentiation, as well as Akt[84]. While it is clear from these studies that Akt is both necessary and sufficient to drive adipogenesis, its downstream targets involved in regulating this differentiation program are not well understood[85].

The forkhead box O1 (FoxO1) family of transcription factors are phosphorylated and inhibited by Akt, exporting it out of the nucleus because its presence in the nucleus strongly attenuates adipocyte differentiation[86]. FoxO1 expression is highest in adipose tissue, but FoxO1 appears to be a strong inhibitor of adipocyte differentiation[87]. Furthermore, FoxO1 has been proposed to directly repress PPARγ transcription[88]. Taken together, these studies suggest that Akt-mediated inhibition of FoxO1 is one mechanism by which Akt induces PPARγ and subsequent adipocyte differentiation[89]. It could be expected that the activation of PKB/Akt by the IGF-I receptor signal leads to the phosphorylation and inactivation of FoxO and removes its braking effect on the adipogenic transcription factors[90].

Other downstream signal of Akt involved in adipogenesis is the mammalian target of rapamycin (mTOR)[91], a critical regulator of mRNA translation and cell growth[92]. Using mTOR-specific inhibitor rapamycin, several studies have concluded that mTOR activity is required for proper differentiation of preadipocyte cell lines and primary cultures[93,94]. The effects of rapamycin were found to correlate with a reduction in PPARγ mRNA and protein levels[95,96,97,98]. Akt activity results in downstream activation of mTOR complex 1 (mTORC1), which is acutely sensitive to rapamycin. A second mTOR-containing protein complex, mTORC2, lies upstream of Akt and contributes to Akt activation by insulin and growth factors by phosphorylating S473 in its hydrophobic regulatory motif[99]. mTORC2 is resistant to the acute effects of rapamycin, but prolonged treatment with rapamycin disrupts mTORC2 and in some lines results in loss of Akt phosphorylation[100,101,102].

Another target of Akt-mediated phosphorylation is GATA2, a transcription factor specifically expressed in the stromal vascular fraction of the adipose tissue where preadipocytes reside. In fact, GATA2 blocks the transition from preadipocyte to adipocyte in part through suppression of PPAR-γ2 expression after being phosphorylated by PI3K/Akt[103, 104].

84. Rosen, E. D. et al. PPARγ: a nuclear regulator of metabolism, differentiation, and cell growth. *J. Biol. Chem.* 2001; 276: 37731-4.
85. Zhang, H. H. et al. Insulin stimulates adipogenesis through the Akt-TSC2-mTORC1 pathway. *PLoS One*. 2009; 10; 4 (7): E6189.
86. Yun, S. J. et al. Isoform- specific regulation of adipocyte differentiation by Akt/protein kinase B α. *Biochem. Biophys. Res. Commun*. 2008; 371: 138-43.
87. Nakae, J. et al. The forkhead transcription factor Foxo1 regulates adipocyte differentiation. *Dev. Cell*. 2003; 4: 119-29.
88. Armoni, M. et al. FoxO1 represses peroxisome proliferator-activated receptor-gamma1 and -gamma2 gene promoters in primary adipocytes. A novel paradigm to increase insulin sensitivity. *J. Biol. Chem*. 2006; 281: 19881-91.
89. Wolfrum, C. et al. Role of Foxa-2 in adipocyte metabolism and differentiation. *J. Clin. Invest*. 2003; 112: 345-56.
90. Jinfei, X. et al. PKB/Akt Plays Pivotal Role in IGF-I Adipocyte Differentiation. *J. Biol. Chem*. 2004; 279 (20): 35914-22.
91. Kim, J. E. et al. Regulation of peroxisome proliferator-activated receptor-γ activity by mammalian target of rapamycin and amino acids in adipogenesis. *Diabetes*. 2004; 53: 2748-56.
92. Wullschleger, S. et al. TOR signalling in growth and metabolism. *Cell*. 2006; 124: 471-84.
93. Bell, A. et al. Rapamycin inhibits human adipocyte differentiation in primary culture. *Obes. Res*. 2000; 8: 249-54.
94. Yeh, W. C. et al. Rapamycin inhibits clonal expansion and adipogenic differentiation of 3T3-L1 cells. *Proc. Natl. Acad. Sci. USA*. 1995; 92: 11086-90.
95. Cho, H. J. et al. Regulation of adipocyte differentiation and insulin action with rapamycin. *Biochem. Biophys. Res. Commun*. 2004; 321: 942-8.
96. Gagnon, A. et al. Rapamycin-sensitive phase of 3T3-L1 preadipocyte differentiation after clonal expansion. *J. Cell. Physiol.* 2001; 189: 14-22.
97. El-Chaar, D. et al. Inhibition of insulin signalling and adipogenesis by rapamycin: effect on phosphorylation of p70 S6 kinase vs eIF4E- BP1. *Int. J. Obes. Relat. Metab. Disord*. 2004; 28: 191-8.
98. Kim, J. E. et al. Regulation of peroxisome proliferator-activated receptor- gamma activity by mammalian target of rapamycin and amino acids in adipogenesis. *Diabetes*. 2004; 53: 2748-56.
99. Sarbassov, D. D. et al. Phosphorylation and regulation of Akt/PKB by the rictor-mTOR complex. *Science*. 2005; 307: 1098-101.
100. Sarbassov, D, D, et al. Prolonged rapamycin treatment inhibits mTORC2 assembly and Akt/PKB. Mol Cell, 2006; 22:159-68.
101. Hahn-Windgassen, A. et al. Akt activates the mammalian target of rapamycin by regulating cellular ATP level and AMPK activity. *J. Biol. Chem*. 2005; 280: 32081-9.
102. Zhang, H. H. et al. Insulin stimulates adipogenesis through the Akt-TSC2-mTORC1 pathway. *PLoS One*. 2009; 10; 4 (7): E6189.
103. Tong, Q. et al. Function of GATA transcription factors in preadipocyte-adipocyte transition. *Science*. 2000; 290: 134-8.
104. Menghini, R. et al. Phosphorylation of GATA2 by Akt increases adipose tissue differentiation and reduces adipose tissue–related Inflammation: a novel pathway linking obesity to atherosclerosis. *Circulation*. 2005; 111: 1946-53.

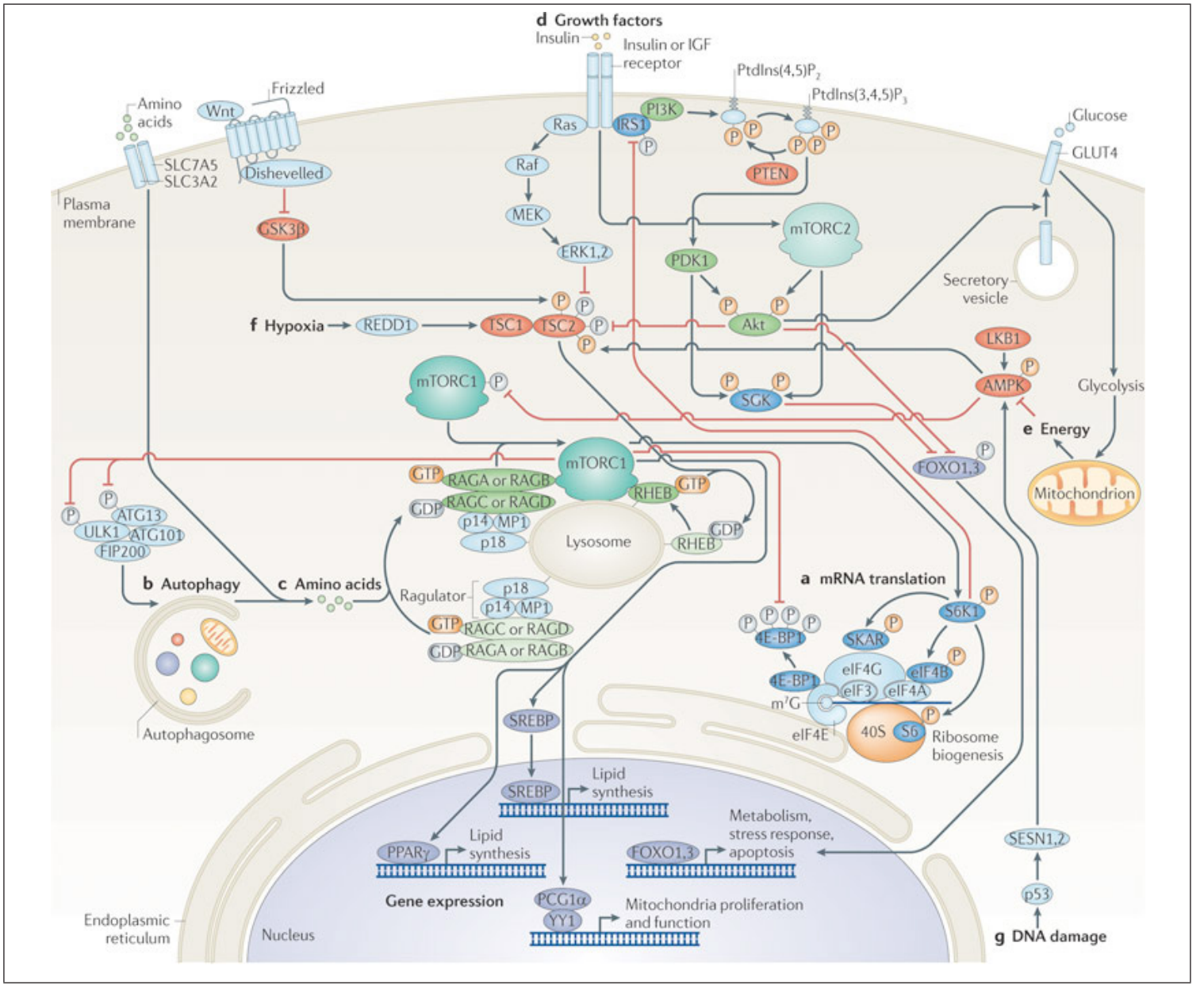

SCHEME-4. Molecular mechanisms implicated in the Akt/mTOR signalling pathway. mTOR promotes mRNAtranslation (**a**) and inhibits autophagy (**b**), by integrating nutrient signals that are generated by amino acids (**c**), growth factors such as insulin and IGFs (**d**), energy signals that act through AMPK (**e**) and various stressors including hypoxia (**f**), and DNA damage (**g**). Akt and ERK1/2 phosphorylate TSC2 inhibiting the GAP activity of TSC1–TSC2 towards Ras homologue enriched in brain (RHEB). By contrast, phosphorylation of TSC2 by AMPK and GSK3β results in the activation of TSC1–TSC2. The hypoxic factor protein regulated in development and DNA damage response 1 (REDD1; also known as DDIT4) promotes the assembly and activation of TSC1–TSC2. A second level of integration occurs at the lysosome: the Rag GTPases [which are held in place by the Ragulator, which consists of p18, p14 and MAPK scaffold protein 1 (MP1)] recruit mTORC1 to the lysosomal surface in response to amino acids (**c**); in turn, lysosomal recruitment enables mTORC1 to interact with GTP-bound RHEB, the end point of growth factor (**d**), energy (**e**) and stress (**f**,**g**) inputs. Growth factor receptors activate mTORC2 near the plasma membrane (**d**), where mTORC2 may be recruited through binding of mammalian stress-activated map kinase-interacting protein 1 (mSIN1; also known as MAPKAP1) to phospholipids. Because of its role in phosphorylating and activating Akt, mTORC2 forms a core component of the phosphoinositide 3-kinase (PI3K) pathway. (Figure extracted from *Nat. Rev. Mol. Cell Biol.* 2011; 12: 21-35)

MYOGENESIS

Types of tissues, characteristics and different functions

There are three major types of muscle structure in our body **(SCHEME-5)**:

1. **Skeletal muscle/voluntary muscle**, responsible for skeletal movement such as locomotion and in maintaining posture and it is the most abundant.
2. **Smooth muscle**, found within the walls of organs and blood vessels, it is not under conscious control.
3. **Cardiac muscle**, an involuntary muscle and is found only in the heart.

Skeletal muscle exhibits a distinctive banding pattern when viewed under the microscope due to the arrangement of cytoskeletal elements in the cytoplasm of the muscle fibers. The structural and functional element of skeletal muscle is the myofiber. Each myofiber is surrounded by the endomysium, also called the basement membrane or basal lamina. Bundles of myofibers are surrounded by the perimysium, while the entire muscle is contained within the epimysium. Each myofiber is anchored at its extremities to tendons or tendon-like fascia at the myotendinous junctions (MTJs). Myofibers are composed mainly of actin and myosin myofibrils (also known as thick and thin filaments, respectively) repeated as a sarcomere, which is the basic functional unit of skeletal muscle. Responding to the signals from motor neurons, myofibers depolarize and release calcium from the sarcoplasmic reticulum (SR). This drives the movement of actin and myosin filaments relative to one another and leads to sarcomere shortening and muscle contraction[105].

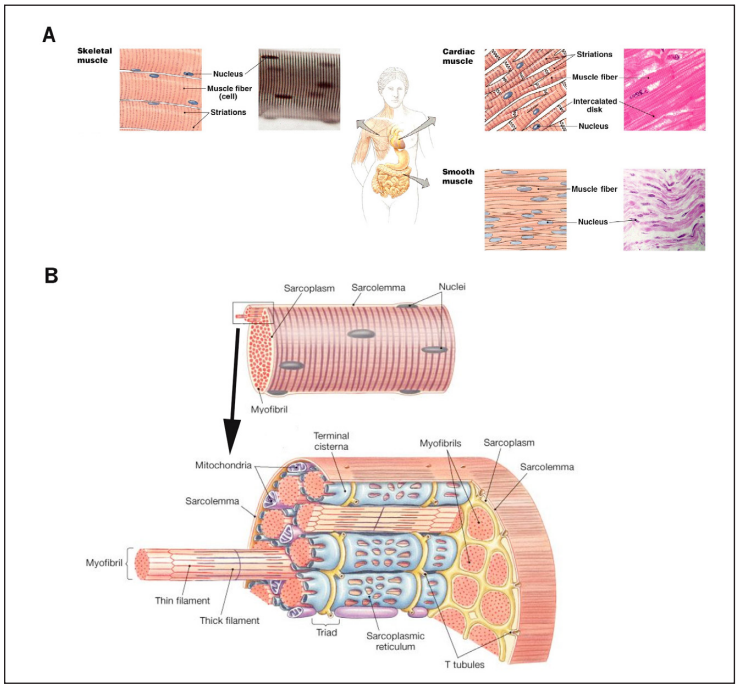

SCHEME-5. Types and anatomical description of the muscle. **(A)** Anatomical location and description of the three main types of muscle: *Cardiac muscle* located in the heart walls has striated, tubular and branched uninucleated fibers; *skeletal muscle* is usually attached to skeleton and has striated, tubular and multinucleated fibers; *smooth muscle* located in walls of internal organs and blood vessels, it has narrow and tapered rod-shaped cells, as well as non striated and uninucleated fibers. **(B)** Scheme of the different parts that conform the skeletal muscle.

Based on their physiological properties, skeletal muscle fibers can be grouped into[106]:

1. **Fast-contracting**, fatigue-susceptible type.
2. **Slow-contracting**, fatigue-resistant type.

Myofibers also vary in terms of their myosin heavy chain (MHC) isoforms (fast or slow) and metabolism types (oxidative or glycolytic), the proportion of each fiber type within a muscle determines its overall contractile property[107].

105. Scott, W. et al. Human skeletal muscle fiber type classifications. *Phys. Ther.* 2001; 81 (11): 1810-6.

106. Zierath, J. R. et al. Skeletal muscle fiber type: influence on contractile and metabolic properties. *PLoS Biol*. 2004; 2 (10): E348.

107. Yin, H. et al. Satellite cells and the muscle stem cell niche. *Physiol. Rev.* 2013; 93: 23-67.

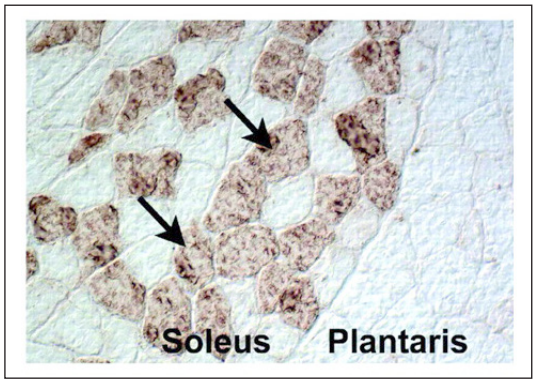

SCHEME-6. Histological section showing the different pattern of fibers distribution. The slow contracting soleus muscle is rich in myofibers expressing the slow type I MHC isoform as illustrated by the mosaic pattern displayed following immunostaining with an antibody specific to slow myosin heavy chain (arrows), whereas the fast contracting plantaris muscle is devoid of slow type I myofibers. (Figure extracted from *Physiol. Rev.* 2004; 84: 209-38)

Skeletal muscle tissue embryonic origin

In mammals, all axial and limb skeletal muscle derives from progenitors originating in the mesoderm, all are finalized during the fetal stage of development. These progenitors arise from the dorsal portion of the somite, the dermomyotome, an epithelial structure formed on the dorsal part of the somite. The dermomyotome contains multipotent progenitor cells, which eventually give rise to multiple adult tissues/cell types. The cell fate decisions largely depend on the relative position of these multipotent progenitor cells with respect to adjacent tissues (notochord, neural tube, dorsal ectoderm, and myotome) that contain the morphogenes that qualitatively trigger different cellular behavioral responses[108]. These cells destined for a muscle fate then undergo the process of myogenesis, it takes place in two successive stages[109]. Briefly, primary myofibers are first formed in the embryonic stage. Later, other signals stimulate a wave of proliferation giving rise to a population of so-called secondary myoblasts that will differentiate to form secondary fibers in the mid and late gestation in humans, and late and neonatal stages in mice[110]. The formation of secondary myofibers overlaps with adipogenesis, and fibrogenesis, which are initiated at mid-gestation in humans and late gestation in rodents[111,112] **(SCHEME-7).**

Summarizing, during myogenesis the progenitors become specified and determined as myoblasts, which in turn differentiate into postmitotic mononuclear myocytes, and these myocytes fuse to one another to form multinucleated myofibers that will be fused among them to assemble the final muscle structure[113]. All along this process different specific factors are expressed: Paired-Homebox Transcription Factors (Pax3/Pax7) are express in the course of the myogenic progenitors development, and basic helix-loop-helix (bHLH) myogenic regulatory factors (MRFs) during the next steps of differentiation. Pax3-positive cells are founder cells, forming a template of initial fibers in the limb to which Pax7-positive cells then contribute by forming secondary fibers[114,115]. The MRFs consist of four proteins: myogenic factor 5 (Myf5), myoblast determination protein 1 (MyoD), Mrf4 (also called Myf6), and myogenin. These factors were originally identified by their in vitro ability to convert 10T1/2 fibroblasts to a myogenic fate[116]. Myf5, MyoD, and Mrf4 are expressed in myoblasts[117,118,119], while myogenin is expressed in myocytes[120,121,122]. In addition, MyoD, Mrf4, and myogenin are all expressed in the myonuclei of differentiated myofibers[123,124,125].

108. Buckingham, M. Myogenic progenitor cells and skeletal myogenesis in vertebrates. *Curr. Opin. Genet. Dev.* 2006; 16: 525-32.
109. Buckingham, M. et al. The formation of skeletal muscle- from somite to limb. *J. Anat.* 2003; 202: 59-68.
110. Ross, J. J. et al. Formation of primary and secondary myotubes in rat lumbrical muscles. *Development*. 1987; 100: 383-94.
111. Michael, V. Dodson, et al. Skeletal muscle stem cells from animals I. Basic Cell Biology. *Int. J. Biol. Sci*. 2010; 6 (5): 465-74.
112. Du, M. et al. Fetal muscle development, mesenchymal multipotent cell differentiation, and associated signalling pathways. *J. Anim. Sci.* 2011; 89: 583-90.
113. Murphy, M. et al. Origin of vertebrate limb muscle- the role of progenitor and myoblast populations. *Curr. Top. Dev. Biol.* 2011; 96: 1-32.
114. McMahon, J. A. et al. Noggin-mediated antagonism of BMP signalling is required for growth and patterning of the neural tube and somite. *Genes Dev.* 1998; 12: 1438-52.
115. Bentzinger, C. F. et al. Building Muscle- Molecular Regulation of Myogenesis. *Cold Spring Harb. Perspect. Biol.* 2012; 4: A008342.
116. Weintraub, H. et al. The myoD gene family: Nodal point during specification of the muscle cell lineage. *Science*. 1991; 251: 761-6.
117. Biressi, S. et al. Intrinsic phenotypic diversity of embryonic and fetal myoblasts is revealed by genome-wide gene expression analysis on purified cells. *Dev. Biol.* 2007; 304: 633-51.
118. Kassar-Duchossoy, L. et al. Mrf4 determines skeletal muscle identity in Myf5: MyoD double-mutant mice. *Nature*. 2004; 431: 466-71.
119. Sassoon, D. et al. Expression of two myogenic regulatory factors myogenin and MyoD1 during mouse embryogenesis. *Nature*. 1989; 341: 303-7.
120. Ontell, M. et al. Contractile protein gene expression in primary myotubes of embryonic mouse hind limb muscles. *Development*. 1993; 117: 1435-44.
121. Ontell, M. P. et al. Modulation of contractile protein gene expression in fetal murine crural muscles: emergence of muscle diversity. *Dev. Dyn*. 1993; 198: 203-13.
122. Ott, M. O. et al. Early expression of the myogenic regulatory gene, myf-5, in precursor cells of skeletal muscle in the mouse embryo. *Development*. 1991; 111: 1097-107.
123. Bober, E. et al. The muscle regulatory gene, Myf-6, has a biphasic pattern of expression during early mouse development. *J. Cell Biol.* 1991; 113; 1255-65.
124. Hinterberger, T. J. et al. Expression of the muscle regulatory factor MRF4 during somite and skeletal myofiber development. *Dev. Biol.* 1991; 147: 144-56.
125. Voytik, S. L. et al. Differential expression of muscle regulatory factor genes in normal and denervated adult rat hind limb muscles. *Dev. Dyn.* 1993; 198: 214-24.

Identification of these molecular markers of the different stages of myogenic cells has been essential for reconstructing how myogenesis occurs.

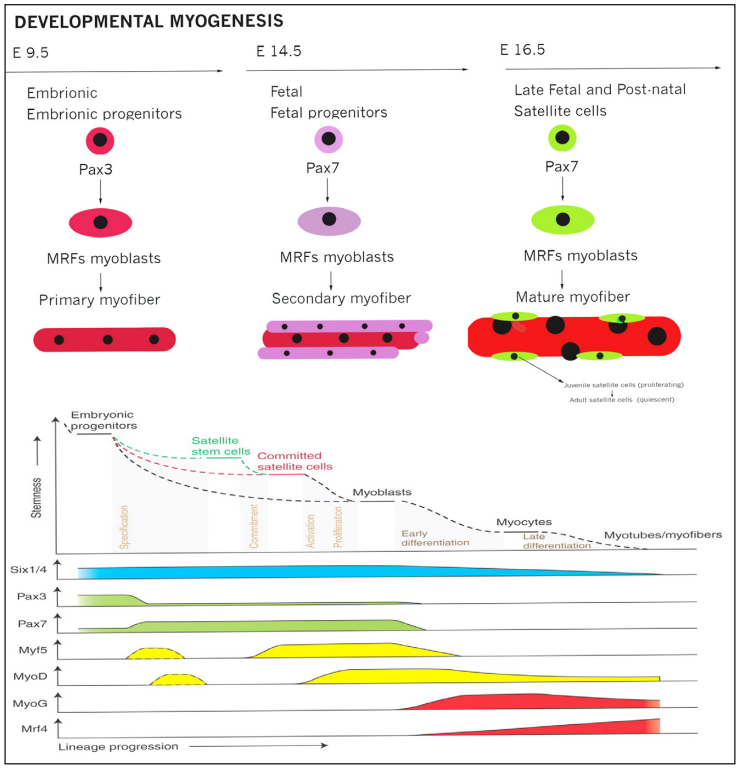

SCHEME-7. Formation and origin of trunk and hind limb mice muscles. Skeletal muscle is established in successive steps involving different types of muscle progenitors: embryonic/primary and fetal/secondary progenitors during development, and SCs in the adult. In mouse embryos, embryonic myogenesis occurs from E9.5 (embryonic day 9.5) to E16.5. From E16.5 to E18.5, fetal myogenesis allows muscle growth in the embryo. From E18.5, SCs appear that are responsible for perinatal growth and muscle regeneration. From 3 weeks postnatal, satellite cells are quiescent. Muscle progenitors that are involved in embryonic muscle differentiation skip the quiescent SCs stage and directly become myoblasts. Some progenitors remain as SCs in postnatal muscle and form a heterogeneous population of stem and committed cells. Activated committed satellite cells (myoblasts) can eventually return to the quiescent state. Six1/4 and Pax3/7 are master regulators of early lineage specification, whereas Myf5 and MyoD commit cells to the myogenic program. Expression of the terminal differentiation genes, required for the fusion of myocytes and the formation of myotubes, are performed by both myogenin and MRF4.

Satellite cells and muscle regeneration

It has been known for more than a century that skeletal muscle has the ability to regenerate new muscle fibers switching on myogenesis process, after it has been damaged by injury or as a consequence of disease such as muscular dystrophy[126]. Recent studies have revealed striking similarities in the mechanisms and the mediators of skeletal myogenesis in the embryo and in adult life[127]. Although skeletal muscle fibers are post-mitotic and unable to divide, a class of steam cells residing on the periphery of the fiber maintains the capacity for tissue remodeling and muscle regeneration[128,129,130,131]. Half a century ago, Alexander Mauro observed a group of mononucleated cells at the periphery of adult skeletal muscle myofibers by electron microscopy[132]. These cells were named satellite cells (SCs) due to their sublaminar location and intimate association with the plasma membrane of myofibers. They reside beneath the surrounding basal lamina and outside the myofiber plasma membrane. The direct juxtaposition of satellite cells and myofibers immediately raised a hypothesis that these progenitors cells may be involved in skeletal muscle growth and regeneration **(SCHEME-8)**. In intact muscle, SCs are sublaminal and mitotically quiescent (G_o phase). Quiescent SCs are characterized by the expression of Pax7 but not MyoD or myogenin[133]. Accumulating evidence indicates that adult SCs originate from the dermomyotome as all the other myogenic cell lineages. $Pax3^+/Pax7^+$ embryonic progenitor cells are the major source of adult SCs in trunk and limb muscles[134]. The quantity of SCs differs between muscles, myofiber types, developmental stages, and species. In general, SCs account for 30–35% of the sublaminal nuclei on myofibers in early post-natal murine muscles, and this number declines to 2-7% in adult muscles[135,136,137,138]. Within the same muscle, the number of SCs found on slow muscle myofibers

126. Tedesco, F. S. et al. Repairing skeletal muscle- regenerative potential of skeletal muscle stem cells. *J. Clin. Invest.* 2010; 120: 11-9.
127. Palacios, D. et al. The epigenetic network regulating muscle development and regeneration. *J. Cell Physiol*. 2006; 207 (1): 1-11.
128. Seale, P. et al. A new look at the origin, function, and "stem-cell" status of muscle satellite cells. *Dev. Biol.* 2000; 218: 115-24.
129. Charge, S. B. et al. Cellular and molecular regulation of muscle regeneration. *Physiol. Rev.* 2004; 84: 209-38.
130. Zammit, P. S. et al. The skeletal muscle satellite cell: the stem cell that came in from the cold. *J. Histochem. Cytochem*. 2006; 54: 1177-91.
131. Mckay, B. R. et al. Satellite cell number and cell cycle kinetics in response to acute myotrauma in humans: immunohistochemistry versus flow cytometry. *J. Physiol.* 2010; 588 (17): 3307-20.
132. Mauro, A. Satellite cell of skeletal muscle fibers. *J. Biophys. Biochem. Cytol.* 1961; 9: 493-5.
133. Yin, H. et al. Satellite cells and the muscle stem cell niche. *Physiol. Rev.* 2013; 93: 23-67.
134. Horst, D. et al. Comparative expression analysis of Pax3 and Pax7 during mouse myogenesis. *Int. J. Dev. Biol.* 2006; 50 (1): 47-54.
135. Allbrook, D. B. et al. Population of muscle satellite cells in relation to age and mitotic activity. *Pathology*. 1971; 3: 223-43.
136. Hellmuth, A. E. et al. Muscle satellite cell numbers during the postnatal period. *J. Anat*. 1971; 110: 503.
137. Rudnicki, M. A. et al. The molecular regulation of muscle stem cell function. *Cold Spring Harb. Symp. Quant Biol.* 2008; 73: 323-31.
138. Schultz, E. A. et al. Quantitative study of the satellite cell population in postnatal mouse lumbrical muscle. *Anat. Rec*. 1974; 180: 589-95.

(type I) is generally higher than those on fast myofibers (type IIa and type IIb)[139,140,141]. It has been reported that the density of SCs is higher at the ends of the myofibers, where the longitudinal growth of skeletal muscle happens[142]. Moreover, SCs have been observed in close proximity to capillaries[143].

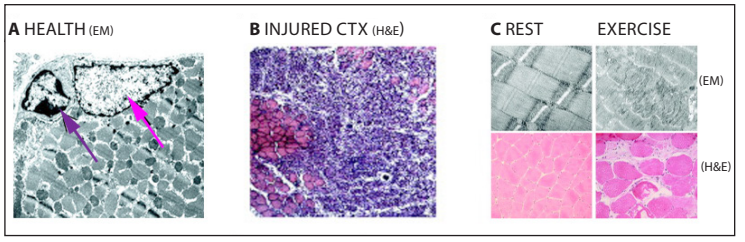

SCHEME-8. Muscle sections showing the different fibers distribution between health and injured muscle. (A) Adult skeletal muscle contains a population of SCs, closely associated with myofibers, located within the same basal lamina as seen by electron microscopy. SCs (violet arrow) can be distinguished from myonuclei (pink arrow) by their abundant heterochromatin reflecting their mitotic quiescence. **(B-C)**. Cardiotoxin versus exercise - induced damage. The extreme nature of the damage caused by cardiotoxin can be easily observed by H&E staining, with an almost complete loss of muscle fibers in the injured area at 4 days post-injection. Contrast with the lower damage caused via exercise observed in **C**. The electronic microscopy images show a clear disruption of Z - bands, indicating damage, which is also clear from the H&E.

Muscle regeneration occurs in three sequential but overlapping stages after a pharmacological or physical damage, excessive exercise or a specific pathology **(SCHEME-9)**:

1. Inflammatory response.
2. Activation, division, migration of SCs.
3. Differentiation and fusion of myotubes.
4. Maturation and remodeling of newly formed myofibers.

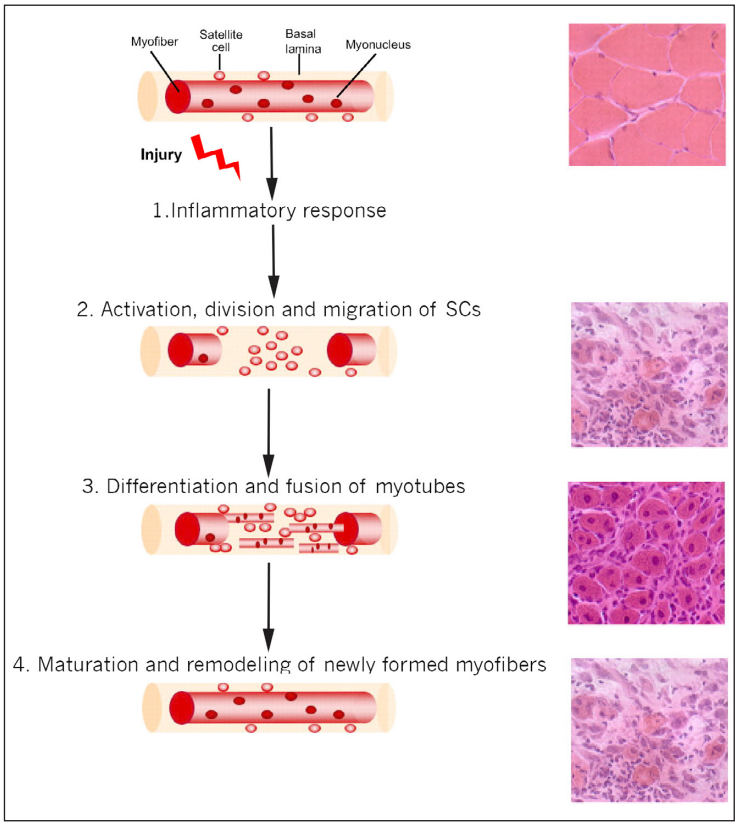

SCHEME-9. Muscle regeneration in adult mouse muscle. Left panel. Each myofiber in adult muscle is surrounded by a basal lamina sheath underneath which lie SCs in close apposition to the fiber. In response to injury, segmental necrosis of the myofiber occurs and SCs begin to proliferate and form myoblasts. These myoblasts differentiate and then migrate, adhere and fuse with one another to form multiple myotubes within the basal lamina sheath. Myoblasts/myotubes fuse with the stumps of the surviving myofiber and myotubes also fuse with each other to repair the injured myofiber. **Right panel.** Regenerated myofibers are easily identified by the presence of centrally located nuclei. For each stage of regeneration in the schematic, a representative mouse muscle section is shown in cross-section and stained with H&E to illustrate the morphological features of the tissue. (Figure extracted from *Development*. 2012; 139: 641-56).

Muscle degeneration begins with necrosis of damaged muscle fibers. This event is initiated by dissolution of the myofiber sarcolemma, which leads to increased myofiber permeability. Disruption of myofiber integrity is reflected by increased plasma levels of muscle proteins and microRNAs, such as creatine kinase (CK)[144] and miR-133a[145], which are usually

139. Gibson, M. C. et al. The distribution of satellite cells and their relationship to specific fiber types in soleus and extensor digitorum longus muscles. *Anat. Rec.* 1982; 202: 329-37.
140. Mackey, A. L. et al. Assessment of satellite cell number and activity status in human skeletal muscle biopsies. *Muscle Nerve*. 2009; 40: 455-65.
141. Okada, S. et al. Muscle fiber type differentiation and satellite cell populations in normally grown and neonatally denervated muscles in the rat. *Acta Neuropathol*. 1984; 65: 90-8.
142. Allouh, M.Z. et al. Pax7 reveals a greater frequency and concentration of satellite cells at the ends of growing skeletal muscle fibers. *J. Histochem. Cytochem*. 2008; 56: 77-87.
143. Christov, C. et al. Muscle satellite cells and endothelial cells: close neighbors and privileged partners. *Mol. Biol. Cell.* 2007; 18: 1397-409.
144. Angelini, C. et al. Relationship of serum enzyme changes to muscle damage in vitamin E deficiency of the rabbit. *Sperimentale*. 1968; 118: 349-69.
145. Laterza, O. F. et al. Plasma MicroRNAs as sensitive and specific biomarkers of tissue injury. *Clin. Chem*. 2009; 55: 1977-83.

restricted to the myofiber cytosol. Moreover, myofiber necrosis is accompanied by increased calcium influx or calcium release from the sarcoplasmatic reticulum (SR), which, in turn, activates calcium-dependent proteolysis and drives tissue degeneration. In this process, calpain, a calcium-activated protease, has been shown to cleave myofibrillar and other cytoskeletal proteins. Myofiber necrosis also activates the complement cascade and induces inflammatory responses[146]. Subsequent to inflammatory responses, chemotactic recruitment of circulating leukocytes occurs at local sites of damage. Neutrophils are the first inflammatory cells to infiltrate the damaged muscle, with a significant increase in their number being observed as early as 1–6 h after myotoxin- or exercise-induced muscle damage[147]. Following neutrophil infiltration, two distinct subpopulations of macrophages (MPs) sequentially invade the injured muscle and become the predominant inflammatory cells[148]. The early invading MPs, characterized by the surface markers cluster of differentiation 68^+ and 163^-($CD68^+/CD163^-$), reach their highest concentration in damaged muscle at 24 h after the onset of injury and thereafter rapidly decline. These $CD68^+/CD163^-$MPs secrete proinflammatory cytokines, such as tumor necrosis factor-α (TNF-α) and interleukin-1 (IL-1), and are responsible for the phagocytosis of cellular debris. A second population of MPs, containing $CD68^+/CD163^-$, reaches their peak at 2–4 days after injury. These MPs secrete anti-inflammatory cytokines, such as interleukin-10 (IL-10), and persist in damaged muscle until the termination of inflammation. Notably, the $CD68^+/CD163^-$-MPs also reportedly facilitate the proliferation and differentiation of SCs[149,150,151,152].

Following muscle damage, SCs activate and undergo rounds of proliferation before differentiating and fusing with existing myofibers[153,154]. SCs activation is not only restricted to the site of muscle damage. In fact, localized damage at one end of a muscle fiber leads to the activation of all satellite cells along the same myofiber and migration of these SCs to the regeneration site[155]. It has been observed that SCs can migrate between myofibers and even muscles across barriers of basal lamina and connective tissues during muscle development, growth, and regeneration [156,157,158]. Recently, sialomucin CD34, whose expression is high on quiescent SCs but dramatically reduced during satellite cell activation, was demonstrated to act as an antiadhesive molecule to facilitate migration and promote the proliferation at very early stages of muscle regeneration[159]. In addition, dynamic regulation of ephrin receptors and ephrin ligands have been shown to direct SCs migration[160]. Progression of SCs through the myogenic program is controlled by the coordinated up- and down-regulation of MRFs. The upregulation of Myf5 marks the earliest phase of myogenic commitment followed by the concomitant expression of MyoD, which together mark the majority of newly activated SCs (myoblasts). Following proliferation, these cells express markers of myoblast differentiation (MRF4 and myogenin) giving rise to nascent myotubes, that will be fused to form new myofibers, aiding in the repair process[161,162].

Similar to embryonic myogenesis, *de novo* formation of myofibers during muscle regeneration happens in two stages. In the first stage, individual differentiated myoblasts fuse to one another and generate nascent myotubes with few nuclei. In the second phase, additional myoblasts incorporate into the nascent myotubes, forming a mature myofiber with increased size and expression of contractile proteins **(SCHEME-10)**. In recent years, studies in

146. Orimo, S. et al. Analysis of inflammatory cells and complement C3 in bupivacaine-induced myonecrosis. *Muscle Nerve*. 1991; 14: 515-20.
147. Fielding, R. A. et al. Acute phase response in exercise. III. Neutrophil and IL-1 beta accumulation in skeletal muscle. *Am. J. Physiol. Regul. Integr. Comp. Physiol.* 1993; 265: R166-R172.
148. Chazaud, B. et al. Dual and beneficial roles of macrophages during skeletal muscle regeneration. *Exerc. Sport. Sci. Rev.* 2009; 37: 18-22.
149. Cantini. M, et al. Macrophage-secreted myogenic factors: a promising tool for greatly enhancing the proliferative capacity of myoblasts in vitro and in vivo. *Neurol. Sci*. 2002; 23: 189-94.
150. Lescaudron, L. et al. Blood borne macrophages are essential for the triggering of muscle regeneration following muscle transplant. *Neuromuscul. Disord*. 1999; 9: 72-80.
151. Merly, F. et al. Macrophages enhance muscle satellite cell proliferation and delay their differentiation. *Muscle Nerve*. 1999; 22: 724-32.
152. Sonnet, C. et al. Human macrophages rescue myoblasts and myotubes from apoptosis through a set of adhesion molecular systems. *J. Cell Sci.* 2006; 119: 2497-507.
153. Holterman, C. E. et al. Molecular regulation of satellite cell function. *Semin. Cell Dev. Biol*. 2005; 16: 575-84.
154. Le Grand, F. et al. Skeletal muscle satellite cells and adult myogenesis. *Curr. Opin. Cell. Biol.* 2007; 19: 628-33.
155. Schultz, E. et al. Response of satellite cell stofocal skeletal muscle injury. *Muscle Nerve*. 1985; 8: 217-22.
156. Hughes, S. M. et al. Migration of myoblasts across basal lamina during skeletal muscle development. *Nature*. 1990; 345: 350-3.
157. Jockusch, H. et al. Migration of adult myogenic precursor cells as revealed by GFP/nLacZ labelling of mouse transplantation chimeras. *J. Cell. Sci.* 2003; 116: 1611-6.
158. Watt, D. J. et al. The movement of muscle precursor cells between adjacent regenerating muscles in the mouse. *Anat. Embryol*. 1987; 175: 527-36.
159. Alfaro, L. A. et al. CD34 promotes satellite cell motility and entry into proliferation to facilitate efficient skeletal muscle regeneration. *Stem Cells*. 2011; 29: 2030-41.
160. Stark, D. A. et al. Eph/ephrin interactions modulate muscle satellite cell motility and patterning. *Development*. 2011; 138: 5279-89.
161. Charge, S. B. et al. Cellular and molecular regulation of muscle regeneration. *Physiol. Rev*. 2004; 84: 209-38.
162. Dhawan, J. et al. Stem cells in postnatal myogenesis: molecular mechanisms of satellite cell quiescence, activation and replenishment. *Trends Cell. Biol*. 2005; 15: 666-73.

myoblast fusion *in vitro* have identified a cadre of cell surface, extracellular, and intracellular molecules, which are important for these two stages of myogenic cell fusion. For example, cell membrane proteins β 1-integrin[163], very late antigen-4 integrin (VLA-4), integrin receptor V-CAM[164], caveolin-3[165], and transcription factor Forkhead in human rhabdomyosarcoma (FKHR) also called FoxO1a have been shown to act in myoblast-to-myoblast fusion. Whereas the cytokine interleukin-4 (IL-4)[166] and calcium and calmodulin activated nuclear factor of activated T cells isoforms (NFATC2) pathway is critical for the fusion of myoblasts with nascent myotubes[167].

Muscle regeneration can be characterized by a series of morphological characteristics based on histological and immunofluorescence staining. On muscle cross-sections, newly formed myofibers can be readily distinguished by their small caliber and centrally located myonuclei. These myofibers are often basophilic in the beginning of regeneration due to protein synthesis and the expression of embryonic/developmental forms of MHC[168,169]. On muscle longitudinal sections and on isolated single myofibers, the centrally localized myonuclei were observed in discrete segments of regenerating myofibers or along the entire new myofiber, which suggests that cell fusion during regeneration happens in a focal, rather than diffuse, manner[170]. Once the regeneration process is completed, the nuclei of new myofibers will move towards the sides, as they reside in the mature fibers.

Skeletal muscle is a dynamic tissue composed of numerous elements including vascular, nervous and connective tissue. It is during skeletal muscle development and regeneration that these elements need to grow or repair in conjunction with the muscle fibers in order to produce a fully functional unit[171]. Numerous studies further revealed that the proliferation and differentiation of SCs during muscle regeneration is profoundly influenced by innervation, the vasculature, hormones, nutrition, and the extent of tissue injury[172,173,174,175,176,177,178]. Therefore *in vitro* and *in vivo* research is focused on trying to mimic the environment of the muscle regeneration process, using different approaches, surgical techniques, implants and co-cultures, with the challenge to get a therapeutic alternative. Several publications have demonstrated the effectiveness *in vitro* and *in vivo* of co-culture rat skeletal muscle SCs and micro vascular fragments (MVF) or MSCs[179] . Other challenge is the transplantation of SCs, a solution after a muscle damaged[180,181,182]. Transplantation of the cultured primary myoblasts into regenerating muscle typically results in extensive loss of the transplanted cells, terminal differentiation of the surviving cells, and virtually no contribution to the SCs compartment[183,184, 185,186,187,188]. By contrast, experiments

163. Schwander, M. et al. Beta1 integrins regulate myoblast fusion and sarcomere assembly. *Dev. Cell*. 2003; 4: 673-85.
164. Rosen, G. D. et al. Roles for the integrin VLA-4 and its counter receptor VCAM-1 in myogenesis. *Cell*. 1992; 69: 1107-19.
165. Galbiati, F. et al. Targeted down-regulation of caveolin-3 is sufficient to inhibit myotube formation in differentiating C2C12 myoblasts. Transient activation of p38 mitogen-activated protein kinase is required for induction of caveolin-3 expression and subsequent myotube formation. *J. Biol. Chem.* 1999; 274: 30315-21.
166. Horsley, V. et al. Forming a multinucleated cell: molecules that regulate myoblast fusion. *Cells Tissues Organs*. 2004; 176: 67-78.
167. Horsley, V. Regulation of the growth of multinucleated muscle cells by an NFATC2-dependent pathway. *J. Cell. Biol.* 2001; 153: 329-38.
168. Hall-Craggs, E. C. et al. Histochemical changes in innervated and denervated skeletal muscle fibers following treatment with bupivacaine (marcain). *Exp. Neurol.* 1975; 46: 345-4.
169. Wheeler, E. F. et al. Spatio temporal patterns of expression of NGF and the low-affinity NGF receptor in rat embryos suggest functional roles in tissue morphogenesis and myogenesis. *J. Neurosci.* 1992; 12: 930-45.
170. Blaveri, K. et al. Patterns of repair of dystrophic mouse muscle: studies on isolated fibers. *Dev. Dyn.* 1999; 216: 244-56.
171. Dodson, M. V. et al. Skeletal Muscle Stem Cells from Animals I. Basic Cell Biology. *Int. J. Biol. Sci*. 2010; 6 (5): 465-74.
172. D'Albis, A. et al. Regulation by thyroid hormones of terminal differentiation in the skeletal dorsal muscle. I. Neonate mouse. *Dev. Biol.* 1987; 123: 25-32.
173. Hansen-Smith, F. M. et al. Muscle satellite cells in malnourished and nutritionally rehabilitated children. *J. Neurol. Sci.* 1979; 41: 207-21.
174. Jirmanova, I. et al. Ultra structural study of experimental muscle degeneration and regeneration in the adult rat. *Z. Zellforsch. Mikrosk. Anat.* 1972; 131: 77-97.
175. McGeachie, J. K. et al. Initiation and duration of muscle precursor replication after mild and severe injury to skeletal muscle of mice. An auto radiographic study. *Cell. Tissue Res.* 1987; 248: 125-30.
176. Mulvaney, D. R. et al. Proliferation of skeletal muscle satellite cells after castration and administration of testosterone propionate. *Proc. Soc. Exp. Biol. Med.* 1988; 188: 40-5.
177. Phillips, W. D. et al. Elimination of distributed synaptic acetylcholine receptor clusters on developing avian fast-twitch muscle fibers accompanies loss of polyneuronal innervation. *J. Neurocytol.* 1987; 16: 785-97.
178. Yinm H. et al. Satellite cells and the muscle stem cell niche. *Physiol. Rev.* 2013; 93: 23-67.
179. Rhoads, R. P. et al. Satellite cell-mediated angiogenesis in vitro coincides with a functional hypoxia-inducible factor pathway. *Am. J. Physiol. Cell. Physiol.* 2009; 296: C1321-C1328.
180. Wallace, G. Q. et al. Long-Term survival of transplanted stem cells in immunocompetent mice with muscular dystrophy. *Am. J. Pathol.* 2008; 173 (3): 792-802.
181. Perie, S. et al. Premature proliferative arrest of cricopharyngeal myoblasts in oculo-pharyngeal muscular dystrophy: therapeutic perspectives of autologous myoblast transplantation. *Neuromuscul. Disord*. 2006; 16 (11): 770-81.
182. Torrente, Y. et al. Autologous transplantation of muscle-derived CD133+ stem cells in Duchenne muscle patients. *Cell. Transplant*. 2007; 16 (6): 563-77.
183. Beauchamp, J. R. et al. Dynamics of myoblast transplantation reveal a discrete minority of precursors with stem cell-like properties as the myogenic source. *J. Cell. Biol.* 1999; 144: 1113-22.
184. El Fahime, E. et al. Tubulyzine, a novel tri-substituted triazine, prevents the early cell death of transplanted myogenic cells and improves transplantation success. *Biochem. Cell. Biol.* 2003; 81: 81-90.
185. Fan, Y. et al. Rapid death of injected myoblasts in myoblast transfer therapy. *Muscle Nerve*. 1996; 19: 853-60.
186. Hodgetts, S. I. et al. Why do cultured transplanted myoblasts die in vivo? DNA quantification shows enhanced survival of donor male myoblasts in host mice depleted of CD4+ and CD8+ cells or Nk1.1+ cells. *Cell. Transplant*. 2000; 9: 489-502.
187. Qu, Z. et al. Development of approaches to improve cell survival in myoblast transfer therapy. *J. Cell. Biol.* 1998; 142: 1257-67.
188. Rando, T. A. et al. Primary mouse myoblast purification, characterization, and transplantation for cell-mediated gene therapy. *J. Cell. Biol*. 1994; 125: 1275-87.

involving transplant of intact fibers carrying SCs[189]or fresh isolated SCs[190] have suggested that at least some portion of SCs have the capacity to repopulate the SCs compartment as well as extensively contribute to regenerating muscle. All of these findings led to an intriguing notion that SCs reside in a especial microenvironment in vivo, which profoundly affects their behavior, their niche is completely crucial for the correct SCs homeostasis[191].

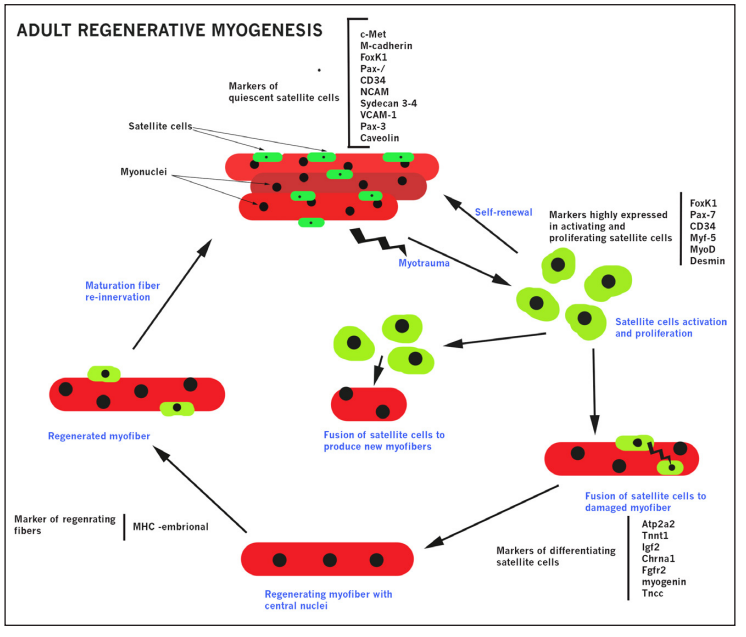

SCHEME-10. Model of adult stem cell-mediated muscle regeneration. Schematic model outlining the different stages (text in blue) of muscle regeneration. At first, activated SCs proliferate, then fuse with existing myofibers, repairing damaged muscle fibers or alternatively fuse to each other to form new myofibers, participating to muscle regeneration and repair. SCs express specific markers during the different stages of muscle regeneration. It is important to note that while these markers are all effective for identifying SCs, most of them are not selectively expressed by SCs (e. g. CD34, syndecan 3 and 4). (Figure extracted from *Ageing Res. Rev*. 2011; 10 (1): 35-42)

Self-renewal and commitment of SCs

SCs are crucial for regeneration following injury but they also have the maintaining muscle homeostasis role, by self-renewing[192]. The fate of daughter cell is determined by their relative orientation within the SCs compartment. Theoretically, sister cells can either be in a planar orientation where both cells remain in direct contact with the basal lamina and host myofiber or in an apical-basal orientation where one daughter cell is pushed toward the basal lamina and the other cell apically toward the host myofiber. Apical-basal location determines self-renewal versus differentiation[193] **(SCHEME-11)**. During regeneration both types of orientation were founded, but doublets are predominantly planar (91%). Planar divisions were observed to give rise almost exclusively to identical daughter cells, trough symmetric division. Apical-basal orientation is performed trough asymmetric division principally[194]. Results regarding asymmetric division revealed that majority of apical-basal oriented doublets contained a $Pax7^{+}/Myf5^{-}$ cell against the basal surface and a $Pax7^{+}/Myf5^{+}$ cell located on the apical side against the muscle fiber. The daughter cell attached to the basal lamina remains $Myf5^{-}$, whereas the daughter that loses contact with the basal lamina upregulates Myf5 and becomes a committed myogenic cell. Presumably, Myf 5 is a marker of SCs commitment. So apical-basal division usually gives rise to two different cells, they divided in an asymmetric mode, allowing to stem cell self- renewal. This finding strongly argues that satellite cell self-renewal is governed by the structure and signalling present in their immediate niche[195]. Trough asymmetric division, satellite stem cells self-renew to replenish the stem cell poll and produce more committed myogenic progenitors that participate in skeletal muscle growth and regeneration. Further investigation has revealed an important role for Wnt7a signalling trough the planar cell polarity pathway, controlling the homeostatic level of satellite steam cells and hence regulates the regenerative potential muscle self-renewal[196,197].

189. Collins, C. A. et al. Stem cell function, self-renewal, and behavioral heterogeneity of cells from the adult muscle satellite cell niche. *Cell*. 2005; 122: 289-301.
190. Montarras, D. et al. Direct isolation of satellite cells for skeletal muscle regeneration. *Science*. 2005; 309: 2064-7.
191. Kuang, S. et al. Asymmetric self-Renewal and commitment of satellite stem cells in muscle. *Cell*. 2007; 129; 999-1010.
192. Watt, F. M. et al. Out of Eden: stem cells and their niches. *Science*. 2000; 287: 1427-30.
193. Yin, H. et al. Satellite cells and the muscle stem cell niche. *Physiol. Rev.* 2013; 93: 23-67.
194. Cossu, G. et al. Oriented cell divisions and muscle satellite cell heterogeneity. *Cell*. 2007; 129 (5): 859-61.
195. Kuang, S. et al. Asymmetric self-renewal and commitment of satellite stem cells in muscle. *Cell*. 2007; 129: 999-1010.
196. Cossu, G. et al. Oriented cell Divisions and Muscle satellite cell Heterogeneity. *Cell.* 2007; 129 (5): 859-61.
197. Le Grand, F. et al. Wnt7a Activates the Planar Cell Polarity Pathway to Drive the Symmetric Expansion of Satellite Stem Cells. *Cell. Stem. Cell.* 2009; 4 (6): 535-47.

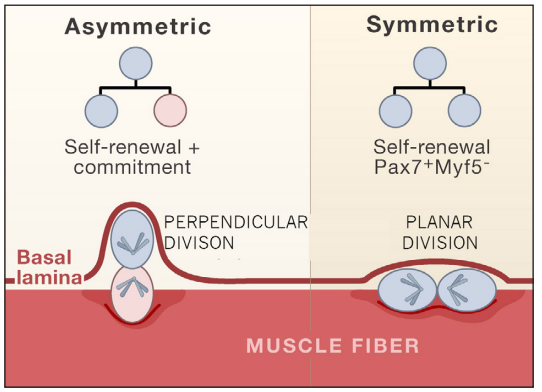

SCHEME-11. Symmetric and asymmetric division of muscle SCs. Asymmetric division of stem cells generates self-renewing and committed daughter cells. Symmetric divisions generate either two self-renewing cells that are $Pax7^{+}/Myf5^{-}$ (green) or two committed cells that are $Pax7^{+}/Myf5^{+}$ (red). In adult skeletal muscle, symmetric divisions (where the mitotic spindle is oriented parallel to the muscle fiber axis) generate two identical (either stem or committed progenitor) daughter cells that both contact the basal lamina and the plasmalemma. Asymmetric division (where the mitotic spindle is oriented perpendicular to the fiber axis) generates one self-renewing cell ($Pax7^{+}/Myf5^{-}$) that remains in contact with the basal lamina and one committed cell ($Pax7^{+}/Myf5^{+}$) that is adjacent to the plasmalemma but has lost contact with the basal lamina. (Figure extracted from *Cell*. 2007; 129: 999-1001)

Autocrine/Paracrine factors involved in myogenesis

Given that skeletal muscle is the largest organ in the human body, the discovery of muscle as a producing organ revealed a whole new paradigm: skeletal muscle is an endocrine organ, which by secretion of hormone-like factors may influence metabolism in tissues and organs. Cytokines and other peptides that are produced, expressed and released by muscle fibers and exert autocrine, paracrine or endocrine effects should be classified as myokines[198]. Myostatin, was the first secreted muscle factor discovered to fulfill the criteria of a myokine[199]. Myostatin is a highly conserved member of the TGF*α* superfamily, is secreted and processed by protein binding and proteolitic cleavage before the active protein can execute its effects by preventing myoblast hyperplasia via the cell cycle progression, and thereby reduce muscle size[200]. Knock-out of the GDF8 gene encoding this protein promotes extensive skeletal muscle hypertrophy in mice, cattle and humans[201]. Contracting human skeletal muscle releases significant amounts of interleukin-6 (IL-6) into the circulation during prolonged single-limb exercise without any sign of muscle damage[202] **(SCHEME-12).** Muscle fibers express the myokine IL-6, which subsequently exerts its effects both, locally within the muscle (e. g. through activation of AMPK) and when released into the circulation peripherally in several organs in a hormone-like fashion. Research during subsequent years highlighted the fact that muscle-derived IL-6 is an important player in metabolism. Moreover, IL-6 increased insulin-stimulated glucose uptake in muscle cells *in vitro*[203]. Specifically in skeletal muscle, IL-6 acts in an autocrine or paracrine manner to signal through a gp130R/IL-6R homodimer, resulting in the activation of AMPK and/or PI3K to increase glucose uptake and fat oxidation[204]. Another interleukin involved in myogenesis is interleukin-7 (IL-7). During differentiation of human myoblasts IL-7 induces a reduction in mRNA levels of the terminal myogenic markers myosin heavy chain 2 and myogenin[205]. There are also other cytokines involved in muscle regeneration in a less manner as IL-8[206] implicated in the further vascularization after muscle damaged, and interleukin-15 (IL-15), that also plays a role in the metabolic relation muscle-adipose tissues[207]. Other molecules were identified as novel muscle secreted factors which enhance muscle regeneration by stimulating the fusion of myoblasts with myotubes[208].They include several growth factors and other molecules as: IGF-I[209,210]; FGF-21[211,212]; vascular endothelial growth

198. Trayhurn, P. et al. Secreted proteins from adipose tissue and skeletal muscle-adipokines, myokines and adipose/muscle cross-talk. *Arch. Physiol. Biochem*. 2011; 117 (2): 47-56.
199. Kocamis, H. et al. Myostatin expression and possible functions in animal muscle growth. *Domest. Anim. Endocrinol*. 2002; 23 (4): 447-54.
200. Rodgers, B. et al. Clinical, agricultural, and evolutionary biology of myostatin: a comparative review. *Endocr. Rev*. 2008; 29: 513-34.
201. McPherron, A. et al. Regulation of skeletal muscle mass in mice by a new TGF-α superfamily member. *Nature*. 1997; 387: 83-90.
202. Steensberg, A. et al. Production of interleukin-6 in contracting human skeletal muscles can account for the exercise-induced increase in plasma interleukin-6. *J. Physiol*. 2000; 529 (1): 237-42.
203. Pedersen, B. K. et al. Muscle as an endocrine organ: focus on muscle-derived interleukin-6. *Physiol. Rev*. 2008; 88: 1379-406.
204. Pedersen, B. K. et al. Point: Interleukin-6 does have a beneficial role in insulin sensitivity and glucose homeostasis. *J. Appl. Physiol*. 2007; 102: 814-6.
205. Haugen, F. et al. IL-7 is expressed and secreted by human skeletal muscle cells *Am. J. Physiol. Cell Physiol*. 2010; 298: C807-16.
206. Keane, M. P. et al. The CXC chemokines, IL-8 and IP-10, regulate angiogenic activity in idiopathic pulmonary fibrosis. *J. Immunol*. 1997; 159: 1437-43.
207. Nielsen, A. R. et al. Expression of interleukin-15 in human skeletal muscle effect of exercise and muscle fiber type composition. *J. Physiol.* 2007; 584: 305-12.
208. Pedersen, B. K. et al. Muscles, exercise and obesity skeletal muscle as a secretory organ. *Nat. Rev. Endocrinol*. 2012; 8: 457-65.
209. Jacquemin, V. et al. IGF -1 induces human myotube hypertrophy by increasing cell recruitment. *Exp. Cell. Res.* 2004; 299 (1): 148-58.
210. Musaro, A. et al. Stem cell-mediated muscle regeneration is enhanced by local isoform of insulin-like growth factor 1. *Proc. Natl. Acad. Sci. USA*. 2004; 101 (5): 1206-10.
211. Dogra, C. et al. Fibroblast growth factor inducible 14 (Fn14) is required for the expression of myogenic regulatory factors and differentiation of myoblasts into myotubes. Evidence for TWEAK-independent functions of Fn14 during myogenesis. *J. Biol. Chem*. 2007; 282 (20): 15000-10.
212. Hojman, P. et al. Fibroblast growth factor-21 is induced in human skeletal muscles by hyperinsulinemia. *Diabetes*. 2009; 58: 2797-801.

factor (VEGF)[213,214]; hepatocitic growth factor (HGF)[215]; TNF-α[216] , and its regulation by tissue inhibitor of metalloproteinase (TIMP-3) is directly implicated in muscle regeneration[217]; brain-derived neurotrophic factor (BDNF)[218]; vasopressin receptor (V1a-R)[219]; hexamethylene bis-acetamide inducible (HEXIM1)[220] ; follistatin-related protein 1[221].

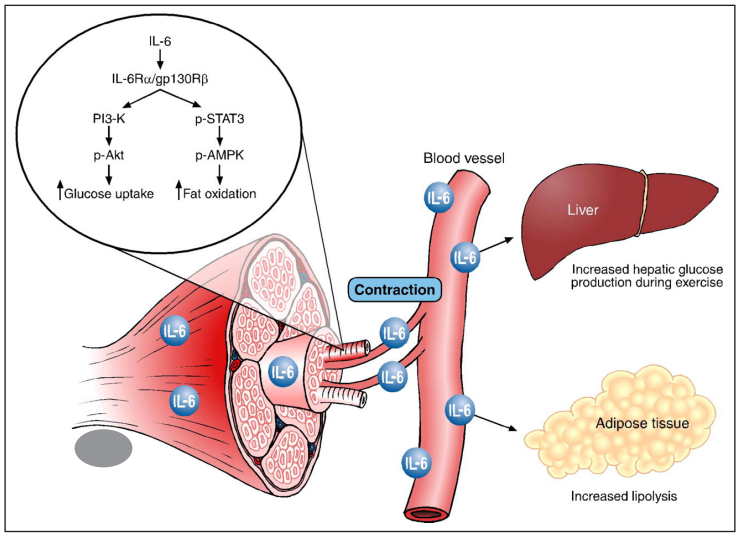

SCHEME-12. Biological role of contraction-induced IL-6. Skeletal muscle expresses and releases myokines into the circulation. In response to muscle contractions, both type I and type II muscle fibers express the myokine IL-6, which subsequently exerts its effects both locally within the muscle (e.g. through activation of AMPK) and when released into the circulation peripherally in several organs in a hormone-like fashion (Figure extracted from *J. Exp. Biol*. 2011; 214: 337-46).

213. Germani, A. et al. Vascular endothelial growth factor modulates skeletal myoblast function. *Am. J. Pathol*. 2003; 163: 1417-28.
214. Bryan, B. A. Coordinated vascular endothelial growth factor expression and signalling during skeletal myogenic differentiation. *Mol. Biol. Cell*. 2008; 19 (3): 994-1006.
215. Sugiura, T. et al. Increased HGF and c-Met in muscle tissues of polymyositis and dermatomyositis patients: beneficial roles of HGF in muscle regeneration. *Clin. Immunol*. 2010; 136 (3): 387-99.
216. Chen, S. E. et al. TNF-alpha regulates myogenesis and muscle regeneration by activating p38 MAPK. *Am. J. Physiol. Cell. Physiol.* 2007; 292 (5): C1660-71.
217. Liu, H. et al. TIMP3: a physiological regulator of adult myogenesis. *J. Cell. Sci.* 2010; 123 (17): 2914-21.
218. Miura, P. et al. Brain-derived neurotrophic factor expression is repressed during myogenic differentiation by miR-206. *J. Neurochem*. 2012; 120 (2): 230-8.
219. Toschi, A. et al. Skeletal muscle regeneration in mice is stimulated by local overexpression of V1a-vasopressin receptor. *Mol. Endocrinol.* 2011; 25: 1661-73.
220. Hong, P. et al. HEXIM1 controls satellite cell expansion after injury to regulate skeletal muscle regeneration. *J. Clin. Invest*. 2012; 122 (11): 3873-87.
221. Ouchi, N. et al. Follistatin-like 1, a secreted muscle protein, promotes endothelial cell function and revascularization in ischemic tissue through a nitric-oxide synthase-dependent mechanism. *J. Biol. Chem*. 2008; 283: 32802-11.

GLUCOSE METABOLISM OF MUSCLE AND ADIPOSSE TISSUE

Development and growth of the different tissues are intimately bounded programs. The role of energy is fundamental to such biological processes, life is dependent on energy transformations, from a variety of metabolic pathways and chemical bonds are broken and made as part of the exchange and transformation of energy. Mammals must consume organic compounds to get energy, these are mostly carbohydrates, fats and proteins[222].

Mammals possess highly integrated systems to regulate energy storage and expenditure. These systems have evolved to promote energy storage during periods of food surplus and mobilization of these stores when food is scarce[223]. Such systems are regulated both at the cellular level and in the whole organism by the coordinated actions of circulating hormones and efferent neural signals from the central nervous system both to higher brain centers and to peripheral tissues, including the liver, muscle, and adipose tissue[224]. When food is abundant, carbohydrates are stored as small reserves of glycogen in the liver and muscle and as a much larger reserve as triglycerides in adipocytes. When food is limited, these stores are mobilized in catabolic pathways to meet energy needs[225,226].

Glucose up-take occurs by diffusion and is mediated by glucose transporters (GLUT). There are over 10 different types of glucose transporters; however, the most significant for study are GLUT1-4[227].

1. **GLUT1** and **GLUT3** are located in the plasma membrane of cells throughout the body, as they are responsible for maintaining a constant basal rate of glucose uptake.
2. **GLUT2** are located in the plasma membranes of hepatocytes and pancreatic beta cells, and they have a lower affinity for glucose.

222. Lehninger, A. L. Bioenergetics: The Molecular Basis of Biological Energy Transformations . Ed. Addison-Wesley. (Indiana, USA) 1971
223. Wahren, J. et al. Splanchnic regulation of glucose production. *Annu. Rev. Nutr.* 2007; 27: 329-45.
224. Wolfgang, M. J. et al. The role of hypothalamic malonyl-CoA in energy homeostasis. *J. Biol. Chem*. 2006; 281: 37265-9.
225. Otto, T. C. et al. Adipose development: from stem cell to adipocyte. *Crit. Rev. Biochem. Mol. Biol.* 2005; 40: 229-42.
226. Cahill, G. F. Jr. Fuel metabolism in starvation. *Annu. Rev. Nutr.* 2006; 26: 1-22.
227. Joost, H. et al. The extended GLUT-family of sugar/polyol transport facilitators: nomenclature, sequence characteristics, and potential function of its novel members. *Mol. Membr. Biol*. 2001; 18 (4): 247-56.

3. **GLUT4** are found in muscle and adipose tissue, it is involved in post-prandial uptake of excess glucose from the bloodstream.

During fasting, some GLUT4 transporters will be expressed at the surface of the cell. However, most will be found within the plasma membranes of cytoplasmic vesicles within the cell. Upon reaching the plasmalemma, the vesicles fuse with the membrane, increasing the number of GLUT4 transporters expressed at the cell surface, and hence increasing glucose uptake. GLUT4 proteins transport glucose and related hexoses according to a model of alternate conformation, which predicts that the transporter exposes a single substrate binding site toward either the outside or the inside of the cell. Binding of glucose to one site provokes a conformational change associated with transport, and releases glucose to the other side of the membrane[228].

Insulin is the most potent anabolic hormone known, it stimulates the uptake of glucose, amino acids and fatty acids into cells, and increases the expression or activity of enzymes that catalyze glycogen, lipid and protein synthesis, while inhibiting the activity or expression of those that catalyze degradation[229].Up to 75% of insulin-dependent glucose disposal occurs in skeletal muscle, whereas adipose tissue accounts for only a small fraction[230]. Insulin regulates the amount of trafficking GLUT from intracellular compartments to the plasma membrane (PM) [231] **(SCHEME-13).** There are also references of GLUT translocation to the membrane after acute exercise[232]. Numerous references reflect the effect of different drugs in GLUT4 membrane translocation, 4-Hydroxyisoleucine[233], triglitazone[234]. Akt is a key node for insulin and glucose metabolism with its consequently redistribution of GLUT4 to the cell. Although the precise molecular mechanisms by which Akt stimulates GLUT4 translocation are still being intensely studied. The Rab GTPase-acting protein (GAP) Akt substrate (AS160), also known as TBC1 domain family member 4 (TBC1D4) has emerged as an important direct target of Akt involved in this process[235]. Five putative Akt sites are phosphorylated on AS160 in response to insulin, of which S588 and T642 are the most important binding sites for its bioactivity. Importantly, mutation of these two sites to alanine significantly blocks insulin-stimulated GLUT4 translocation[236]. The current model is that Akt-mediated phosphorylation of some combination of the sites on AS160 inhibits its GAP activity; thereby allowing a GAP to become GTP loaded and stimulate GLUT4 vesicle translocation.

Inside the cell, depending on the homeostasis, glucose is converted to glucose 6-phosphate that can be stored by conversion to glycogen in the muscle, or catabolized to produce cellular energy trough glycolysis, to pyruvate, which then enters the Krebs cycle in the mitochondria and is catabolized to acetyl-CoA-carboxilase (ACC), which is a feed stock for the fatty acid synthesis pathway, so they stored by conversion to triglycerides in the adipocytes, or in case, catabolized until the end of the catabolic process to get energy in form of ATP, all these processes under the control of Akt signalling[237]. Glycogen storage needs phosphorylation and consequent inactivation of GSK3 α/β. This inactivation leads to a decrease in the phosphorylation of glycogen synthase (GS) resulting in its activation, thereby stimulating glycogen synthesis[238]. Apart from GS, eukaryotic translation initiation factor 2B (eIF2B) can be also activated in a similar way leading to an increase in the glycogen synthesis and the protein synthesis[239]. Furthermore, inactivation of GSK3 has been shown to avoid degradation of the sterol regulatory element-binding proteins (SREBPs), which are transcription factors that trigger the expression of genes involved in cholesterol and fatty acid biosynthesis[240].

Storage in the adipose tissue as triglycerides is an important source of energy because they are both reduced and anhydrous. The energy yield from a gram of fatty acids is approximately 9 Kcal (37 kJ), compared to 4 Kcal/g (17 kJ/g) for carbohydrates[241].

228. Bell, G. et al. Molecular biology of mammalian glucose transporters. *Diabetes Care*. 1990; 13 (3): 198-208.
229. Saltiel, A. R. et al. Insulin signalling and the regulation of glucose and lipid metabolism. *Nature*. 2001; 414 (6865): 799-806.
230. Klip, A. et al. Glucose transport and glucose transporters in muscle and their metabolic regulation. *Diabetes Care*. 1990; 13: 228-43.
231. Pessin, J. E. et al. Molecular basis of insulin-stimulated GLUT4 vesicle trafficking. Location! Location! Location! *J. Biol. Chem*. 1999; 274: 2593-6.
232. Kennedy, J. W. et al. Acute exercise induces GLUT4 translocation in skeletal muscle of normal human subjects and subjects with type 2 diabetes. *Diabetes*. 1999; 48 (5): 1192-7.
233. Jaiswal, N. et al. 4-Hydroxyisoleucine stimulates glucose uptake by increasing surface GLUT4 level in skeletal muscle cells via phosphatidylinositol-3-kinase-dependent pathway. *Eur. J. Nutr*. 2012; 51 (7): 893-8.
234. Yonemitsu, S. et al. Troglitazone induces GLUT4 translocation in L6 myotubes. *Diabetes*. 2001; 50 (5): 1093-101.
235. Eguez, L. et al. Full intracellular retention of GLUT4 requires AS160 Rab GTPase activating protein. *Cell Metab*. 2005; 2: 263-72.
236. Sano, H. et al. Insulin-stimulated phosphorylation of a Rab GTPase-activating protein regulates GLUT4 translocation. *J. Biol. Chem*. 2003; 278: 14599-602.
237. Manning, B. D. et al. Akt/PKB signalling: navigating downstream. *Cell*. 2007; 129: 1261-74.
238. Kim, Y. M. et al. Roles of GSK3 in metabolic shift toward abnormal anabolism in cell senescence. *Ann. NY Acad. Sci*. 2010; 1201: 65-71.
239. Rayasam, G. V. et al. Glycogen synthase kinase 3: more than a namesake. *Br. J. Pharmacol*. 2009; 156: 885-98.
240. Sundqvist, A. et al. Control of lipid metabolism by phosphorylation-dependent degradation of the SREBP family of transcription factors by SCF(Fbw7). *Cell Metab*. 2005; 1: 379-91.
241. Zechner, R. et al. Lipolysis: pathway under construction. *Curr. Opin. Lipidol*. 2005; 16: 333-40.

Triglycerides storage is regulated by adenosine monophosphate-activated protein kinase (AMPK) pathway, a serine/threonine protein kinase that senses the immediate availability of cellular energy. AMPK is switched on when the ratio ADP: ATP is decreased, to get energy and consequently switching on catabolic pathways and switching off anabolic pathways[242]. However, in case of overfeeding conditions, the glucose up-take is very high, there is an increase of ATP, so energy needs to be storage. This situation triggers out the dephosphorylation of AMPK that leads to a reduction in ACC phosphorylation, and thus an increase in the activity of this enzyme. Enhanced ACC activity consequently leads to increased malonyl Co-A levels, which mediate an inhibitory effect on cholinephosphotransferase 1 (CPT-1), preventing fatty acid transport into mitochondria and fatty acid oxidation, promoting fatty acid synthesis and the consequently adipogenesis[243]. Therefore, both Akt and AMPK are involved in glucose metabolism, but their expression in overfeeding conditions is inverse, Akt regulates the intracellular ATP level and acts as a negative regulator of AMPK[244]. Akt has been shown to be an upstream negative regulator of AMPK and tuberous sclerosis protein 2 (TSC2) and, in that capacity, induces the full inhibition of TSC2 and activation of mTOR in lung cancer[245]. Conversely, Akt dephosphorylation often occurs concomitantly with AMPK activation when cells are treated with phenformin, an anti-diabetic drug, suggesting that these drugs do not only affect AMPK but also cause a coordinated inverse regulation of AMPK and Akt[246].

Both pathways, GS or AMPK, favor glycogen/fat deposition respectively, with the consequent inhibition of breakdown plus burning stored energy and reduction of body weight. There is a main difference between muscle and adipose tissue glucose metabolism. In the first case, muscle metabolism does not implicate myogenesis, however in adipose tissue, an increase in glucose uptake involve the adipogenesis process and the consequently enhance of adipose tissue size. Despite these control mechanisms to survive feast or famine situations, lifestyles in developed societies have led to excessive consumption of energy rich foods and sedentary behavior. Accumulation of excess fat in visceral compartment, even if subcutaneous fat mass is normal, carries greater metabolic risk as consequence of obesity, and its accompanying pathological consequences, most notably insulin resistance, the precursor to type 2 diabetes, and heart disease, that have become serious medical problems[247]. Conversely, in comparison with visceral adipose tissue, the subcutaneous depots appear less metabolically active[248]. When the capacity of WAT to store FFAs is exceeded, as occurs in some forms of obesity (when WAT expandability is exhausted) or in lipodystrophy (when WAT is partially or completely absent), extra-adipose lipid accumulation, lipotoxicity, insulin resistance and ectopic lipid accumulation ensues[249].

The increase of intermuscular adipose tissue (IMAT) could play a crucial pathogenic role and represents a negative prognostic factor for several myopathies, metabolic diseases, and aging. Therefore, the origin and biology of this adipose depot could represent a promising pharmacological target. It is possible to speculate that a primary insult to the muscle could induce its differentiation toward adipose tissue. In fact, high-glucose-induced muscle stem cell to enter the adipogenic lineage[250]. On the other hand, the expansion of IMAT could induce some changes in muscle metabolism and insulin sensitivity because of the release of adipokines and metabolites from fat cells surrounding muscle fibers. There are clear evidences of signalling interaction between myogenic cells and adipocytes, playing a significant role in the rate and extent of adipogenesis, myogenesis, and lipogenesis/lipolysis [251,252,253]. A fibro/adipogenic progenitor cell population may exist in skeletal muscle, having impacts on intramuscular fat accumulation as well as fibrosis in disease states[254]. Switching the commitment of these stem cells from myogenesis to adipogenesis in pathological situations, may increase intramuscular fat, an event associated with muscle

242. Osawa, Y. et al. Acid sphingomyelinase regulates glucose and lipid metabolism in hepatocytes through Akt activation and amp-activated protein kinase suppression. *FASEB J*. 2011; 25 (4): 1133-44.
243. Munday, M. R. Regulation of mammalian acetyl-CoA carboxylase. *Biochem. Soc. Trans*. 2002; 30: 1059-64.
244. Hahn-Windgassen, A. et al. Akt activates the mammalian target of rapamycin by regulating cellular ATP level and AMPK activity. *J. Biol. Chem.* 2005; 280 (37): 32081-9.
245. Quanri, J. et al. Implication of AMP-activated protein kinase and Akt-regulated survivin in lung cancer chemopreventive activities of deguelin. *Cancer Res.* 2007; 67 (24): 11630-9.
246. King, T. D. et al. AMP-activated protein kinase (AMPK) activating agents cause dephosphorylation of Akt and glycogen synthase kinase-3. *Biochem. Pharmacol*. 2006; 71 (11): 1637-47.
247. Wolfgang, M. J. et al.. Control of energy homeostasis: role of enzymes and intermediates of fatty acid metabolism in the central nervous system. *Annu. Rev. Nutr.* 2006; 26: 23-44.
248. Tang, Q. Q. et al. Adipogenesis: From Stem Cell to Adipocyte. *Annu. Rev. Biochem*. 2012; 81: 715-36.
249. Christodoulides, C. et al. Adipogenesis and WNT signalling. *Trends Endocrinol. Metab.* 2009; 20 (1): 16-24.
250. Aguiari, P. et al. High glucose induces adipogenic differentiation of muscle-derived stem cells. *Proc. Natl. Acad. Sci. USA*. 2008; 105: 1226-31.
251. Boone, C. et al. The adipose conversion process: regulation by extracellular and intracellular factors. *Reprod. Nutr. Dev.* 2000; 40: 325-58.
252. Diamond, F. The endocrine function of adipose tissue. *Growth Genet. Hormones*. 2002; 18: 17-23.
253. Fruhbeck, G. et al. The adipocyte: a model for integration of endocrine and metabolic signalling in energy metabolism regulation. *Am. J. Physiol*. 2001; 280: E827-47.
254. Pisani, D. F. et al. Isolation of a highly myogenic CD34-negative subset of human skeletal muscle cells free of adipogenic potential. *Stem Cells*. 2010; 28:753-64.

insulin resistance due to the paracrine effect of intramuscular adipocytes[255,256,257]. Because of their particular position close to muscle fibers, it is possible to hypothesize that the biology of intramuscular adipocytes may differ from that of adipocytes from other sites, but only a few data have been reported in animals[258,259] , and no data are available in humans[260].

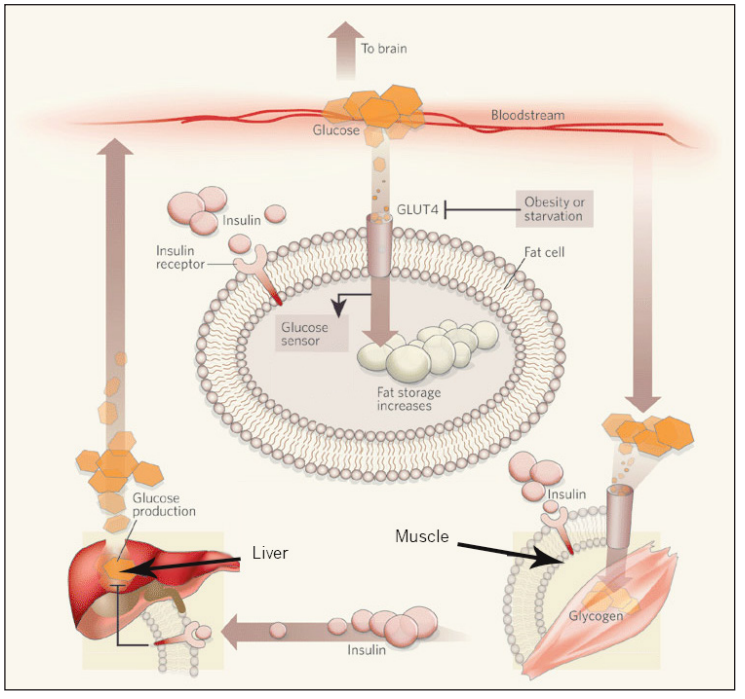

SCHEME-13. Glucose uptake and metabolism in the different organs. In normal individuals, binding of insulin to its receptor on the cell membrane stimulates glucose uptake into muscle and fat cells through the GLUT4 transporter. It also inhibits glucose production in liver, thereby maintaining normal glucose levels in the blood. In adipose tissue, glucose provides fuel for the synthesis of fat stores, which serve as the body's main energy reservoir. In muscle glucose provides energy and it is storage as glycogen, as a first energy source. Summarizing glucose uptake by insulin activates lipogenesis in adipose tissue, glycogenesis in muscle tissue and inhibits gluconeogenesis in liver (Figure extracted from *Nature*. 2005; 436:337-338).

255. Uezumi, A. et al. Mesenchymal progenitors distinct from satellite cells contribute to ectopic fat cell formation in skeletal muscle. *Nat. Cell Biol.* 2010; 12: 143-52.
256. Joe, A. W. et al. Muscle injury activates resident fibro/dipogenic progenitors that facilitate myogenesis. *Nat. Cell Biol*. 2010; 12: 153-63.
257. Kokta, T. A. et al. Intracellular signalling between adipose tissue and muscle tissue. *Domest. Anim. Endocrinol*. 2004; 27: 303-31.
258. Pond, C. M. et al. The effects of noradrenaline and insulin on lipolysis in adipocytes isolated from nine different adipose depots of guinea-pigs. *Int. J. Obes*. 1991; 15: 609-18.
259. Gardan, D. et al. Lipid metabolism and secretory function of porcine intramuscular adipocytes compared with subcutane- ous and perirenal adipocytes. *Am. J. Physiol. Endocrinol. Metab.* 2006; 291: E372-E380.
260. Vettor, R. The origin of intermuscular adipose tissue and its pathophysiological implications. *Am. J. Physiol. Endocrinol. Metab*. 2009; 297: E987-E998.

OBESTATIN, THE GREAT MISSUNDERSTOOD

Preproghrelin, the origin

Preproghrelin is a polypeptide encoded by the gene GHRL, which is located on chromosome 3, band p25–26, and it has 4 exons and 3 introns[261]. It is composed of 117 amino acids, with 23 amino acids conforming the signal sequence and 94 the proghrelin **(SCHEME-14).** After translation, the signal sequence is eliminated subsequently in the endoplasmatic reticulum (ER) and then a proteolitic processing occurs giving two mature peptides: ghrelin and obestatin[262]. It has been identified and described different and multiple ghrelin-derived molecules produced by post-translational processing, on the basis of amino acid length and by type of acylation at serine [263].

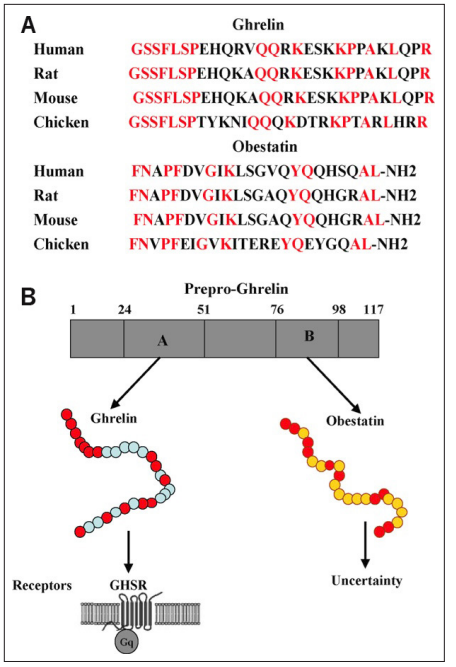

SCHEME-14. The sequences of obestatin and ghrelin. **A.** Comparison of amino acid sequences of human, rat, mouse, chicken obestatin and ghrelin peptides. **B.** Amino acid segments and receptors of obestatin and ghrelin. A: Amino acid segment of ghrelin; B: Amino acid segment of obestatin. Conserved amino acids in all species are represented as red letters. (Figure extracted from *Peptides.* 2008; 29: 639-45)

261. Kojima, M. et al. Ghrelin: structure and function. *Physiol. Rev.* 2005; 85: 495-522.
262. Gualillo, O. One ancestor, several peptides post-translational modifications of preproghrelin generate several peptides with antithetical effects. *Mol. Cell. Endocrinol*. 2006; 256: 1-8.
263. Hosoda, H. et al. Structural divergence of human ghrelin. Identification of multiple ghrelin-derived molecules produced by post-traslational processing. *J. Biol. Chem*. 2003; 278: 64-70.

Ghrelin and its receptor

The ghrelin hormone was discovered in gastric extracts as the natural ligand of the orphan growth hormone secretagogue receptor type 1a (GHSR1a) using reverse pharmacology[264]. Ghrelin is a 28 amino acidic peptide hormone, mainly produced in the stomach by the enteroendocrine X/A-like cells in the oxyntic mucosa[265], in other organs and tissues, to a lesser extent, as other parts of gastrointestinal tract, pancreas, kidney, pituitary and hypothalamus[266]. Additionally, to increase food intake and body weight in rodents after central as well as peripheral administration[267], ghrelin possess other no endocrine activities such as the control of body energy, gastric motility, acid-gastric secretion, influence on pancreatic activity and glucose metabolism, reproductively, cardiovascular effects and proliferative and antiproliferative effects on different cell lines[268,269].

Ghrelin undergoes a post-translational modification, O-n-octanoylation at Ser 3, essential for the binding to the GHSR-1a, for the release of growth hormone (GH) both *in vivo* and *in vitro* and for the most of the other endocrine actions[270]. Recently, the enzyme that catalyzes ghrelin acylation has been discovered using a bioinformatics approach. The ghrelin O-acyl transferase (GOAT) belongs to the membrane bound O-acyl transferases (MBOAT), specifically MBOAT4[271] **(SCHEME-15)**. In mouse, GOAT is located in the ER and its distribution is well defined across the gastrointestinal tract and testis. In humans, it is expressed in stomach and pancreas[272]. Another difference between rodents and humans is that GOAT catalyzes the binding of n-octanoic acid to the Ser 3 in a specific way in the former one, meanwhile in humans this binding can occur with other different fatty acids[273]. The acylation occurs before pro-ghrelin is transported to the Golgi and it starts after the signal sequence is cleaved by a signal peptide peptidase. Then, GOAT, which is located in the membrane of the ER compartment, mediates the translocation of the octanoyl-CoA from the cytosolic side to the ER lumen. Once the pro-ghrelin precursor reaches the trans-Golgi compartment, it is cleaved by prohormone convertase 1/3 (PC1/3), releasing the ghrelin peptide to the blood stream[274]. In addition to this acylated ghrelin, exists another form of ghrelin, commonly named des-acyl ghrelin or unacylated ghrelin (UAG), which circulates in a greater amount respect to acylated ghrelin (AG), it does not present the acylation on Ser 3 but nevertheless it has biological functions[275]. Des-acyl ghrelin has different no endocrine functions like cardiovascular and antiproliferative effects[276, 277] and numerous reports point to the existence of another receptor, different to the GHSR-1a, for the des-acyl ghrelin[278,279].

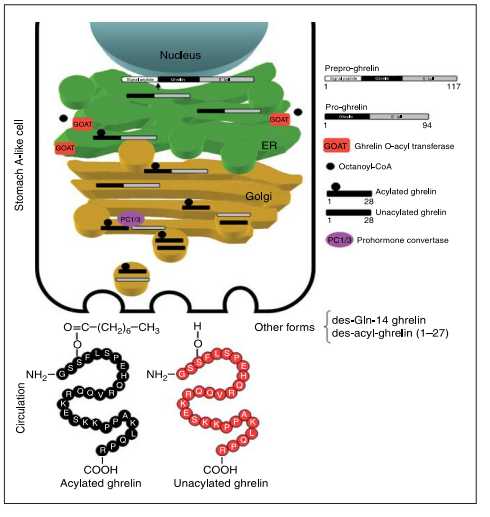

SCHEME-15. Posttranslational processing of the different peptides that are cleaved from preproghrelin. The figure represents the posttranslational processing and acylation of the pro-ghrelin peptide. The acylation of pro-ghrelin occurs after the signal sequence is cleaved by a signal peptide peptidase. GOAT seems to be located at the ER compartment and mediates the translocation of the octanoyl-CoA from the cytosolic side. Once the pro-ghrelin precursor reaches the trans-Golgi compartment, it might be cleaved by PC1/3 convertase, packaged in vesicles, and released to the blood. Different forms of ghrelin are released to the circulation: acylated, unacylated, and other shorter forms whose role is still unknown (Figure extracted from *Eur. J. Endocrinol*. 2010; 163(1):1-8).

264. Kojima, M. et al. Ghrelin is a growth-hormone-releasing acylated peptide from stomach. *Nature*. 1999; 402: 656-60.
265. Kojima, M. et al. Ghrelin: discovery of the natural endogenous ligand for the growth hormone secretagogue receptor. *Trends Endocrinol. Metab.* 2001; 12: 118-22.
266. Horvath, T. L. et al. Minireview: ghrelin and the regulation of energy balance: a hypothalamic perspective. *Endocrinology.* 2001; 142: 4163-9.
267. Inui, A. Ghrelin: an orexigenic and somatotrophic signal from the stomach. *Nat. Rev.* 2001; 2: 551-60.
268. García, M. C. et al. Role of ghrelin in reproduction. *Reproduction*. 2007; 133: 531-40.
269. Camina, J. P. Cell biology of the ghrelin receptor. *J. Neuroendocrinol.* 2006; 18: 65-76.
270. Kojima, M. et al. Ghrelin: discovery of the natural endogenous ligand for the growth hormone secretagogue receptor. *Trends Endocrinol. Metab.* 2001; 12: 118-22.
271. Yang, J. et al. Identification of the acyltransferase that octanoylates ghrelin, an appetite-stimulating peptide hormone. *Cell*. 2008; 132: 387-96.
272. Sakata, I. et al. Colocalization of ghrelin O-acyltransferase and ghrelin in gastric mucosal cells. *Am. J. Physiol. Endocrinol. Metab.* 2009; 297 (1): E134-E141.
273. Gutierrez, J. A. et al. Ghrelin octanoylation mediated by an orphan lipid transferase. *Proc. Natl. Acad. Sci. USA.* 2008; 105: 6320-5.
274. Romero, A. et al. GOAT: the master switch for the ghrelin system? *Eur. J. Endocrinol*. 2010; 163: 1-8.
275. Cederberg, H. et al. Unacylated ghrelin is associated with changes in insulin sensitivity and lipid profile during an exercise intervention. *Clin. Endocrinol*. 2012; 76 (1): 39-45.
276. Korbonits, M. et al. Ghrelin: a hormone with multiple functions. *Front. Neuroendocrinol*. 2004; 25: 27-68.
277. Bowers, C. Y. Unnatural growth hormone-releasing peptide begets natural ghrelin. *J. Clin. Endocrinol. Metab*. 2001; 86: 1464-69.
278. Baldanzi, G. et al. Ghrelin and des-acyl ghrelin inhibit cell death in cardiomyocytes and endothelial cells through ERK1/2 and PI 3-kinase/Akt. *J. Cell Biol*. 2002; 159: 1029-37.
279. Toshinai, K. et al. Des-acyl ghrelin induces food intake by a mechanism independent of the growth hormone secretagogue receptor. *Endocrinology*. 2006; 147: 2306-14.

Obestatin discovery

In 2005, based on bioinformatic predictions, Zhang and colleagues discovered that the ghrelin gene encoded another secreted and bioactive peptide[280]. They isolated a peptide called obestatin, a contraction of obese, from the Latin *"obedere,"* meaning to devour, and *"statin,"* denoting suppression. It showed actions opposite to ghrelin on food intake, body weight, and gastric emptying. This peptide derived from proghrelin (amino acids 76-98) has 23 amino acids with a glycine residue on the carboxy-terminal domain that can be amidated. Obestatin was originally isolated from stomach, showing to be a circulating peptide whose secretion is pulsatile and displays an ultradian rhythmicity similar to ghrelin and GH secretion[281]. Concentrating immunoreactive obestatin from the stomach of 30 rats and verifying its unique sequence according to Edman sequencing[282], it was found that in the first 20 amino acids sequenced, two residues are distinct from those of human obestatin and matched with the rat sequence. At the time, no rodent obestatin was synthesized[283]. Although a recent report could not detect endogenous immunoreactive obestatin in rat stomach extracts[284], another study demonstrated the existence of alternatively spliced ghrelin transcripts in the human stomach, encoding exclusively obestatin together with a signal peptide for secretion[285]. Future studies are needed to reveal the regulation of obestatin biosynthesis, processing, and secretion. Further investigations, found expression in other tissues as small intestines, stomach, spleen, cerebral cortex of rats[286], perinatal rat pancreas[287], myenteric plexus, and in the Leydig cells of the testis in mice/ rats with in vivo and in vitro techniques[288,289].

280. Zhang, J. V. et al. Obestatin, a peptide encoded by the ghrelin gene, opposes ghrelin's effects on food intake. *Science*. 2005; 310: 996-9.
281. Zhu, X. et al. On the processing of proghrelin to ghrelin. *J. Biol. Chem.* 2006; 281: 38867-70.
282. Zhang, J. V. et al. Obestatin, a peptide encoded by the ghrelin gene, opposes ghrelin's effects on food intake. *Science*. 2005; 310: 996-9.
283. Zhang, J. V. et al. Obestatin induction of early-response gene expression in gastrointestinal and adipose tissues and the mediatory role of G protein-coupled receptor, GPR39. *Mol. Endocrinol.* 2008; 22: 1464-75.
284. Bang, A. S. et al. Characterization of proghrelin peptides in mammalian tissue and plasma. *J. Endocrinol.* 2007; 192: 313-23.
285. Seim, I. et al. Revised genomic structure of the human ghrelin gene and identification of novel exons, alternative splice variants and natural antisense transcripts. *BMC Genomics*. 2007; 8: 298-314.
286. Zhang, J. V. et al. Obestatin, a peptide encoded by the ghrelin gene, opposes ghrelin's effects on food intake. *Science*. 2005; 310: 996-9.
287. Chanoine, J. P. et al. Obestatin acylated and total ghrelin concentrations in the perinatal rat pancreas. *Horm. Res.* 2006; 66 (2): 81-8.
288. Dun, S. L. et al. Distribution and biological action of obestatin in the rat. *J. Endocrinol.* 2006; 191: 481-9.
289. Grönberg, M. et al. Distribution of obestatin and ghrelin in human tissues: immunoreactive cells in the gastrointestinal tract, pancreas, and mammary glands. *J. Histochem. Cytochem.* 2008; 56: 793-801.

Obestatin and its receptor

Obestatin was originally reported to be the ligand for the orphan receptor GPR39[290]. GPR39 was first cloned in 1997, before obestatin discovery, from a fetal brain cDNA library, by hybridization at low stringency. Due to the sequence similarity, GPR39, along with another GPCR cloned at that time, was considered related to the GHSR1a, the motilin receptor (GPR38, cloned at the same time as GPR39), neurotensin receptors or neuromedin-U receptors, whose agonists included synthetic peptides and non-peptide GH secretagogues[291]. Later the natural endogenous ligand for GHS-R was discovered, named ghrelin[292], and GPR39 was speculated to have a ligand of a peptide regulating gastrointestinal functions, since all the other receptors homologous to GHS-R have such ligands[293]. GPR39 had been considered, however, an orphan GPCR until 2005, when Zhang and colleagues discovered obestatin encoded by the ghrelin gene. Based on the data of radiolabeled ligand binding assays, it was proposed that the new hormone was a cognate ligand of GPR39[294].

The human GPR39 is 435-amino acid long and has seven-transmembrane helices. Its gene is located in chromosome 2, band q21–q22, consisting of two exons[295].The first exon encodes residues 1 to 285, corresponding to the N-terminal region and the first five transmembrane helices, and the second exon encodes residues 286 to 435, corresponding to the last two transmembrane helices and the C-terminal region. Between the two exons there is an intron as large as 200 kb, whose analogue appears in the genes of the ghrelin receptor and the motilin receptor. The second exon of GPR39 shares a segment of DNA with LYPD1 gene: GPR39 is encoded by the forward strand of DNA, while LYPD1 is transcribed from the reverse strand. The two-exon structure and LYPD1 gene-overlapping pattern are conserved among several species. The maximal promoter activity resides in the 5'-UTR region. Such a region in U-138 cell lines was reported to be from 673 to 14 from the

290. Zhang, J. V. et al. Obestatin, a peptide encoded by the ghrelin gene, opposes ghrelin's effects on food intake. *Science*. 2005; 310: 996-9.
291. McKee, K. K. et al. Cloning and characterization of two human G protein-coupled receptor genes (GPR38 and GPR39) related to the growth hormone secretagogue and neurotensin receptors. *Genomics*. 1997; 46: 426-34.
292. Kojima, M. et al. Ghrelin: discovery of the natural endogenous ligand for the growth hormone secretagogue receptor. *Trends Endocrinol. Metab.* 2001; 12: 118-22.
293. Kojima, M. et al. Ghrelin: structure and function. *Physiol. Rev.* 2005; 85: 495-522.
294. Zhang, J. V. et al. Obestatin, a peptide encoded by the ghrelin gene, opposes ghrelin's effects on food intake. *Science*. 2005; 310: 996-9.
295. Nogueiras, R. et al. Biomedicine. Separation of conjoined hormones yields appetite rivals. *Science*. 2005; 310: 985-6.

translation initiation codon, while in HepG2 cell from "573 to"14. Although the negative regulatory elements have not yet been determined, there was such an element from 673 to 573 in HepG2 cells. The translation initiation codon is at 469 nucleotides downstream of the transcriptional start site[296].

GPR39 is expressed in many organs and various tissues, especially in stomach, white adipose tissue, and hypothalamus[297,298,299]. The colocalization of immunoreactive obestatin and its receptor GPR39 in the gastric mucosa and intestinal tissues implies its involvement in energy homeostasis[300]. Of interest, GPR39 expression in white adipose tissues of rats was up-regulated during fasting whereas GPR39 levels were decreased in cultured mouse embryonic fibroblast cell lines during adipogenesis[301]. In human adipose tissue, decreased GPR39 expression was found in patients with obesity-associated type 2 diabetes mellitus[302].

Beside the canonical form of GPR39 (named GPR39-1a), a splice variant GPR39-1b has been identified, which is encoded by the first exon and thus truncated after the fifth transmembrane helix, but at the present there is no references of functionality[303,304,305].

Obestatin and its controversial bioactivity through GPR39 receptor

The relationship of obestatin and GPR39 was later challenged stating that obestatin did not bind GPR39 and induce any effects on GPR39-transfected cells[306]. This hypothesis was also previously reinforced by two groups that claimed that zinc ion (Zn^{2+}) is a physiologically relevant agonist of GPR39[307,308]. Both groups emphasized that obestatin did neither bind to GPR39-expressing cells nor display any effect such as cAMP production. In response, Zhang and colleagues found out that the interaction of obestatin and GPR39 could not be reproduced due to the instable bioactivity of iodinated obestatin[309]. Just followed up their response about the bioactivity of obestatin, Zhang and colleagues found out that mono-iodinated obestatin can bind to GPR39, but not over-iodinated obestatin. They also demonstrated in the same work that that c-fos expression, a transcription factor as a marker of activity in gastrointestinal, was induced by obestatin in wild-type mice but not in GPR39 null mice, suggesting that activities of obestatin depended on GPR39, and in cultured 3T3-L1 cells, treatment with obestatin induced c-fos expression and activated the MAPK pathway, providing a cell model by which to study obestatin-signalling mechanisms[310]. Previously other group constructed GPR39-knockout mice and partially confirmed the *in vivo* effects of obestatin depending on GPR39[311]. The differences in energy homeostasis included: accelerated gastric emptying, increased gastric secretion, higher mature body weights and body fat compositions, reduced hyperphagia after fasting, and increased cholesterol levels. Despite the initial enthusiasm about the potential of this molecule as a physiological opponent of ghrelin, several observations related to this point have set its effectiveness into question. Consequently, the state-of-knowledge on obestatin suffers from serious gaps, especially for the lack of reproducibility of its central activities[312, 313,314, 315,316] and the

296. Egerod, K. L. et al. GPR39 splice variants versus antisense gene LYPD1: expression and regulation in gastrointestinal tract, endocrine pancreas, liver, and white adipose tissue. *Mol. Endocrinol.* 2007; 21: 1685-98.
297. Jackson, V. R. et al. GPR39 receptor expression in the mouse brain. *Neuroreport.* 2006; 17: 813-6.
298. Zhao, C. M. et al. Characterization of obestatin- and ghrelin-producing cells in the gastrointestinal tract and pancreas of rats: an immunohistochemical and electron-microscopic study. *Cell. Tissue Res.* 2008; 331: 575-87.
299. Dun, S. L. et al. Distribution and biological activity of obestatin in the rat. *J. Endocrinol.* 2006; 191: 481-9.
300. Zhang, J. V. et al. Obestatin receptor in energy homeostasis and obesity pathogenesis. *Prog. Mol. Biol. Transl. Sci.* 2013; 114: 89-107.
301. Egerod, K. L. et al. GPR39 splice variants versus antisense gene LYPD1: expression and regulation in gastrointestinal tract, endocrine pancreas, liver, and white adipose tissue. *Mol. Endocrinol.* 2007; 21: 1685-8.
302. Catalán, V. et al. The obestatin receptor (GPR39) is expressed in human adipose tissue and is down-regulated in obesity-associated type 2 diabetes mellitus. *Clin. Endocrinol.* 2007; 66: 598-601.
303. Popovics, P. et al. GPR39: a $Zn(2^+)$-activated G protein-coupled receptor that regulates pancreatic, gastrointestinal and neuronal functions. *Cell. Mol. Life Sci.* 2011; 68: 85-95.
304. Zhang, J. V. et al. Obestatin receptor in energy homeostasis and obesity pathogenesis. *Prog. Mol. Biol. Transl. Sci*. 2013; 114: 89-107.
305. Sheng-Qiu, T. et al. Obestatin- Its physicochemical characteristics and physiological functions. *Peptides*. 2008; 29: 639-645.
306. Chartrel, N. et al. Comment on "Obestatin, a peptide encoded by the ghrelin gene, opposes ghrelin's effects on food intake". *Science*. 2007; 315: 766 [author reply 766].
307. Lauwers, E. et al. Obestatin does not activate orphan G protein-coupled receptor GPR39. *Biochem. Biophys. Res. Commun.* 2006; 351: 21-5.
308. Holst, B. et al. GPR39 signalling is stimulated by zinc ions but not by obestatin. *Endocrinology*. 2007; 148: 13-20.
309. Zhang, J. V. et al. Response to comment on "Obestatin, a peptide encoded by the ghrelin gene, opposes ghrelin's effects on food intake". *Science*. 2007; 315: 766.
310. Zhang, J. V. et al. Obestatin induction of early-response gene expression in gastrointestinal and adipose tissues and the mediatory role of G protein-coupled receptor, GPR39. *Mol. Endocrinol*. 2008; 22: 1464-75.
311. Moechars, D. et al. Altered gastrointestinal and metabolic function in the GPR39-obestatin receptor-knockout mouse. *Gastroenterology*. 2006; 131: 1131-41.
312. Seoane, L. M. et al. Central obestatin administration does not modify either spontaneous or ghrelin-induced food intake in rats. *J. Endocrinol. Invest.* 2006; 29: RC13-RC15.
313. Chartrel, N. et al Comment on "Obestatin, a peptide encoded by the ghrelin gene, opposes ghrelin's effects on food intake". *Science*. 2007; 315: 766.
314. Nogueiras, R. et al. Effects of obestatin on energy balance and growth hormone secretion in rodents. *Endocrinology*. 2007; 148: 21-26.
315. Gourcerol, G, et al. Lack of interaction between peripheral injection of CCK and obestatin in the regulation of gastric satiety signalling in rodents. *Peptides*. 2006; 27: 2811-19.
316. Tremblay, F, et al. Normal food intake and body weight in mice lacking the G protein-coupled receptor GPR39. *Endocrinology*. 2006; 148: 501-6.

exactly receptor that triggers out the obestatin bioactivity is still unknown[317].

Obestatin bioactivity

Keeping aside its controversial anorexigenic activity, accumulating publications have confirmed the initial role of obestatin in regulating energy homeostasis and its association with obesity, among many other physiological functions. Studies demonstrated that intraperitoneal injection (IP) of obestatin suppressed basal or ghrelin-stimulated food intake in mice[318,319] and rats[320]. Further studies explained that obestatin was involved in other different activities as, inhibiting thirst[321] decreasing anxiety and improving memory[322], regulating sleep[323], increasing vasopressin secretion[324], activating cortical neurons[325]. Obestatin also reduced adipocyte apoptosis and inflammation in metabolic tissues, as well as reduces insulin resistance[326]. Other studies on bone metabolism[327] and term pregnancy[328] have shown the correlation of expression levels of obestatin and GPR39.

Obestatin is also considered for its mitogenic effect, described in pancreatic β cells[329]; in 3T3-L1 preadipocytes[330], bounding to GPR39 is reported to stimulate the phosphorylation of ERK1/2 and potentially Akt, the downstream signalling partners[331]. In primary cultures of human retinal pigmented epithelial cells (hRPEs), the results showed that this peptide induced cell proliferation in a dose-dependent manner with MEK/ERK 1/2 phosphorylation, the obestatin transmembrane signalling pathway involved the consecutive activation of Gi, PI3K, novel PKC (probably PKCε), and Src for ERK 1/2 activation[332]. This mitogenic mechanism was also supported in long-white piglet liver and adipose cells. Obestatin-stimulated the mechanisms signalling pathway during ERK 1/2 activation in cells, activates a PI3K through a PTX-sensitive G-protein. The activation of PI3K results in the phosphorylation of PKCε, which would activate Src. The latter would activate Raf-dependent ERK 1/2 activation via Ras or by a direct activation of Raf. After activation, ERK 1/2 are translocated to the nucleus, where they phosphorylate and activate transcription factors that lead to the mitogenic activity[333].

The same mitogenic result trough ERK signalling pathway was discovered in human gastric carcinoma, KATOIII [334]. Lately, the same group, discovered a transmembrane signalling pathway responsible for obestatin induced-Akt activation in human gastric carcinoma cells, KATOIII and AGS **(SCHEME-16).** The results show that Akt activation requires the phosphorylation of T308 in the A-loop by the phosphoinositide-dependent kinase 1 (PDK1) and S473 within the HM by the mammalian target of rapamycin (mTOR) kinase complex 2 (mTORC2: Rictor, mLST8, mSin1, mTOR kinase) with participation neither of $G_{i/o}$-protein nor G_{β} dimers. Obestatin induces the association of GPR39/beta-arrestin 1/Src signalling complex resulting in the transactivation of the epidermal growth factor receptor (EGFR) and downstream Akt signalling. Upon administration of obestatin, phosphorylation of mTOR (S2448) and p70S6K1 (T389) rise with a time course that parallels that of Akt activation. Based on the experimental data obtained, a signalling pathway involving a beta-arrestin 1 scaffolding complex and EGFR to activate Akt signalling is proposed[335].

317. Zhang, J. V. et al. Obestatin receptor in energy homeostasis and obesity pathogenesis. *Prog. Mol. Biol. Transl. Sci.* 2013; 114: 89-107.
318. Green, B. D. et al. Direct and indirect effects of obestatin peptides on food intake and the regulation of glucose homeostasis and insulin secretion in mice. *Peptides*. 2007; 28: 981-7.
319. Zizzari, P. et al. Obestatin partially affects ghrelin stimulation of food intake and GH secretion in rodents. *Endocrinology*. 2007; 148: 1648-53.
320. Bresciani, E. et al. Obestatin inhibits feeding but does not modulate GH and corticosterone secretion in the rat. *J. Endocrinol. Invest.* 2006; 29: RC16-RC18.
321. Samson, W. K. et al. Obestatin acts in brain to inhibit thirst. *Am. J. Physiol. Regul. Integr. Comp. Physiol.* 2007; 292 (1): R637-643.
322. Carlini, V. P. et al. Obestatin improves memory performance and causes anxiolytic effects in rats. *Biochem. Biophys. Res. Commun*. 2007; 352: 907-12.
323. Szentirmai, E. et al. Obestatin alters sleep in rats. *Neurosci. Lett.* 2006; 404: 222-6.
324. Samson, W. K. et al. Obestatin inhibits vasopressin secretion: evidence for a physiological role in the control of fluid homeostasis. *J. Endocrinol*. 2008; 196: 559-64.
325. Dun, S. L. et al. Distribution and biological activity of obestatin in the rat. *J. Endocrinol*. 2006; 191: 481-9.
326. Green, B. D. et al. Direct and indirect effects of obestatin peptides on food intake and the regulation of glucose homeostasis and insulin secretion in mice. *Peptides.* 2007; 28 (5): 981-7.
327. Pacheco-Pantoja, E. L. et al. Receptors and effects of gut hormones in three osteoblastic cell lines. *BMC Physiol*. 2011; 11:12-52.
328. Fontenot, E. et al. Obestatin and ghrelin in obese and in pregnant women. *Peptides.* 2007; 28: 1937-44.
329. Granata, R. et al. Obestatin promotes survival of pancreatic β-cells and human islets and induces expression of genes involved in the regulation of β-cell mass and function. *Diabetes*. 2008; 57: 967-79.
330. Zhang, J. V. et al. Obestatin induction of early-response gene expression in gastrointestinal and adipose tissues and the mediatory role of G protein-coupled receptor, GPR39. *Mol. Endocrinol.* 2008; 22: 1464-75.
331. Granata, R. et al. Obestatin promotes survival of pancreatic beta-cells and human islets and induces expression of genes involved in the regulation of beta-cell mass and function. *Diabetes.* 2008; 57: 967-79.
332. Camiña, J. P. et al. Obestatin-mediated proliferation of human retinal pigment epithelial cells: regulatory mechanisms. *J. Cell. Physiol.* 2007; 211 (1): 1-9.
333. Dong, X. Y. Ghrelin and its biological effects on pigs. *Peptides.* 2009; 30 (6): 1203-11.
334. Pazos, Y. et al. Stimulation of extracellular signal-regulated kinases and proliferation in the human gastric cancer cells KATO-III by obestatin. *Growth Factors*. 2007; 25: 373-81.
335. Alvarez, C. J. et al. Obestatin stimulates Akt signalling in gastric cancer cells through β-arrestin-mediated epidermal growth factor receptor transactivation. *Endocr. Relat. Cancer*. 2009; 16: 599-611.

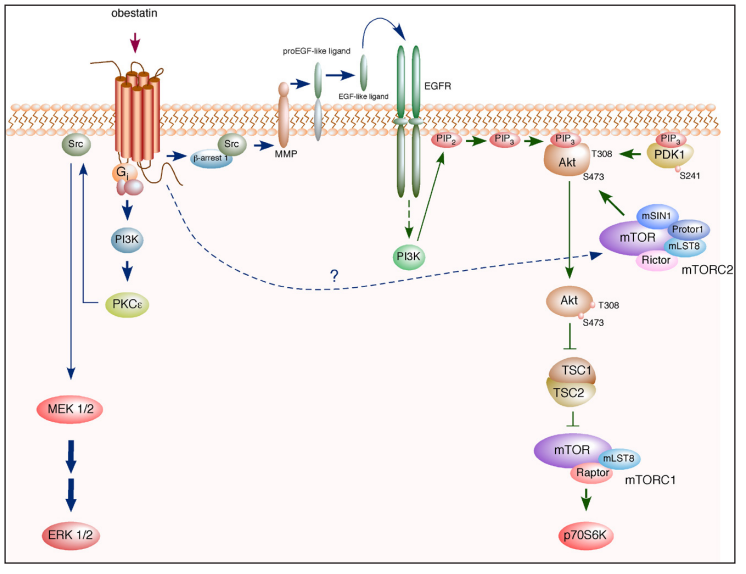

SCHEME-16. Proposed model of signalling pathway for Akt and ERK1/2 activation in response to obestatin in KATO-III and AGS cells. Translocation of β-arrestins 1 to obestatin receptor (GPR39) allows its association with Src. β-arrestin 1 activates Src (phosphorylation at Y416) that initiates the transactivation of EGFR and subsequent downstream Akt signalling (Figure extracted from *Endocr. Relat. Cancer.* 2009; 16: 599-611).

Obestatin/GPR39 structure-bioactivity relationship

A structure-activity relationship for obestatin has been derived by employing this peptide and several analogues as ligands for the seven-transmembrane receptor GPR39 **(SCHEME-17).** The analysis of the data suggested that amidation at the C-terminus of human obestatin was essential for this molecule to adopt an α-helix structure. This α-helix exists between Ser20 and Leu23 and from Gly8 to Lys11. The presence of this structure correlated with the stabilization of the GPR39 conformations that were necessary for the full range of receptor activities, e.g., G protein-dependent and β-arrestin-dependent signalling. Indeed, the change of this α-helix to a 3_{10} helix or the loss of this α-helical pattern was correlated with the absence of complete activation, as observed for non-amidated obestatin. Additionally, GPR39 showed to adopt multiple active conformations, which were related to the activation of specific signalling mechanisms. In particular, human (11–23)-obestatin wass able to induce selective coupling to a portion of the downstream signalling pathways, e.g., β-arrestin-dependent signalling. This observation supported the idea that human (11–23)-obestatin stabilizes a receptor conformation different from that induced by human obestatin. Most likely, this activity was related to the presence of the α-helix segment from Tyr16 to Leu23. Because this peptide is present in the stomach, it was proposed as the first example of an endogenous biased ligand for GPR39. Aditionally, mouse and human obestatin exhibited clear conformational differences beyond their differences in primary structure. The mouse analogue adopts a distinct three-dimensional structure, which could not activate human GPR39. This evidence supported the existence of a species-specific activity[336].

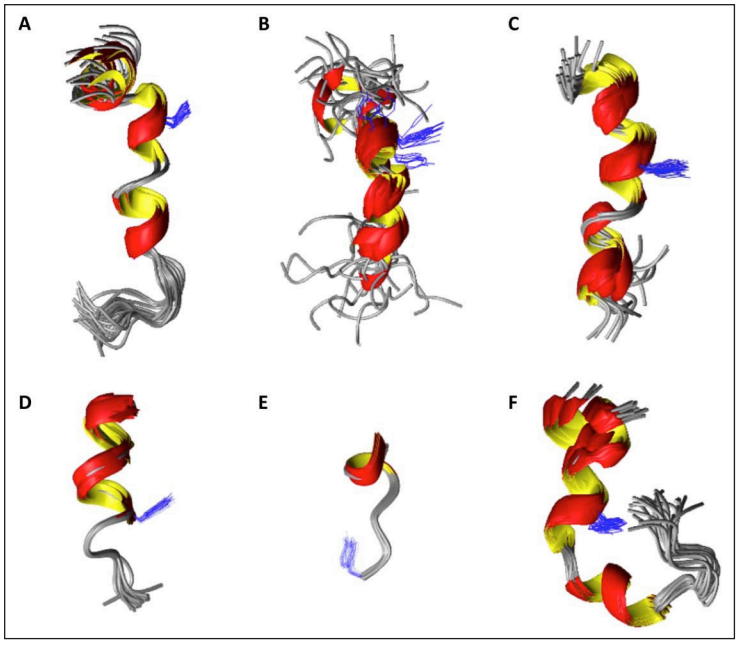

SCHEME-17. Superimposition of the 20 best representative structures of peptides 1 to 6, which possessed the lowest total energies, as calculated from the NMR data for the peptides in SDS micelles. (A) Human obestatin (1), (B) human non-amidated obestatin (2), (C) human (6–23)-obestatin (3), (D) human (11–23)- obestatin (4), (E) human (16–23)-obestatin (5) and (F) mouse obestatin (6). The Tyr16 side chain is shown in blue. (Figure extracted from *PLoS One*. 2012; 7(10):e45434.)

Identification of other hypothetical receptors that mediated obestatin effects

It was recently proposed that obestatin action might be meadiated at least partly by the glucagon-like peptide-1 (GLP-1) receptor (GLP-1R) in pancreatic β cells, which would explain to

336. Alén, B.O. et al. The NMR structure of human obestatin in membrane-like environments: insights into the structure-bioactivity relationship of obestatin. *PLoS One*. 2012; 7 (10): E45434.

some extent its insulinotropic and survival effects[337,338]. The cDNA of GLP-1R was first isolated from a pancreatic islet cDNA library from rats, and its function as a receptor for GLP-1 was confirmed by binding experiments with radiolabeled GLP-1[339]. The cDNA of human GLP-1R was isolated by several groups in 1993[340,341]. At the same time, two exogenous ligands were identified: exendin-4 (Ex-4) and exendin-(9–39)[342]. The interaction between GLP-1R to obestatin was proposed based on binding displacement assays of radiolabeled GLP-1 by obestatin[343]. However, these results were rapidly questionated based on results obtained from INS-1 β and HEK cells overexpressing GLP-1R in which obestatin did not displace radiolabeled GLP-1 binding[344]. Thus, the possible implication of GLP-1R still needs to be clarified .

337. Granata, R. et al. Obestatin promotes survival of pancreatic beta-cells and human islets and induces expression of genes involved in the regulation of beta-cell mass and function. *Diabetes.* 2008; 57: 967-97.
338. Favaro, E. et al. The ghrelin gene products and exendin-4 promote survival of human pancreatic islet endothelial cells in hyperglycaemic conditions, through phosphoinositide 3-kinase/Akt, extracellular signal-related kinase (ERK)1/2 and cAMP/protein kinase A (PKA) signalling pathways. *Diabetologia*. 2012; 55 (4): 1058-70.
339. Thorens, B. Expression cloning of the pancreatic beta cell receptor for the gluco-incretin hormone glucagon-like peptide 1. *Proc. Natl. Acad. Sci. USA.* 1992; 89: 8641-5.
340. Dillon, J. S. et al. Cloning and functional expression of the human glucagon-like peptide-1 (GLP-1) receptor. *Endocrinology*. 1993; 133: 1907-10.
341. Graziano, M. P. et al. Cloning and functional expression of a human glucagon-like peptide-1 receptor. *Biochem. Biophys. Res. Commun.* 1993; 196: 141-6.
342. Thorens, B, et al. Cloning and functional expression of the human islet GLP-1 receptor. Demonstration that exendin-4 is an agonist and exendin-(9-39) an antagonist of the receptor. *Diabetes*. 1993; 42: 1678-82.
343. Granata, R. et al. Obestatin promotes survival of pancreatic beta-cells and human islets and induces expression of genes involved in the regulation of beta-cell mass and function. Diabetes. 2008; 57: 967-97.
344. Unniappan, S. et al. Metabolic effects of chronic obestatin infusion in rats. *Peptides*. 2008; 29: 1354-61.

MATERIALS & METHODS

MATERIALS

Peptides

Rat/mouse obestatin was obtained from California Peptide Research (CA, USA). Mouse ghrelin and des-acyl ghrelin were purchased from Global Peptides (Co, USA). Insulin was obtained from NovoNordisk (Bagsvaerd, Dk).

Antibodies

ANTIBODY	USE	DILUTION	SUPPLIER	REF
Actin	WB	1:5000	Abcam	ab1801
Akt	WB	1:1000	Cell Signalling	4685
Alexa Fluor 594	IF	1:500	Invitrogen	A11012
Alexa Fluor 647	IF	1:1000	Abcam	ab150115
Anti-mouse HRP	WB	1:10000	Jackson	115-035-003
Anti-rabbit HRP	WB	1:10000	Jackson	111-035-003
C/EBPα	WB	1:500	Santa CruzBiotechnology Inc.	sc-61
C/EBPβ	WB	1:500	Santa CruzBiotechnology Inc.	sc-150
C/EBPσ	WB	1:500	Santa CruzBiotechnology Inc.	sc-151
Col1a2	WB	1:5000	Abcam	ab34710
Cyclin D1	WB	1:1000	Cell Signalling	2978
eMHC	IHF	1:20	Hibridoma Bank	F1652
ERK 1/2	WB	1:1000	Cell Signalling	9102
FAT/CD36	WB	1:500	Santa CruzBiotechnology Inc.	sc-9154
FATP1	WB	1:500	Santa CruzBiotechnology Inc.	sc-25670
FATP4	WB	1:500	Santa CruzBiotechnology Inc.	sc-31954
FITC-488	IF	1:1000	Abcam	ab150089
FoxO1	WB	1:1000	Cell Signalling	9454
GADPH	WB	1:5000	Abcam	ab9485
GHSR1a	WB	1:500	Santa CruzBiotechnology Inc.	sc-20748
GLUT1	WB	1:500	Santa CruzBiotechnology Inc.	sc7903
GLUT4	IHF	1:100	Cell signalling	2299
GLUT4	WB	1:1000	Cell Signalling	2299
GPR39	IHC	1:100	Abcam	ab39227
GPR39	IHF	1:250	Abcam	ab39227
GPR39	WB	1:1000	Abcam	ab39227
IGF-R	WB	1:1000	Cell Signalling	3027
IRS1	WB	1:500	Santa CruzBiotechnology Inc.	sc-560

ANTIBODY	USE	DILUTION	SUPPLIER	REF
Isolectin	IHF	2µg/mL	Invitrogen	132450
Laminin	IHF	1:2000	Abcam	ab14055
MBOAT4	IHC	1:100	Santa CruzBiotechnology Inc.	sc87999
MBOAT4	WB	1:500	Santa CruzBiotechnology Inc.	sc87999
Miostatin	WB	1:100	Abcam	ab98337
Myf5	FC	(1 µg/10^6 cells)	Invitrogen	SAP 4501943
Myf5	WB	1:500	Santa CruzBiotechnology Inc.	sc-302
Myf6	WB	1:500	Santa CruzBiotechnology Inc.	sc-301
MyoD	IHC	1:100	Santa CruzBiotechnology Inc.	Sc-304
MyoD	WB	1:1000	Santa CruzBiotechnology Inc.	Sc-304
Myogenin	IHC	1:100	Santa CruzBiotechnology Inc.	sc-576
Myogenin	WB	1:1000	Hibridoma Bank	F5D
MHC	IHF	1:20	Hibridoma Bank	MF20
MHC	WB	1:500	Hibridoma Bank	MF20
Obestatin	IHC	1:100	ADI	GPR391-A
Obestatin	IHF	1:50	Abcam	41704
Obestatin	Neutralization assay	5µg/mL	Abcam	41704
Obestatin	WB	1:500	Abcam	41704
P21-waf	FC	0,6µg/ml	Abcam	ab7960
P21-waf	WB	1:1000	Abcam	ab7960
p-38	WB	1:500	Santa CruzBiotechnology Inc.	sc-535
p-ACC(S79)	WB	1:1000	Cell Signalling	3661
p-Akt (S473)	WB	1:1000	Cell Signalling	9271
p-AMPKα(T172)	WB	1:1000	Cell Signalling	2535
p-AS160(T642)	WB	1:1000	Cell Signalling	4288
Pax7	IHF	1:20	Hibridoma Bank	Pax7

ANTIBODY	USE	DILUTION	SUPPLIER	REF
Pax7	WB	1:500	Hibridoma Bank	Pax7
Pax7-FITC	FC	(1 µg/10^6 cells)	Hibridoma Bank	Pax7-FITC
PC 1/3	IHC	1:100	Santa CruzBiotechnology Inc.	sc-15922
PC 1/3	WB	1:500	Santa CruzBiotechnology Inc.	sc-15922
p-cJun(S63)	WB	1:1000	Cell Signalling	3270
p-CamKII (T286)	WB	1:1000	Cell Signalling	3361
PE	IF	1:1000	Abcam	ab7004
PEDF	WB	1:500	Santa CruzBiotechnology Inc.	sc-25594
p-ERK 1/2 (T202/Y204)	WB	1:1000	Cell Signalling	9101
p-FoxO1/FoxO3a	WB	1:1000	Cell Signalling	9464
p-GSK3α/β(S21/9)	WB	1:1000	Cell Signalling	9331
p-IGF-R	WB	1:1000	Cell Signalling	6113
p-IRS1	WB	1:1000	Cell Signalling	2388
p-mTOR(S2448)	WB	1:1000	Cell Signalling	2971
p-p38 (T180/Y182)	WB	1:1000	Cell Signalling	9211
PPARγ	WB	1:500	Santa CruzBiotechnology Inc.	sc-7196
Preproghrelin	IHC	1:100	Santa CruzBiotechnology Inc.	sc-10368
Preproghrelin	IHF	1:100	Santa CruzBiotechnology Inc.	sc-10368
Preproghrelin	WB	1:200	Santa CruzBiotechnology Inc.	sc-10368
pS6K1(S371)	WB	1:1000	Cell Signalling	9205
S6K1	WB	1:1000	Cell Signalling	2217
Six-1	WB	1:500	Santa CruzBiotechnology Inc.	sc-9127
Tubulin	WB	1:5000	Cell Signalling	T9026
VEGF	WB	1:500	Santa CruzBiotechnology Inc.	sc-152
VEGF-R2	WB	1:500	Santa CruzBiotechnology Inc.	sc-504
Ki67	FC	1:100	Abcam	ab15580
Ki67	WB	1:500	Abcam	ab15580

ANIMALS

This study was carried out in strict accordance with the recommendations in the Guide for the Care and Use of Laboratory Animals of the Faculty Animal Committee at the University of Santiago de Compostela (Santiago de Compostela, Spain) and Spienza-Università di Roma (Roma, Italy). Experiments were performed in agreement with the Rules of Laboratory Animal Care and International Law on Animal Experimentation and all efforts were made to minimize suffering.

Subcutaneous mini-pump implantation animal model

Adult male Sprague–Dawley rats (250 g) were housed in 12 h light/12 h darkness cycles with free access to standard rat chow diet and water. Alzet® mini-pumps (model 1003D, CA, USA) were subcutaneous (SC) implanted. Animals were assigned to one of four-matched experimental groups (n=10/group): 1) 24 h mini-pump SC implanted group [containing obestatin (300 nmol/kg body weight/24 h)]; 2) 24 h mini-pumps SC control group (containing saline); 3) 72 h mini-pump SC implanted group [containing obestatin (300 nmol/kg body weight/24 h)]; and 4) 72 h mini-pumps SC control group (containing saline). These mini-pumps hold 100 µL volume and deliver 1 µL/h. After 24 or 72 h, rats were euthanatized to obtain omental, subcutaneous, gonadal adipose tissues, and gastrocnemius and soleus muscles. All tissues were washed with ice-cold Krebs–Ringer–HEPES buffer [KREBS buffer: HEPES (pH 7,4), 25 mM; NaCl, 125 mM; KCl, 5 mM; $MgSO_4$, 1,2 mM; $CaCl_2$, 2 mM; KH_2PO_4, 2 mM; glucose, 6 mM]. Immediately adipose tissue samples were snap-frozen in liquid nitrogen for its posterior use. Muscles tissue samples for histologic analysis, were mounted in tissue freezing medium (tragacanth paste) and frozen in isopentane. For western blot (WB) analysis, muscles were snap-frozen in liquid nitrogen.

High-fat diet (HFD) mice model

Adult Swiss male mice (30 g, 8 weeks old) were housed in 12 h light/12 h darkness cycle. Animals were assigned to one of two-matched experimental groups (n=10/group): 1) fed with standard diet (SD, control) or 2) high-fat diet (HFD) for 12 weeks (D12451, Research Diets, Inc., New Brunswick, NJ, USA). Food intake and body weight were measured weekly during the experimental phase. Animals were sacrificed when they were 20 weeks old.

Excised WAT, omental and subcutaneous, were washed with ice-cold KREBS buffer and immediately tissue samples were snap-frozen in liquid nitrogen for its posterior use.

Cardiotoxin-induced muscle injury in rat

Adult male Sprague–Dawley rats (250 g) were housed in 12 h light/12 h darkness cycles with free access to standard rat chow diet and water. Gastrocnemius muscles from rats were impaired, along their entire length, with four intramuscular injections per muscle with cardiotoxin (CTX) purchased from Sigma-Aldrich (Missouri, USA) (10 μM CTX; 2 μl/g body weight) or equal volume of PBS to ensure equal distribution throughout the muscle[1]. At different times after injury (6, 24, 48, and 72 h; n=5 per time point), rats were sacrificed, and gastrocnemius muscles were dissected and divided for histological and WB analyses. For histologic analysis, muscle tissue samples were mounted in tissue freezing medium (tragacanth paste) and frozen in isopentane. For WB analysis, muscles were snap-frozen in liquid nitrogen.

Freeze-induced muscle injury in mice

Adult female Swiss mice (30 g) were housed in 12 h light/12 h dark cycles with free access to standard mice chow diet and water. Under anesthesia, mice hind limbs were shaved and both tibialis anterior (TA) muscles were exposed via a 1-cm-long incision in aseptically prepared skin overlying the muscle. Traumatic freeze injury was induced by applying directly a 120-mm-diameter steel probe, pre-chilled on dry ice, to the belly of the TA muscle for 5 s[2]. During the regeneration time, mice were injected into the TA muscle with obestatin (300nmol/Kg body weight/24 h; 20 μL; treated group) or equal volume of PBS (control group) each 24 h during 5 days. The muscles were harvested at different time points after injury (12, 24, 48, 72, 96, 168 and 240 h; n=5 per time point). Muscle tissue samples were divided for WB, histological and flow cytometry (FC) analysis. For WB analysis, muscles were snap-frozen in liquid nitrogen. For histologic analysis, muscle tissue samples were mounted in tissue freezing medium (tragacanth paste) and frozen in isopentane. For FC analysis samples were transported in PBS, as intact as possible, and then digested enzymatically.

Electroporation and muscle injury regeneration

Adult female Swiss mice (30 g) were housed in 12h light/12 h dark cycles with free access to standard mice chow diet and water. After anesthesia, TA were injected with specific cDNA as indicated: for *in vivo* electroporation, 20 μg of plasmid DNA [mouse preproghrelin and GPR39 cDNAs were obtained from Origene (MD, USA)] or pCMV6 (Origene; MD, USA) combined with 5 μg of pCDNA 3.1-SNAP-GFP, marker of transfection efficacy, (kindly provided by Prof. Pozzan, University of Ferrara-Italy) diluted in 20 μL of Dulbecco's phosphate buffer solution [PBS: KCl, 0.2 g/L; KH_2PO_4, 0.2 g/L; NaCl, 8.0 g/L; Na_2HPO_4, 1.2 g/L (pH 7,2)]. All the plasmids were amplified in XL1-Blu competent cells purchased from Life Technologies, Invitrogen (NY, USA), and purified using the Plasmid Maxi Kit (Qiagen, Crawley, UK). The electric pulses were delivered using 3 × 5 mm GenePaddle electrodes (BTX, CA, USA) placed on either side of the muscle. Electroporations were performed 10 days before muscle injury, by delivering six electric pulses of 20 V each (three with the anode placed on the front of the injured TA, followed by three pulses with the polarity inverted). This protocol of gene delivery by electroporation guarantees stable DNA expression for more than 4 months[3]. Mice were sacrificed at 96 h (n=5 per group: control, preproghrelin; GPR39 and preproghrelin+GPR39) and 7 days (n=5 per group) after injury.

CELLS

Cell culture and differentiation induction of 3T3-L1 mouse pre-adipocytes

3T3-L1 cells were cultured as described by the supplier (European Collection of Cell Cultures, Wiltshire, UK). Briefly, 3T3-L1 cells were maintained in Dulbecco's Modified Eagle Medium (DMEM) containing 10% FBS (v/v), both purchased from Lonza (Basel, Switzerland), 100 U/mL penicillin and 100 U/mL streptomycin both purchased from Biowest (Nuaille, France). For routine differentiation, 80% confluent cells were treated with 0.5 mM IBMX, 25 μM DEX both from purchased from Sigma-Aldrich (Missouri, USA) and 861 nM (5 μg/mL) insulin for 3 days and maintained in DMEM containing 10% FBS, 100 U/mL penicillin,

1. Toschi, A. et al. Skeletal muscle regeneration in mice is stimulated by local overexpression of V1a-vasopressin receptor. *Mol. Endocrinol.* 2011; 25: 1661-73.
2. Melissa, W. et al. Early life nutrition modulates muscle stem cell number: implications for muscle mass and repair. *Stem Cells. Dev.* 2011; 20 (10): 1763-9.
3. Moresi, V. et al. Modulation of caspase activity regulates skeletal muscle regeneration and function in response to vasopressin and tumor necrosis factor. *PLoS ONE*. 2009; 4 (5): E5570.

100 U/mL streptomycin and supplemented with 172 nM (1 µg/mL) insulin for 7 days after the beginning of differentiation unless otherwise stated. Before each experiment, 3T3-L1 pre-adipocytes or adipocyte cells were serum-starved 12 h in DMEM.

Cell Culture and differentiation induction of L6E9 rat myoblasts

L6E9 were cultured as described by the supplier (European Collection of Cell Cultures, Wiltshire, UK). L6E9 myoblasts were maintained in growth medium (GM) containing DMEM supplemented with 10% FBS, 100 U/mL penicillin, and 100 U/mL streptomycin. For routine differentiation, cells were grown to 80% confluence, and GM was replaced with differentiation medium (DM), DMEM supplemented with 2% FBS, 100 U/mL penicillin, and 100 U/mL streptomycin for 7 days unless otherwise stated.

Cell Culture and differentiation induction of C2C12 mouse myoblasts

C2C12 were cultured as described by the supplier (European Collection of Cell Cultures, Wiltshire, UK). C2C12 myoblasts were maintained in GM containing DMEM supplemented with 10% FBS, 100 U/mL penicillin, and 100 U/mL streptomycin. For routine differentiation, cells were grown to 80% confluence, and GM was replaced with DM for 7 days unless otherwise stated.

Fibers mice isolation

For fiber isolation, the plastic and glass material is necessary to coat all with 5% FBS in PBS. Gastrocnemius and TA muscles were dissected carefully, cutting tendons trying to keep the muscle as much intact as possible, avoiding muscle stretching. Muscles were washed with PBS and transfer them immediately to 1mL of collagenase type I enzymatic solution purchased from Worthington (NJ, USA) in DMEM(400 U/mL) incubating tubes for 1h at 37°C in a cell incubator. After, muscles were rocked for 30 min at 37°C . After digestion, the medium was enriched with 10% FBS, to block enzymatic action. Finally, all the solution was discarded in a pre-coated 100 mm cell dish, and with a pre-coated pasteur pippete medium was blown against the muscle to release the single fibers[4].

Measurement of SCs division in fibers

Isolated fibers were plated in a pre-coated dishes with growth factor–reduced Matrigel purchased from Life Technologies, Invitrogen (NY, USA) and DMEM with 10% FBS in a cell incubator (30 miofibers per well in 6 multiwell). Fibers were stimulated with obestatin 5 nM and cultured for 24 h. After incubation time, fibers were treated for immunofluorescence (IF) as explained below[5].

REAL TIME QUANTITATIVE REVERSE TRANSCRIPTION PCR (QRT-PCR)

For qRT-PCR, total RNA was isolated with Trizol purchased from Life Technologies, Invitrogen (NY, USA) and DNA-free kit (Applied Biosystems/Ambion, TX, USA) to generate first-strand cDNA synthesis performed with High-capacity cDNA Reverse Transcription kit (Applied Biosystems/Ambion, TX, USA). qRT-PCR was performed using an ABI PRISM 7300 HT Sequence Detection System (Applied Biosystems/Ambion, TX, USA). For the analysis of the preproghrelin gene, ACTB was used as housekeeping gene (TaqMan: Applied Biosystems/Ambion, TX, USA). The fold change in gene expression was calculated using the $2^{-\Delta\Delta Ct}$ relative quantitation method according to the manufacturer's guidelines (Applied Biosystems/Ambion, TX, USA).

IMMUNOBLOT ANALYSIS

Immunoblot analysis of proteins

Tissue samples or cells were directly lysed in ice-cold radioimmune precipitation buffer [Tris-HCl (pH 7.2), 50 mM; NaCl, 150mM; EDTA, 1mM; Nonidet P-40, 1% (v/v); sodium deoxycholate, 0.25% (w/v); protease inhibitor mixture and phosphatase inhibitor mixture, both inhibitors from purchased from Sigma-Aldrich (Missouri, USA)]. Lysates were clarified by centrifugation (14.000 rpm for 15 min at 4 °C), and the protein concentration was quantified using the QuantiProTM BCA assay kit purchased from Sigma-Aldrich (Missouri, USA). For immunoblotting, equal amounts of protein were fractionated by SDS-PAGE and transferred onto nitrocellulose

4. Rosenblatt, J. D. et al. Culturing satellite cells from living single muscle fibre explants. *In Vitro Cell. Dev. Biol.* 1995, 31: 773–779.

5. Kuang, S. et al. Asymmetric self-renewal and commitment of satellite stem cells in muscle. *Cell*. 2007; 129; 999-1010.

membranes. Immunoreactive bands were detected by enhanced chemiluminescence ECL Western blotting Substrate; purchased from Thermo Fisher Scientific-Pierce (Massachusetts, USA).

Immunoblot analysis of GLUT1, GLUT4, FAT/CD36, FATP1 and FATP4 in plasma membrane

Treated cells were harvested by scraping. After centrifugation, pellets were resuspended in homogenization buffer [HEPES (pH 7.4), 20 mM; sucrose, 255 mM; EDTA, 2 mM; protease and phosphatase inhibitor cocktail]. Homogenized with eight strokes, and then centrifuged at 1200 rpm for 5 min at 4°C to remove nuclei and unbroken cells. The supernatant was then centrifuged at 195,000 x g for 60 min at 4°C to obtain total membranes. The final pellet was resuspended in homogenization buffer and used for WB analysis[6].

SMALL INTERFERING RNA ASSAYS

Small interfering RNA assays in 3T3-L1 cells

Chemically synthesized double-stranded small interfering RNA (siRNA) duplexes (Santa Cruz Biothecnology, CA, USA) were for mouse preproghrelin: 3'-CAGAGAAAGGAAUCCAAGA-5', 3'-CCUUCGAUGUUGGCAUCAA-5' and 3'-CUCUCCUACCACUUUAAGA-5'. Mouse GPR39 targeted siRNAs (siRNA sequence numbers s89441, s89442, s89443) were selected from Silencer® Pre-designed sequences from Applied Biosystems/Ambion (TX, USA). Cells were transfected with Lipofectamine 2000 purchased from Life Technologies, Invitrogen (NY, USA).

siRNA assays in L6E9 cells

Chemically synthesized double-stranded siRNA duplexes targeting either preproghrelin or GPR39 were selected from ON-TARGETplus SMARTpool siRNA from Thermo Fisher-Dharmacon (Massachusetts, USA), (preproghrelin, CCAAGAAGCCACCA-GCUAA, CUGCUGACUUACAAAUAAA, CAGAGGAGGAG- CUGGAAAU, and UCAAAGAGGCGCCAGCUAA; GPR39, ACAAGGGACUCAACUGUAA, UUACGCAGGUAUUGCA- GAA, CCUGCAAGCUCCACACACGUU, and AGUUUGGCU- UGUUCAGAUA). An ON-TARGET*plus* non-targeting siRNA was used as a control for all siRNA experiments. All experiments were transfected with Lipofectamine 2000 purchased from Life Technologies, Invitrogen (NY, USA).

IMMUNOCHEMISTRY AND HISTOCHEMISTRY

Immunochemistry

Cells (preadipocytes, adipocytes, myoblasts and myotubes) were fixed on cover slips in 96% ethanol. WAT samples were fixed by immersion in 4% (w/v) buffered paraformaldehyde (PFA)-PBS for 24 h, dehydrated and embedded in paraffin by a standard procedure. Muscle samples were mounted in tissue freezing medium (tragacanth paste) and snap-frozen in nitrogen-cooled isopentane. Sections, 8 µm thick, were mounted on Histobond Adhesion Microslides (Marienfeld, Lauda-Königshofen, Germany), dewaxed and rehydrated. Slides were consecutively incubated with: 1) anti-obestatin, anti-GPR39, anti-preproghrelin, anti-MBOAT4, anti-PC1/3, anti-MyoD and anti-myogenin in Dako ChemMate antibody diluent (Dako, Glostrup, Denmark); 2) EnVision peroxidase rabbit (Dako, CA, USA) used as the detection system and 3) 3,3'-diaminobenzidine-tetrahydrochloride (Dako liquid DAB + substrate-chromogen system). Cell and tissue sections were faintly counterstained with Harris' hematoxylin. Immunochemistry (IC) controls were performed applying the primary antibody plus control antigen peptide (10 nmol/mL) to positive samples.

Quantification of myofiber cross-section area

Serial muscle cryostat sections were stained with hematoxylin/eosin, and five randomly chosen microscopic fields from five different sections in each tissue block were examined using ImageJ64 analysis software.

Heidenhain´s AZAN trichrome stain

Serial muscle cryostat sections were stained with azocarmine G for 15min at 60°C. Cryosections were sequentially washed with water, aniline alcohol, acetate alcohol, phosphotungstic acid and water. Cryosections were counter-stained with aniline, orange G and acetic acid for 30 min. Samples were finally dehydrated with alcohol and xilol before mounting. Five randomly chosen microscopic fields from three different sections in each cryosection were examined using ImageJ64 analysis software.

6. Nishiumi, S. et al. Rapid preparation of a plasma membrane fraction from adipocytes and muscle cells: application to detection of translocated glucose transporter 4 on the plasma membrane. *Biosci. Biotechnol. Biochem*. 2007;71(9):2343-6.

IMMUNOFLUORESCENCE ANALYSIS

Immunofluorescence analysis of GLUT translocation in 3T3-L1 adipocytes

Cells were cultured on cover slips and differentiated into adipocytes. Serum-starved cells were treated with obestatin (100 nM) or insulin (172 nM) for 30 min. Intact cells were fixed with 4% (w/v) PFA-PBS for 15 min, washed, permeabilized and blocked with PBS-Triton X-100 (PBT) [PBT: Triton X-100, 1% (v/v); Tween-20, 1% (v/v); heat inactivated normal goat serum, 5% (v/v); BSA, 0.2% (w/v) in PBS] for 30 min, and then incubated with anti-GLUT4 in PBT overnight at 4°C. After three washes with PBS, cells were incubated with the secondary antibody in PBT for 45 min at 37°C. IF images were captured with a Leica TCS SP 2 (Leica Microsystems, Heidelberg, Germany) confocal laser scanning micro-scope mounted on an Leica DM IRBE inverted microscope (Leica Microsystems, Heidelberg, Germany).

Analysis of differentiation and fusion indexes in L6E9 cells

L6E9 were cultured on coverslips and differentiated into myotubes under DM supplemented with obestatin (5 nM) for 6 days. Intact cells were fixed with 4% PFA-PBS for 15 min, washed, permeabilized, and blocked with PBT for 30 min and then incubated with anti-MHC diluted in PBT overnight at 4 °C. After three washes with PBS, cells were incubated with the secondary antibody in PBT for 45 min at 37 °C. DAPI was used to counter-stain the cell nuclei purchased from Life Technologies, Invitrogen (NY, USA). Digital images of cell cultures were acquired with a Leica TCS-SP2 spectral confocal microscope (Leica Microsystems, Heidelberg, Germany). Five fields from three independent experiments were randomly taken for each treatment. The differentiation grade was evaluated based on the number of MHC-positive cells above the total number of nuclei. The number of nuclei within individual myotubes (≥2 nuclei) was counted for 20–50 myotubes. Myotubes were grouped into two categories, those with 2–3 nuclei and those with 4 or more nuclei, and the percentage of myotubes in each category was calculated relative to untreated cells[7].

Analysis to differentiate between hypertrophic growth and myoblast fusion in C2C12 cells

C2C12 were cultured on coverslips and differentiated into myotubes in different groups: 1) differentiating cells under DM supplemented with obestatin (5 nM) for 7 days; 2) differentiating cells under DM supplemented with obestatin (5 nM) the first three days of differentiation; 3) differentiating cells under DM supplemented with obestatin (5 nM) the last four days of differentiation; 4) differentiating cells under DM supplemented with obestatin (5 nM) the first three days of differentiation and addition of arabinofuranosyl cytidine (AraC, 50μM) purchased from Pfizer (NY, USA), a DNA synthesis suppressor, the second day of differentiation, and, 5) differentiating cells under DM supplemented the last four days of differentiation with obestatin (5 nM) and AraC (50μM) the second day of differentiation[8,9]. Intact cells were fixed with 4% buffered PFA-PBS for 15 min, washed, permeabilized, blocked with PBT for 30 min, and then incubated with anti-MHC diluted in PBT overnight at 4 °C. After three washes with PBS, cells were incubated with the secondary antibody in PBT for 45 min at 37 °C. DAPI was used to counterstain the cell nuclei purchased from Life Technologies, Invitrogen (NY, USA). Digital images of cell cultures were acquired with a Leica TCS-SP2 spectral confocal microscope (Leica Microsystems, Heidelberg, Germany). Five fields from three independent experiments were randomly taken for each treatment. The differentiation grade was evaluated based on the number of MHC-positive cells and the total number of nuclei as indicated . The number of nuclei within individual myotubes (≥2 nuclei) was counted for 20–50 myotubes. Myotubes were grouped into two categories, those with 2–3 nuclei and those with 4 or more nuclei, and the percentage of myotubes in each category was calculated relative to untreated cells[10].

IF in TA cross sections

Muscle samples were mounted in tissue freezing medium (tragacanth paste) and snap frozen in nitrogen-cooled isopentane. Sections, 8 μm thick, were mounted on Histobond Adhesion Microslides (Marienfeld, Lauda-Königshofen, DE). Muscle sections

7. Horsley, V. et al. Regulation of the growth of multinucleated muscle cells by an NFATC2-dependent pathway. *J. Cell. Biol.* 2001; 153: 329-38.

8. Von Maltzahn, J. et al. Wnt7a–Fzd7 signalling directly activates the Akt/mTOR anabolic growth pathway in skeletal muscle. *Nat Cell Biol.* 2012; 14 (2): 186-92.

9. Crescenzi, M. J. et al. Transformation by myc prevents fusion but not biochemical differentiation of C2C12 myoblasts: mechanisms of phenotypic correction in mixed culture with normal cells. *Cell. Biol.* 1994; 125 (5): 1137-45.

10. Horsley, V. et al. Regulation of the growth of multinucleated muscle cells by an NFATC2-dependent pathway. *J. Cell. Biol.* 2001; 153: 329-38.

were permeabilized and blocked with PBT for 30 min, and incubated with primary antibodies [anti-Pax7, anti-embrional myosin, anti-GPR39, anti-preproghrelin and anti-isolectin diluted in PBT overnight at 4 °C], washed with PBS and then incubated with the appropriate secondary antibody for 45 min at 37 °C. DAPI was used to counterstain the cell nuclei purchased from Life Technologies, Invitrogen (NY, USA). Quantification of SCs was performed by counting $Pax7^+$ cells in a whole section using ImageJ64 analysis software. At least 4 sections from each muscle were analysed and the mean results of sections from each muscle were further calculated as mean value of muscles. For vessel counting, the total number of $isolectin^+$ vessels and the total number of laminin myofibers were measured for each cross-section. Five fields from three independent experiments were randomly taken for each treatment.

IF of SCs in fibers

The IF analysis was developed based on the protocol described elsewhere[11]. Fibers were collected on pre-coated glass tubes. After centrifugation for 7 min at 1000 rpm, fibers were treated with 4% PFA for 10 min and then with a solution of 2N HCl supplemented with 0,5% (v/v) Triton X-100 for 30 min at room temperature (RT). Tubes were centrifuged and washed three times at 1000 rpm during 7 min with PBS. Fibers were treated with blocking buffer (BF) for 30 min [BF: goat serum, 10 % (v/v); and, FBS, 10 % (v/v) in PBS], and incubated with primary antibodies [anti-Pax7 and anti-laminin diluted in BF overnight overnight at 4 °C], washed with PBS and then incubated with the appropriate secondary antibody for 1 h. DAPI was used to counterstain the cell nuclei. Fibers were finally washed with PBS, and transferred to microscope slides and mounted with Mowioll reagent (Calbiochem-Millipore; CA, USA). For SCs counting, the total number of $Pax7^+$ cells per length were measured for each fiber using ImageJ64 analysis software.

FLOW CYTOMETRY ANALYSIS

TA muscles samples from injured mice were transported freshly to the laboratory. SCs isolation method is described in detail elsewhere[12]. Briefly, the plastic and glass material was coated with 5% FBS in PBS. TAs were minced and the enzymatic digestion was done by treatment with a solution of collagenase-dispase [2.5 U/mL; Roche (Basel, Switzerland)] in DMEM for 1 h at 37 °C in a water bath rocking. After tissue digestion, FBS 10% (v/v) was added to inactivate the enzymes. Minced muscles were resuspended with a pipette to obtain an homogeneous solution to assure enzyme inactivation. The solution was filtered (74 μm), washed twice with PBS and centrifuged at 1500 rpm for 7 min. Cells were fixed with 1% PFA-PBS for 10 min and permeabilized with 70% (v/v) freeze ethanol and stored overnight at -20 °C. The day after samples were blocked for 15 min with PBS plus 5% BSA (w/v), and then incubated with the corresponding primary conjugated antibodies [Pax7-FITC and Myf5-Alexa Fluor 647] for 1 h. After three washes with PBS plus 5% BSA (1500 rpm for 7 min), cells were incubated with propidium iodide (PI) (40 μg/mL final concentration) purchased from Sigma-Aldrich (Missouri, USA) for 20 min. Events were acquired on a FACS Calibur four colours cytometer (B. Dickinson, Belgium) and analysed using Cell-Quest software. Gates were set to include only cells with DNA (PI positive), thus gating out cellular debris commonly observed in isolating cells from solid tissues.

MIGRATION/INVATION ASSAY

In vitro migration assay in L6E9 cells

Cells were seeded on 6-well plates, grown to 100% confluence in GM, and then wounded with a sterile pipette tip to remove cells by linear scratches. The cells were washed and maintained in GM or GM +5 nM obestatin. The progress of migration was photographed immediately after injury and at 8 and 24 h after wounding, near the crossing point. The wound was calculated by tracing along the border of the scratch using the ImageJ64 analysis software and using the following equation: percentage of wound closure = ((wound area (0 h) - wound area (x h))/wound area (0 h)) x 100[13].

Ex vivo migration assays in TA mice muscles

Minced fresh mice gastrocnemius were inverted harvested in 8 μm pore size transwell purchased from Corning (NY, USA)

11. Rosenblant, J. D. Culturing satellite cells from living single muscle fiber explants. *In Vitro Cell. Dev. Biol.* 1995, 31: 773-9.
12. Pasut, A. et al. Isolation of muscle stem cells by fluorescence activated cell sorting cytometry. *Methods Mol. Biol*. 2012; 798: 53-64.
13. Goetsch, K. P. et al. Optimization of the scratch assay for in vitro skeletal muscle wound healing analysis. *Anal. Biochem*. 2011; 411: 158-60.

and were allowed to migrate and invade into growth factor–reduced matrigel using obestatin (25 nM) as a chemoattractant. After 7 days, transwells were stained with 4 mmol/L calcein-acetoxymethyl ester purchased from Life Technologies, Invitrogen (NY, USA), and visualized by confocal microscopy (Leica TCS SP2 confocal microscope) using a 10x objective. Optical sections were scanned at 5 μm intervals moving up from the underside of the membrane into the matrigel. The fluorescence from each optical section was quantified with LCS Lite software (Leica Microsystems)[14].

QUANTIFICATION AND STAINING OF LIPIDS WITH OIL RED O

Treated cells were fixed for 1 h with 4% buffered paraformaldehyde-PBS. Each dish was rinsed three times with Milli-Q water and then with 60% iso-propanol (5 min at RT). Lipid droplets were stained for 10 min at room temperature with a working solution of 60% Oil Red O. For quantification, cells were washed extensively with water to remove unbound dye, and iso-propanol was added to the stained culture plates and then analyzed by spectrophotometry at 520 nm.

GLUCOSE UPTAKE ASSAYS

In vitro assays in 3T3-L1 and L6E9 cells

Cells were cultured in six-well culture plates. Serum-starved cells (12 h) were washed with PBS buffer and then cells were either unstimulated or stimulated with obestatin or insulin at the indicated concentrations for 30 min. Glucose transport was determined by addition of 2-[^{3}H]deoxyglucose (0.5 μCi/mL) from GE-Amersham (Buckinghamshire, UK). The uptake was stopped after 5 min by aspiration, and cells were washed three times with ice-cold PBS. Cells were lysed in 1% SDS, and deoxyglucose uptake was determined by scintillation counting in triplicate. Non-specific uptake was measured in the presence of 20 μM cytochalasin B (cyB) purchased from Sigma-Aldrich (Missouri, USA).

DOGU *ex vivo* in gastrocnemius rat muscle

Gastrocnemius were removed from hind limbs and cleaned from all adipose tissue and vessels. After washing muscles twice with PBS, gastrocnemius were placed on six-well culture plates for 30 min in DMEM for stabilization in a culture incubator. After that, muscles were either unstimulated or stimulated with obestatin or insulin at the indicated concentrations for 30 min. Glucose transport was determined by addition of 2-[^{3}H]deoxyglucose (0.5 μCi/mL) from GE-Amersham (Buckinghamshire, UK). The uptake was stopped after 5 min by aspiration, and muscles were washed three times with ice-cold PBS. Cells were lysed in 1% SDS, and deoxyglucose uptake was determined by scintillation counting in triplicate.

DATA ANALYSIS

All values are presented as mean ± standard error of the mean (s.e.). Student t test were performed to assess the statistical significance of 2-way analysis. For multiple comparisons, ANOVA was employed. $P < 0.05$ was considered as statistically significant (*,#,##).

14. Muinelo-Romay, L. et al. High-Risk Endometrial Carcinoma Profiling Identifies TGF-b1 as a Key Factor in the Initiation of Tumor Invasion. *Mol. Cancer*. 2011; 10 (8): 1357-66.

RESULTS

CHAPTER 1

OBESTATIN AS A REGULATOR OF ADIPOCYTE METABOLISM AND ADIPOGENESIS

Obestatin activates Akt phosphorylation and AMPK dephosphorylation in 3T3-L1 adipocyte cells

First, the dose dependence of Akt activation by obestatin was examined in 3T3-L1 adipocytes. Akt phosphorylation at C-terminal hydrophobic motif (S473) [HM(S473); p-Akt(S473)] was observed using 10 nM obestatin, and the level of p-Akt(S473) plateaued at 100–200 nM (data not shown). Next, we examined the kinetic of Akt activation in response to obestatin. Significant p-Akt(S473) augment was observed 10 min after addition of obestatin (100 nM), being sustained by 60 min (Fig. 1.1A). Parallel to Akt activation, obestatin (100 nM) triggered the phosphorylation of a broad range of Akt downstream substrates: GSK3 α/β (S21/9), AS160 (T642) mTOR(S2448) and S6K1(T384) (Fig. 1.1B and C). Importantly, dephosphorylation of p-AMPKα (T172) and its downstream substrate ACC (S79) was observed in response to obestatin (100 nM) (Fig. 1.1C).

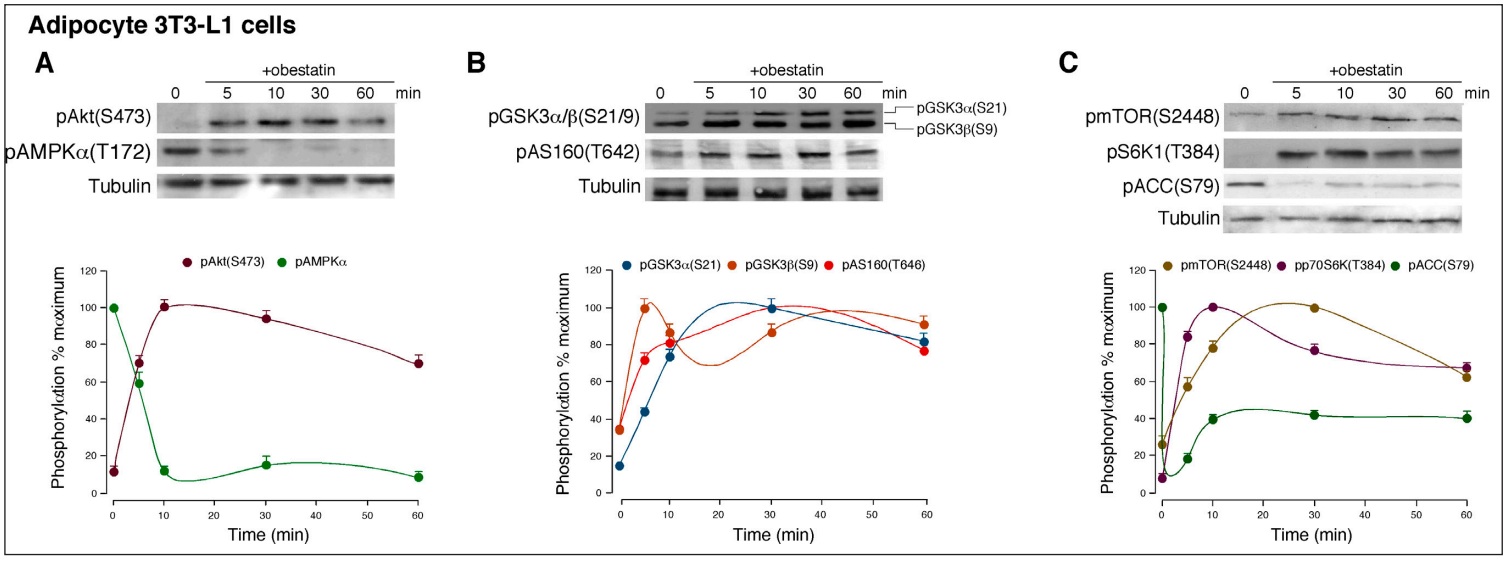

Fig. 1.1 Time-course of the effect of obestatin (100 nM) 3T3-L1 adipocytes: **(A)** p-Akt(S473) and p-AMPKα (T172); **(B)** p-GSK3 α/β (S21/9) and p-AS160(T642) and **(C)** p-mTOR(S2448), p-S6K1(T384) and p-ACC(S79). Phosphorylation was expressed as a percentage of the maximal phosphorylation obtained for each residue (n=3; mean± S.E.).

Obestatin activates Akt phosphorylation and AMPK dephosphorylation in WAT

For *in vivo* obestatin administration, osmotic mini pumps were selected based on the short half-life of this peptide (~22 min)[1]. Male rats received a 24 h continuous subcutaneous (*sc*) infusion of obestatin (300 nmol/kg body weight/24 h) and dissected WATs were processed for WB analysis. Obestatin significantly activated Akt, measured as p-Akt (S473), in subcutaneous, gonadal and omental WAT (Fig. 1.2A). p-AMPKα (T172) was decreased by 20% to basal phosphorylation in omental WAT with no effect in subcutaneous and gonadal WAT (Fig. 1.2A). A 72 h continuous *sc* infusion of obestatin (300 nmol/kg body weight/24 h) increased p-Akt (S473) and decreased p-AMPKα (T172) in subcutaneous, gonadal and omental WAT (Fig. 1.2B). The divergence between 24 and 72 h might be explained by the stress generated by mini-pump implantation.

Fig. 1.2 Obestatin activates Akt phosphorylation and AMPK dephosphorylation in WAT. (A) Effect of 24 h continuous *sc* infusion of obestatin (300 nmol/kg body weight/24 h; n=10) on p-Akt(S473) and p-AMPKα (T172) from subcutaneous, gonadal and omental WAT obtained from male rats. **(B)** Effect of 72 h continuous *sc* infusion of obestatin (300 nmol/kg body weight/24 h; n=10) on p-Akt(S473) and p-AMPKα (T172) from subcutaneous, gonadal and omental WAT obtained from male rats. Phosphorylation was expressed as a percentage of control obtained from 24 h or 72 h mini pump *sc* implanted saline group (n=10; mean± S.E.). Asterisk (*) denotes P< 0.05 when comparing obestatin-treated group with untreated control group (saline).

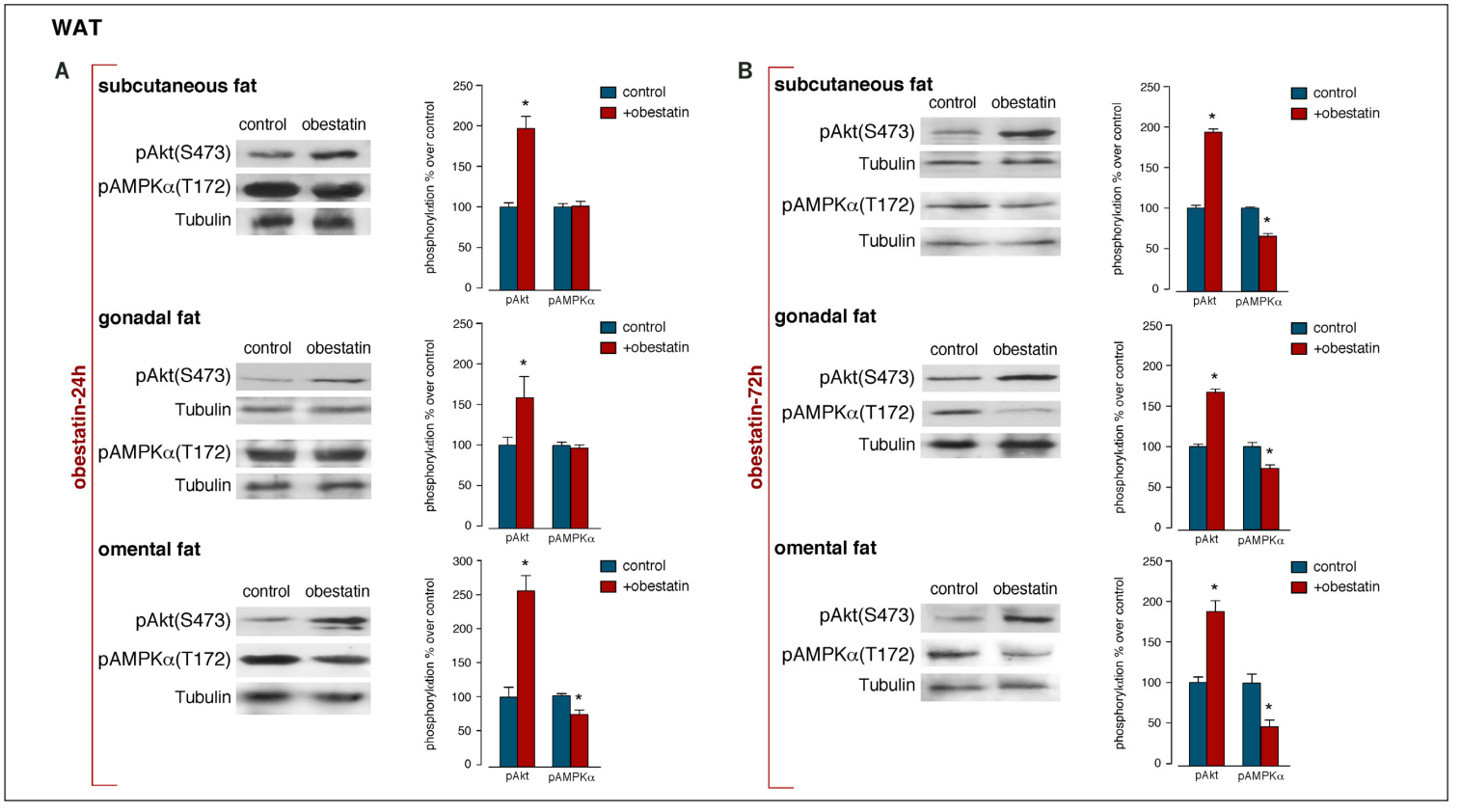

1. Zizzari, P. et al. Obestatin partially affects ghrelin stimulation of food intake and growth hormone secretion in rodents. *Endocrinology*. 2007; 148: 1648-53.

Obestatin increases GLUT4 levels in plasma membranes and glucose uptake in 3T3-L1 adipocyte cells

The amplitude of Akt activation was evaluated on the basis of GLUT1 and GLUT4 translocation to plasma membrane in 3T3-L1 adipocyte cells. Acute treatment with obestatin (100 nM, 30 min) resulted in an increase in GLUT4 translocation to the plasma membrane by ~1.9-fold (Fig. 1.3A). Intriguingly, a modest GLUT1 redistribution was observed in response to 100 nM obestatin (30 min) in 3T3-L1 adipocyte cells (~1.3-fold; Fig. 1.3A). Insulin (172 nM, 30 min) caused a higher increase of GLUT4 levels at the plasma membrane than obestatin in 3T3-L1 adipocyte cells (~2.8-fold) with no significant effect on GLUT1 translocation (Fig. 1.3A). The effect of obestatin in the translocation of GLUT4 to the plasma membrane was confirmed by specific immunofluorescence staining (Fig. 1.3B). In quiescent 3T3-L1 adipocyte cells, the fluorescence was distributed throughout the cytoplasm. After exposure to obestatin (100 nM, 30 min), the fluorescence almost completely disappeared from the cytoplasm to be redistributed in the plasma membrane. The effect of obestatin on DOGU was examined in 3T3-L1 adipocyte cells. Cells were incubated with different concentrations of obestatin (0.001–200 nM) for 30 min, resulting in a dose- dependent increase in DOGU with a maximal effect at 100 nM obestatin (~2.0-fold; Fig. 1.3C). Insulin treatment (172 nM) caused an increase of DOGU by ~2.8-fold in adipocyte cells (Fig. 1.3C).

Obestatin shows no effect on FATP1, FATP4 and FAT/CD36 translocation to plasma membrane in 3T3-L1 adipocyte cells

The levels of long chain fatty acid transport proteins 1 and 4 (FATP1 and FATP4) and fatty acid translocase (FAT/CD36) at plasma membrane were examined by subcellular fractionation. As shown in Fig. 1.4, obestatin (100 nM, 30 min) did not modify FATP1, FATP4 and FAT/CD36 levels at the plasma membrane in 3T3-L1 adipocyte cells. Remarkably, FATP1 and FATP4 redistribution was significantly affected in response to insulin (172 nM, 30 min) in ~2.3- and 2.6-fold, respectively. In contrast to the FATP observation, FAT/CD36 redistribution was unaffected in response to insulin (172 nM, 30 min; Fig. 1.4).

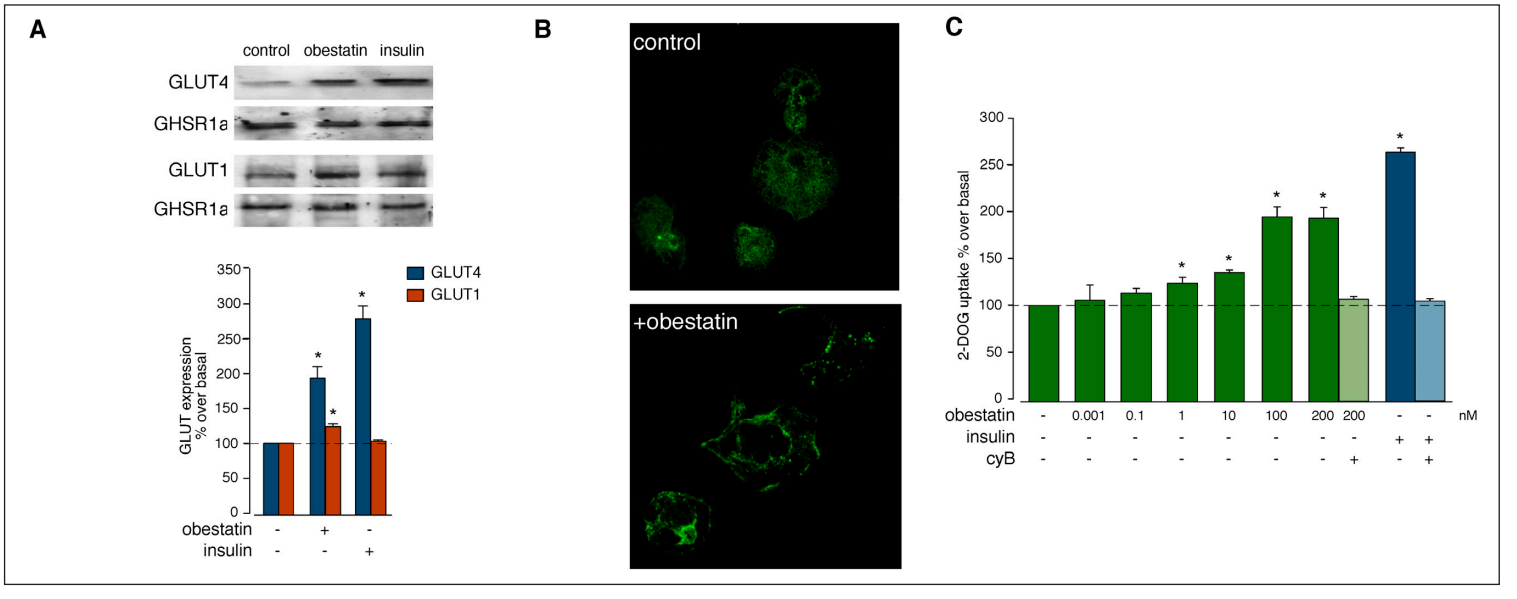

Fig. 1.3 Effect of obestatin in glucose up-take. (A) WB analysis of GLUT4 and GLUT1 expression in membrane from 3T3-L1 adipocyte cells treated with obestatin (100 nM) or insulin (172 nM) for 30 min. GLUT expression was expressed as a percentage of basal expression obtained in control cells (n=3; mean± S.E.). **(B)** Immunofluorescence analysis of obestatin-induced GLUT4 translocation in 3T3-L1 adipocyte cells. Serum-starved cells were stimulated with obestatin (100 nM, 30 min) and the amount of GLUT4 was determined by labeling with anti-GLUT4 antibody in combination with Alexa 594-conjugate goat anti- rabbit antibody in permeabilized cells. **(C)** Obestatin dose dependently stimulated 2-[^{3}H]deoxyglucose uptake in 3T3-L1 adipocyte cells (n=3; mean± S.E.). Non-specific uptake was measured in the presence of 20 μM cytochalasin B (CyB).

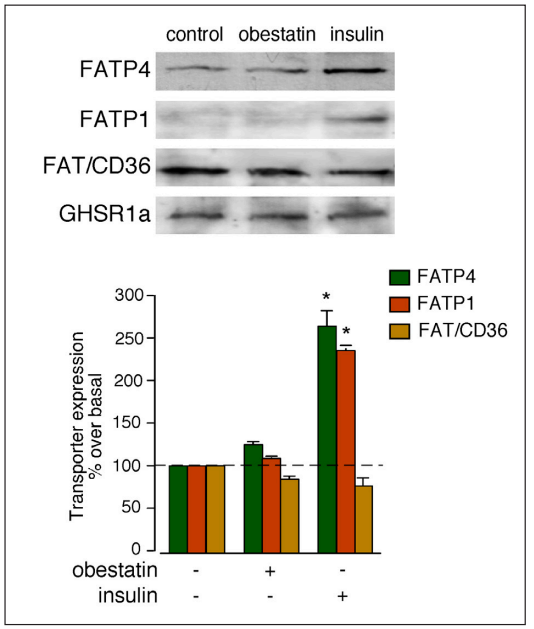

Fig. 1.4. Effect of obestatin on fatty acid transporters. WB analysis of FATP1, FATP4 and FAT/CD36 expression in membrane from 3T3-L1 adipocyte cells treated with 100 nM obestatin or with 172 nM insulin for 30 min. FATP1, FATP4 and FAT/CD36 expression were expressed as a percentage of basal expression obtained in control cells (n=3; mean± S.E.). Expression of GHSR1a was determined to ensure equal membrane protein loading. Blots are representative of three independent experiments. Asterisk (*) denotes P<0.05 when comparing obestatin-treated group with untreated control group.

Obestatin promotes adipogenesis *in vitro*

To initiate the 3T3-L1 adipocyte differentiation process, IBMX, DEX and insulin are used. Among these three compounds, only insulin is capable of activating Akt system through IGF-1 receptor playing a pivotal role in adipogenesis[2]. Consistent with the effect on 3T3-L1 adipocytes (Fig.1.1A), obestatin (100 nM) induced significant Akt(S473) phosphorylation, which was parallel to AMPK dephosphorylation at T172 in 3T3-L1 preadipocyte cells. To ascertain the effect of obestatin on adipogenesis, we first analyzed the effect of obestatin on Akt activation in 3T3-L1 preadipocytes (Fig 1.5A). The effect of acute GPR39 deficiency was determined by means of siRNA in 3T3-L1 preadipocyte cells. Under these conditions, the constructs decreased GPR39 expression by 50±10% (Fig. 1.5B). In the presence of a non-targeting control siRNA. Silencing of GPR39 in preadipocyte cells decreased subsequent p-Akt(S473) with respect to siRNA control (47±2% under treatment with obestatin (100 nM) for 5 min; Fig. 1.5B).

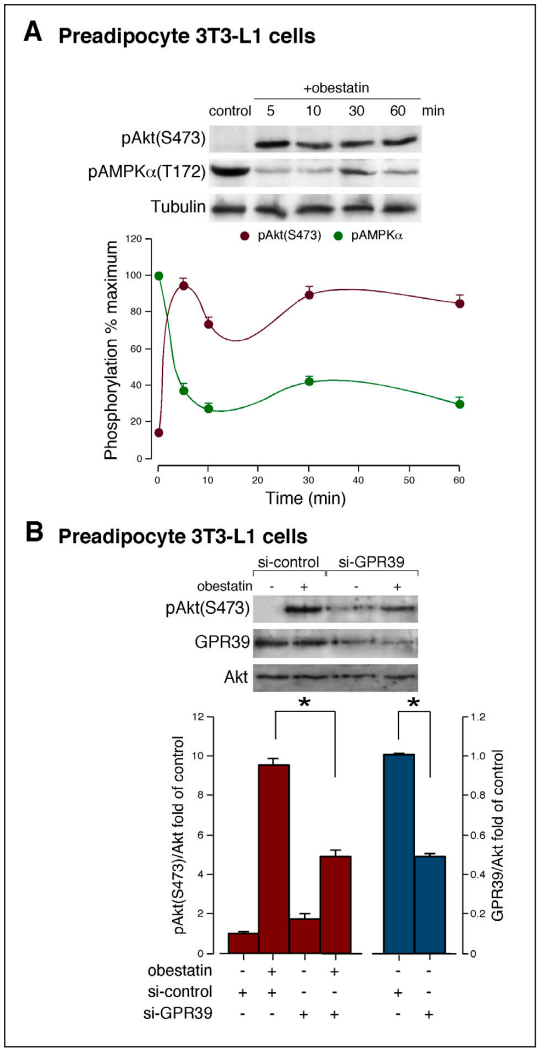

Fig.1.5 Effect of obestatin on preadipocytes trough GPR39. (A) Time-course of the effect of obestatin (100 nM) on p-Akt(S473) and p-AMPKα(T172) in 3T3-L1 preadipocyte cells. Phosphorylation was expressed as a percentage of the maximal phosphorylation obtained for each residue (n=3; mean± S.E.). **(B)** Effect of siRNA depletion of GPR39 on obestatin-activated p-Akt(S473) (100 nM, 5 min) in 3T3-L1 preadipocyte cells. Expression of p-Akt(S473) and GPR39 was expressed as fold of their levels in control siRNA-transfected cells (n=3; mean± S.E.).

Next, we examined the role of obestatin as promoter of terminal adipocyte differentiation working with 3T3-L1 preadipocyte cells maintained in DMEM containing 10% FBS with obestatin (0.001–200 nM), ghrelin (0.001–200 nM) or insulin (172 nM) for 7 days after induction of differentiation under combination of 0.5 mM IBMX, 25

2. Xu, J. et al. Protein kinase B/Akt 1 plays a pivotal role in insulin-like growth factor- 1 receptor signalling induced 3T3-L1 adipocyte differentiation. *J. Biol. Chem.* 2004; 279: 35914-22.

μM DEX and 861 nM insulin for 3 days. Oil red O staining revealed that the accumulation of lipid droplets was dose-dependent for obestatin or ghrelin treatments being maximal at 10 nM for both peptides (~3.6-fold; Fig. 1.6A). Insulin (172 nM) treatment increased the formation of lipid droplets (~7.8-fold; Fig. 1.6A). Co-treatment with obestatin or ghrelin (1 or 10 nM) and a half-dose of insulin (86 nM) further stimulated adipocyte differentiation compared to the treatments with obestatin or ghrelin alone (Fig. 1.6A).

The capability of obestatin as initiator of adipocyte differentiation was explored by the combination of IBMX, DEX and obestatin (1.96 μM obestatin for 3 days and then maintained in DMEM containing 10% FBS with 392 nM obestatin for 7 days; Fig. 1.6B). Obestatin-stimulated adipocyte differentiation was detected at 10 nM, but maximal effects were observed at pharmacological levels for *in vitro* assays (≥1 μM). Obestatin treatment (1.96 μM) for 3 days (Group 2, Fig. 1.6B) induced more lipid droplets (~1.6-fold) than insulin treatment (Group 1, Fig. 1.6B). The accumulation was higher in cells maintained in DMEM/10% FBS with obestatin (392 nM) for 7 days after induction of differentiation (Group 3, Fig. 1.6B), but fewer than that observed in full dose insulin-treated cells (172 nM) for 7 days (Group 4, Fig. 1.6B).

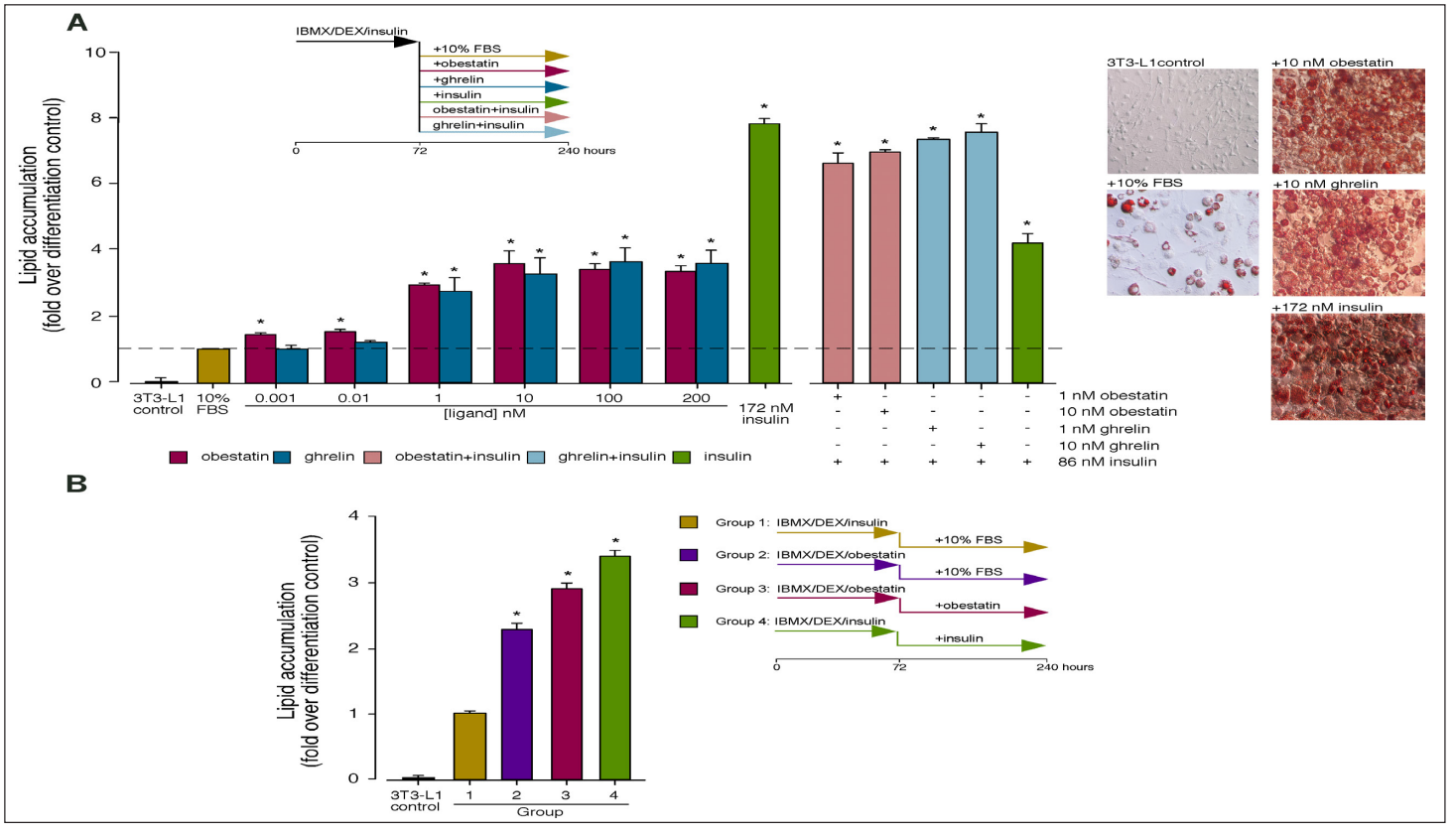

Fig.1.6. Effect of obestatin as a promoter or initiator of adipogenesis: **(A)** 3T3-L1 cells display an obestatin-dependent increase in adipogenesis. 3T3-L1 preadipocyte cells were maintained in DMEM containing 10% FBS with different concentrations of obestatin, ghrelin or insulin (172 nM) for 7 days after induction of differentiation by combination of 0.5 mM IBMX/25 μM DEX/861 nM insulin for 3 days. Lipid droplet accumulation was analyzed by spectrophotometry at 520 nm by Oil red O staining. Results are expressed as a fold of lipid accumulation over differentiation control (cells maintained in DMEM/10% FBS/172 nM insulin for 7 days after induction of differentiation under treatment with 0.5 mM IBMX/25 μM DEX/861 nM insulin for 3 days; n=3; mean± S.E.). Representative microscope fields of view (right) are shown at the same magnification. **(B)** Effect of obestatin as initiator of adipogenesis. 3T3-L1 preadipocyte cells were maintained in DMEM containing 10% FBS with obestatin (392 nM) or insulin (172 nM) for 7 days after induction of differentiation by treatment with 0.5 mM IBMX, 25 μM DEX, 861 nM insulin or 1.96 μM obestatin for 3 days. Lipid droplet accumulation was analyzed by spectrophotometry at 520 nm by Oil red O staining. Results are expressed as fold of lipid accumulation over differentiation control (cells maintained in DMEM/10% FBS/172 nM insulin for 7 days after induction of differentiation by treatment with 0.5 mM IBMX/25 μM DEX/861 nM insulin for 3 days; n=3; mean± S.E.). Asterisk (*) denotes P<0.05.

Supporting this scenario, in obestatin-treated 3T3-L1 differentiating adipocytes, C/EBPβ protein expression markedly increased at 24 h for p32 and p35 isoforms, respectively (Fig. 1.7A). Furthermore, C/EBPδ protein expression peaked around 6 h after obestatin treatment (Fig. 1.7B). Consistently, obestatin treatment strongly increased the expression of PPARγ proteins peaking at 48 and 144 h of differentiation for PPARγ1 and PPARγ2 isoforms, respectively (Fig. 1.7C). In addition, this treatment also increased the expression of C/EBPα proteins peaking at 24 and 72 h for p30 and p42 isoforms, respectively (Fig. 1.7D).

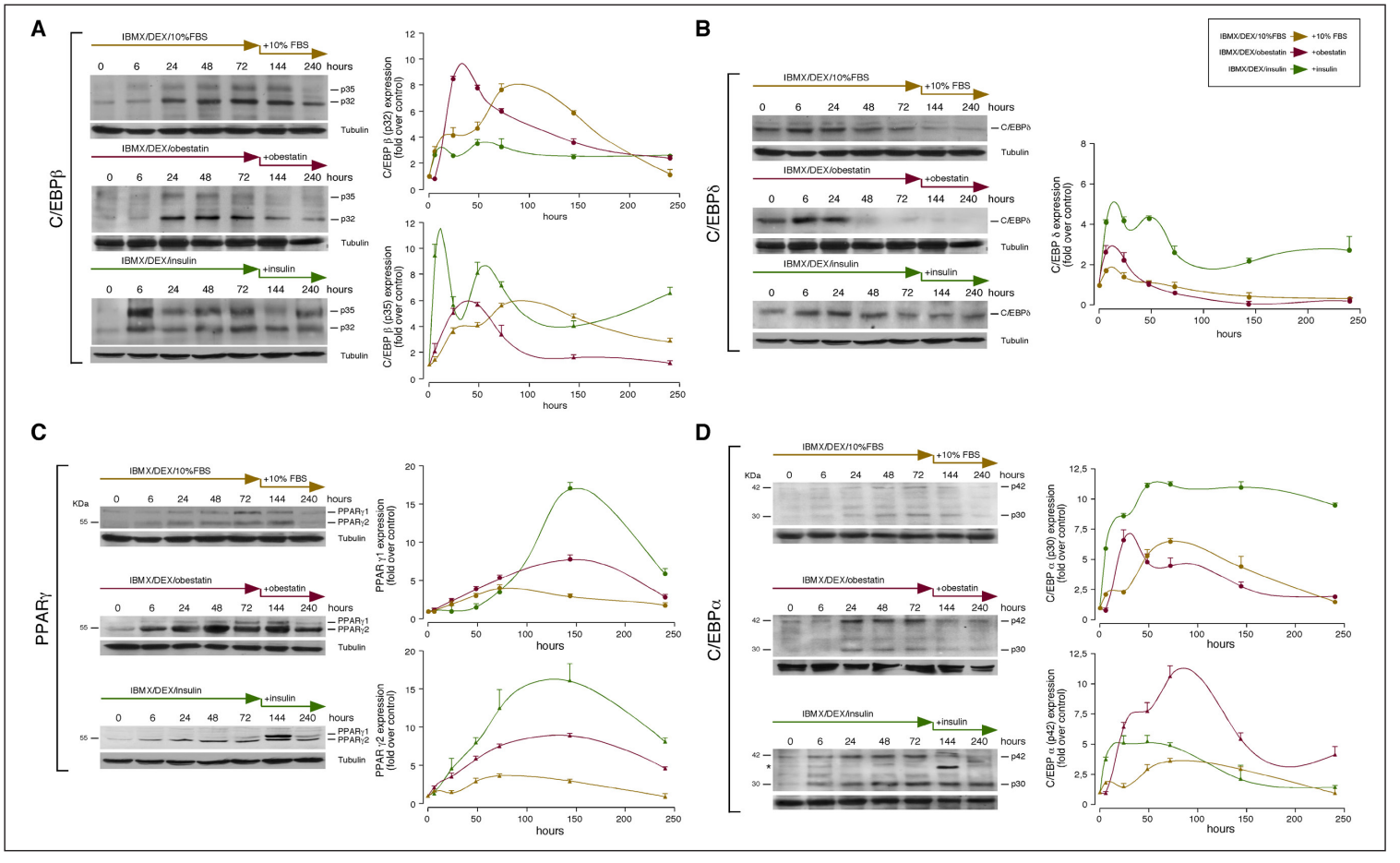

Fig. 1.7 Obestatin regulation of transcription factors during adipogenesis: (A) C/EBPβ, **(B)** C/EBPδ , **(C)** PPARγ and **(D)** C/EBPα. 3T3-L1 preadipocyte cells were maintained in DMEM containing 10% FBS, obestatin (392 nM) or insulin (172 nM) for 7 days after induction of differentiation by treatment with 0.5 mM IBMX, 25 μM DEX, 10% FBS, 861 nM insulin or 1.96 μM obestatin for 3 days [in **(D)**, asterisk (*) denotes unspecific band]. Data were expressed as percentage of control expression (n=3; mean± S.E.). Blots are representative of three independent experiments.

Preproghrelin expression increases throughout adipogenesis

We first examine obestatin expression in 3T3-L1 preadipocyte and adipocyte cells at protein level, utilizing immunocytochemistry. 3T3-L1 adipocyte cells showed a stronger obestatin expression (Fig. 1.8B) compared to that observed in 3T3-L1 preadipocyte cells (Fig. 1.8A). No immunostaining was found with obestatin antibody pre-adsorption control in 3T3-L1 adipocyte cells (Fig. 1.8C). This result leads us to focus on preproghrelin expression along adipogenesis as source of obestatin. Preproghrelin expression was examined at mRNA and protein level, by RT-PCR and immunoblot, respectively, in 3T3-L1 preadipocyte cells. The cells were maintained in DMEM containing 10% FBS with insulin (172 nM) for 7 days after induction for 3 days (0.5 mM IBMX, 25 µM DEX and 861 nM insulin). The amount of preproghrelin mRNA showed a biphasic pattern of expression. A rapid augment was observed at 6 h (~1.7-fold; Fig. 1.8D), to reach values bellow basal by 24 h after the induction of differentiation. Preproghrelin mRNA expression increased from 48 h, becoming maximal 72 h after induction to be sustained throughout terminal differentiation. As Fig. 1.8E shows, there is a rapid augment of preproghrelin protein expression at the time of differentiation into adipocytes (~4.0-fold, 6 h after induction) reaching a maximum 24 h after induction of differentiation (~5.8-fold) concomitant with the minimum of preproghrelin mRNA expression (Fig. 1.8D). Intriguingly, preproghrelin protein expression decreased 48 h after induction of differentiation to be sustained along terminal differentiation being higher than that in preadipocyte cells (~2.4-fold at 240 h). Furthermore, GPR39 protein expression decreased in terminal differentiation compared to undifferentiated 3T3-L1 cells (~40% reduction, 240 h after induction; Fig. 1.8F), showing two maximal expression levels concomitant with the maximum of preproghrelin expression (Fig. 1.8D).

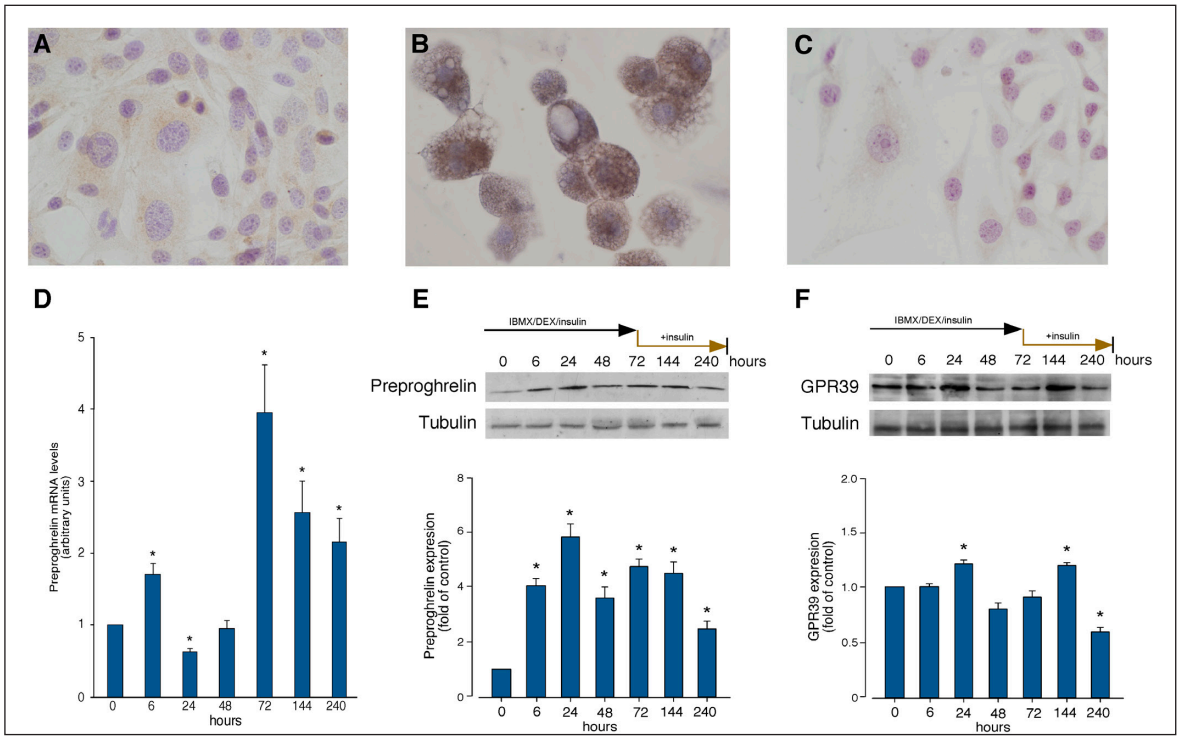

Fig.1.8 Obestatin expression along adipogenesis. Immunocytochemical detection of obestatin in 3T3-L1 preadipocyte **(A)** and adipocyte cells **(B)** (objective magnification 40x). Obestatin immunostaining was mainly localized in the cytoplasm of 3T3-L1 adipocytes while it was faint in 3T3-L1preadipocyte cells. **(C)** Pre-adsorption control with mouse obestatin (10 nmol/mL) showed no positive immunostaining. **(D)** Preproghrelin mRNA levels in the course of adipogenesis. WB analysis of preproghrelin **(E)** and GPR39 **(F)** expression in the course of adipogenesis. Preproghrelin expression at mRNA or protein levels, were examined in 3T3-L1 preadipocyte cells maintained in DMEM containing 10% FBS with insulin (172 nM) for 7 days after induction for 3 days (0.5 mM IBMX, 25 µM DEX and 861 nM insulin). Protein expression was expressed as a fold over control cells (n=3; mean± S.E.). mRNA was quantified by RT-PCR and expressed as arbitrary units (n=5; mean± S.E.). Asterisk (*) denotes $P<0.05$ when comparing obestatin-treated group with untreated control group.

Consistent with the results from cultured cells, immunohistochemical analysis confirmed the expression of obestatin in subcutaneous, gonadal and omental WAT obtained from male ad libitum rats (Fig 1.9 A–C, respectively).

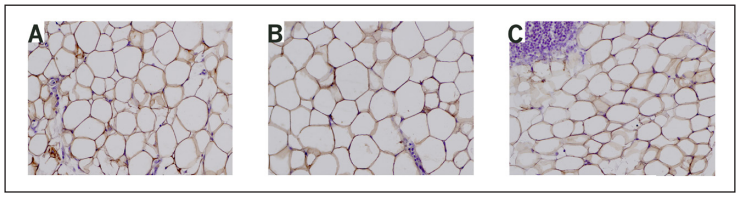

Fig.1.9 Immunohistochemical detection of obestatin in WAT : subcutaneous **(A)**, gonadal **(B)** and omental **(C)** WAT (objective magnification 20x).

Autocrine/paracrine role of obestatin on adipogenesis

The autocrine/paracrine role of obestatin on adipogenesis was tested *in vitro* performed with a neutralizing obestatin antibody (anti-obestatin Ab). As shown in the Fig. 1.10 (*left panel*) neutralization of obestatin (100 nM) by pre-incubation with anti-obestatin Ab (1.3 µg/mL) reduced by ~70±3% the level of p-Akt (S473) in 3T3-L1 preadipocyte cells. By contrast, insulin-induced Akt activity was not affected by pre-incubation with anti-obestatin Ab. The autocrine/paracrine role on adipogenesis was then tested by combination of 24 and 48 h serum-free conditioned medium (CM) of 3T3-L1 adipocyte cells with neutralizing obestatin antibody (5 µg/mL), Fig. 1.10 (*right panel*). 3T3-L1 preadipocyte cells were maintained in DMEM containing 0.1% BSA with obestatin (392 nM; Group 2), anti- obestatin Ab, (Group 3), obestatin (392 nM)+anti-obestatin Ab (Group 4), CM-24h (Group 5), CM-24h+anti-obestatin Ab (Group 6), CM-48h (Group 7) or CM-48h+anti-obestatin Ab (Group 8) for 7 days after induction of differentiation under treatment with 0.5 mM IBMX, 25 µM DEX and 861 nM insulin for 3 days. Oil Red O staining revealed that incubation with neutralizing obestatin Ab reduced by 35±3% accumulation of lipid droplets compared to 3T3-L1 preadipocyte cells maintained in DMEM/0.1% BSA/392 nM obestatin (Fig. 1.10, Group 3 versus Group 2). Neutralization of obestatin (392 nM) by pre-incubation with anti-obestatin Ab reduced by 35±8% accumulation of lipid droplets compared to 3T3-L1 preadipocyte cells maintained in DMEM/0.1% BSA/392 nM obestatin (Group 4 versus Group 2; Fig. 1.10). Serum-free conditioned medium, CM-24h or CM-48h, also activated accumulation of lipid droplets (~2.0- and ~2.5-fold, respectively; Groups 5 and 7 versus Group 1; Fig. 1.10). Pre-incubation of the CM-24h or CM-48h with anti-obestatin Ab reduced accumulation of lipid droplets by 21±4% and 20±6%, respectively (Groups 6 versus Groups 5, and Group 8 versus Group 7, Fig. 1.10).

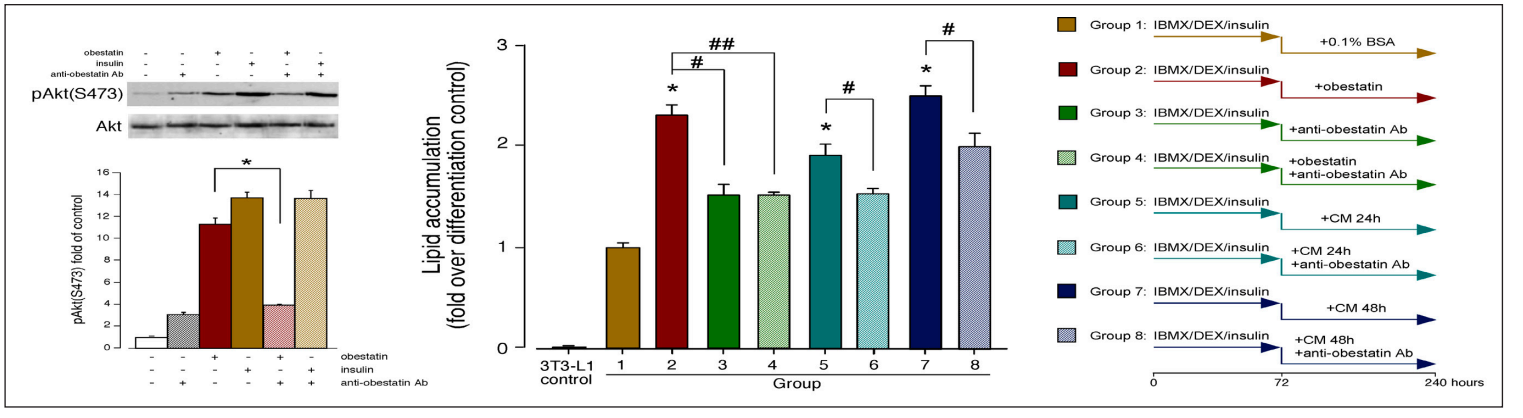

Fig. 1.10 Autocrine/paracrine role of obestatin on adipogenesis. (Left panel) Anti-obestatin antibody specificity. Effect of anti- obestatin antibody (1.3 µg/mL), obestatin (100 nM), insulin (100 nM), anti-obestatin antibody+ obestatin and anti-obestatin antibody+ insulin on p-Akt(S473) in 3T3-L1 preadipocytes. **(Right panel)** 3T3-L1 preadipocyte cells were maintained in DMEM containing 0.1% BSA with obestatin (392 nM; Group 2), anti-obestatin antibody (5 µg/mL; anti-obestatin Ab; Group 3), obestatin (392 nM)+anti-obestatin Ab (5 µg/mL; Group 4), CM-24h (Group 5), CM-24h+anti-obestatin Ab (5 µg/mL; Group 6), CM-48h (Group 7) or CM-48h+anti-obestatin Ab (5 µg/mL; Group 8) for 7 days after induction of differentiation by treatment with 0.5 mM IBMX, 25 µM DEX and 861 nM insulin for 3 days. Lipid droplet accumulation was analyzed by spectrophotometry (520 nm) by Oil red O staining. Results are expressed as fold of lipid accumulation over differentiation control (Group 1; cells maintained in DMEM/0.1% BSA for 7 days after induction of differentiation by treatment with 0.5 mM IBMX/25 µM DEX/861 nM insulin for 3 days; mean± S.E. of three independent experiments). Asterisk (*) denotes P<0.05 when comparing treated groups with control group; daggers (#, ##) denote P < 0.05 when comparing treated groups with antibody-treated groups. Phosphorylation was expressed as fold of control (n=3; mean± S.E.). Blot is representative of three independent experiments. Asterisk (*) denotes P<0.05 when comparing obestatin-treated group with anti-obestatin ab+ obestatin group.

The effect of acute obestatin deficiency was determined by knock-down of preproghrelin by means of siRNA prior to induction of adipocyte differentiation. Under these conditions, the constructs decreased preproghrelin expression by 58±6% (Fig. 1.11, *left panel*). Silencing of preproghrelin in preadipocyte cells decreased subsequent adipocyte differentiation with respect to siRNA control [43±5% and 48±4% for 3T3-L1 preadipocyte cells under treatment with 0.5 mM IBMX, 25 µM DEX, and insulin (861 nM) for 3 days and then maintained in DMEM containing 10% FBS or insulin (172 nM) for 7 days, respectively (Fig. 1.11, *right panel*)].

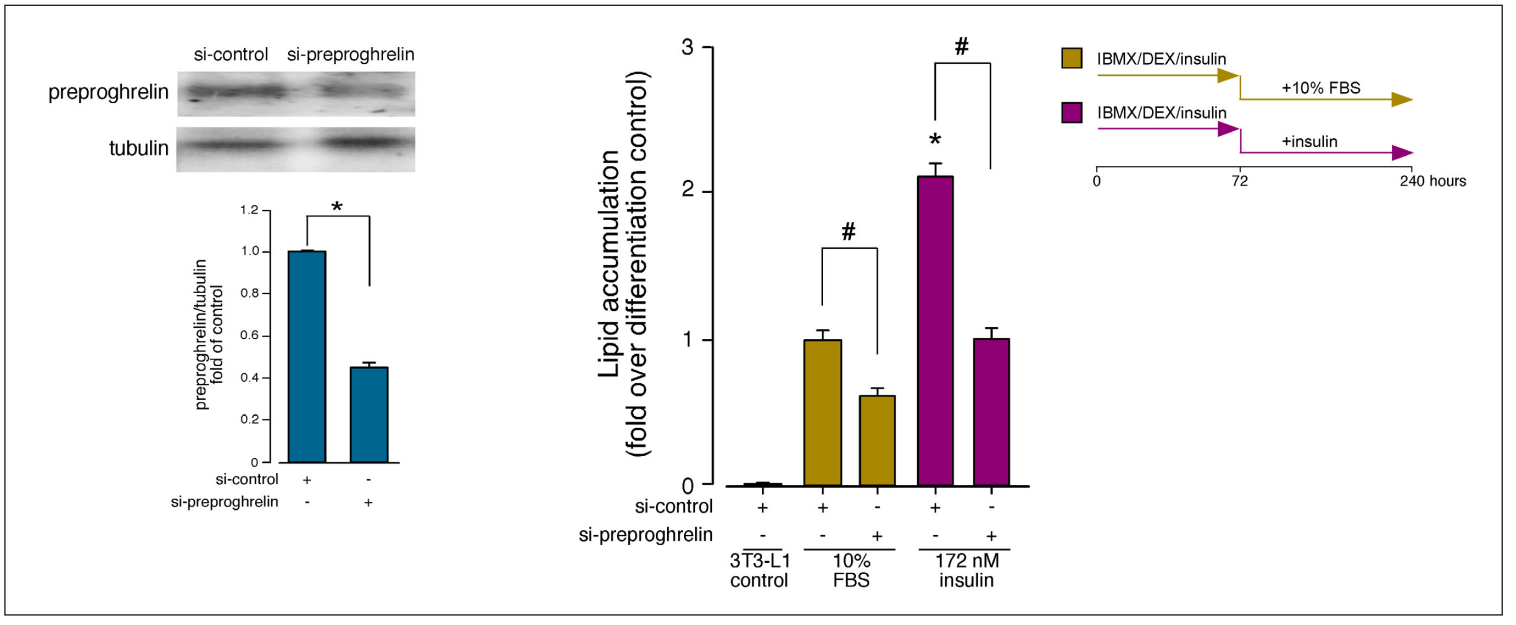

Fig.11 Effect of siRNA depletion of preproghrelin on adipogenesis. (Left panel) 3T3-L1 cells transfected with preproghrelin siRNA prior to induction of adipocyte differentiation (DMEM/10% FBS with insulin (172 nM) for 7 days after induction for 3 days under 0.5 mM IBMX, 25 µM DEX and 861 nM insulin). Equal amounts of protein in each sample were used to assess the expression of preproghrelin by WB. Expression of preproghrelin was expressed as fold of the level of preproghrelin in control siRNA-transfected cells (mean± S.E.). **(Right panel)** Lipid droplet accumulation was analyzed by spectrophotometry at 520 nm by Oil red O staining. Results are expressed as fold of lipid accumulation over differentiation control. Asterisk (*) denotes P<0.05 when comparing treated control siRNA group with control siRNA group; dagger (#) denotes P<0.05 when comparing preproghrelin siRNA group with control siRNA group.

CHAPTER 2

PREPROGHRELIN EXPRESSION IS A KEY TARGET FOR INSULIN ACTION ON ADIPOGENESIS

Expression of preproghrelin, PC1/3, and MBOAT4 throughout adipogenesis in 3T3-L1 cells

Preproghrelin, PC1/3, and MBOAT4 proteins were found to predominate in 3T3-L1 adipocyte cells compared to preadipocyte cells as indicated in Fig. 2.1. To ascertain whether insulin determines this pattern of expression, mRNA and protein expression of preproghrelin, PC1/3, and MBOAT4 were analyzed in insulin-induced adipogenesis and compared to that with no insulin treatment (group A: DEX, IBMX and group B: insulin, DEX and IBMX) (Fig. 2.2). In Fig. 2.2A we showed that meanwhile the preproghrelin mRNA showed a maximum at 144 h in group A, insulin-stimulated group showed two peaks of expression at 6 and 144 h being ~1.7- and 1.5-fold higher compared with the former. The PC1/3 mRNA levels significantly augmented for all times tested in the group A, although this pattern of expression was clearly regulated under insulin treatment in group B with a maximal display at 144 h (~3.5-fold). The MBOAT4 mRNA levels increased 24 h after treatment to return to near basal levels over 144h in group A (Fig. 2.2A). By contrast, insulin treatment inhibited MBOAT4 mRNA throughout adipogenesis to return to basal levels in terminal differentiation (Fig. 2.2A). Results of WB analysis (Fig. 2.2B) showed that the preproghrelin protein level markedly increased at 6 h (~4.5-fold) which was sustained along terminal differentiation in group B. A similar temporal profile was observed for PC1/3 protein showing two maximal expression levels concomitant with the maximum of preproghrelin expression (~2.5- and 2.0-fold at 6 and 144 h respectively), whereas MBOAT4 protein was apparent within 24 h and increased in abundance throughout adipogenesis reaching maximal values in terminal differentiation (~3.0-fold at 240 h). In marked contrast, the amount of preproghrelin, PC1/3, and MBOAT4 protein was not significantly affected in the absence of insulin treatment (group A).

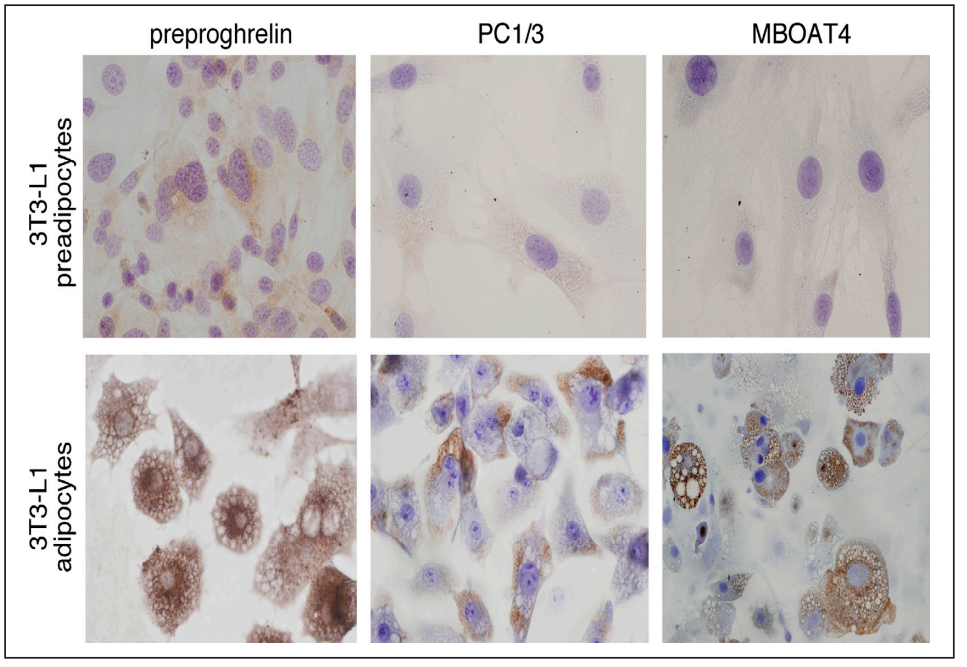

Fig. 2.1 Immunohistochemical detection of preproghrelin derived enzymes. Preproghrelin, PC1/3, and MBOAT4 in 3T3-L1 preadipocyte and adipocyte cells (objective magnification 40x).

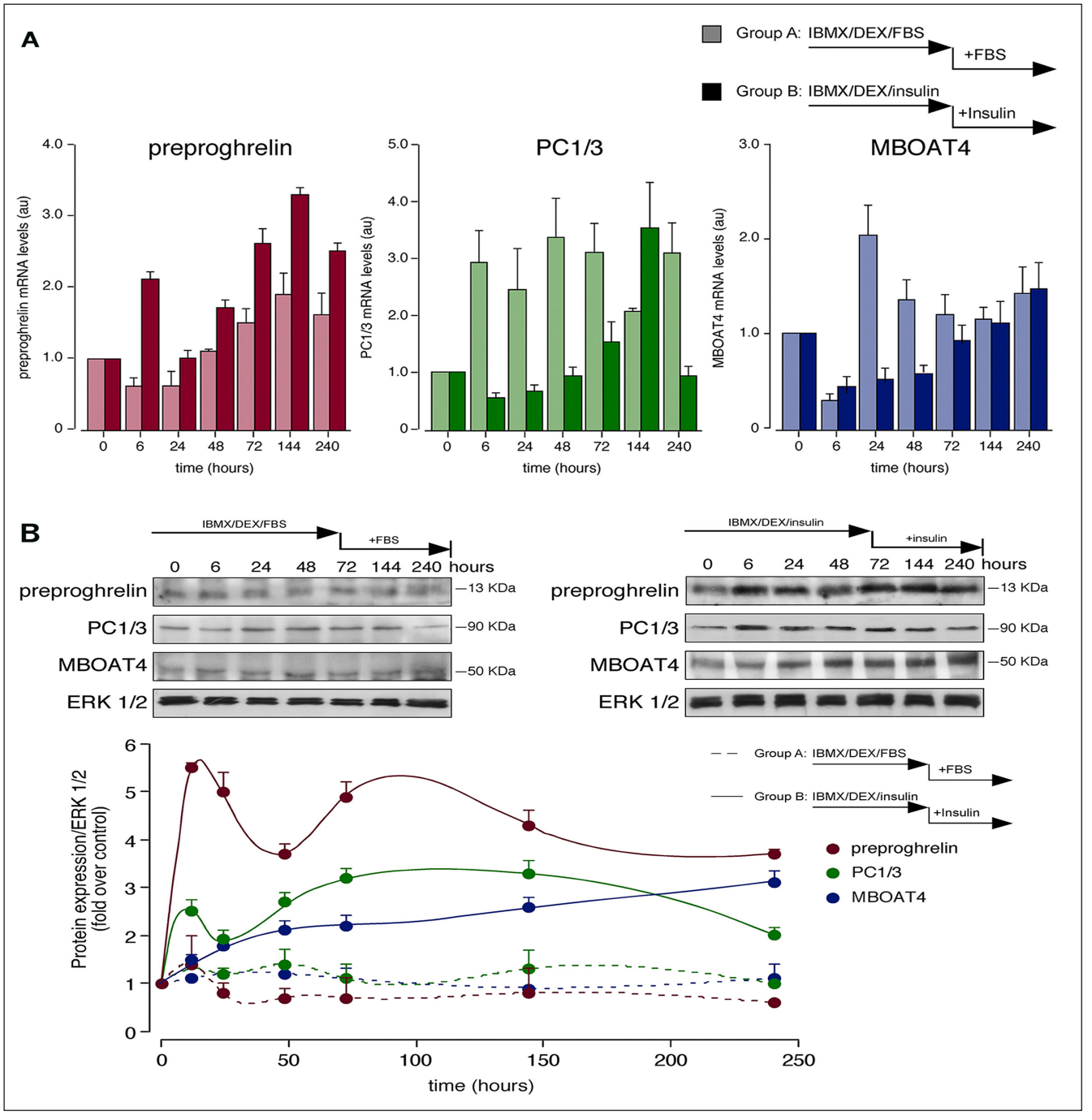

Fig. 2.2 Quantitative analysis of mRNA and protein levels of preproghrelin and its derived enzymes during differentiation (A) Preproghrelin, PC1/3, and MBOAT4 mRNA levels in the course of adipogenesis. Data were normalized to levels of ACTB and expressed as mean± S.E.M. (n=6). **(B)** WB analysis of preproghrelin, PC1/3, and MBOAT4 in adipogenesis. mRNA or protein levels were examined in group A (3T3-L1 preadipocyte cells maintained in DMEM containing 10% FBS for 7 days after treatment for 3 days with 0.5 mM IBMX, 25 mM DEX) and group B (3T3-L1 preadipocyte cells maintained in DMEM containing 10% FBS, insulin (172 nM) for 7 days after induction for 3 days (0.5 mM IBMX, 25 mM DEX, and 861 nM insulin)). For **B** data are expressed as mean± S.E.M. (n=3). For all experiments *P<0.05 versus control values.

mTOR/56K1 pathway is involved in preproghrelin derived peptides regulation

To further explore the mechanism involved in the control of protein translation, the effect of rapamycin treatment (25 nM) was examined 2 h prior to insulin-induced adipocyte differentiation. Inhibition of mTORC1/S6K1 pathway significantly reduced the preproghrelin, MBOAT4, and PC1/3 protein expression at 72 h after insulin-activated adipogenesis (Fig. 2.3). Rapamycin treatment did not significantly alter the expression of analyzed proteins in 3T3-L1 preadipocyte-treated controls.

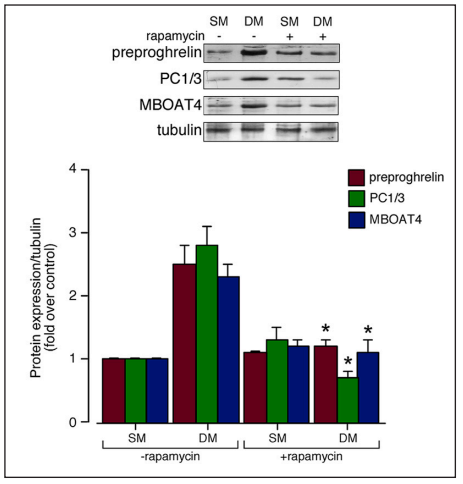

Fig. 2.3 Preproghrelin, and its derived enzymes, protein expression in absence or presence of rapamycin. After pretreatment with rapamycin (25 nM, 2 h), 3T3-L1 preadipocyte cells were maintained for 72 h in DMEM containing 10% FBS, 0.5 mM IBMX, 25 mM DEX, 861 nM insulin (differentiation medium, DM), or DMEM containing 10% FBS (standard medium, SM). Data are expressed as mean± S.E.M. (n=3). *P<0.05 versus control values.

Auto/paracrine role of preproghrelin-derived peptides in adipogenesis in 3T3-L1 cells

To define the auto/paracrine role of preproghrelin-derived peptides in adipogenesis, the effect of preproghrelin siRNA was first examined. Transfection of 3T3-L1 preadipocytes prior to induction of adipogenesis with siRNA designed against preproghrelin reduced target protein expression by 51±2% (Fig. 2.4). The effect of preproghrelin deficiency decreased MBOAT4 and PC1/3 with respect to siRNA control (49±3 and 61±3% respectively; Fig. 2.4, *above panel*). Oil Red O staining revealed that preproghrelin knock-down significantly reduced insulin-mediated adipogenesis by at least 30±1 and 50±5% for 3T3-L1 preadipocyte cells under treatment with IBMX, DEX, and insulin for 3 days and then maintained in DMEM containing 10% FBS or insulin for 7 days respectively (Fig. 2.4, *below panel*).

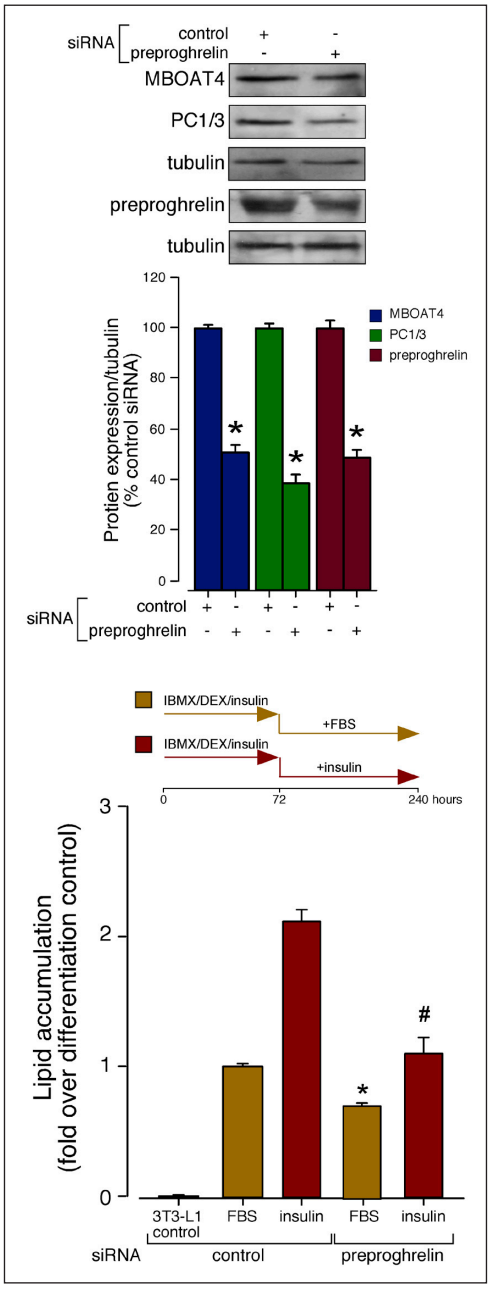

Fig. 2.4. Effect of siRNA depletion of preproghrelin on adipogenesis. (Above panel) 3T3-L1 cells transfected with preproghrelin siRNA prior to induction of adipocyte differentiation (DMEM/10% FBS or DMEM/10% FBS with insulin (172 nM) for 7 days after induction for 3 days under 0.5 mM IBMX, 25 mM DEX, and 861 nM insulin). Equal amounts of protein in each sample were used to assess the expression of MBOAT 4, PC1/3, and preproghrelin by WB. **(Bellow panel)** Lipid droplet accumulation was analyzed by spectrophotometry at 520 nm by Oil red O staining. Data are mean± S.E.M. of three independent experiments (*,P<0.05 versus control values).

Similar results were obtained by neutralization of endogenous obestatin or UAG/AG using anti-obestatin (5 µg/mL) or anti-ghrelin (5 µg/mL; antibody raised against a peptide mapping within an internal region of ghrelin) antibodies (Ab; Fig. 2.5A). The differentiation-associated lipid accumulation was significantly reduced by anti-obestatin Ab (25±4%). A larger effect was observed with anti-ghrelin Ab (39±2%). These effects were reverted neutralizing the primary antibody with its respective antigen peptide (obestatin, AG or UAG, 5 µg/mL). The expression pattern of GHSR1a and GPR39 was further analyzed in Fig. 2.5B. The GHSR1a protein levels were concomitant with the maximum of preproghrelin expression (Fig. 2.2B)(~1.7- and 1.4-fold at 6 h and 144 h respectively; Fig. 2.5B). The GPR39 levels showed a more sustained expression throughout adipogenesis with two maximal levels (~2.3- and 2.2-fold at 48 h and 144 h respectively; Fig. 2.5B).

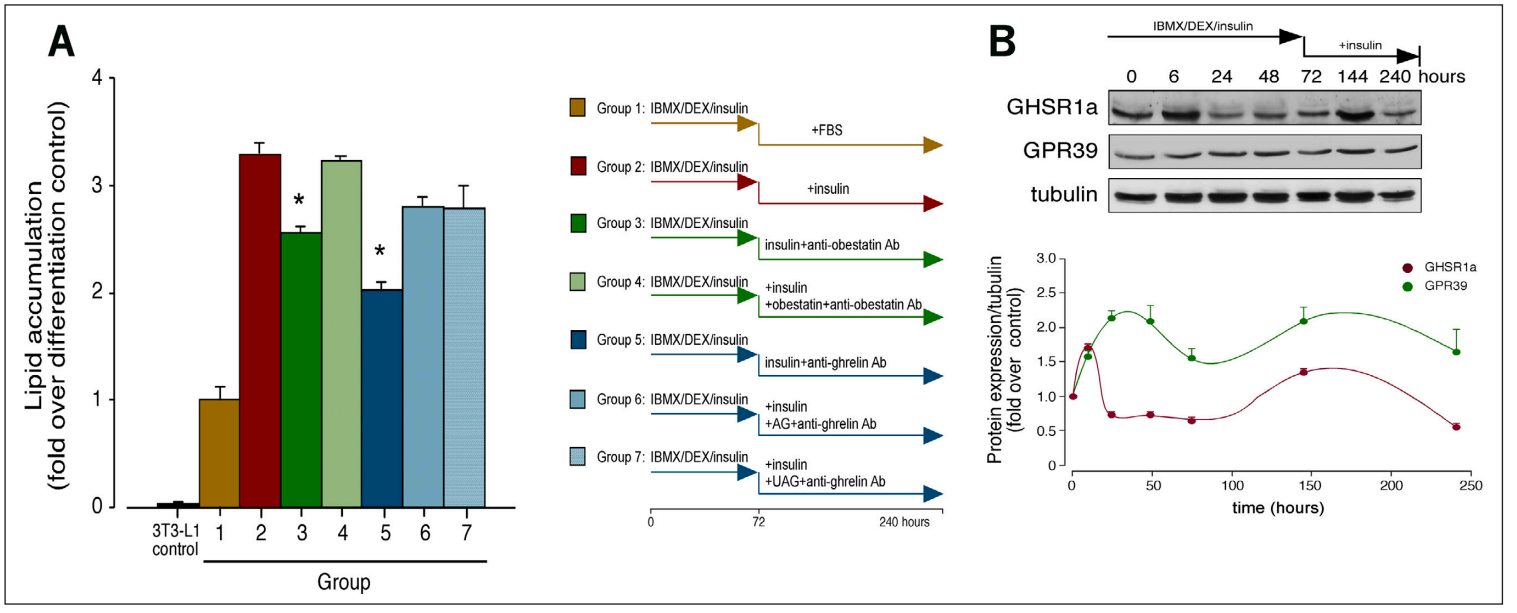

Fig. 2.5 Autocrine/paracrine role of obestatin and ghrelin/O-acyl ghrelin on adipogenesis. (A) 3T3-L1 preadipocyte cells were maintained in DMEM containing 10% FBS (group 1), 10% FBS+ insulin (172 nM; group 2), 10% FBS+ insulin (172 nM)+anti-obestatin Ab (5 µg/mL; group 3), 10% FBS+ insulin (172 nM)+anti-obestatin Ab (5 µg/mL)+obestatin (5 µg/mL; group 4), 10% FBS+ insulin (172 nM)+anti-ghrelin Ab (5 µg/mL; group 5), 10% FBS+ insulin (172 nM)+anti-ghrelin Ab (5 µg/mL)+AG (5 µg/mL; group 6) or 10% FBS+ insulin (172 nM)+anti-ghrelin Ab (5 µg/mL)+UAG (5 µg/mL; group 7) for 7 days after induction of differentiation by treatment with 0.5 mM IBMX, 25 mM DEX, and 861 nM insulin for 3 days**. (B)** WB analysis of GHSR1a and GPR39 along adipogenesis. Data are mean± S.E.M. of three independent experiments (*P<0.05 versus control values).

Preproghrelin, PC1/3, and MBOAT4 expression in WAT

Preproghrelin, PC1/3, and MBOAT4 were detected immunohistochemically in omental and subcutaneous WAT obtained from mice under normal chow (control; Fig. 2.7A). WB analysis comparing WAT obtained from mice under normal chow and HFD showed that preproghrelin expression was enhanced in subcutaneous WAT of HFD mice relative to WAT of control mice (~0.5-fold), although its expression was not altered in omental WAT of HFD mice (Fig. 2.7B). PC1/3 levels were enhanced in both omental and subcutaneous WAT of HFD mice (~1.5- and 0.6-fold respectively). MBOAT4 levels were also augmented in both omental and subcutaneous WAT of HFD mice (~0.8- and 0.4-fold respectively; Fig. 2.7B).

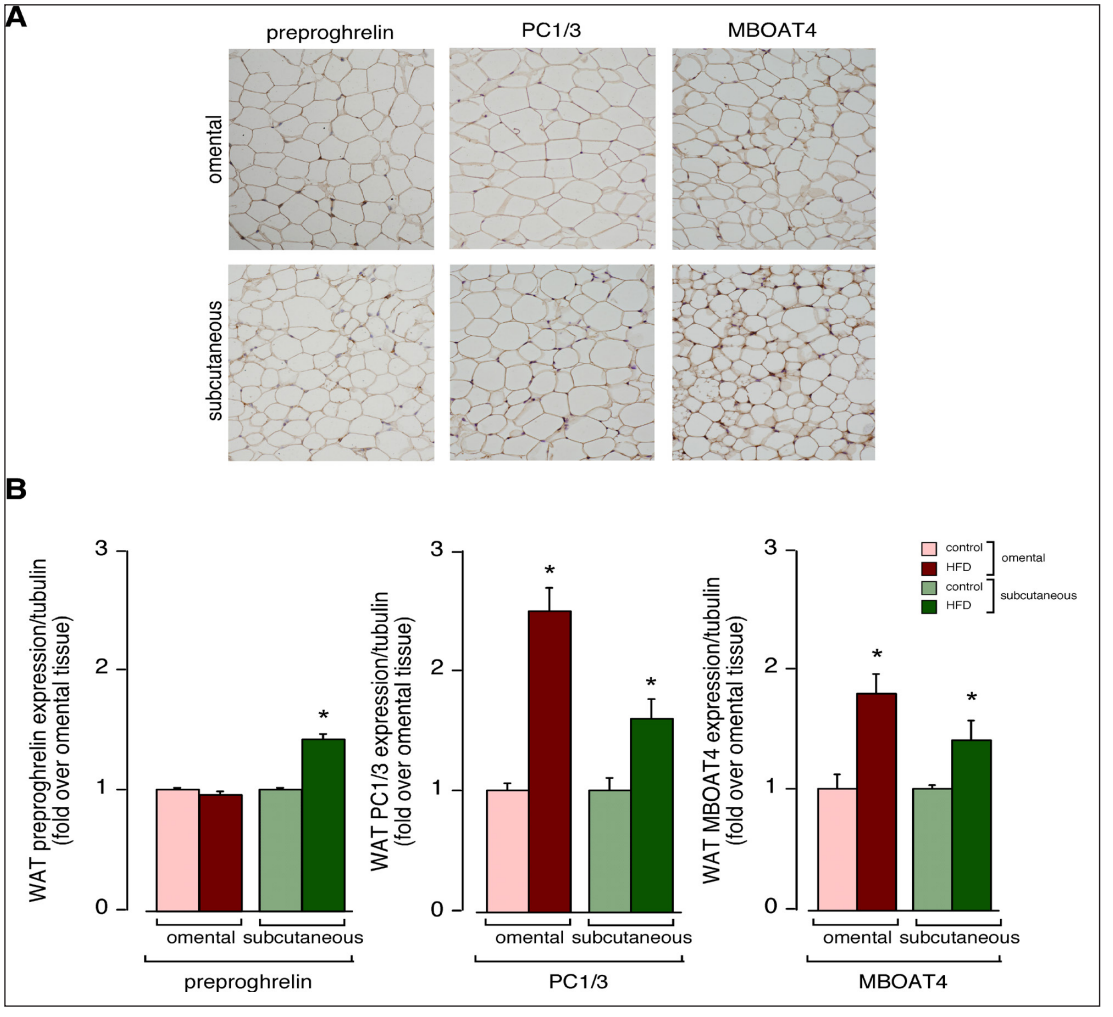

Fig. 2.7. Detection of preproghrelin and its derived enzymes in WAT
(A) Immunohistochemical analysis of preproghrelin, PC1/3, and MBOAT4 in omental and subcutaneous WAT obtained from control mice (objective magnification 20x). **(B)** WB analysis of preproghrelin, PC1/3, and MBOAT4 in omental and subcutaneous WAT obtained from control and HFD mice (n=10 per group). Data are mean± S.E.M. *P<0.05 versus control values.

CHAPTER 3

THE OBESTATIN/GPR39 SYSTEM IS UP-REGULATED BY MUSCLE INJURY AND FUNCTIONS AS AN AUTOCRINE REGENERATIVE SYSTEM

The Obestatin/GPR39 system is expressed in adult skeletal muscle

The expression of the obestatin/ GPR39 system was detected in adult gastrocnemius skeletal muscle from male *ad libitum* rats by IHC (Fig. 3.1.1 and 3.1.4, respectively). No immunostaining was found when obestatin or GPR39 antibodies were preadsorbed with homologous peptides (Fig. 3.1.2 and 3.1.5, respectively). In contrast, immunostaining was observed when obestatin antibody was preadsorbed with ghrelin peptide (Fig. 3.1.3). A comparative study with WB analysis demonstrated moderate obestatin expression in the gastrocnemius when compared with the stomach (~0.4-fold; Fig. 3.1, *right panel*). In contrast, higher GPR39 expression in the gastrocnemius than in the stomach was detected (~1.4-fold).

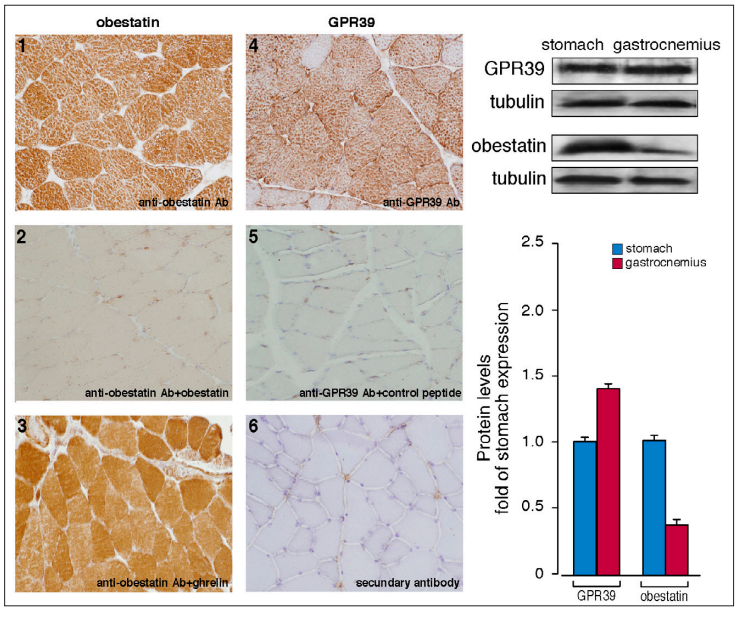

Fig. 3.1 Expression of obestatin and GPR39 in muscle and stomach. (Left panel) Immunohistochemical detection of obestatin (1.1) and GPR39 (1.4) in gastrocnemius muscle (objective magnification 20x). Preadsorption controls were performed, applying the primary antibody plus obestatin (1.2), ghrelin (1.3), or GPR39 control peptide (1.5) (10 nmol/mL per control peptide) to positive samples. Immunohistochemistry was also performed in the absence of primary antibody (1.6). **(Right panel)** WB analysis of obestatin and GPR39 of extracts from stomach and gastrocnemius muscle of control rats (n=5). Results were expressed as a -fold of protein levels in the stomach.

Obestatin/GPR39 system is up-regulated in skeletal muscle upon CTX injury

To examine the obestatin/GPR39 regulation in a model of skeletal muscle injury and regeneration, CTX solution (10 µM CTX; 2 µl/g body weight)[1] or an equal volume of PBS was injected into the gastrocnemius muscle. Tissues were analyzed at 6, 24, 48, and 72 h after treatment (n=5 at each time point). As shown in Fig. 3.2A WB analysis revealed that the maximal expression of preproghrelin (~4.5- fold), obestatin (~1.7-fold), and GPR39 (~2.1-fold) occurred at 24 h after CTX treatment. Maximal protein expression of the myogenic nuclear factors MyoD (~2.9-fold) and myogenin (~2.4-fold) paralleled with the expression of preproghrelin, obestatin, and GPR39 at the 24 h time point (Fig. 3.2A, *left panel*). Immunohistochemical analysis of obestatin, GPR39, MyoD, and myogenin was also performed at the 24 h time point (Fig. 3.2B.3–3.2B.6). The strongest signal for both obestatin (Fig. 3.2.3) and GPR39 (Fig. 3.2.4) occurred in damaged myofibers (Fig. 3.2.5 and 3.2.6).

1. Zeng, L. et al. Insulin-like 6 is induced by muscle injury and functions as a regenerative factor. *J. Biol. Chem.* 3010; 285: 36060-9.

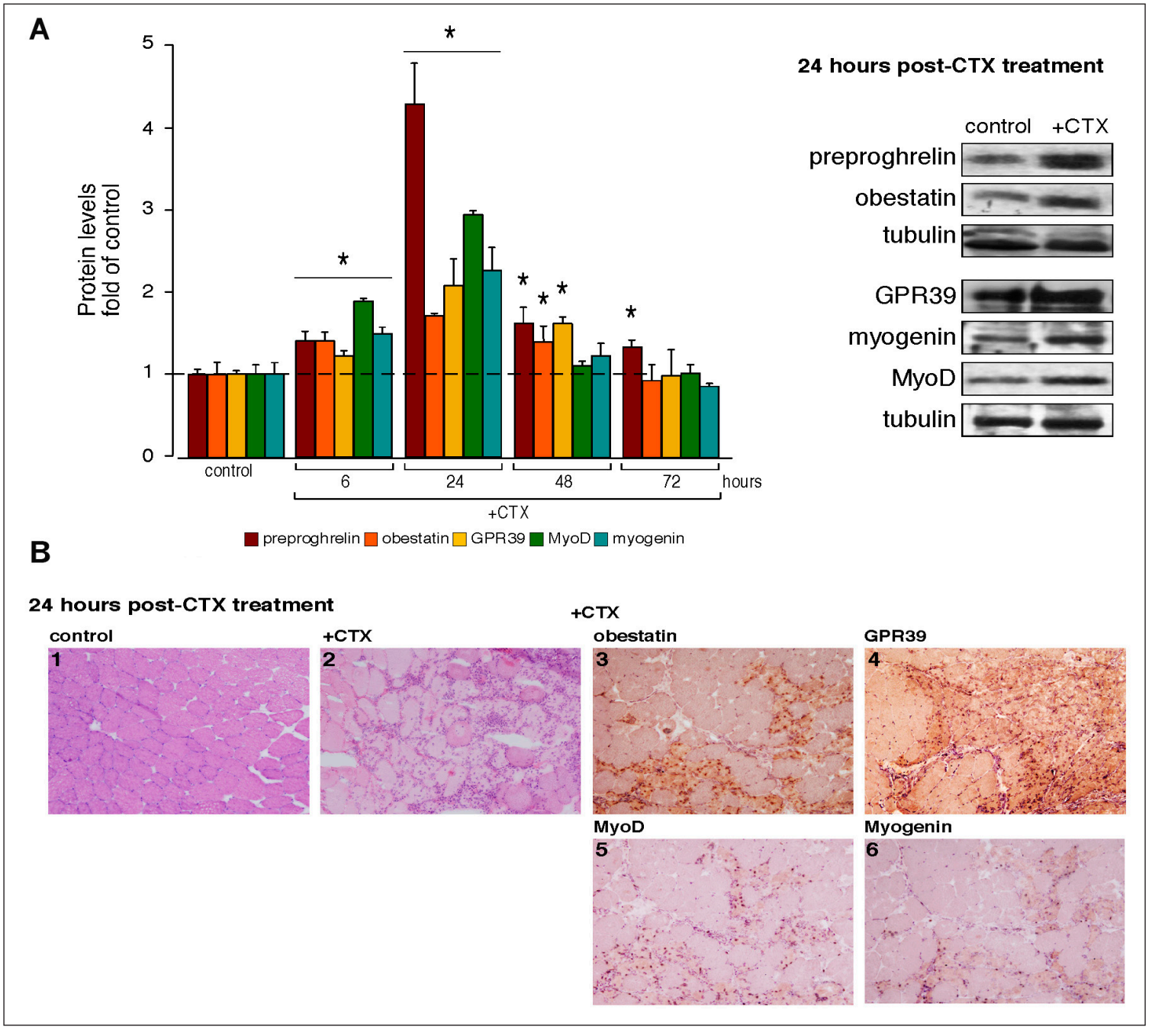

Fig.3.2 (A) *Left panel:* Relative protein expression of preproghrelin, obestatin, GPR39, MyoD, and myogenin in CTX- or PBS-injected gastrocnemius muscle was assessed at the indicated time points by WB (n = 5 per group and time point). Protein expression was expressed as a -fold over PBS control muscle**.** *Right panel:* Representative WB images of gastrocnemius muscle sections 24 h after PBS or CTX injection. **(B).** Representative images of gastrocnemius muscle sections 24 h after PBS or CTX injection: hematoxylin/eosin (2.1, control, and 2.2, +CTX); immunohistochemical detection of obestatin, GPR39, MyoD, and myogenin after CTX injection (2.3, 2.4, 2.5, and 2.6, respectively; objective magnification 20x). WB are representative of three independent experiments. Data were expressed as the mean ±S.E. *, P <0.05 versus control values.

Obestatin is up-regulated during myogenic differentiation *in vitro*

To elucidate the role of this system in myogenesis, an *in vitro* cell culture model that closely recapitulates the formation and maintenance of skeletal muscle was utilized: the rat skeletal muscle L6 myoblasts (subclone E9, L6E9 cells)[2]. Upon reaching confluence, serum was withdrawn to induce the differentiation of L6E9 cells from proliferative myoblasts into terminally differentiated myotubes to permit fusion and form multinucleated cells that express markers of differentiated skeletal muscle. As shown in Fig.3.3, L6E9 myotubes, obtained during a 6-day differentiation period, showed a stronger obestatin expression when compared with that observed in L6E9 myoblast cells (Fig. 3.3.3 when compared with Fig. 3.3.1). In contrast, GPR39 was detected in L6E9 in both myoblast and myotube cells (Fig. 3.3.2 and 3.3.4, respectively).

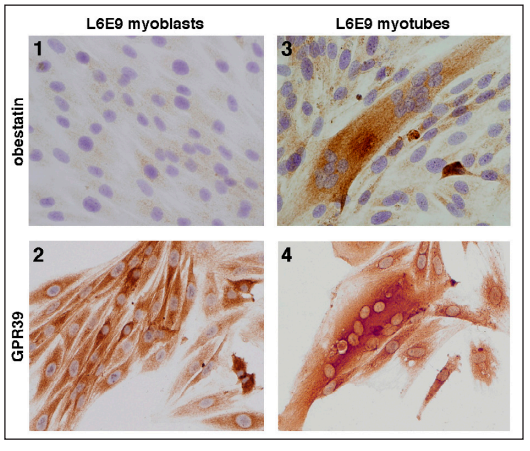

Fig.3.3 Immunocytochemical detection of obestatin and GPR39 in myoblast and myotube L6E9 cells (objective magnification 40x)

These results led us to focus on preproghrelin expression during myogenesis as a source of obestatin. Preproghrelin expression was examined at the mRNA and protein levels by real-time PCR and WB, respectively, from samples taken at the proliferative state and throughout differentiation. Within 6 h of differentiation, the preproghrelin mRNA levels experienced a rapid increase (~1.6-fold; Fig. 3.4A), which subsequently returned to basal level values by 48 h of induction. Transcript expression increased again from 72 h, reaching maximal levels at 144 h after induction of differentiation (~2.3-fold). As shown in Fig. 3.4B, WB analysis confirmed the dynamic regulation of preproghrelin expression at the time of differentiation into myotubes, with a rapid increase at the 6 h time point, reaching a maximum at 24 h after induction of differentiation (~4.4- fold) concomitant with the rise of preproghrelin mRNA expression. Intriguingly, preproghrelin protein expression began to decrease 48 h after induction of differentiation (~2.1-fold at 144 h), remaining at sustained but reduced levels during terminal differentiation; however, the levels remained higher than in myoblast cells (Fig. 3.4B). Obestatin peptide expression closely paralleled the expression of preproghrelin (~4.5- and 3.0-fold at 24 and 144 h, respectively). GPR39 protein expression showed maximal expression levels at two time points: 6 and 144 h (~2.9- and 2.6-fold, respectively), concomitant with maximum expression levels of the myogenic transcription factor myogenin (Fig. 3.4B). The expression of MHC reached maximal levels 72 h after induction, which marked the progression of terminal differentiation (Fig. 3.4B).

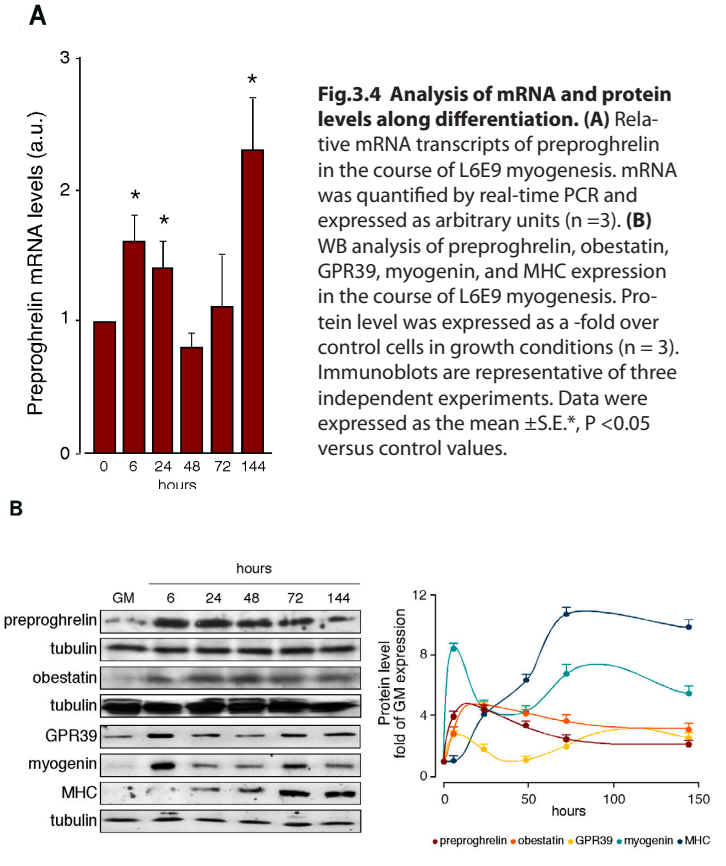

Fig.3.4 Analysis of mRNA and protein levels along differentiation. (A) Relative mRNA transcripts of preproghrelin in the course of L6E9 myogenesis. mRNA was quantified by real-time PCR and expressed as arbitrary units (n =3). **(B)** WB analysis of preproghrelin, obestatin, GPR39, myogenin, and MHC expression in the course of L6E9 myogenesis. Protein level was expressed as a -fold over control cells in growth conditions (n = 3). Immunoblots are representative of three independent experiments. Data were expressed as the mean ±S.E.*, P <0.05 versus control values.

2. Nadal-Ginard, B. Commitment, fusion, and biochemical differentiation of a myogenic cell line in the absence of DNA synthesis. *Cell*. 1978; 15: 855-64.

Autocrine/Paracrine role of obestatin on myogenesis *in vitro*

The effect of acute obestatin deficiency was first determined by preproghrelin knock-down by means of siRNA prior to induction of myogenic differentiation. Under these conditions, the constructs decreased preproghrelin level by 57±2% relative to siRNA control (si-control; Fig. 3.5A) during a 96 h differentiation period. Silencing of preproghrelin (si-preproghrelin) decreased myogenin and MHC expression levels with respect to si-control (46±6 and 33±7%, respectively; Fig. 3.5A). Correspondingly, the cell cycle arrest protein p21 expression was decreased in the presence of si-preproghrelin (26 ± 2%; Fig. 3.5A). The individual autocrine role of obestatin was tested using a neutralizing obestatin antibody (Ab)[3]. L6E9 cells were maintained in GM and DM, anti-obestatin Ab (5 µg/mL) in DM, obestatin + anti- obestatin Ab (1:1, w/w) in DM, or pre-immune IgG (5 µg/mL) in DM during a 6 day differentiation period in which DM plus reactive were replaced every 24 h. As shown in Fig. 3.5B, anti- obestatin Ab reduced myogenin and MHC expression levels with respect to standard differentiation conditions (40±3 % and 89±2%, respectively), whereas obestatin + anti-obestatin Ab or pre-immune IgG treatments, used as Ab controls, did not affect the differentiation marker levels. Simultaneously, Akt phosphorylation at the C-terminal hydrophobic motif (Ser- 473) (HM(S-473); p-Akt(S-473)) and p38 phosphorylation at T-182 (p-p38(T-182)) showed significant decrease in the presence of the obestatin neutralizing Ab (60±2 and 30±3%, respectively; Fig. 3.5B). Furthermore, the presence of the anti- obestatin Ab reduced p21 expression (32±1%; Fig. 3.5B).

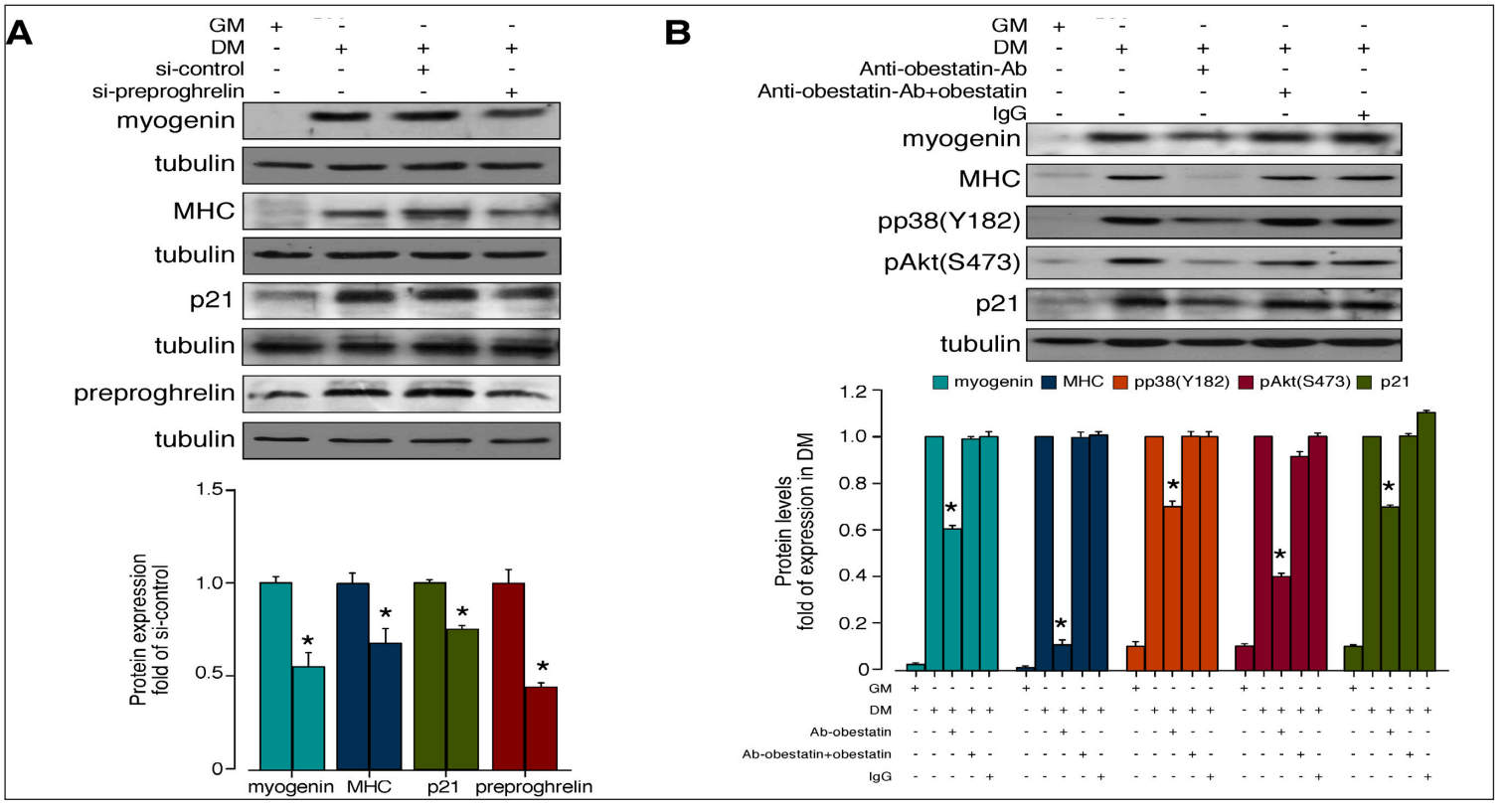

Fig 3.5. Effect of siRNA depletion of preproghrelin on myogenesis. (A) L6E9 cells were transfected with preproghrelin siRNA prior to induction of myogenesis for 96 h. Expression of myogenin, MHC, p21, and preproghrelin was denoted as a -fold of the respective levels in control siRNA-transfected cells (n=3). **(B)** Differentiating L6E9 cells were maintained in DM, DM supplemented with anti-obestatin antibody (5 µg/mL; anti-obestatin Ab), obestatin + anti-obestatin Ab (1:1, w/w), or pre-immune IgG (5 µg/mL) for 6 days. Expression of p-p38(T-182), p-Akt(S-473), or p21 is expressed as a -fold of respective expressions in DM control (n = 6). Data were expressed as the mean ± S.E. *, $p < 0.05$ *versus* control values.

3. Gurriarán-Rodríguez, U. et al. Obestatin as a regulator of adipocyte metabolism and adipogenesis. *J. Cell. Mol. Med.* 2011; 15: 1927–40.

GPR39 regulates myogenesis *in vitro*

First, the effect of acute GPR39 deficiency on obestatin signalling was determined by treatment of L6E9 myoblast cells with siRNA (si-GPR39). Under these conditions, the constructs decreased GPR39 expression by 69±2% (Fig. 3.6A). In the presence of si-control, obestatin-activated Akt(S-473) and p38(T-182) phosphorylation was identical to levels observed with un-transfected cells. Silencing of GPR39 decreased subsequent p-Akt(S-473) and p-p38(T-182) with respect to si-control by 61±2 % and 52±1% with treatment of obestatin (5 nM, 10 min; Fig. 3.6A), respectively. Second, the effect of acute GPR39 deficiency on myogenesis was further evaluated on myogenic differentiation. Under these conditions, the constructs decreased GPR39 expression by 50±3% (Fig. 3.6B) during a 96 h differentiation period. The GPR39 knock-down decreased the expression levels of myogenin and MHC by 40±5 % and 41±4% with respect to si-control, respectively (Fig. 3.6B).

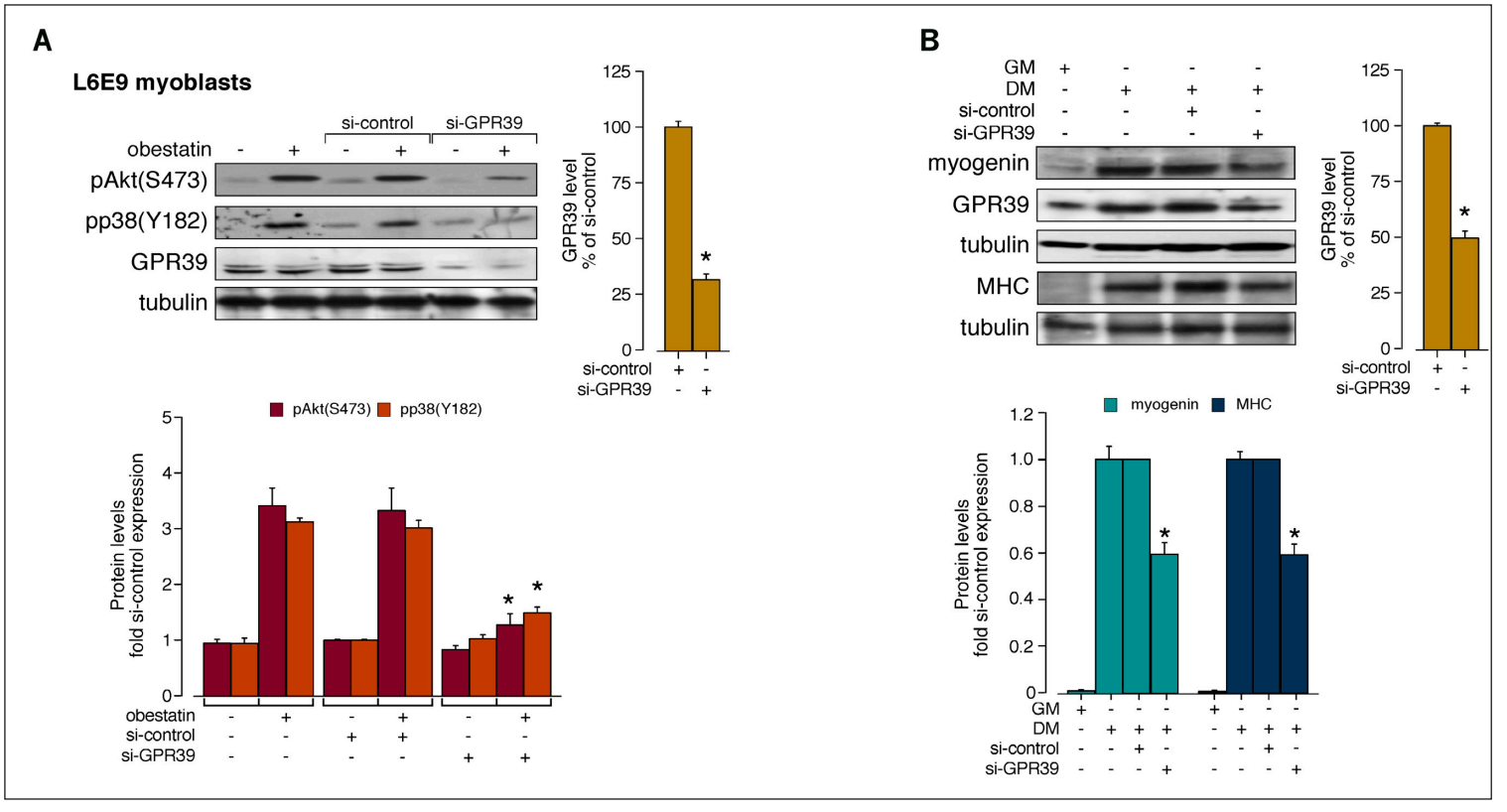

Fig. 3.6 **Effect of GPR39 knock-down by siRNA (A)** On obestatin-activated p-Akt(S-473) and p-p38(T-182) in L6E9 myoblast cells (5 nM, 5 min). GPR39 was expressed as a -fold of its level to control siRNA-transfected cells (*n* =3). Activation of Akt and p38 was expressed relative to control siRNA-transfected cells. **(B)** Effect of siRNA depletion of GPR39 on myogenesis. L6E9 cells were transfected with GPR39 siRNA prior to induction of myogenesis for 96 h. Expression of myogenin and MHC was expressed as a -fold of the respective levels to control siRNA-transfected cells (*n*= 3). Immunoblots are representative of three independent experiments. Data were expressed as the mean ± S.E. *, $p < 0.05$ *versus* control values.

Obestatin enhances myogenic proliferation *in vitro*

To ascertain the influence of obestatin on myogenesis, the effect of obestatin (0.001–100 nM) on intracellular targets leading to either proliferation (ERK1/2) or differentiation (p38 and Akt) was first assayed in L6E9 myoblasts. P-Akt (S-473), p-p38 (T-182), and p-ERK1/2 (W-202/T-204) were observed using different concentrations of obestatin (0.001–100 nM), and the level of phosphorylation peaked at 5 nM in L6E9 myoblasts (data not shown). Fig. 3.7A shows that myoblast treatment with obestatin (5 nM) elicited a time-dependent increase in p-Akt(S-473), p-ERK1/2 (W-202/T-204), and p-p38 (T-182) protein levels, which reached a maximum at 10 min. Mitogenic action was then explored by dose-effect experiments performed on myoblasts treated with a range of obestatin concentrations (0.01– 100 nM) in GM (proliferating conditions; Fig. 3.7B). Maximal effect in the cell number was observed at 5 nM obestatin (~2.2- fold). This mitogenic effect was compared with that induced by ghrelin, under the same range of concentrations (0.01–100 nM) in GM. As shown in Fig. 3.7C, ghrelin showed proliferative capability in L6E9 myoblast cells, although its effect was lower than that of obestatin for all doses tested.

Obestatin enhances migration/invasion *in vitro*

We performed invasion/migration assays on L6E9 myoblast cells supplemented with obestatin (5 nM). Confluent monolayers of cells were physically wounded with a scratch and allowed to migrate to heal for 8 and 24 h, eliminating the possibility of proliferation accounting for the wound closure. As shown in Fig. 3.8, at 8 h after initial scratch, obestatin-treated cells exhibited an ~53% increase in the invasion/migration capability when compared with the control. At 24 h after scratch, the increase was ~21% for obestatin-treated cells when compared with control.

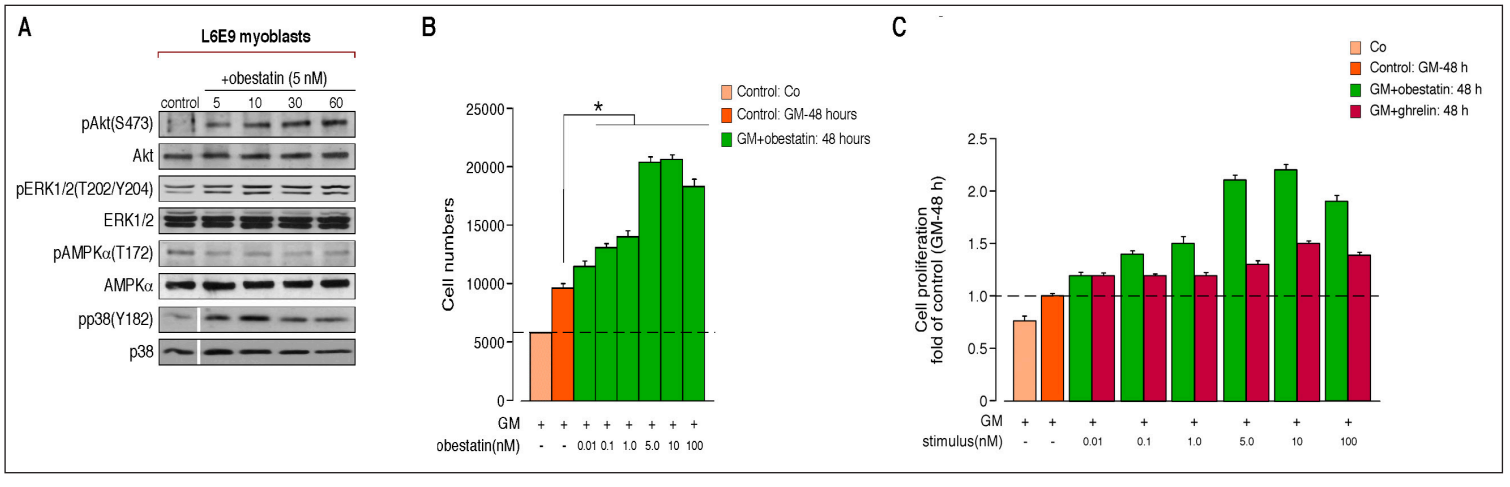

Fig. 3.7 (A) Time course of the effect of obestatin (5 nM) in L6E9 myoblast cells on p-Akt(S-473), p-ERK1/2(W-202/T-204), p-AMPK(W-172), and p-p38(T-182) ($n = 3$). AMPK, AMP-activated protein kinase. **(B)** Dose-response effect of obestatin (0.01–100 nM) on L6E9 myoblast cell proliferation (48 h, $n = 5$). **(C)** Dose-response effect of obestatin/ghrelin (0.01–100 nM) on L6E9 myoblast cell proliferation (48 h, $n = 5$). *Co*: cells initially seeded. *Control*: cells maintained 48 h in GM. Immunoblots are representative of three independent experiments.

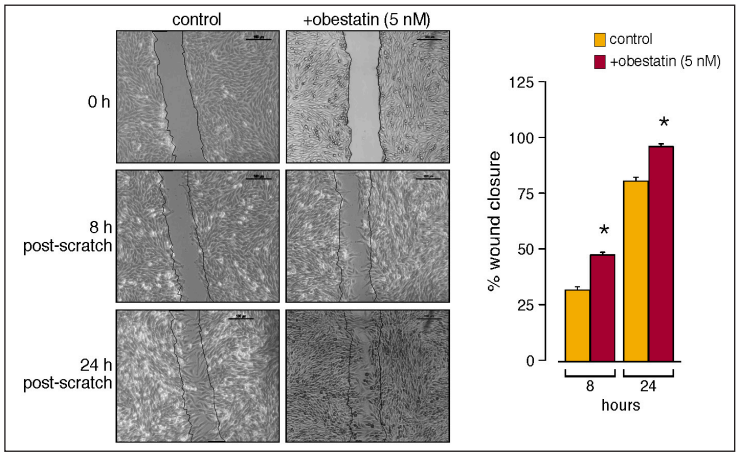

Fig.3.8 Evaluation of invasion/migration obestatin role: (Left panel) L6E9 myoblast cells at 100% confluence were wounded with a sterile pipette tip to remove cells. Photographs were taken (objective magnification 10x) at 0, 8, and 24 h after injury. **(Right panel)** wound closure was evaluated using the equation described in the chapter of "Material and Methods." For these panels, data were expressed as the mean± S.E.

Obestatin enhances myogenic differentiation *in vitro*

To assess the activity of obestatin as a promoter of the differentiation process, L6E9 cells were switched to DM supplemented with obestatin at a range of concentrations (0.001–100nM) for 7 days. As shown in Fig. 3.9A, the protein levels of myogenin and MHC, as detected by immunoblot, were dose-dependent and up-regulated with the maximal effect at 5 nM for both differentiation markers (~1.7- and 1.6-fold, respectively). The possibility that obestatin accelerates differentiation was also investigated (DM + 5 nM obestatin for 7 days). WB analyses revealed normal kinetics with enhanced protein level of both myogenin and MHC when compared with control cells (DM for 7 days; supplemental Fig. 3.9B). To confirm the observation that obestatin activates the differentiation program, the ability of this peptide to activate the differentiation program under GM (GM + 5 nM obestatin) was evaluated in L6E9 myoblast cells for 7 days. The protein levels of myogenin and MHC, as detected by immunoblot, were significantly increased when compared with control cells in GM (~4.2- and 14-fold, respectively; Fig. 3.9C). The expression for both differentiation markers was induced to similar levels upon 7 days of treatment with ghrelin (5 nM; supplemental Fig. 3.9C).

Fig.3.9 Obestatin as a enhancer of myogenesis.(A) Dose-response effect of obestatin (0.01–100 nM) on differentiating L6E9 cells for 7 days (*n*=6). Levels of myogenin and MHC were represented as a -fold of respective expression in GM. **(B)** Time course along differentiation adding obestatin 5nM on differentiating L6E9 cells for 7 days (*n*=6). Levels of myogenin and MHC were represented as a -fold of respective expression in GM. **(C)** Effect of obestatin on myogenic differentiation in GM conditions on L6E9 cells for 7 days (*n*=6). Levels of myogenin and MHC were represented as a -fold of respective expression in GM without obestatin.

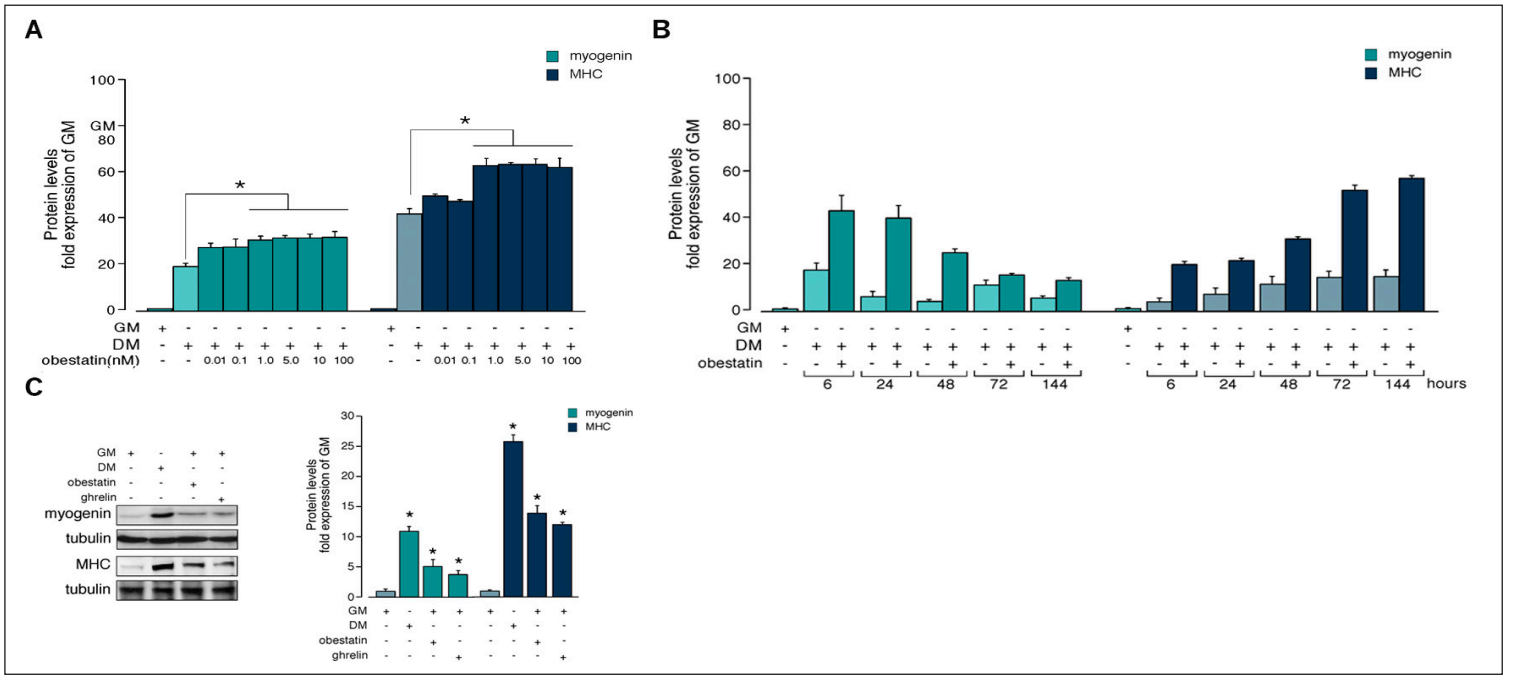

These results were confirmed by quantifying the differentiation grade by immuno- fluorescence. After 7 days, obestatin-treated cells (DM + 5 nM obestatin) increased by ~250% in myotube number when compared with control cells (DM; Fig. 3.10A). Moreover, myotubes were grouped into two categories, those with 2–3 nuclei and those with 4 or more nuclei[4]. As shown in Fig. 3.10B, ~22% of control myotubes contained ≥4 nuclei, *versus* ~67% of obestatin-treated cells (DM +5 nM obestatin). This effect represents an increase of ~3.4-fold respect to control cells (DM).

Obestatin regulates myogenic and angiogenic markers *in vivo* with an hypertrophic effect

Based on the short half-life of this peptide (~22 min), osmotic mini-pumps were selected for *in vivo* obestatin administration[5]. Male rats received a 72 h continuous subcutaneous infusion of obestatin (300 nmol/kg of body weight/24 h), and dissected gastrocnemius and soleus tissues were processed for WB analysis. Levels of Pax7, Myf5, MyoD, myogenin, Myf6, and MHC were up-regulated in gastrocnemius and soleus muscle tissues from obestatin-treated rats when compared with control tissues (Fig. 3.11A, *left panel*). Pax7 increased expression was demonstrated also by IF, showing a pronounced enhanced expression after obestatin infusion (Fig. 3.11A, *right panel*). Moreover, obestatin treatment resulted in a significant up-regulation of the VEGF and VEGF-R2 (VEGF receptor) expression in both gastrocnemius and soleus muscle when compared with controls (Fig. 3.11B). Conversely, the plateled endothelial growth factor (PEDF) expression level was significantly down-regulated in gastrocnemius and soleus muscle under obestatin treatment (Fig. 3.11B).

It is noteworthy that after 72 h of infusion, a significant increase in myofiber diameters was observed in gastrocnemius muscle (Fig. 3.12). A minor effect was observed in the soleus myofiber area (Fig. 3.12).

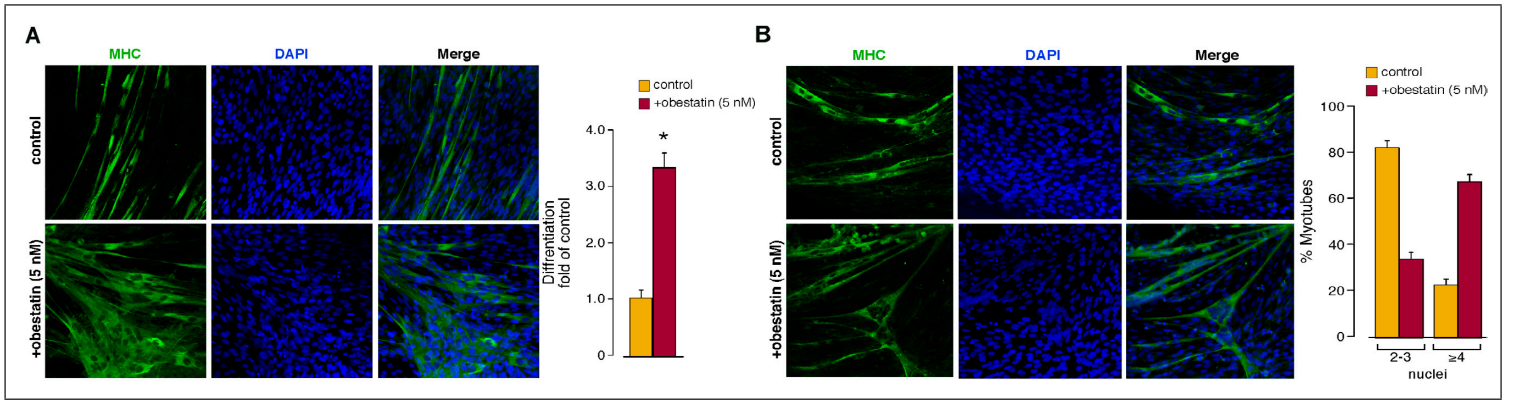

Fig. 3.10 IF analysis of obestatin as a myogenic enhancer: (A) *Left panel* immunofluorescence detection of MHC and DAPI (objective magnification 20x) in L6E9 myotube cells under DM (control) or DM + obestatin (5 nM) at the 7-day point after stimulation. *Right panel,* the differentiation grade was evaluated based on the number of MHC-positive cells above total nuclei and expressed as a -fold of control. **(B)** Representative images used to determined the number of nuclei within individual myotubes (at least two nuclei) in L6E9 myotube cells under DM (control) or DM + obestatin (5 nM) at the 6-day point after stimulation (*left panel*, objective magnification 20x). Myotubes were grouped into two categories, and the percentage of myotubes in each category was determined (*right panel*). Data were expressed as the mean ± S.E. as described under "Experimental Procedures." *, $p < 0.05$ *versus* control values.

4. Horsley, V. et al. Regulation of the growth of multinucleated muscle cells by an NFATC2-dependent pathway. *J. Cell Biol.* 2001; 153: 329-38.

5. Zizzari, P. et al. Obestatin partially affects ghrelin stimulation of food intake and growth hormone secretion in rodents. *Endocrinology*. 2007; 148: 1648-53.

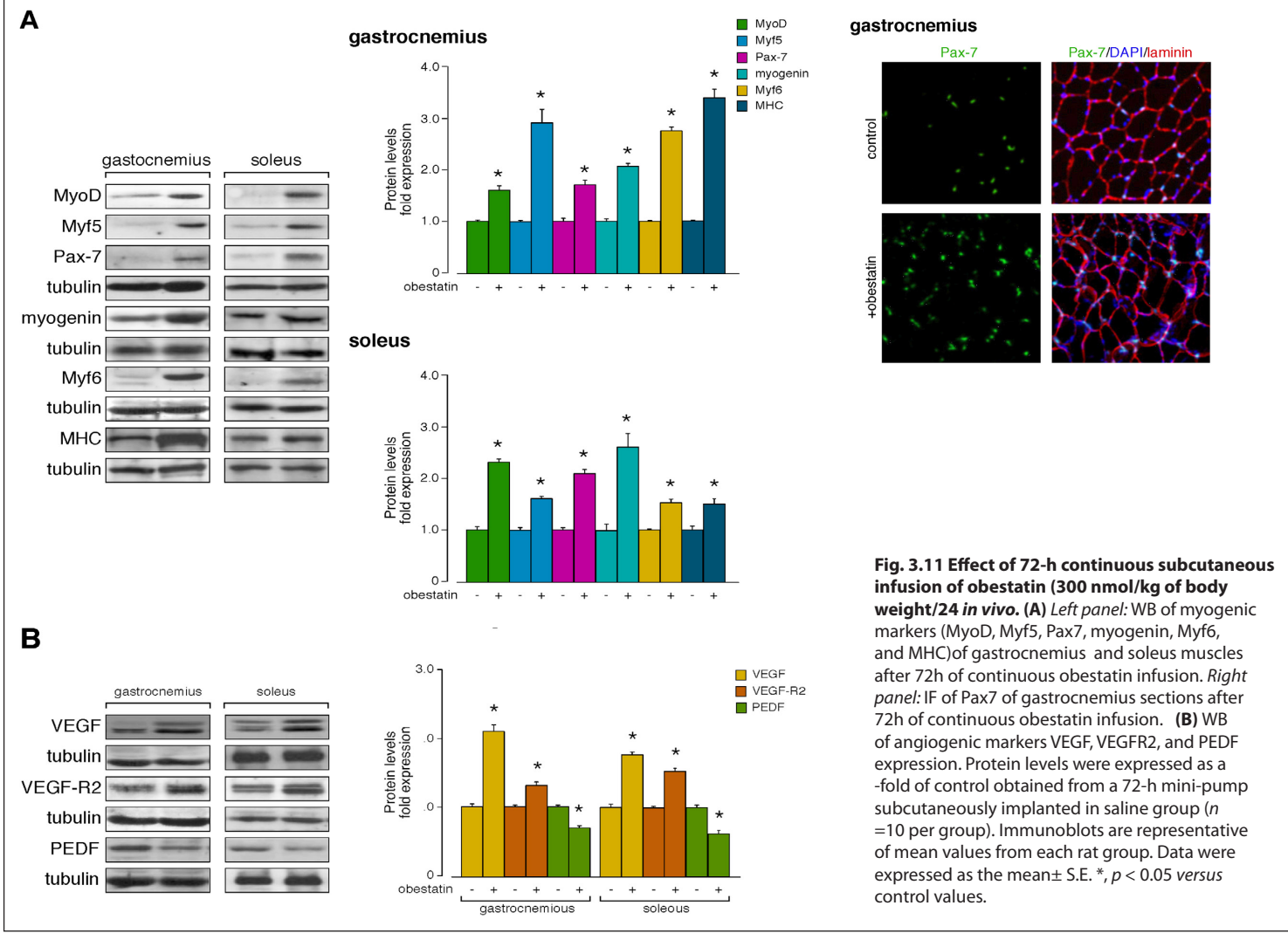

Fig. 3.11 Effect of 72-h continuous subcutaneous infusion of obestatin (300 nmol/kg of body weight/24 *in vivo*. **(A)** *Left panel:* WB of myogenic markers (MyoD, Myf5, Pax7, myogenin, Myf6, and MHC)of gastrocnemius and soleus muscles after 72h of continuous obestatin infusion. *Right panel:* IF of Pax7 of gastrocnemius sections after 72h of continuous obestatin infusion. **(B)** WB of angiogenic markers VEGF, VEGFR2, and PEDF expression. Protein levels were expressed as a -fold of control obtained from a 72-h mini-pump subcutaneously implanted in saline group (*n* =10 per group). Immunoblots are representative of mean values from each rat group. Data were expressed as the mean± S.E. *, $p < 0.05$ *versus* control values.

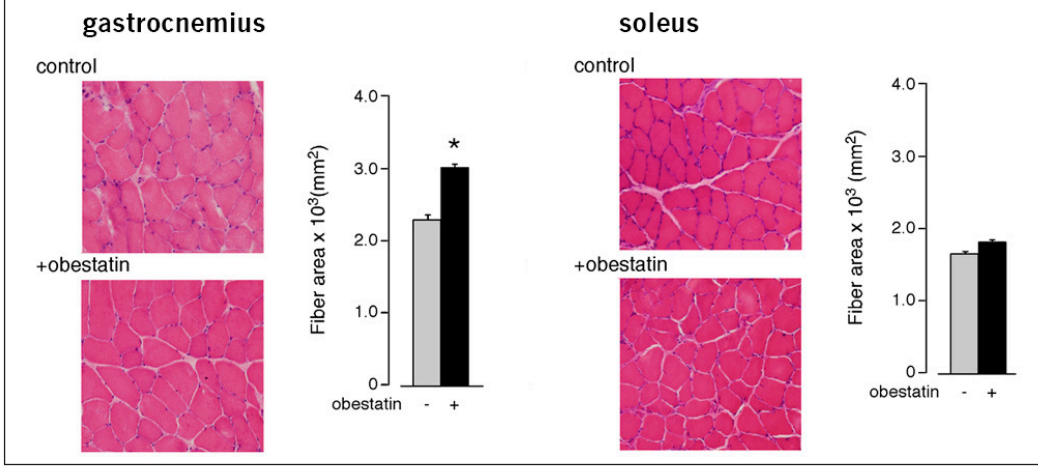

Fig.3.12 Hematoxylin/eosin-stained myofiber cross-section area of gastrocnemius and soleus. Sections are representative of the mean value of total cross-section area. Data were expressed as the mean± S.E. *, $p < 0.05$ *versus* control values.

CHAPTER 4

OBESTATIN AS A REGULATOR OF MYOTUBES AND MUSCLE METABOLISM

Obestatin activates Akt downstream targets and inactivates AMPK in L6E9 myotube cells and skeletal muscle tissue

As previously described in L6E9 myoblast cells (Fig.3.7) the kinetic of Akt activation in response to obestatin (5 nM) in L6E9 myotube cells showed significant pAkt(S473) augment at 10 min post-treatment reaching a maximum at 30min being sustained by 60 min (Fig. 4.1A). Parallel to Akt activation, obestatin triggered the phosphorylation of a broad range of Akt downstream substrates: GSK3 α/β (S21/9), AS160 (T642) and S6K1(T384) (Fig. 4.1B and D). Importantly, dephosphorylation of p-AMPKα (T172) (Fig. 4.1A) and its downstream substrate ACC (S79) was observed in response to obestatin (Fig. 4.1C).

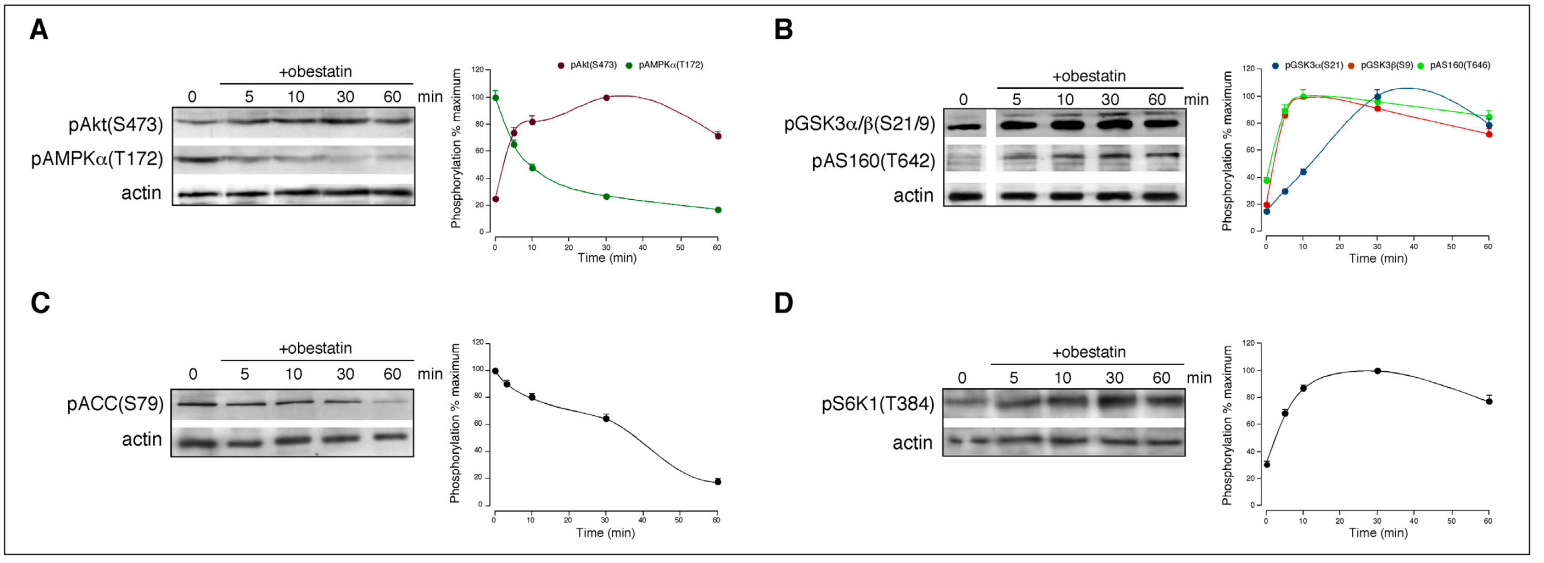

Fig. 4.1 Time-course of the effect of obestatin L6E9 myotubes: **(A)** p-Akt(S473) and p-AMPKα (T172); **(B)** p-GSK3 α/β (S21/9) and p-AS160(T642); **(C)** and p-ACC(S79) and **(D)** p-S6K1(T384) Phosphorylation was expressed as a percentage of the maximal phosphorylation obtained for each residue (n=3; mean± S.E.).

For *in vivo* obestatin administration, osmotic mini pumps were selected based on the short half-life of this peptide (~22 min)[1]. Male rats received a 24 h continuous *sc* infusion of obestatin (300 nmol/kg body weight/24 h) and dissected muscles were processed for WB analysis. Obestatin significantly activated at 24 h Akt, measured as p-Akt (S473), by 60% to basal phosphorylation in soleus and gastrocnemius muscles (Fig. 4.2A). p-AMPKα (T172) was decreased by 20% to basal phosphorylation in soleus with no effect in gastrocnemius (Fig. 4.2A). At 72 h continuous *sc* infusion of obestatin (300 nmol/kg body weight/24 h) increased p-Akt (S473) by 50% in soleus and more than 400% in gastrocnemius muscles over basal phosphorylation and decreased p-AMPKα (T172) by 50% in soleus and in gastrocnemius decreased almost to control levels(Fig. 4.2B). The divergence between 24 and 72 h might be explained by the stress generated by mini-pump implantation.

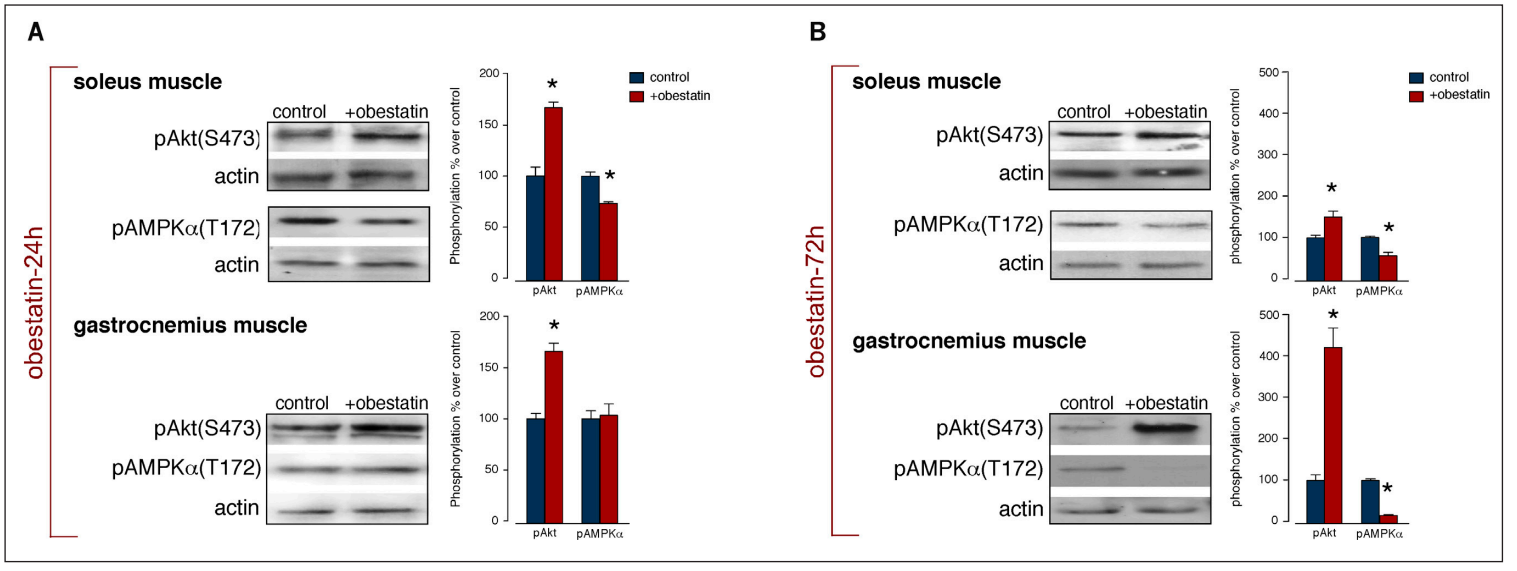

Fig. 4.2 Obestatin activates Akt phosphorylation and AMPK dephosphorylation in muscle. (A) Effect of 24 h continuous *sc* infusion of obestatin (300 nmol/kg body weight/24 h; n=10) on p-Akt(S473) and p-AMPKα (T172) from soleus and gastrocnemius muscles obtained from male rats. **(B)** Effect of 72 h continuous *sc* infusion of obestatin (300 nmol/kg body weight/24 h; n=10) on p-Akt(S473) and p-AMPKα (T172) from soleus and gastrocnemius muscles obtained from male rats. Phosphorylation was expressed as a percentage of control obtained from 24 h or 72 h mini pump *sc* implanted saline group (n=10; mean± S.E.). Asterisk (*) denotes P< 0.05 when comparing obestatin-treated group with untreated control group (saline).

1. Zizzari, P. et al. Obestatin partially affects ghrelin stimulation of food intake and growth hormone secretion in rodents. *Endocrinology*. 2007; 148: 1648-53.

Obestatin increases GLUT4 levels in plasma membranes and glucose uptake *in vitro* and *ex vivo*

The amplitude of Akt activation was evaluated on the basis of GLUT1 and GLUT4 translocation to plasma membrane in L6E9 myotubes cells. Acute treatment with obestatin (5 nM, 30 min) resulted in an increase in GLUT4 translocation to the plasma membrane by ~1.9-fold, this increase in GLUT4 translocation was equal to the one produced for the positive control insulin (172 nM, 30 min) (Fig. 4.3A). Intriguingly, there is not GLUT1 redistribution in response to obestatin (30 min) neither to insulin (172 nM, 30 min) in L6E9 myotubes (Fig. 4.3A). The divergence between GLUT4 and GLUT1 might be explained by the different roles on glucose uptake depending on the type of glucose transporter and the tissue expression. The effect of obestatin on DOGU was examined *in vitro* in L6E9 myotubes cells. Cells were incubated with different concentrations of obestatin (0.001–200 nM) for 30 min, resulting in a dose- dependent increase in DOGU with a maximal effect at 10 nM obestatin (~3.0-fold; Fig. 4.2C). Surprisingly insulin treatment (172 nM) caused an equal increase of DOGU in L6E9 myotubes cells (Fig. 4.3C). *Ex vivo* DOGU experiments with soleus and gastrocnemius muscles, showed after treatment (obestatin 172 nM and insulin 172nM both 30 min) an equal 50% increase in gastrocnemius muscle for both treatments over non-treated muscles. In the soleus case the increase with obestatin treatment was lower by a ~1.2-fold and with insulin was by ~1.5-fold. The divergence between soleus and gastrocnemius might be explained by the different type of fibers depending on the muscle and its different glucose metabolism.

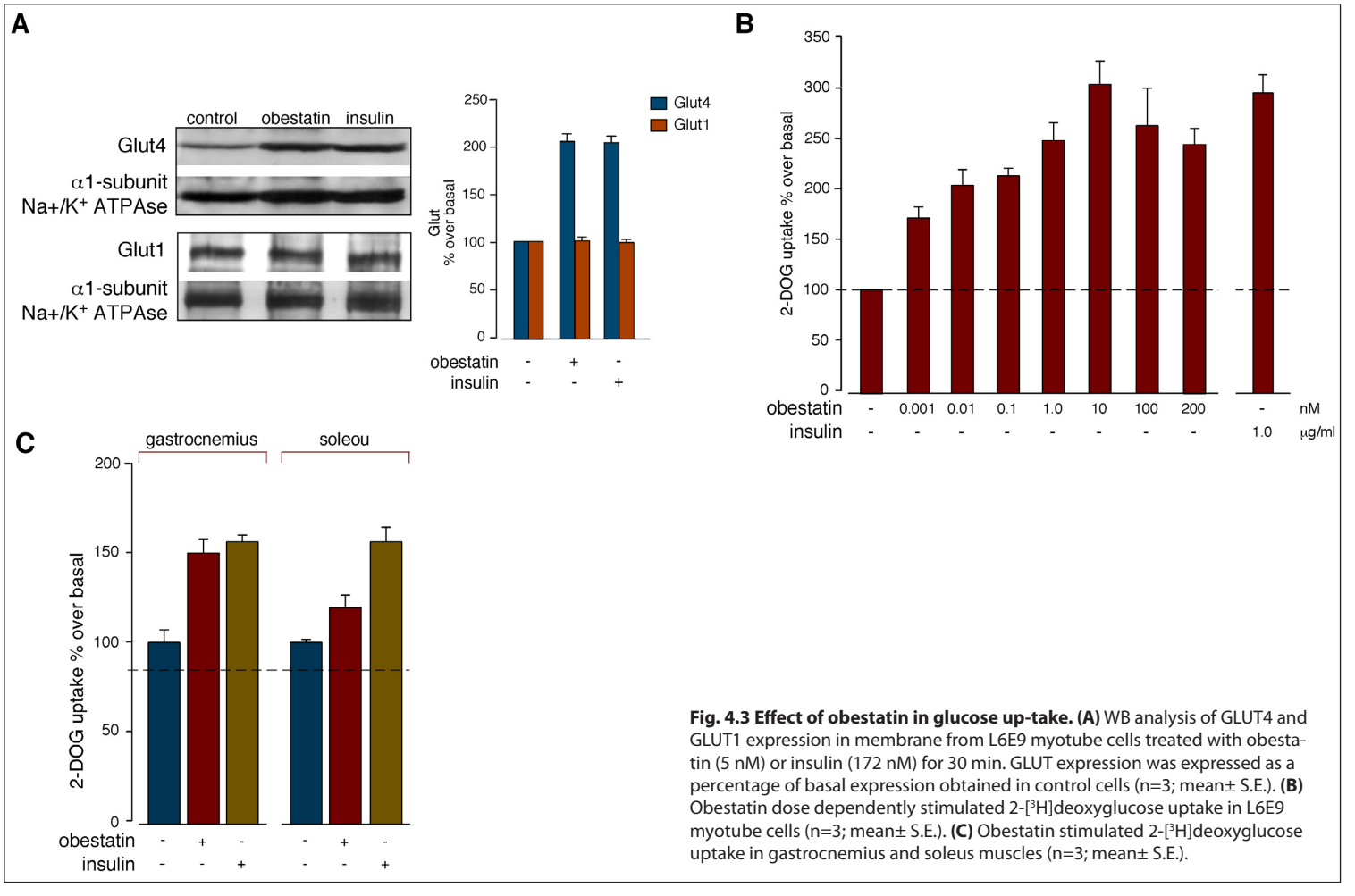

Fig. 4.3 Effect of obestatin in glucose up-take. (A) WB analysis of GLUT4 and GLUT1 expression in membrane from L6E9 myotube cells treated with obestatin (5 nM) or insulin (172 nM) for 30 min. GLUT expression was expressed as a percentage of basal expression obtained in control cells (n=3; mean± S.E.). **(B)** Obestatin dose dependently stimulated 2-[^{3}H]deoxyglucose uptake in L6E9 myotube cells (n=3; mean± S.E.). **(C)** Obestatin stimulated 2-[^{3}H]deoxyglucose uptake in gastrocnemius and soleus muscles (n=3; mean± S.E.).

CHAPTER 5

REPAIRING THE SKELETAL MUSCLE: REGENERATIVE POTENCTIAL OF THE OBESTATIN/GPR39 SYSTEM

Overexpression of the preproghrelin/GPR39 system *in vivo* enhances muscle regeneration

To investigate the role of the obestatin/GPR39 system in muscle regeneration *in vivo*, preproghrelin, and thus obestatin, was overexpressed by electroporation of a CMV-preproghrelin expression plasmid into TA muscles of 8 week-old mice. Freeze muscle injury was chosen because of the significantly reduced inflammatory response relative to other methods such as CTX injection. Changes in protein expression were analysed at 96 h post-injury, corresponding to the acute phase of regeneration, and at 168-h post-injury when satellite cells have returned to a quiescent stage. Histological analysis of muscles electroporated with pCMV6 revealed no regeneration deficit as compared to saline electroporation (Fig. 5.1A). In addition, immunostaining of cryosections of TA muscles 168 h following electroporation with the CMV plasmids exhibited overexpression levels of preproghrelin, GPR39 or both (*left panels* of Fig. 5.1B-D, respectively). TA muscles electroporated with CMV-preproghrelin exhibited an increase in protein expression of Pax7, MyoD, myogenin and eMHC (Fig. 5.1B) at 96 and 168 h time points. At the same times, overexpression of CMV-GPR39 resulted in an increased of these myogenic markers(Fig. 5.1C). Notably, TA muscles electroporated with both CMV-preproghrelin and CMV-GPR39 revealed a larger increase of Pax7, MyoD, myogenin and embryonic myosin heavy chain (eMHC) (Fig. 5.1D) at 96 and 168 h time points. Taken together, these results indicate that overexpression of preproghrelin and/or GPR39 enhance muscle regeneration, as evidenced by the increase of the expression of myogenic markers. Nonetheless, the electroporation conditions used also result in an injury to the muscle, raising the question of whether active regeneration is a direct consequence of the obestatina/GPR39 response.

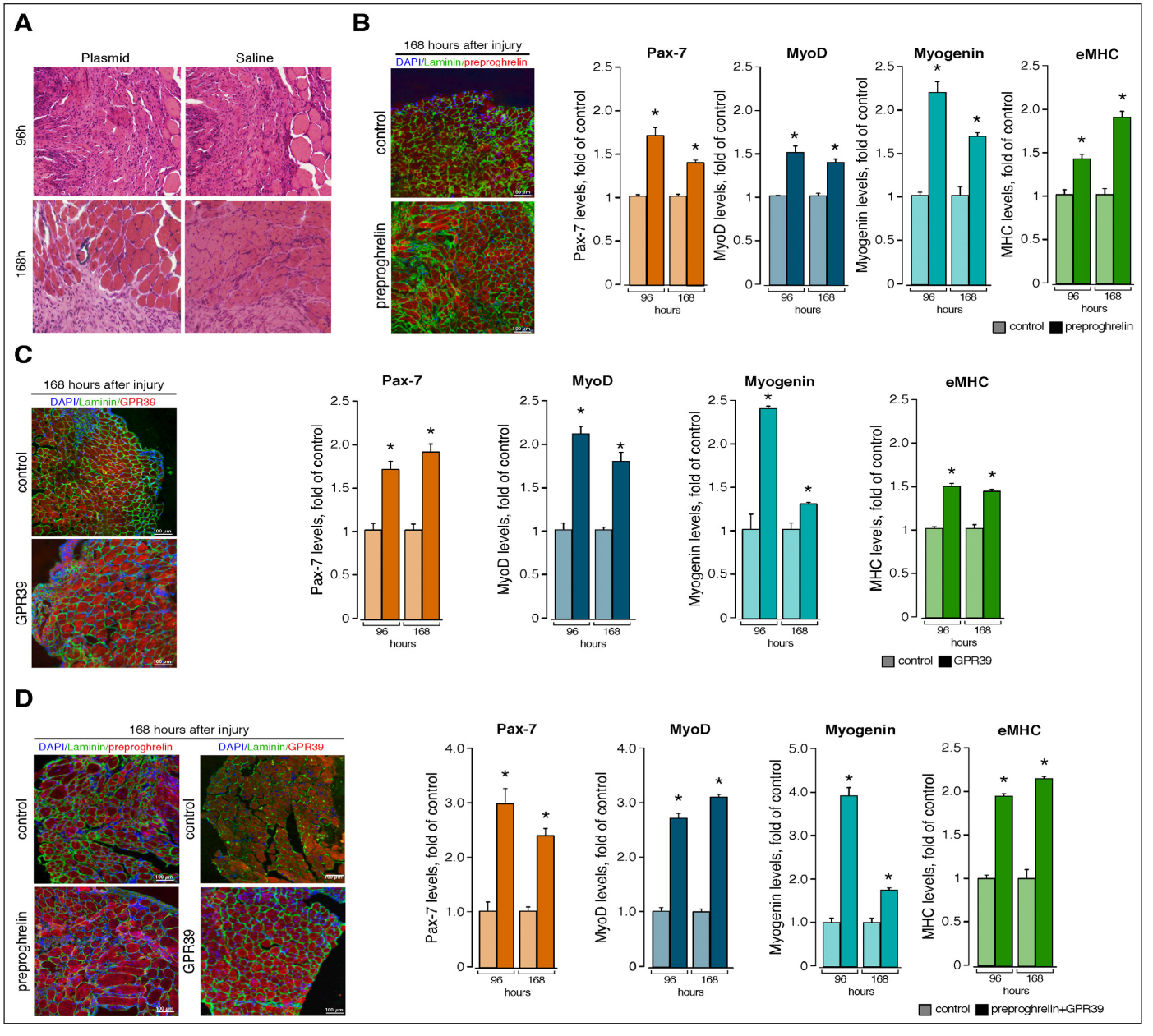

Fig. 5.1. Overexpression of preproghrelin/GPR39 in electroporated TA. **(A)** Representative H&E stained TA cross-sections at 96 h or168 h after freeze injury, comparing electroporated-TA with control CMV plasmid to TA under vehicle administration. **(B)** *Left panel*: immunostaining of cryosections of TA muscles 168 h following electroporation with the control or preproghrelin CMV plasmids demonstrating overexpression of preproghrelin at 168 h post-injury. *Right panel:* WB quantification of Pax7, MyoD, myogenin and eMHC expression in TA muscles electroporated with CMV-preproghrelin at 96 and 168 h post-injury. **(C)** *Left panel*: immunostaining of cryosections of TA muscles 168 h following electroporation with the control or GPR39 CMV plasmids demonstrating overexpression of GPR39 at 168 h post-injury. *Right panel:* WB quantification of Pax7, MyoD, myogenin and eMHC expression in TA muscles electroporated with CMV-GPR39 at 96 and 168 h post-injury. **(D)** *Left panel*: immunostaining of cryosections of TA muscles 168 h following electroporation with the control or preproghrelin and GPR39 CMV plasmids demonstrating overexpression of both preproghrelin and GPR39 at 168 h post-injury. *Right panel:* WB quantification of Pax7, MyoD, myogenin and eMHC expression in TA muscles electroporated with both CMV-preproghrelin and CMV-GPR39 at 96 and 168 h post-injury. Data were expressed as mean± S.E. (n=10 per time point). Asterisk (*) denotes P< 0.05 when comparing mice electroporated with CMV plasmid to CMV-preproghrelin, -GPR39 or –preproghrelin plus-GPR39.

Obestatin enhances muscle regeneration *in vivo*

To address whether the exogenous administration of obestatin is capable of stimulating productive regeneration, obestatin (300 nmol/kg body-weight) or vehicle was directly injected into TA of 2-month-old mice (n=35/group). Histological analysis revealed (Fig. 5.2A). WB analysis showed a significant increase, as compared to control, in the protein expression of Pax7, MyoD, myogenin eMHC for the time tested (Fig. 5.2A-D). To confirm eMHC up-regulation during muscle regeneration, IF analyses were performed on cryosections of freeze-injured TA fixed 96 h post-injury (Fig. 5.2E). In control TA muscle, eMHC was expressed at detectable levels in regenerating fibers (Fig. 5.2E, *left)*. By contrast eMHC was markedly up-regulated in obestatin-treated TA muscles (Fig. 5.2E, *right*).

Fig. 5.2 Effect of intramuscular administration of obestatin in freeze-injured TA. WB analysis of Pax7 (**A**), MyoD (**B**), myogenin (**C**) and eMHC (**D**) at different time points during the muscle regeneration under intramuscular administration of vehicle or obestatin (n=10 per time point corresponding to n=5 per group). (**E**) IF analysis of eMHC in freeze-injured TA at 96 h under obestatin or vehicle administration. The images are representative of five independent experiments. For A-D, *denotes P< 0.05 when comparing control muscle (undamaged) *versus* treated-muscles (vehicle- or obestatin-treated muscles). # denotes P<0.05 when comparing vehicle- and obestatin-treated muscle at each time point.

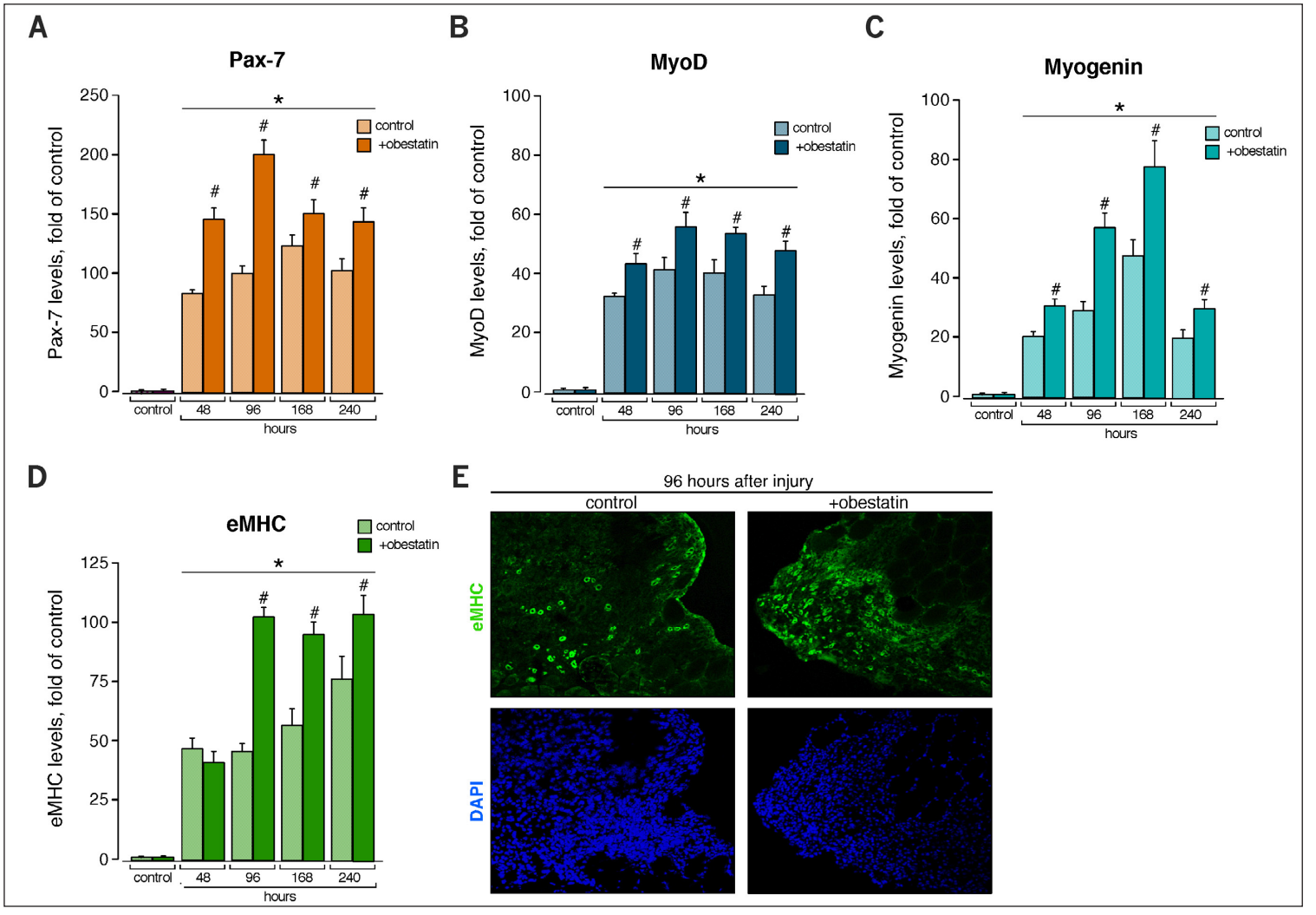

Obestatin enhances hypertrophy *in vivo*

Histological analysis revealed that treated-to-control ratios of regenerating fibre cross-section areas were 62 and enhances 28% larger in obestatin-treated mice (324±29 and 755±42 μm^2) than in control mice (199±22 and 588±88 μm^2) at 96 and 168 h after injury, respectively (Fig. 5.3B). At 240 h post-injury, cross-section area analysis revealed a significant increases, as compared to control, in the % of myofibers of larger area (Fig. 5.3C): 24% *vs.* 3% of fibers in a range between 4-3x10^3 μm^2, 56% *vs.* 39% between 2-1x10^3 μm^2, and 18% *vs.* 56% between 1-0.5x10^3 μm^2, respectively. Consistent with these results, the number of myonuclei per myofiber were significantly increased by 91% in obestatin-treated TA (481±19 cells per muscle section) compared to control TA muscles (251±17 cells per muscle section) 240 h after injury (Fig. 5.3D). Taken together, these data indicate that obestatin delivered by intramuscular injection markedly enhances muscle regeneration, as evidenced by up-regulation of the expression of specific myogenic factors and the significantly increased size of myofibers.

Fig. 5.3 Effect of intramuscular administration of obestatin in freeze-injured TA. (A) Time course analysis by H&E of muscles cryosection along the regeneration process under vehicle or obestatin treatment (n=10 per time point). **(B)** Measurement of regenerating myofibers as cross-sectional area (μm^2) at 96 and 168 h post injury. **(C)** Analysis the percentage of fibers associated to different cross-sectional area groups at 240 h post injury under vehicle or obestatin treatment,. **(D)** Analysis by IF expression of myonuclei (DAPI) per 100 myofibers in cryosections at 240 h post-injury under vehicle or obestatin treatment. For A and D, the images are representative of five independent experiments. Data were expressed as the mean ± S.E. (n=5 per group; *, $p < 0.05$).

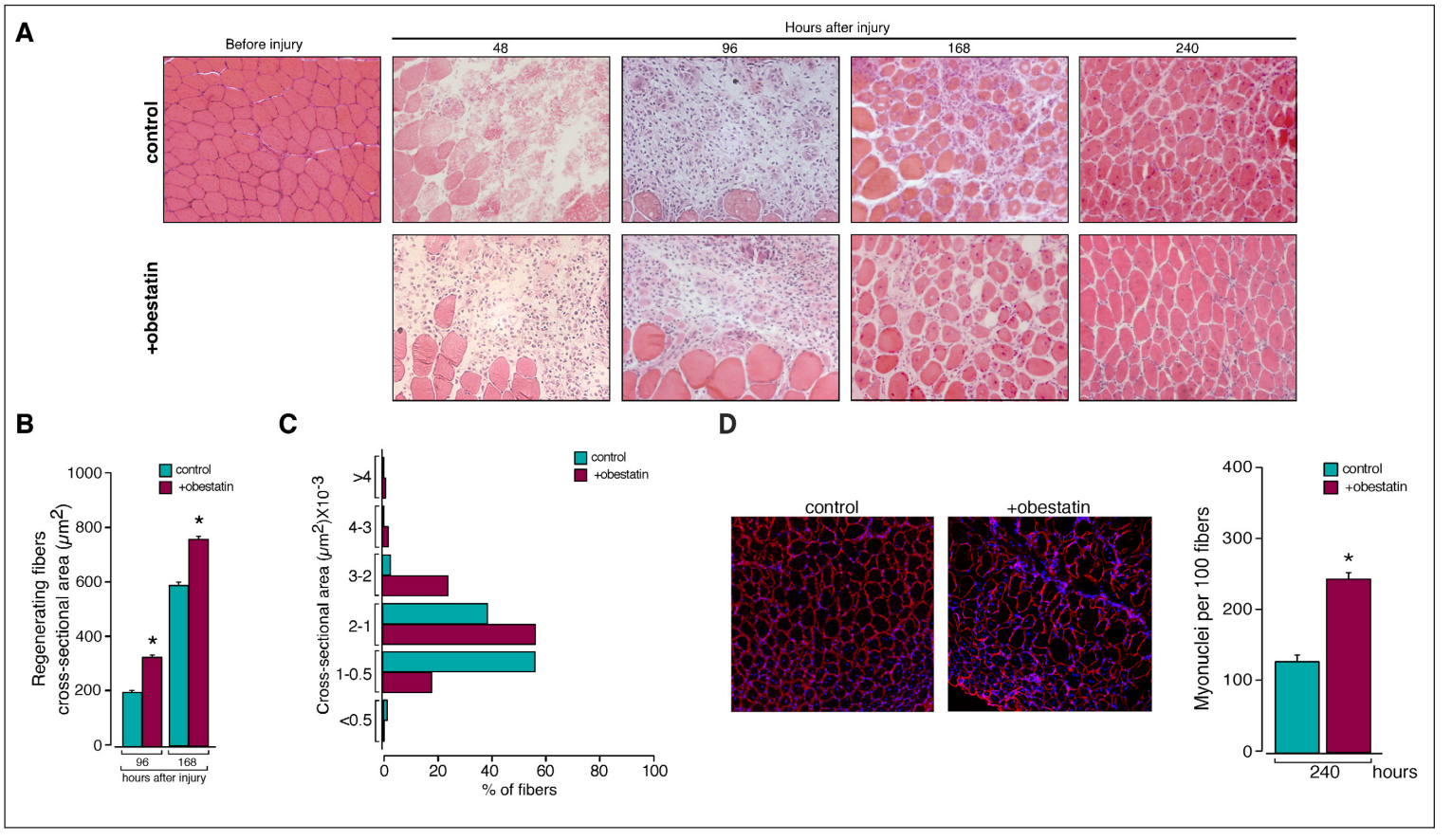

Obestatin enhances satellite cell activation after muscle injury

Based on the up-regulation of Pax7, an specific SCs marker, in obestatin-treated TA muscles, SCs were quantified on muscle sections 96 h post-injury (Fig. 5.4A). The density of SCs in obestatin-treated TA muscles harbored ~2.3-fold more Pax7$^+$ cells per section (427±7 cells per muscle section) than control TA muscles (189±12 cells per muscle section) 96 h after injury. In addition, myofibers were isolated from obestatin-treated and control TA muscles 96 h after injury (Fig. 5.4B). The number of activated satellite cell (Pax7$^+$) normalized to myofiber length was correspondingly higher in myofibers obtained from obestatin-treated muscles than in control (~2.2-fold; Fig. 5.4B). These results demonstrate that obestatin stimulates sc division and consequently drive the expansion of SCs pool.

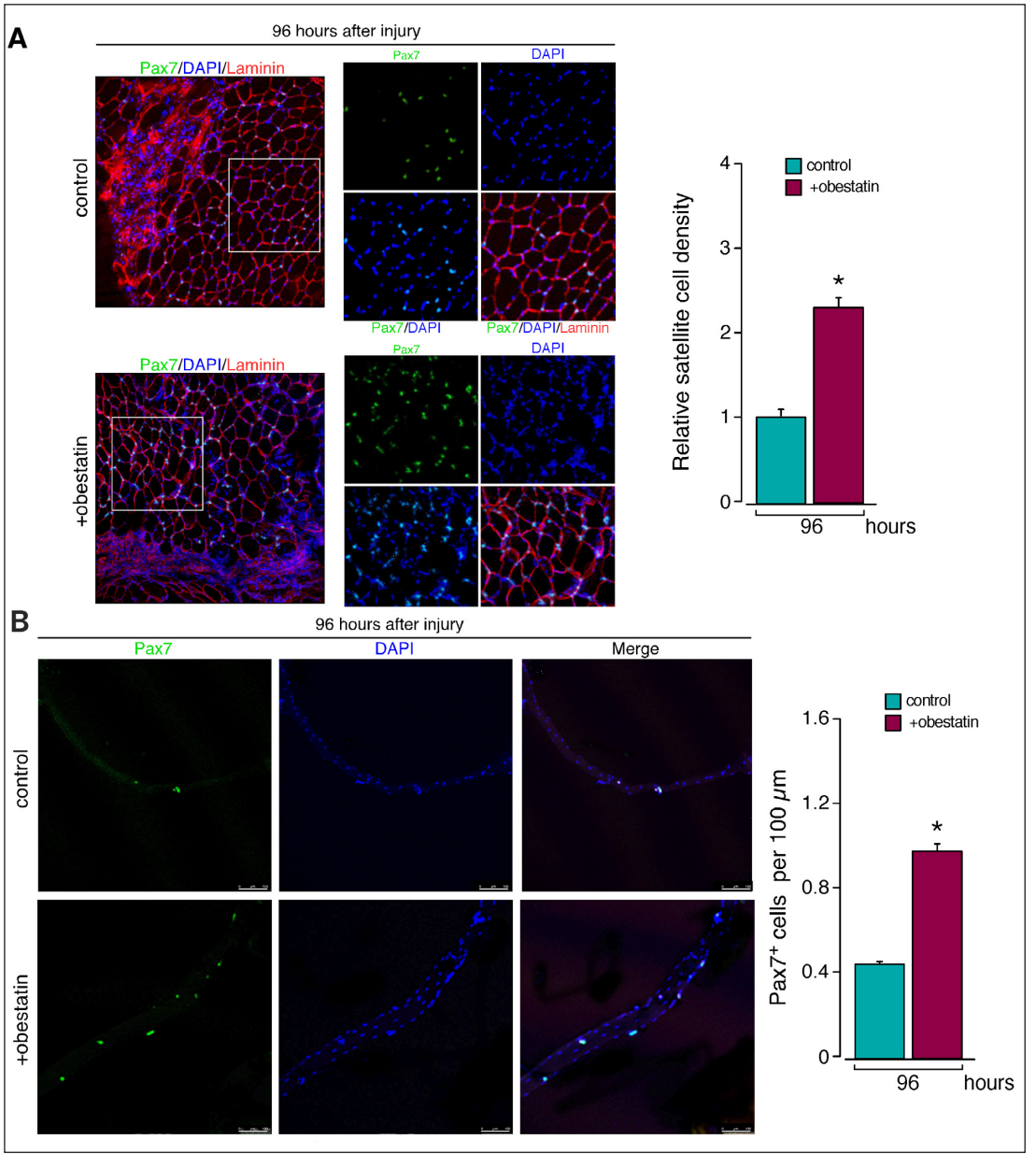

Fig. 5.4 Analysis of Pax7 expression in obestatin-treated TA muscle or isolated-myofibers. (A) IF analysis of Pax7 in TA cryosections at 96h post-injury under vehicle or obestatin administration (*left panel*, objective magnification 20x; *middle panel*, magnification of a significative area). **(B)** IF expression of pax7 in TA isolated-myofibers at 96 h post-injury under vehicle or obestatin administration. IF images are representative of five independent experiments. Data were expressed as the mean ± S.E. (*, $p < 0.05$).

Obestatin enhances Ki67 and Cyclin D1 in early stages of muscle regeneration

As previously indicated, obestatin treatment stimulates the expansion of SCs, which would then give rise to transient amplifying progenitors that undergo normal proliferation and differentiation. The elevated protein level of Ki67, 2.3-fold higher in obestatin-treated TA muscles than in control muscles (Fig. 5.5A), implies enhanced proliferation 96 h after muscle injury. Added to this fact, the elevated protein expression of Cyclin D1, 2.2-fold higher in obestatin-treated TA muscles than in control muscles, demonstrated enhanced proliferation during regeneration (Fig. 5.5B). Together, these data demonstrate that obestatin enhances cell proliferation during early stages of muscle regeneration.

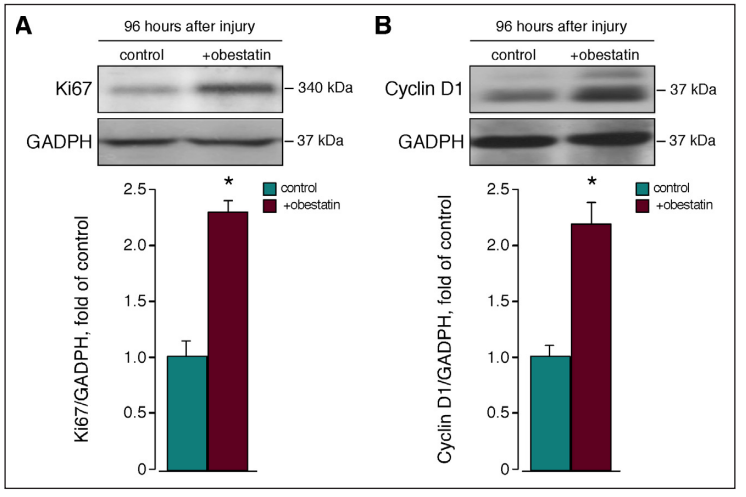

Fig. 5.5 Expression of mitogenic markers in obestatin-treated TA at 96 h after freeze injury. WB analysis of Ki67 (**A**) or cyclin D1 (**B**) in TA under vehicle or obestatin administration. Immunoblots are representative of five independent experiments (n=5 per group; mean± S.E.; *denotes P< 0.05).

Obestatin affects the essential network for regenerating muscle fibre growth

Obestatin-treatment-to-control ratios of VEGF and VEGF-R2 protein levels were 130 and 80% higher in obestatin-treated TA compared than in control TA muscles 96-h after injury, respectively (Fig. 5.6A). Vessel counting, evaluated as isolectin^{+} per myofiber, showed differences in capillary density in obestatin-treated TA (1.5±0.06) compared to control TA muscles (0.5±0.01) 96 h post-injury (Fig. 5.6B). These data indicated that obestatin contributed to the restoration of VEGF/VEGF-R2 tissue levels and to the subsequent dynamic process of capillary formation and muscle regeneration. Protein levels of myostatin, measured as precursor, latency-associated peptide (LAP) and dimer, were respectively 20, 30 and 60% lower in obestatin-treated TA than in control TA muscles 96-h after injury (Fig. 5.6C), which corroborated the obestatin role on muscle regeneration and growth. Of note, is that there was no significant elevation of collagen 1α2 (Col1α2) 96 and 240 h after injury (Fig. 5.7, *right panel*). This result was endorsed by Azan trichrome staining of muscle sections 240-h after injury (Fig. 5.7F, *left panel*). This indicated that fibrosis in obestatin-treated muscles is not enhanced during regeneration and did not contribute to the increases size of regenerated muscle.

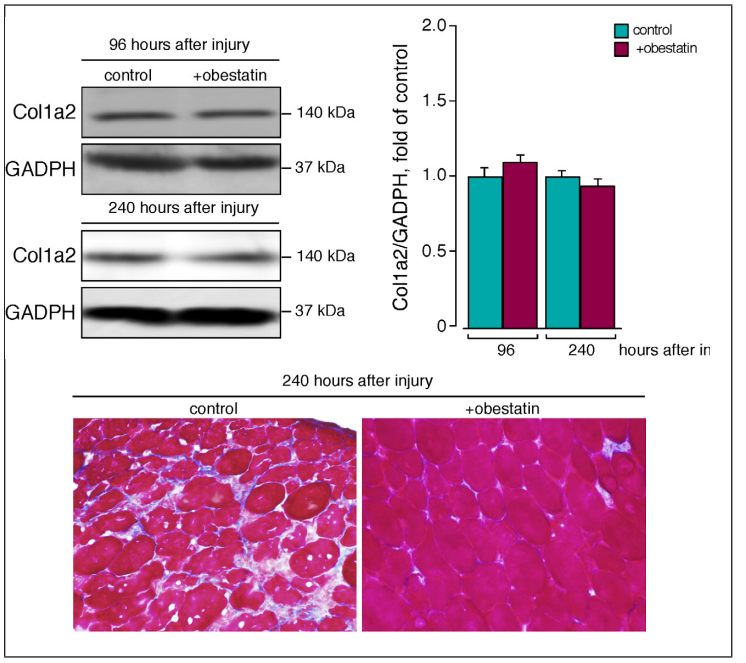

Fig. 5.7 Expression of fibrogenic markers. WB analysis of collagen 1α-2 isoforms at 96 h and 240 h after TA freeze injury (*left panel*). Analysis of fibrosis by Azan trichrome stain in vehicle- and obestatin–treated TA at 240 h after reeze injury (*right panel*). Immunoblots are representative of five independent experiments (n=5 per group; mean± S.E.).

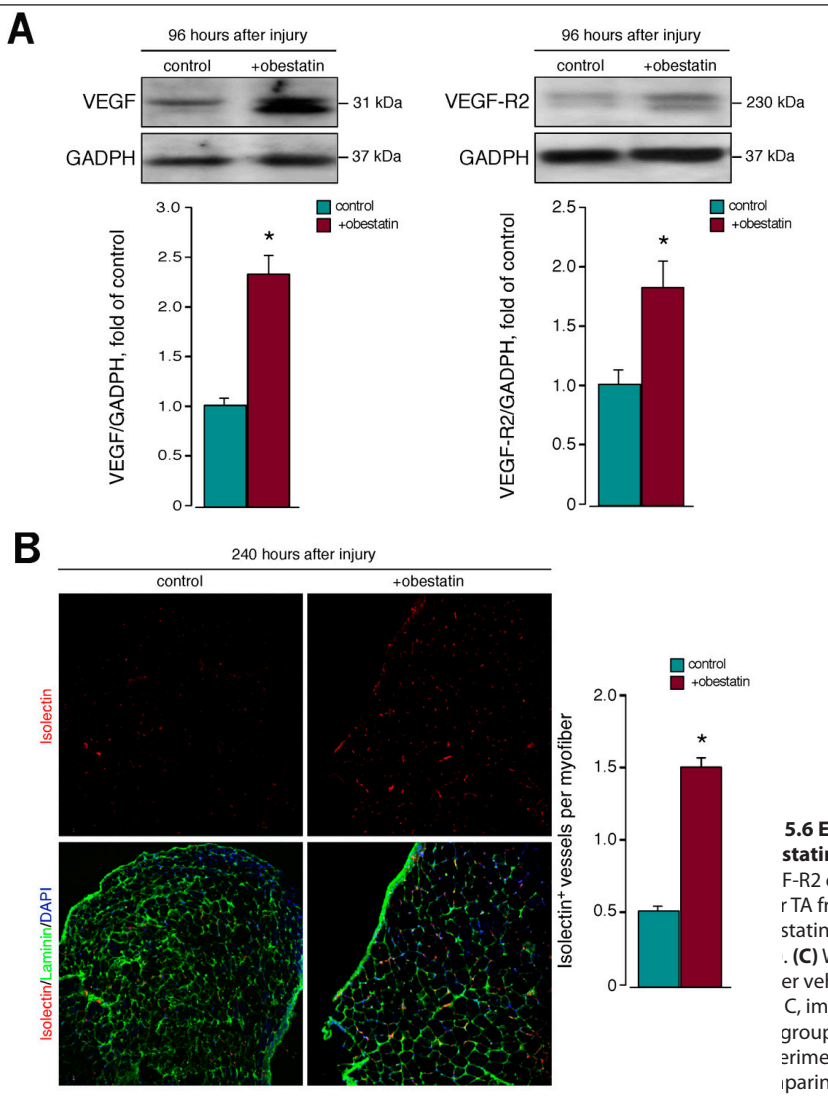

5.6 Evaluation of microvascularization and miostatin expression in statin-treated TA after muscle damage (A) WB analysis of VEGF and F-R2 expression in TA under vehicle or obestatin administration at 96 h r TA freeze injury. **(B)** IF analysis of isolectin⁺ cells in TA under vehicle or statin administration at 96 h after TA freeze injury (objective magnification . **(C)** WB analysis of myostatin isoforms (precursor, LAP and dimer) in TA er vehicle or obestatin administration at 96 h after TA freeze injury. For A C, immunoblots are representative of five independent experiments (n=5 group; mean± S.E.). For B, IF images are representative of five independent eriments (n=5 per group; mean± S.E.). Asterisk (*) denotes P< 0.05 when paring obestatin-treated with vehicle-treated groups.

Obestatin regulates mitogenesis and myogenesis during differentiattion

The elevated protein levels of Ki67 and Cyclin D1 in TA muscle under obestatin treatment, implies an enhance proliferation during the early stage of regeneration. To ascertain this possibility, the mitogenic action was explored by dose-effect experiments performed on cultured C2C12 myoblasts treated with a range of obestatin concentrations (0.1–100 nM) in GM (proliferating conditions; Fig. 5.8A). Maximal effect in the cell number was observed at 5 nM obestatin (2.4-fold). During the differentiation process, immunoblot analysis of Ki67 and p21 revealed elevated protein expression when compared obestatin-treated cells (DM+5 nM obestatin) with control cells (DM; Fig. 5.8B). At 24 h, Ki67 showed maximal expression levels, followed by an increase in the expression of p21 that reached maximal levels at 48 h, reflecting growth arrest to promote cellular differentiation. In fact, the protein levels of myogenin and MHC were up-regulated, displaying maximal levels at 72 and 96 h respectively (Fig. 5.8B). It is noteworthy that, both proliferating and myogenic markers, displayed normal kinetics with enhanced protein levels when compared obestatin-treated with control cells, aiming that obestatin exerts a double mitogenic and myogenic effect.

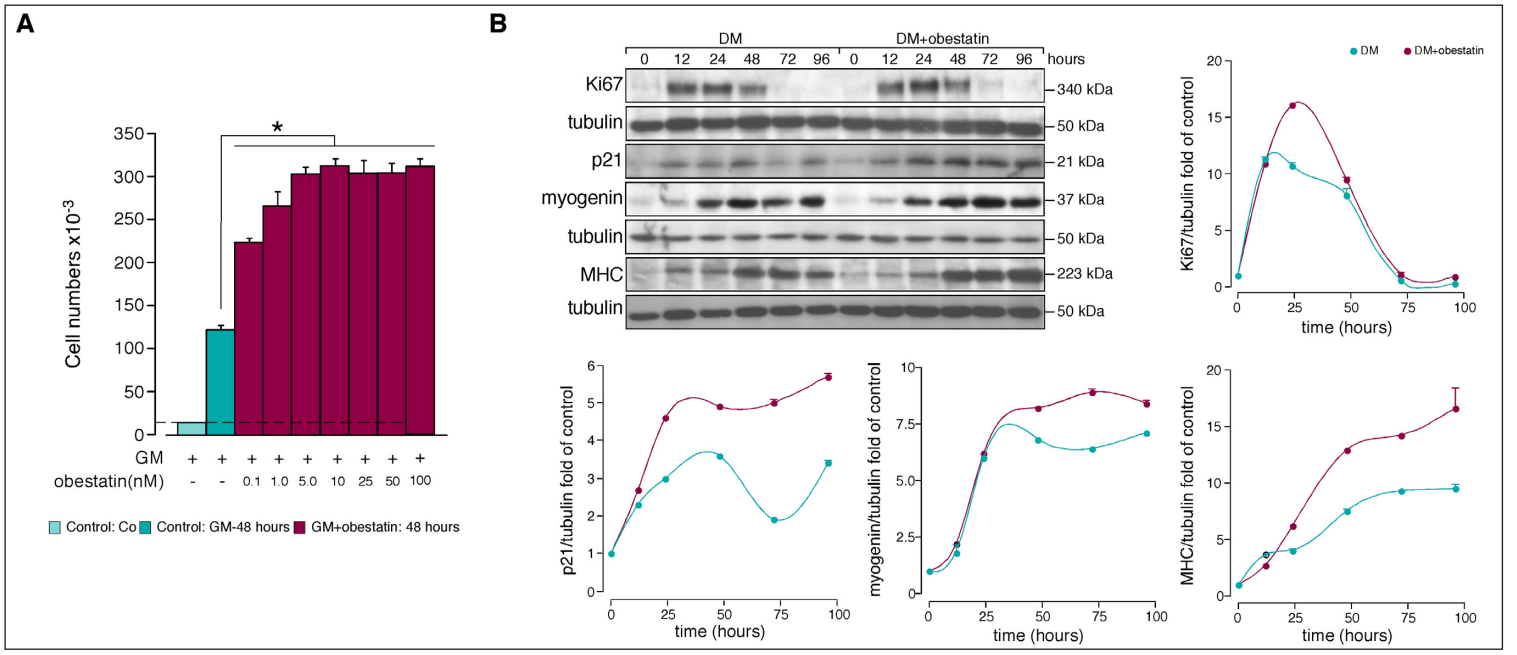

Fig.5.8 Effect of obestatin on mitogenesis and myogenesis. (A) Dose-response effect of obestatin (0.01–100 nM) on C2C12 myoblast cell proliferation (48 h, *n* = 5). **(B)** Time course on C2C12 of Ki67, p21, myogenin and MHC along differentiation. Protein level was expressed as a -fold over control cells in growth conditions (n = 3). Immunoblots are representative of three independent experiments. Data were expressed as the mean ±S.E.*, P <0.05 versus control values.

Hipertrophic effect triggered by obestatin is independent of mitogenic effect

Exogenous administration of obestatin to TA during regeneration enhanced the area and the number of myonuclei per myofiber. To investigate whether obestatin was in fact stimulating hypertrophic growth of myofibres, C2C12 myoblasts were treated with obestatin (Fig. 5.9A). Myotube areas were 110% larger in obestatin-treated cells (DM+5 nM obestatin; 941±4 μm^2) than in control cells (DM; 449±3 μm^2) 168-h after differentiation. Moreover, myotubes were grouped into two categories, those with 2–3 nuclei and those with 4 or more nuclei. ~30% of control myotubes contained 4 nuclei, *versus* 73% of obestatin-treated cells. This effect represents an increase of ~2.43-fold respect to control cells (Fig. 5.9A). Having shown that obestatin increased myotube size with associated enhancement of nuclei number, we assessed whether hypertrophy was dependent on mitogenic effect. To reach this point, obestatin was administrated 3 days after differentiation when myoblasts withdrawal the cell cycle (Fig. 5.9 B). In this case, myotube areas were ~80% larger in obestatin-treated cells (DM for 72 h followed by DM+5 nM obestatin for 96 h; 736±7 μm^2) than in control cells (DM; 409±6 μm^2) at 168 h after differentiation. Under this conditions, ~25% of control myotubes contained 4 nuclei *versus* 77% of obestatin-treated cells. Furthermore, myotubes were treated with obestatin after administration of cytosine arabinoside (AraC), an inhibitor of DNA replication[1]. Of note, is that obestatin-treated cells displayed ~92% larger in myotubes areas (DM for 72 h followed by DM+AraC+5 nM obestatin for 96 h; 853±3 μm^2; Fig. 5.9C) than in control cells (DM; 444±4 μm^2) at 168 h. Obestatin treatment led to a ~69% of myotubes contained 4 nuclei *versus* 11% of control cells. Furthermore, immunoblot analyses revealed no differences in myogenin and MHC levels between both groups: DM+obestatin and DM+AraC+obestatin (Fig. 5.9D). Therefore, obestatin increases myoblast fusion and acts on established myotubes to induce hypertrophy independently of the mitogenic effect produced in the first three days of differentiation.

1. Von Maltzahn, J. et al. Wnt7a-Fzd7 signalling directly activates the Akt/mTOR anabolic growth pathway in skeletal muscle. *Nat. Cell. Biol*. 2011; 14(2):186-91.

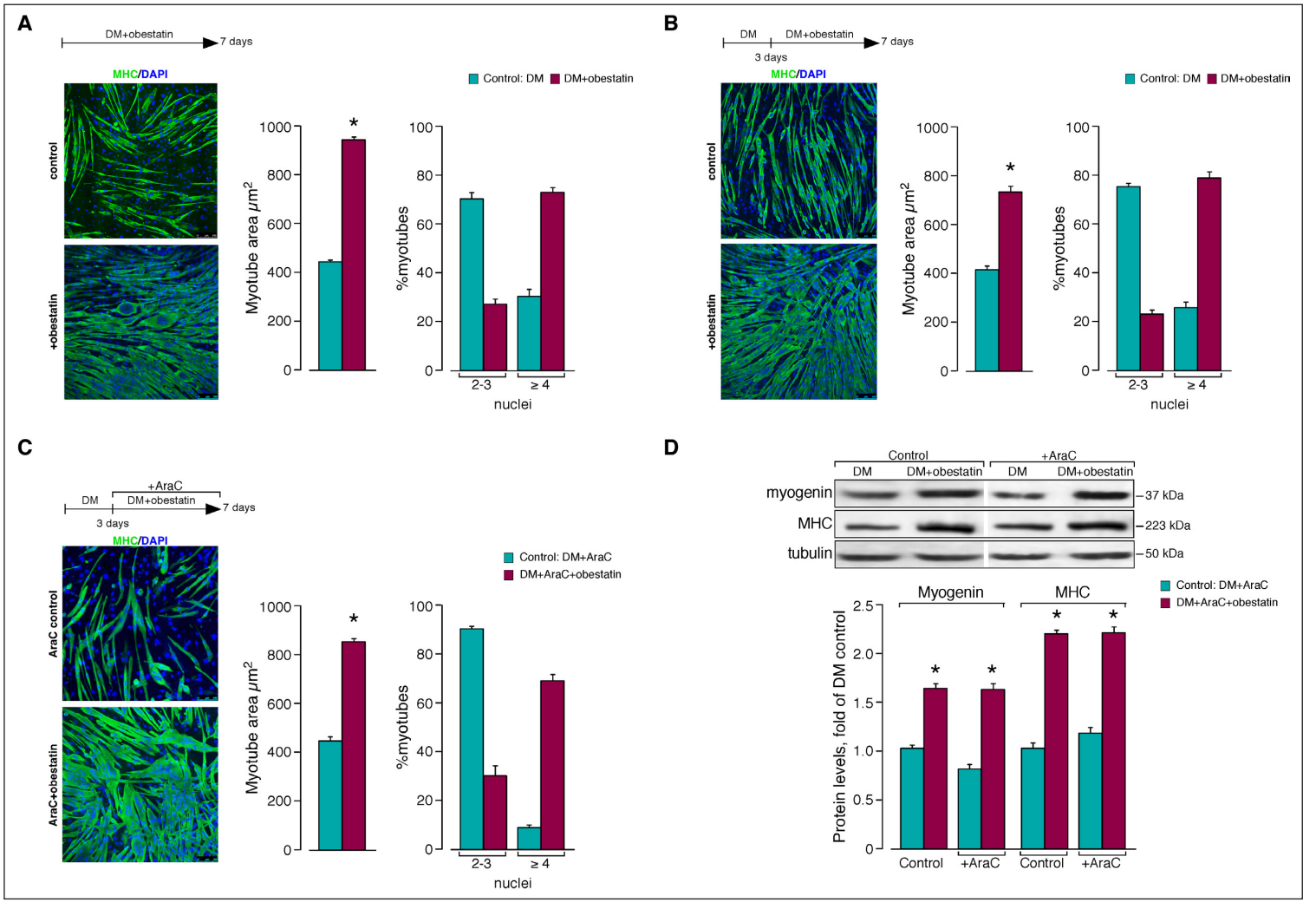

Fig. 5.9 Role of obestatin in myotube hypertrophic response. (A) Representative images used to determine the myotube area (μm^2; *left panel*; objective magnification 20x) and the number of nuclei within individual myotubes (at leats two nuclei) in C2C12 myotube cells under DM (control) or DM + obestatin (5 nM) at the 7 day point after stimulation. **(B)** Representative images used to determine the myotube area (μm^2; *left panel*; objective magnification 20x) and the number of nuclei within individual myotubes (at leats two nuclei) in C2C12 myotube cells under DM (control) or DM + obestatin (5 nM) three days after differentiation. **(C)** Representative images used to determine the myotube area (μm^2; *left panel*; objective magnification 20x) and the number of nuclei within individual myotubes (at leats two nuclei) in C2C12 myotube cells under DM (control) or DM + AraC (50 μM)+obestatin (5 nM) three days after differentiation **(D)** WB analysis of the expression of myogenin and MHC C2C12 myotube cells under DM (control) or DM + AraC (50 μM) + obestatin (5 nM) three days after differentiation. Immunoblots are representative of three independent experiments. Data were expressed as the mean ±S.E.*, P <0.05 versus control values.

Obestatin controls myogenesis by regulating Akt, ERK1/2, p38 and CamkII activity

To establish the molecular events activated by obestatin to drive myogenic process, the activity of Akt/mTOR signalling was examined in differentiating C2C12 cells during 168 h (Fig. 5.10A). Obestatin treatment (5 nM) resulted in markedly elevated levels of phosphorylated Akt [pAkt(S473)] and its downstream target S6K1 [pS6K1(S371)] during myogenesis. Despite the increased Akt activity under obestatin treatment, lower levels of pFoxO1(T24) and pFoxO3a(T32) were observed obestatin-treated cells than control cells (DM). Obestatin increased ERK1/2 activity [pERK1/2(T202/Y204)] in early steps of differentiation

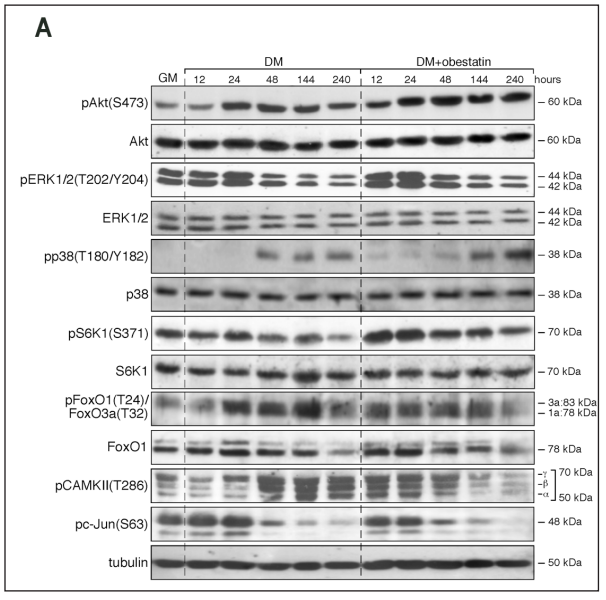

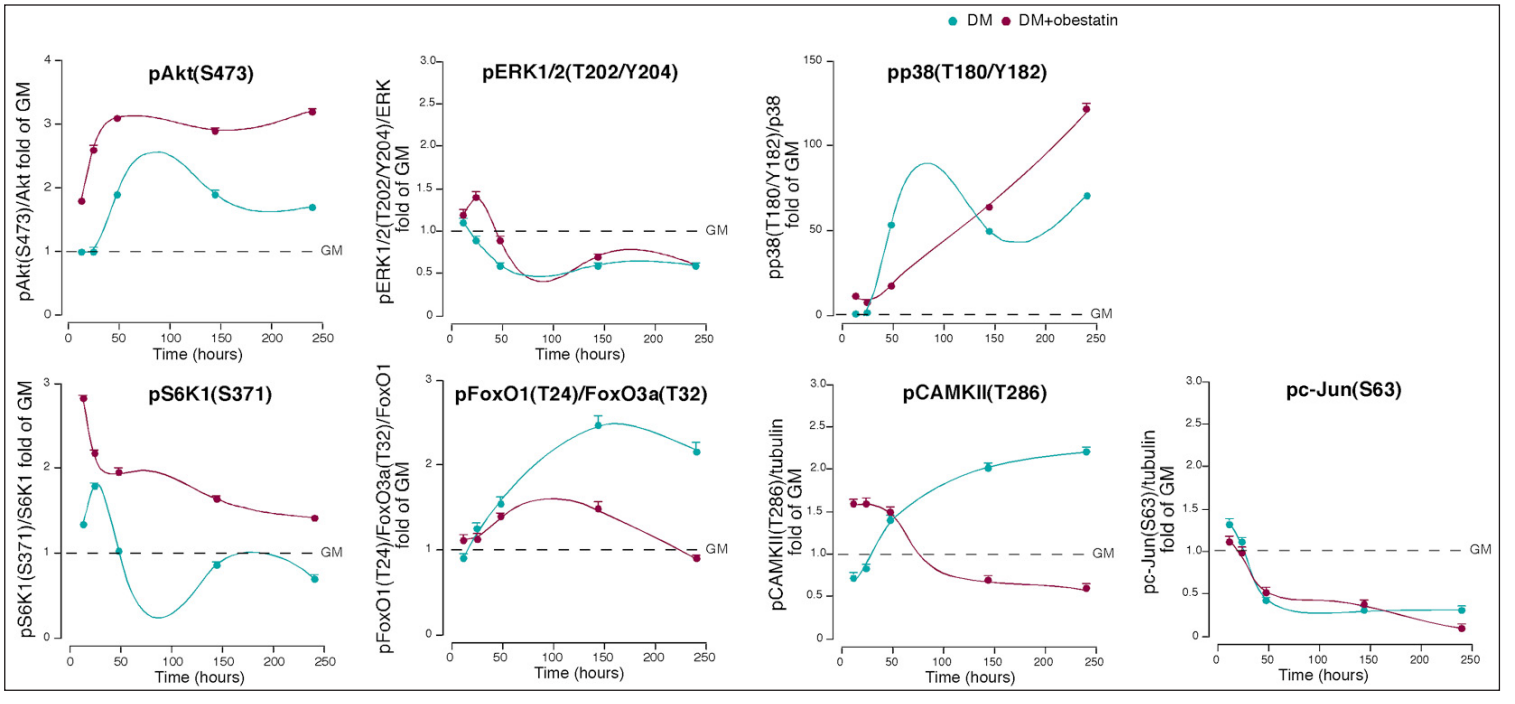

program. Strikingly, obestatin markedly elevated levels of phosphorylated p38 [pp38(T180/Y182)] during differentiation. The phosphorylation levels of c-Jun [pc-Jun(S63)] showed no significant differences following obestatin treatment. By contrast, the phosphorylation pattern of CamkII [pCamkII(T286)] showed clear differences under obestatin treatment. Gradual increase of pCamkII (T286) was observed in control cells reaching maximal levels at 240 h. Under obestatin treatment, maximal levels were showed at early time points, 12-48 h, to decline to basal phosphorylation after 48 h. In regenerating TA muscle, obestatin treatment resulted in robust activation of Akt and S6K1 96 h after injury (Fig. 5.10B). None of the other components, ERK1/2, FoxO1, FoxO3a, p38, c-Jun and CamKII, showed to be significantly phosphorylated at this time. Together, the obestatin action is determined by a kinase hierarchy that coordinates myogenesis in a manner analogous to the myogenic transcription factors. Initially, obestatin appears to activate ERK1/2, CamkII and Akt to promote proliferation. Akt/mTOR and p38 activity drive differentiation, fusion and hypertrophy at later points. Finally, p38 activity promotes the mid to late stages of differentiation. Based on these results, the central signalling node implicated in the regulation of myogenesis by obestatin appears to be Akt.

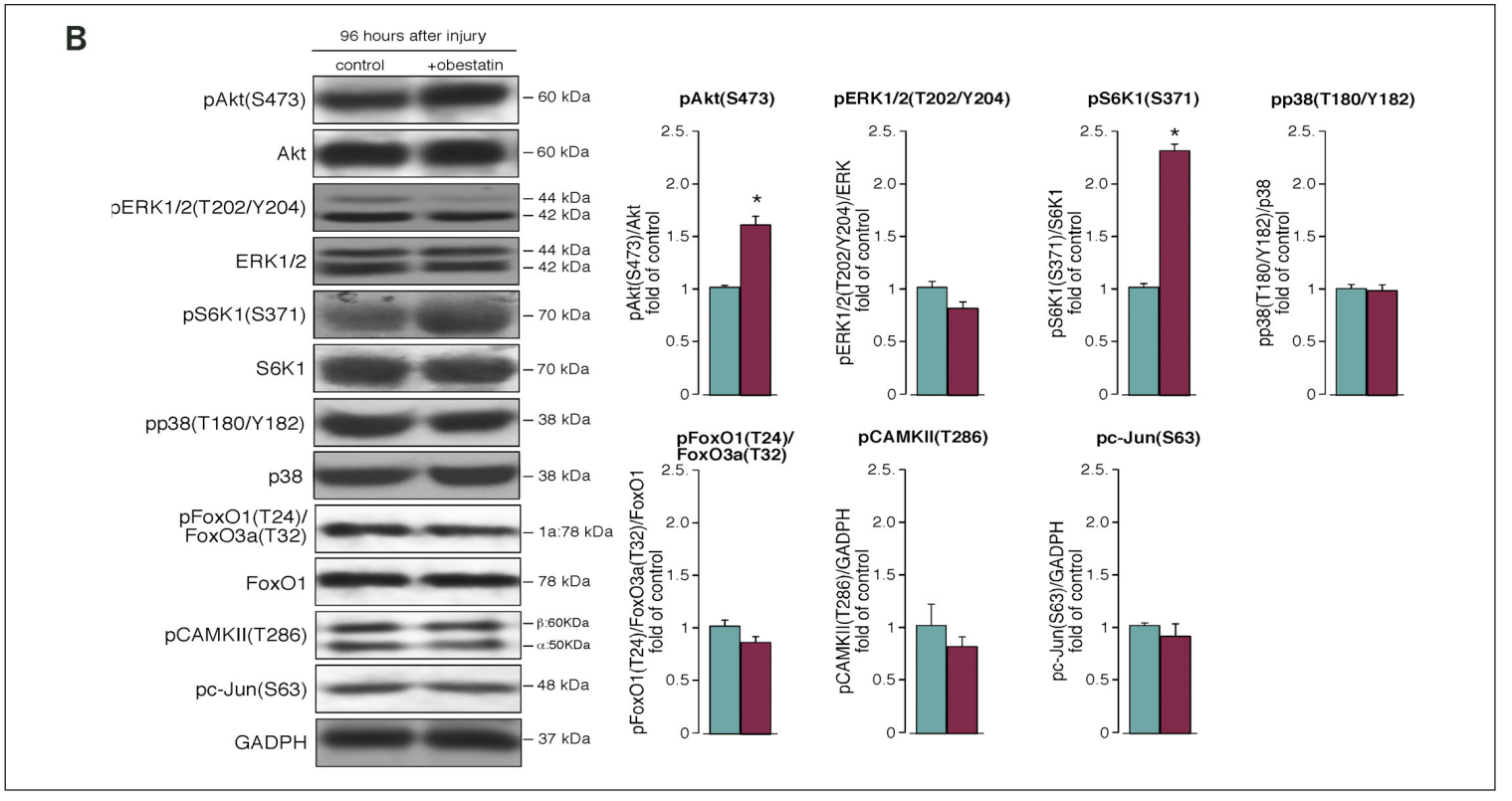

Fig.5.10 Obestatin-activated intracellular signalling nodes in C2C12 and TA during the myogenesis and regeneration programs. (A) WB analysis of p-Akt (S473), p-ERK ½ (T202/Y204), p-p38 (T180/Y180), p-S6K1 (S371), p-FoxO1 (T24)/FoxO3a (T32), P-CamKII and p-cJun (S63), and its respective non phosphorilated forms, in obestatin-treated C2C12 cells (5 nM) along myogenesis. **(B)** WB analysis of p-Akt (S473), p-ERK ½ (T202/Y204), p-p38 (T180/Y180), p-S6K1 (S371), p-FoxO1 (T24)/FoxO3a (T32), P-CamKII and p-cJun (S63), and its respective non phosphorilated forms, in mouse TA under treatment of obestatin (300 nmol/Kg) at 96 h after freeze injury. Immunoblots are representative of three independent experiments. Data were expressed as the mean ±S.E.*, P <0.05 versus control values.

Obestatin regulates myogenesis by limiting IGFR/IRS1 activity

Obestatin signals to activate the Akt/mTOR pathway through cross-talk with tyrosine kinase receptors, i.e. EGFR. To investigate the possibility that obestatin was indirectly activating the Akt/mTOR pathway through IGFR, activation of IGFR, measured as phosphorylated IGFR [p-IGFR(Y1316)], was examined in differentiating C2C12 cells during 168 h (Fig. 5.11A). Obestatin showed to increase the level of p-IGFR (Y1316) at early time points (12-48 h). However, under these conditions there was a substantial increase of the IRS-1 phosphorylation at S636/639 [pIRS-1(S636/639)], sites shown to inhibit PI3K binding to IRS-1 and consequent activation of Akt-associated IGFR signalling (Fig. 5.11A). In regenerating TA muscle, obestatin treatment showed to enhance the levels of p-IGFR(Y1316) and p-IRS-1(S636/639) 96-h after injury (Fig. 5.11B). Therefore, obestatin action on Akt/mTOR pathway is independent of IGFR/IRS1 activity.

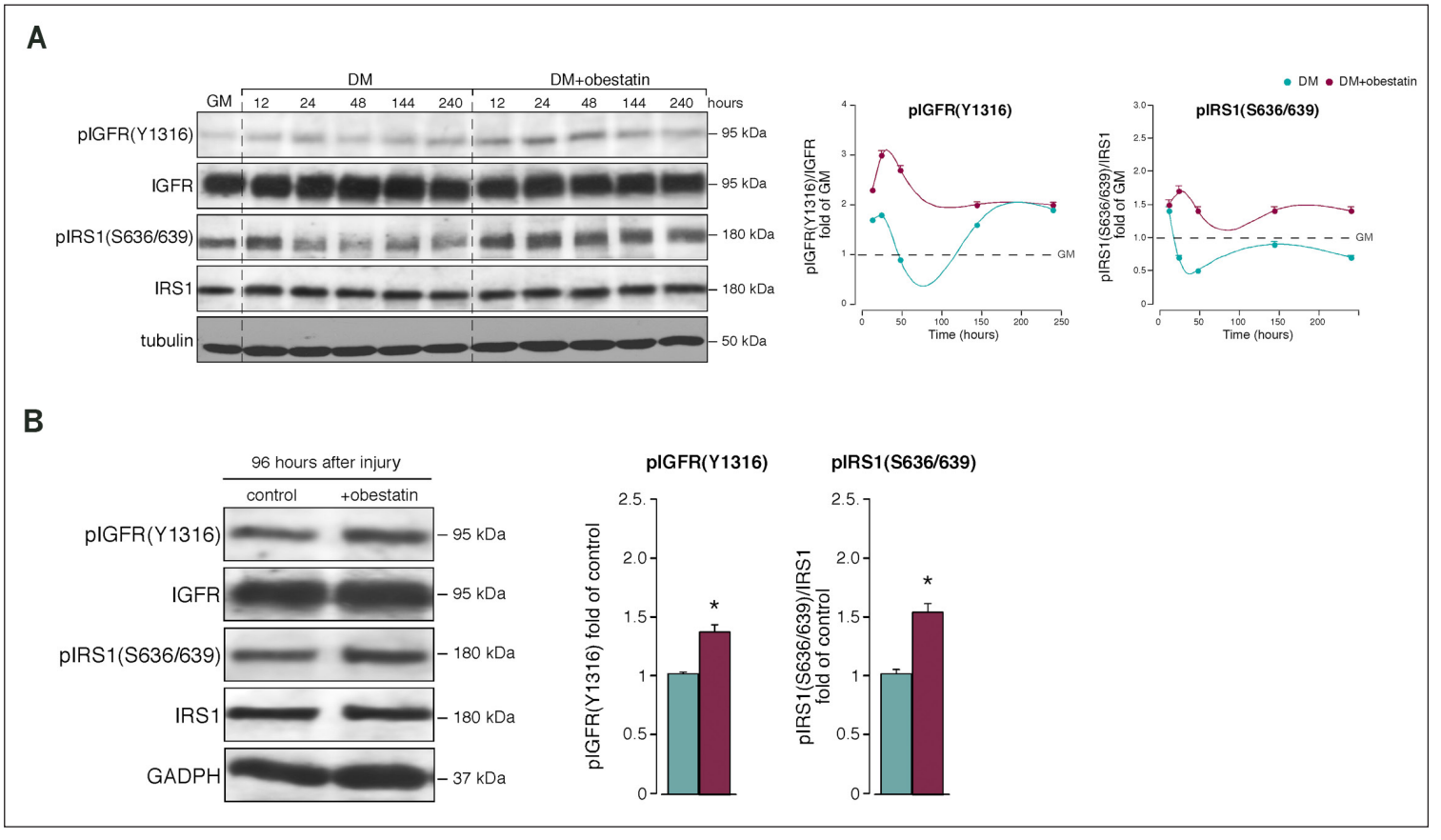

Fig. 5.11 Obestatin regulation of IGFR and IRS1 (A) WB analysis of p-IGFR (Y1316) and p-IRS1 (S636/639) in C2C12 cells along differentiation. **(B)** WB analysis of p-IGFR (Y1316) and p-IRS1 (S636/639) in mice TA 96h after freeze injury. Immunoblots are representative of three independent experiments. Data were expressed as the mean ±S.E.*, P <0.05 versus control values.

CHAPTER 6

OBESTATIN/GPR39 AN AUTOCRINE/PARACRINE SYSTEM INVOLVED IN SCs MYOGENIC REGULATION

GPR39 is expressed in SCs on *ex vivo* myofibers

To elucidate the autocrine/paracrine role of obestatin/GPR39 system on SCs activation, a culture model of *ex vivo*-isolated myofibers that closely recapitulates the SCs niche was utilized. IF analysis of myofibers fixed immediately following isolation from TA muscles revealed that SCs expressed detectable levels of GPR39 (Fig. 6.1A). In contrast, no immunostaining was found for obestatin (Fig. 6.1B).

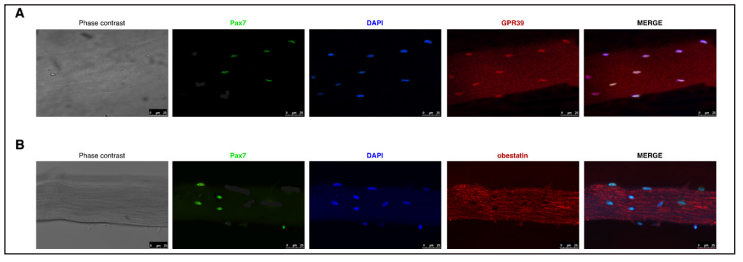

Fig. 6.1 Expression of obestatin and GPR39 in SCs muscle fibers. Immunofluorescence detection of obestatin **(A)** and GPR39 **(B)** in Pax7$^+$ SCs (objective magnification 20x).

Obestatin enhances SCs apical-basal division versus planar division on *ex vivo* myofibers

The specific expression of GPR39 in SCs suggested that obestatin might be involved in regulating muscle stem cell function in a paracrine mode, due to the expression of obestatin in mature fibers. Differences in the behavior of daughter cells from planar *versus* vertical division have yielded evidences that the orientation of cell division with respect to the myofiber may indicate or convey asymmetry in the two daughter cells[1,2]. Therefore, we examined the ability of obestatin to alter the ratio between planar and apical-basal cell divisions of SCs *in vitro*. Myofibers were isolated from TA muscle and cultured under non-adherent conditions. In this culture system, quiescent SCs become activated following myofiber isolation. Thus, we first visualized the outcome of the first division by fixing and immunostaining the myofibers after 24 h of culture. When stimulated with obestatin (5 nM), we observed an increase of 52% in the proportion of total SCs divisions in obestatin treated fibers *versus* control fibers (Fig.6.2, *left panel)*. Regarding the type of division, the percentage of planar division in control fibers was a 74% *versus* 41,9 % in the obesatin-treated fibers. In the case of apical-basal divisions it is noteworthy that obestatin-treated fibers had a percentage of 58,1% *versus* 25,5% showed in control fibers (n=5, n≥ x pairs; Fig. 6.2 *right panel*). These data reinforced the fact that obestatin favoured the commitment of SCs *versus* the stemness.

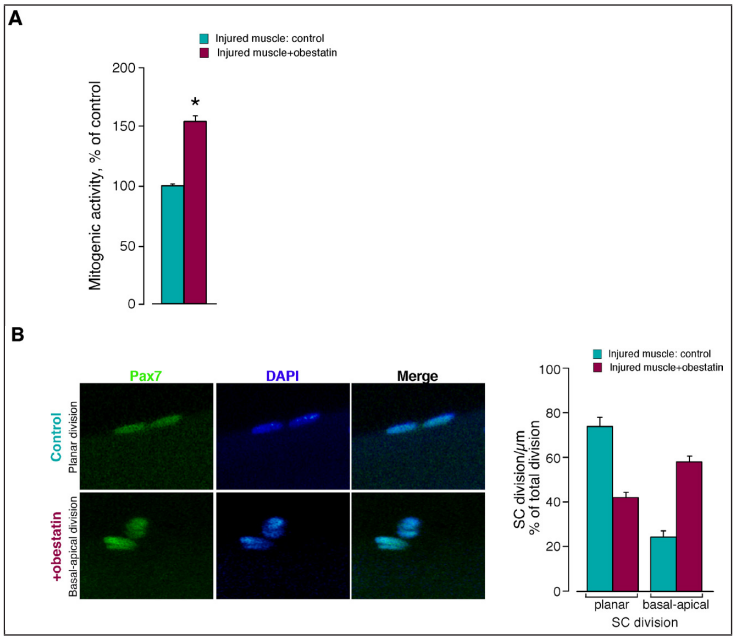

Fig. 6.2 Quantification of SCs divisions. (**A**) Immunofluorescence quantification of total SCs divisions per myofiber length (µm). (B) Orientation of cell division within the SCs niche. *Left panel:* IF examples of dividing SCs in planar division and apical-basal obestatin division (objective magnification 63x). *Right panel:* Relative quantification of planar division versus apical-basal comparing control and obestatin-treated myofibers, respectively (objective magnification 63x). Quantification is representative of seven independent experiments. Data were expressed as the mean ±S.E.*, P <0.05 versus control values.

Ex vivo migration of myoblasts is promoted by obestatin

To examine whether obestatin was capable of inducing myoblast migration in a 3-dimensional culture assay an inverted version of the classical Boyden chamber invasion assay was used. SC-derived cells (myoblasts) from muscle were able to migrate through the membrane and to invade into the Matrigel as an extracellular matrix, when obestatin was applied on top of the Matrigel as a chemoattractant being ~8.0-fold higher compared to control cells

1. Sambasivan, R. et al. Skeletal muscle stem cell birth and properties. *Semin. Cell. Dev. Biol.* 2007; 18: 870-82.
2. Siegel, A. et al. Muscle satellite cell proliferation and association: new insights from myofiber time-lapse imaging. *Skeletal Muscle.* 2011; 1 (1):1-7.

at 7 days (Fig. 6.3). These data demonstrated: (1) an anti-apoptotic effect; and, (2), more importantly, obestatin promoted migration of myoblasts, a critical step in muscle regeneration, reinforcing previous data.

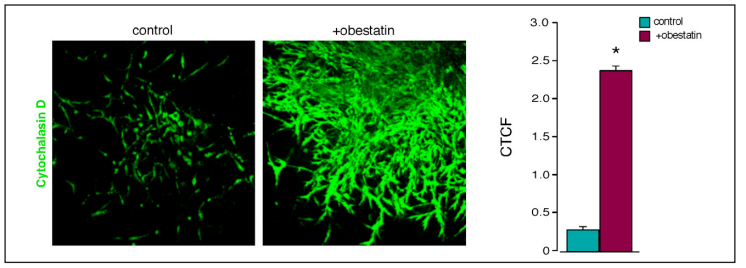

Fig. 6.3 Effect of obestatin on myoblast migration. *Left panel:* Representative images of calcein-satined myoblasts migrated into the upper chamber (objective magnification 20x) at 7 days. *Right panel:* Quantification of the maximal myoblast calcein staining. Quantification is representative of five independent experiments. Data were expressed as the mean ±S.E.*, P <0.05 versus control values.

Obestatin enhanced different SC populations during *in vivo* muscle regeneration

SCs were initially considered to be a homogeneous population of committed muscle progenitors[3]. However, several studies have pointed to a heterogeneous population[4,5]. SCs cells (Myf5$^-$) are capable of either symmetrical cell division to give rise to two Myf5$^-$ daughter cells, or asymmetric cell division to give rise to one Myf5$^-$ stem cell and one Myf5$^+$ committed precursor[6]. Kuang S. et al described that the 82% of apical-basal oriented doublets contained a Pax7$^+$/Myf5$^-$ cell against the basal surface and a Pax7$^+$/ Myf5$^+$ cell located on the apical side against the muscle fiber and 92% of planar divisions give rise to two symmetrical cells.[7]. To know the ratio between Pax7$^+$/Myf5$^-$ and Pax7$^+$/ Myf5$^+$ cells, these populations were measured along the regeneration process by FC. To reach this aim, DNA synthesis was first examined by propidium iodide (PI) staining at different time points, 12-168 h, during the regeneration process in order to discard apoptotic cells and to evaluate the cell cycle. Within the early stage of regeneration, 12 h, of obestatin treatment (300 nmol/kg body-weight) after muscle injury, ~60 % of cells exhibited PI staining related to uninjured muscle. Cells exposed to vehicle alone showed a ~90% PI staining (Fig. 6.4A). However, this difference was not kept along muscle regeneration in which obestatin treatment showed to increase PI staining related to control injured muscle. It is important to note that at the end of the regeneration process (168 h), corresponding to late stage of the regeneration program, ~30 % of cells exhibited PI staining compared to ~58 % of cells exposed to vehicle alone (Fig. 6.4A and 6.4B).

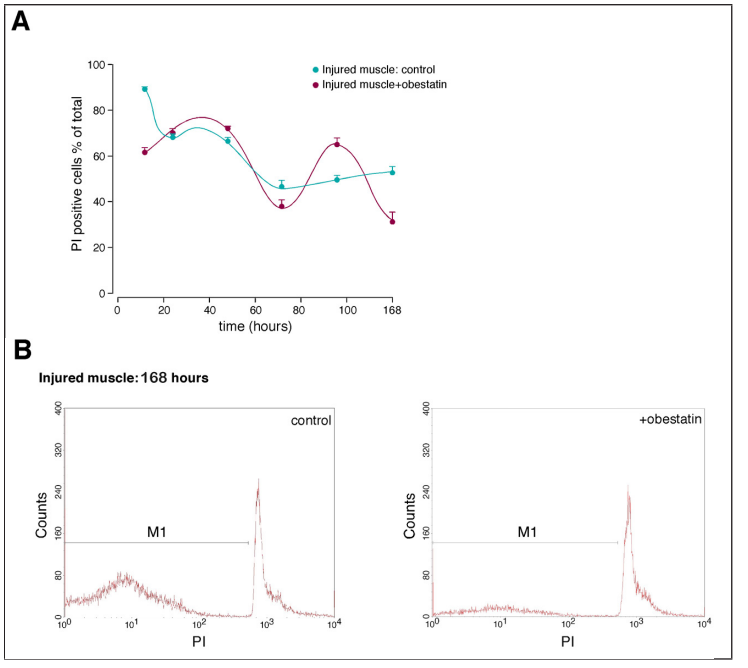

Fig. 6.4 Evaluation of the effect of obestatin treatment on PI positive cells during muscle regeneration. (A) Time course of PI staining comparing cells treated with obestatin or vehicle alone obtained from freeze injured TA. These PI staining was related to control injured TA. Data were expressed as the mean ±S.E representative of five independent experiments. **(B)** Representative DNA histogram of the apoptosis at 168 h after freeze injuried TA comparing control (vehicle) *versus* obestatin treatment.

An analysis of the cell cycle of living cells by FC demonstrated that within the early stage of regeneration, 12-48 h post-injury, obestatin treatment (300 nmol/kg body-weight) increased the percentage of cells in G_o phase related cells exposed to vehicle alone (~82% *versus* ~50% at 12 h, respectively; Fig. 6.5A). Furthermore, obestatin showed to enhance the percentage of cells in S phase during the late stages of regeneration, corresponding to 72-168 h (~85% for obestatin-treated cells

3. Bischoff, R. The satellite cell and muscle regeneration. In Myology. Ed. A.G. Engel and C. Franzini-Armstrong, McGraw-Hill. (New York,USA). 1994.
4. Schultz, E. Satellite cell proliferative compartments in growing skeletal muscles. *Dev. Biol*. 1996; 175: 84-94.
5. Beauchamp, J. R. et al. Expression of CD34 and myf5 defines the majority of quiescent adult skeletal muscle satellite cells. *J. Cell. Biol*. 2000; 151: 1221-34.
6. Cossu, G. et al. Oriented cell divisions and muscle satellite cell heterogeneity. *Cell*. 2007; 129 (5): 859-61.
7. Kuang, S. et al. Asymmetric self-renewal and commitment of satellite stem cells in muscle. *Cell*. 2007; 129: 999-1010.

versus ~60% for vehicle-treated cells; Fig. 6.5B) correlating to the minimum of G_o phase at 72 h for obestatin-treated cells (Fig. 6.5A and Fig. 6.5D). No significant differences in the percentage of cells in G_1 phase between the groups of obestatin- and vehicle-treated cells (Fig. 6.5C). The biggest divergence in cell cycle phases between treated and non-treated groups was produced at 72 h after freeze injury (Fig. 6.5D).

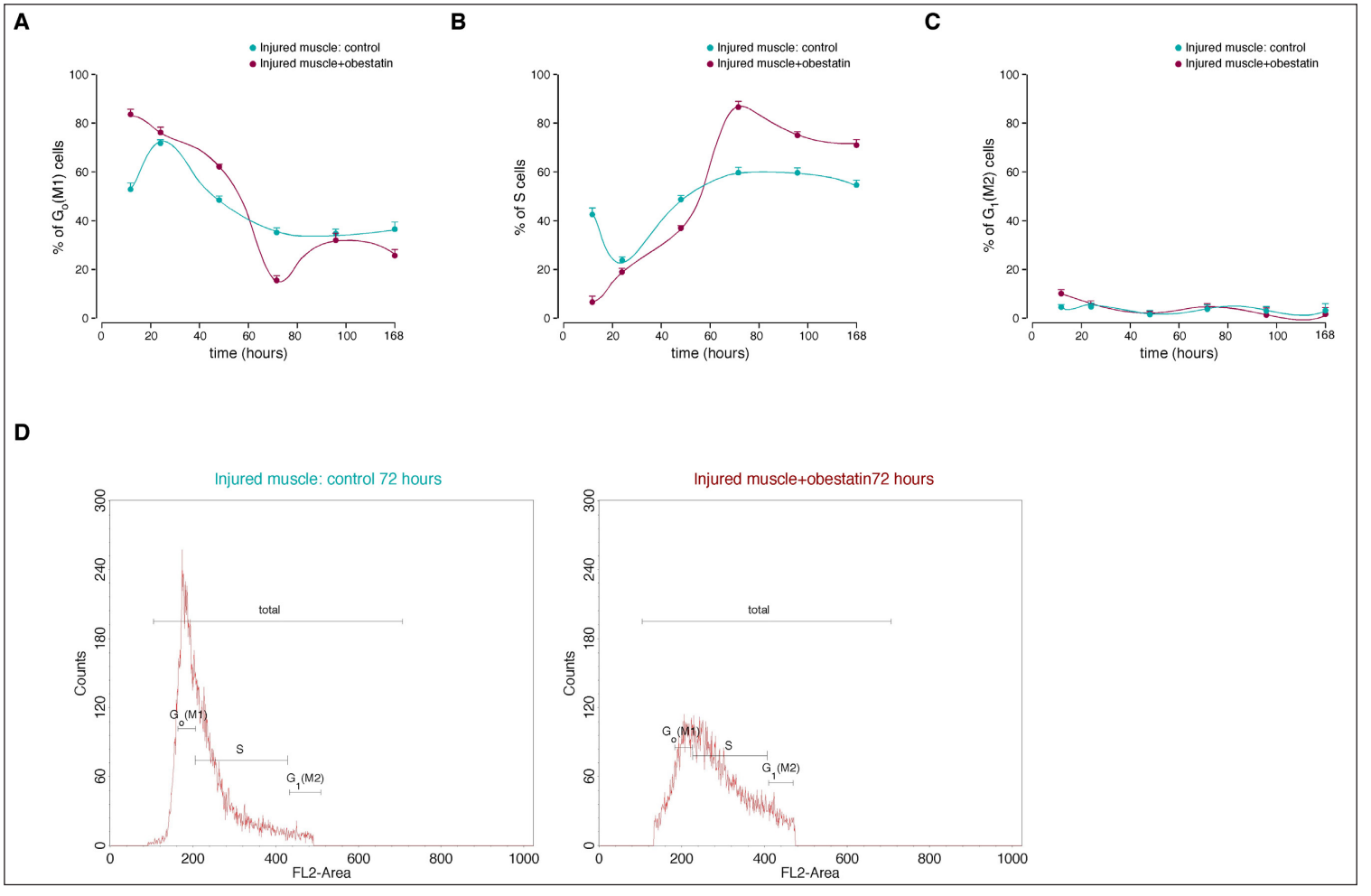

Fig.6.5 Time course of cell cycle during the regeneration process of total mononuclear cells isolated from freeze- injuried TA under obestatin or vehicle administratioin. Quantification of cells in G_o(M1) phase **(A)** S phase (**B**) and G_1(M2) phase (**C**). Data were expressed as the mean ±S.E representative of five independent experiments. **(D)** Representative DNA histograms of vehicle- (*left panel*) and obestatin-treated cells (*right panel)* showing the cell cycle phases at 72 h post-injury.

Finally, SCs from injured mice TA were immunostained with Pax7, Myf5 and Pax7/Myf5 over gated PI whole cell lysates (Fig. 6.6A-C). The population of Pax7^{+} and Myf5^{+} cells increased during regeneration showing maximal levels 96 h post-injury (~30% and ~9% for obestatin *versus* 15% and 3% for vehicle-treated cells, respectively). Furthermore, the population of Pax7^{+}/Myf5^{+} was also increased at the late stage of myogenic program being ~5 fold higher in for obestatin treatment related to control at 168 h post-injury (Fig. 6.6C). This pattern expression was demostrated after FC analysis with IF using the same samples from FC, showing the different ratio of myogenic markers expression (Fig. 6.6E).

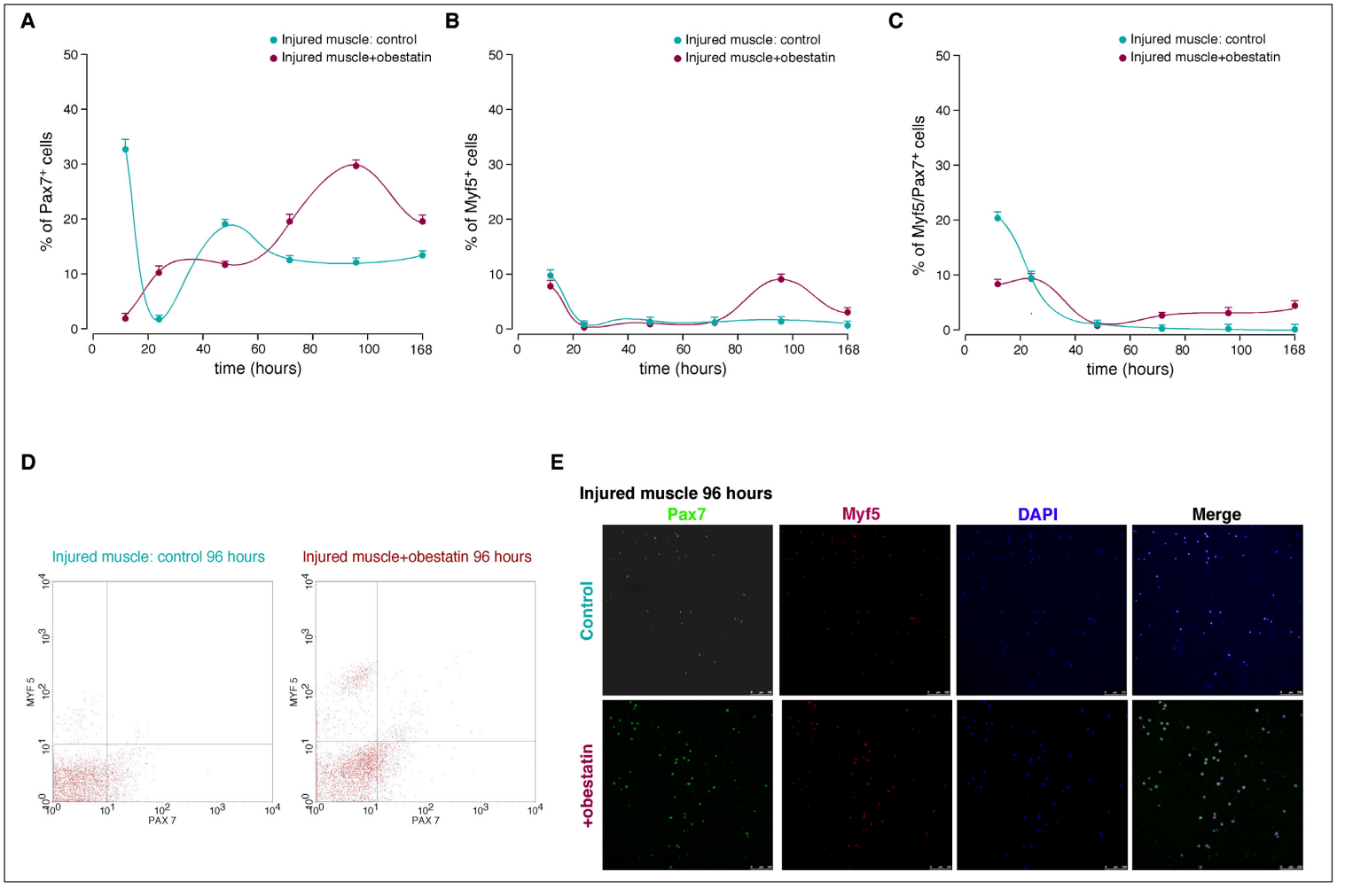

Fig. 6.6 Time course of the cell population expressing Pax7 (Pax7^{+}, **A**), Myf5 (Myf 5^{+}, **B**) and Myf5/Pax7 (Myf 5^{+}/ Pax7^{+}, **C**). Cells, obtained from injured-TA treated with vehicle (control) or obestatin (300 nmol/kg body-weight) and analysed by FA as indicated in Method section. **(D)** Representative flow cytometry histograms of gated PI samples, comparing the Pax7^{+}, Myf 5^{+} and Myf 5^{+}/ Pax7^{+} in whole lysates of cells, obtained from injured-TA treated with vehicle (control) or obestatin (300 nmol/kg body-weight) at 96h post-freeze injury. **(E)** Immunofluorescence detection of Pax7, Myf5 and myonuclei (DAPI) myoblast-derived SCs obtained from injured TA treated with vehicle (control) or obestatin (300 nmol/kg body-weight) at 96 h post-injury.

DISCUSSION

CHAPTER 1

We provided the first evidence that obestatin regulates adipocyte metabolism and adipogenesis. Preproghrelin expression, and thus obestatin, increased during adipogenesis being sustained throughout terminal differentiation of 3T3-L1 cells. In vitro 3T3-L1 cells secreted obestatin whose effects on adipocyte differentiation were neutralized by an obestatin antibody. Preproghrelin knock-down experiments revealed that obestatin contributes to adipogenesis, a fact that is supported by the effect of exogenous obestatin on the expression of C/EBPβ, C/EBPδ, C/EBPα and PPARγ and, consequently, lipid accumulation. In 3T3-L1 adipocyte cells, obestatin activated Akt phosphorylation and its downstream targets, GSK3α/β, mTOR, S6K1 and inhibited AMPK activity. This fact was confirmed *in vivo* in omental, subcutaneous and gonadal WAT obtained from male rats under continuous *sc* infusion of obestatin. The relevance of obestatin as regulator of preadipocyte/adipocyte metabolism was also supported by AS160 phosphorylation, GLUT4 translocation and augment of glucose uptake in 3T3-L1 adipocyte cells. By contrast, obestatin failed to modify translocation of fatty acid transporters, FATP4 and FAT/CD36, to plasma membrane.

Exposure of 3T3-L1 cells, a well-characterized model for studying the differentiation of white adipocytes, to obestatin regulates Akt activity. This study also demonstrated that chronic *in vivo* obestatin administration in male rats enhanced Akt activity in omental, subcutaneous and gonadal fat. It is well known that Akt regulates mammalian cell cycle progression and cell survival[1]. Furthermore, there is strong evidence, including results obtained from genetic mouse models, supporting the concept that Akt is a key node for regulation of a multitude of metabolic events such as glucose uptake, glycogen synthesis, gluconeogenesis, lipid metabolism, protein synthesis and differentiation processes as adipogenesis[2,3,4,5,6]. One of the physiological functions of Akt is to stimulate glucose uptake by GLUT4 trafficking through GAP known as AS160[7,8,9]. Our results showed that obestatin increased AS160 phosphorylation on Thr 642, consistent with Akt mediating obestatin-induced phosphorylation. AS160 keeps a GAP domain that maintains its target Rab(s) in their inactive GDP-state. AS160 phosphorylation suppresses its GAP activity, shifting the equilibrium of its targets Rab(s) to an active GTP form, enabling it to mediate GLUT4 trafficking[10]. Indeed, obestatin increased GLUT4 membrane translocation and glucose transport in 3T3-L1 adipocyte cells, although in smaller extension to that of insulin. Inside the cell, glucose is converted to glucose 6-phosphate that can be stored by conversion to glycogen or catabolized by glycolysis, both processes under the control of Akt signalling[11]. In this sense, obestatin inactivated GSK3α/β, an Akt substrate, through phosphorylation in 3T3-L1 adipocyte cells. This inactivation leads to a decrease in the phosphorylation of GS resulting in its activation, thereby stimulating glycogen synthesis. Consequently, Akt-directed signalling coordinates the obestatin-evoked glucose uptake and storage as glycogen in adipose tissue by regulation of AS160 and GSK3. In addition to glucose uptake, obestatin showed to regulate mTORC1/S6K1 signalling, a critical element integrating cellular metabolism with growth factor signalling[12]. mTORC1 controls many aspects of cellular metabolism including adipose tissue metabolism[13]. In particular, mTORC1/S6K1 plays an important role in adipogenesis and, thus, in lipid accumulation[14]. Loss of mTORC1/S6K1 activity correlates with a decrease in adipocytes accumulation, suggesting that the mTOR pathway is required for fat accumulation[15]. Furthermore, activation of mTORC1 signalling is a critical step in adipocyte differentiation[16]. The capacity of obestatin to modulate Akt activity in preadipocyte and adipocyte cells is not an isolated fact since this kinase is also activated by this peptide in pancreatic®-cell lines, human islets[17] and gastric cell lines[18]. In gastric cell lines, a signalling pathway involving a β-arrestin 1 scaffolding complex and EGFR to activate Akt signalling was

1. Manning, B. D. et al. Akt/PKB signalling: navigating downstream. *Cell*. 2007; 129: 1261-74.
2. Xu, J. et al. Protein kinase B/Akt 1 plays a pivotal role in insulin-like growth factor- 1 receptor signalling induced 3T3-L1 adipocyte differentiation. *J. Biol. Chem*. 2004; 279: 35914-22.
3. Chen, W. S. et al. Growth retardation and increased apoptosis in mice with homozygous disruption of the Akt1 gene. *Genes Dev*. 2001; 15: 2203-8.
4. Cho, H. et al. Akt1/PKBalpha is required for normal growth but dispensable for maintenance of glucose homeostasis in mice. *J. Biol. Chem*. 2001; 276: 38349-52.
5. Garofalo, R. S. et al. Severe diabetes, age-dependent loss of adipose tissue, and mild growth deficiency in mice lacking Akt2/PKB beta. *J. Clin. Invest*. 2003; 112: 197-208.
6. Berggreen, C. et al. Protein kinase B activity is required for the effects of insulin on lipid metabolism in adipocytes. *Am. J. Physiol. Endocrinol. Metab*. 2009; 296: E635-46
7. Kane, S. et al. A method to identify serine kinase substrates. Akt phosphorylates a novel adipocyte protein with a Rab GTPase-activating protein (GAP) domain. *J. Biol. Chem*. 2002; 277: 22115-8.
8. Eguez, L. et al. Full intracellular retention of GLUT4 requires AS160 Rab GTPase activating protein. *Cell Metab*. 2005; 2: 263-72.
9. Larance, M. et al. Characterization of the role of the Rab GTPase-activating protein AS160 in insulin-regulated GLUT4 trafficking. *J. Biol. Chem*. 2005; 280: 37803-13.
10. Zaid H, et al. Insulin action on glucose transporters through molecular switches, tracks and tethers. *Biochem. J*. 2008; 413: 201-15.
11. Manning, B. D. et al. Akt/PKB signalling: navigating downstream. *Cell*. 2007; 129: 1261-74.
12. Um, S. H. et al. Nutrient overload, insulin resistance, and ribosomal protein S6 kinase 1, S6K1. *Cell Metab*. 2006; 3: 393-402.
13. Dann, S. G. et al. mTOR complex1-S6K1 signalling: at the cross- roads of obesity, diabetes and cancer. *Trends Mol. Med*. 2007; 13: 252-9.
14. Kim, J. E. et al. Regulation of peroxisome proliferator-activated receptor-gamma activity by mammalian target of rapamycin and amino acids in adipogenesis. *Diabetes*. 2004; 53: 2748-56.
15. Um, S. H. et al. Absence of S6K1 protects against age- and diet-induced obesity while enhancing insulin sensitivity. *Nature*. 2004; 431: 200-5.
16. Zhang, H. H. et al. Insulin stimulates adipogenesis through the Akt- TSC2-mTORC1 pathway. *PLoS One*. 2009; 4: E6189.
17. Granata, R. et al. Obestatin promotes survival of pancreatic beta-cells and human islets and induces expression of genes involved in the regulation of beta-cell mass and function. *Diabetes*. 2008; 57: 967-79.
18. Pazos, Y. et al. Stimulation of extracellular signal-regulated kinases and proliferation in the human gastric cancer cells KATO-III by obestatin. *Growth Factors*. 2007; 25: 373-81.

proposed, as previously described[19]. It will clearly be of interest to establish whether this also occurs in adipose cells.

Parallel to Akt activation, AMPK inactivation was triggered by obestatin in 3T3-L1 pre-adipocyte and adipocyte cells. Similarly, 72 h continuous *sc* infusion of obestatin *in vivo* resulted in decreased AMPK activity in WAT similar to that observed *in vitro*. Thus, a decline in AMPK phosphorylation would be expected to lead to a reduction in ACC phosphorylation, and thus an increase in the activity of this enzyme. Accordingly, we found that ACC phosphorylation was also decreased by obestatin in this study. Based on it, increased ACC activity consequently leads to increased malonyl Co-A levels, which mediate an inhibitory effect on CPT-1, preventing fatty acid transport into mitochondria and fatty acid oxidation, promoting fatty acid synthesis[20]. Thus, Akt activation and AMPK inactivation seem to be inversely correlated during obestatin stimulation. This fact was confirmed *in vivo* in omental, subcutaneous and gonadal WAT obtained from male rats under continuous *sc* infusion of obestatin. This enzymatic activity favors fat deposition with the consequent inhibition of breakdown plus burning stored fat and reduction of body weight. Furthermore, obestatin works in a rapid, hormone-like manner, being its effect insulin independent.

This study demonstrates a novel role for obestatin as an adipogenic molecule. Based on the promoter role exerted by obestatin on insulin-induced adipogenesis and the fact that obestatin expression increased in adipocytes compared to preadipocyte cells, we postulated that obestatin might exert an autocrine/paracrine effect on the differentiation process. The fact that preproghrelin expression increased in the course of differentiation process being sustained throughout terminal differentiation of 3T3-L1 cells supports our hypothesis. Furthermore, preproghrelin knock-down experiments revealed its contribution to adipogenesis, although it would involve both ghrelin and obestatin. The implication of obestatin seems to be confirmed by neutralization of obestatin with specific antibody in 3T3-L1 cells that reduced their adipogenic potential. This is further supported by the effect of exogenous obestatin on the expression of master regulators of adipocyte fate, C/EBPβ, C/EBPδ, C/EBPα and PPARγ[21]. We can hypothesize that ghrelin and obestatin mutually contribute to adipogenesis as pro-adipogenic factors promoting lipogenesis. Indeed, it has been shown that ghrelin stimulates lipid accumulation *in vitro*[22,23], and *in vivo* [24,25]. Thus, the original concept that these two peptides derived from the same gene show opposite actions is not completely correct. Interestingly, ghrelin and obestatin knock-down by preproghrelin siRNA revealed a key contribution of both peptides to insulin-induced terminal adipogenesis suggesting that the insulin effect might be mediated by expression and secretion of both peptides on the late stage of adipogenesis.

The expression of GPR39 in 3T3-L1 cells and its expression changes during adipogenesis suggests its implication in adipocyte differentiation. This fits well with the expression pattern of GPR39 in mouse embryonic fibroblast cells during adipocyte differentiation[26]. This hypothesis seems to be consistent with the up-regulation of preproghrelin expression and, in consequence, with the increase of the biosynthesis and secretion of obestatin by adipocytes, which exerts a paracrine control on pre-adipocyte via a GPR39-dependent mechanism.

In summary, in this report we describe a novel role of obestatin in the autocrine/paracrine regulation of adipogenesis. The adipogenic role of obestatin is supported by: 1) the activation of Akt signalling, 2) the regulation of adipocyte metabolism and, 3) the inhibition of adipogenesis by disruption of preproghrelin or neutralization of obestatin. Intriguingly, circulating obestatin and ghrelin levels do not increase in obese subjects, a fact shared with ghrelin[27,28,29]. Therefore, neither obestatin nor ghrelin appear to be determinant in maintaining obesity. Nonetheless this fact does not rule out a function for obestatin in the development of obesity. In this sense, it is remarkable that the magnification of WAT is related to the development of the metabolic disorders, and the identification of factors that participate to this phenomenon would provide new aspects for the understanding of adipogenesis as well as the pathogenesis of obesity and associated comorbidities.

19. Alvarez, C. J. et al. Obestatin stimulates Akt signalling in gastric cancer cells through beta-arrestin-mediated epidermal growth factor receptor transactivation. *Endocr. Relat. Cancer*. 2009; 16: 599-611.
20. Munday, M. R. Regulation of mammalian acetyl-CoA carboxylase. *Biochem. Soc. Trans*. 2002; 30: 1059-64.
21. Rosen, E. D. et al. Adipocyte differentiation from the inside out. *Nat. Rev. Mol. Cell Biol*. 2006; 7: 885-96.
22. Kim, M. S. et al. The mitogenic and anti-apoptotic actions of ghrelin in 3T3-L1 adipocytes. *Mol. Endocrinol*. 2004; 18: 2291-301.
23. Rodríguez, A. et al. Acylated and desacyl ghrelin stimulate lipid accumulation in human visceral adipocytes. *Int. J. Obes*. 2009; 33: 541-52.
24. Davies, J. S. et al. Ghrelin induces abdominal obesity via GHS-R-dependent lipid retention. *Mol. Endocrinol*. 2009; 23: 914-24.
25. Wells T. Ghrelin—defender of fat. *Prog. Lipid. Res*. 2009; 48: 257-74.
26. Egerod, K. L. et al. GPR39 splice variants versus antisense gene LYPD1: expression and regulation in gastrointestinal tract, endocrine pancreas, liver, and white adipose tissue. *Mol. Endocrinol*. 2007; 21: 1685-8.
27. Vicennati, V. et al. Circulating obestatin levels and the ghrelin/obestatin ratio in obese women. *Eur. J. Endocrinol*. 2007; 157: 295-301.
28. Huda, M. S. et al. Plasma obestatin levels are lower in obese and post-gastrectomy subjects, but do not change in response to a meal. *Int. J. Obes*. 2008; 32: 129-35.
29. Zamrazilová, H. et al. Plasma obestatin levels in normal weight, obese and anorectic women. *Physiol. Res*. 2008; 57: S49-55.

CHAPTER 2

In this chapter, we have demonstrated that preproghrelin plays a critical role in the process of adipogenesis. We have shown that insulin-induced adipocyte conversion is impaired in the absence of preproghrelin. Furthermore, neutralization of preproghrelin-derived peptides displays defective accumulation of lipid droplets. Thus, preproghrelin is a key source of autocrine peptides involved in adipocyte differentiation. Furthermore, we have identified that preproghrelin and the enzymatic machinery associated to the processing of this peptide into UAG and AG are up-regulated during adipose conversion. This enzymatic system includes PC1/3, which cleaves after Arg. 28 of proghrelin leading to the production of the mature 28 amino acid peptide[30] and MBOAT4, a polytopic membrane-bound enzyme that attaches the octanoyl residue to Ser 3 in AG[31,32]. The changes in mRNA and protein expression were further associated with insulin action, although transcription and translation of these targets showed different regulatory systems. In addition, acute inhibition of mTORC1 activity in the presence of rapamycin led to decreased levels of these proteins. These data suggest the involvement of the mTORC1/S6K1 pathway in the regulation of preproghrelin, PC1/3, and MBOAT4 translation during the early steps of adipogenesis. This point disagree with the findings that inhibition of mTORC1 stimulates gastric and pancreatic preproghrelin expression[33,34]. Indeed, it is likely that the mTORC1/S6K1 pathway and preproghrelin interact in a tissue-specific manner. In addition, the type of pharmacological treatment, chronic versus acute, might also explain this paradigm. In this sense, it is important to note that chronic rapamycin treatment can inhibit both mTORC1 and mTORC2 activities[35,36].

The potential role of preproghrelin as source of auto/paracrine peptides has remained unstudied in adipose tissue, possibly as a result of the perception that preproghrelin is not substantially expressed in this tissue. As reported here and elsewhere[37,38], however, adipose tissue expresses relatively high levels of preproghrelin. This peptide undergoes stepwise processing to produce UAG, AG, and obestatin[39]. AG is widely known for its role in adipogenesis and lipid storage in WAT in both rodents[40] and humans[41]. By contrast, the role of UAG in adipogenesis is not clear, because there are reports showing that UAG suppressed adipogenesis and lipid accumulation[42,43], whereas others showed that UAG increased adipogenesis and lipid accumulation in both rodents[44] and human adipocytes[45]. In this study, we found that the net effect of these secreted preproghrelin- derived peptides favors adipocyte conversion. This fact appears to be a consequence of the Akt activation by both AG and obestatin in adipose tissue[46,47]. There is strong evidence, including results obtained from genetic mouse models, supporting the concept that Akt is a key node for regulation of the transcriptional program required for adipogenesis[48,49,50,51,52,53] .Interestingly, knock-down experiments by preproghrelin siRNA displayed defective adipocyte differentiation. We propose that insulin activates preproghrelin expression and consequent secretion of preproghrelin-derived peptides, which intensify insulin signalling to Akt in an autocrine manner in preadipocyte cells. The co-expression of GHSR1a and GPR39 supports this autocrine function. These peptides further determine the progressive expression of PC1/3 and MBOAT4 related to adipocyte differentiation defining the secretion rate between AG and UAG. Through a paracrine action, preproghrelin-derived peptides impact on adipocytes leading to Akt signalling favoring regulation processes such as hypertrophy. Thus, it is likely that the insulin effect is mediated by expression and secretion of these peptides on the late stage of adipogenesis.

30. Zhu, X. et al. On the processing of proghrelin to ghrelin. *J. Biol. Chem*. 2006, 281: 38867-70.
31. Gutierrez, J. A. et al. Ghrelin octanoylation mediated by an orphan lipid transferase. *PNAS*. 2008; 105: 6320-5.
32. Yang, J. et al. Identification of the acyltransferase that octanoylates ghrelin, an appetite-stimulating peptide hormone. *Cell*. 2008; 132: 387-96.
33. Xu, G. et al. Gastric mammalian target of rapamycin signalling regulates ghrelin production and food intake. *Endocrinology*. 2009; 150: 3637-44.
34. An, W. et al. Modulation of ghrelin O-acyltransferase expression in pancreatic islets. *Cell. Physiol. Biochem*. 2010; 26: 707-16.
35. Sarbassov, D. D. et al. Prolonged rapamycin treatment inhibits mTORC2 assembly and Akt/PKB. *Molecular Cell*. 2006; 22: 159-68.
36. Laplante, M. et al. mTOR signalling at a glance. *J. Cell Sci*. 2009; 122: 3589-94.
37. Gnanapavan, S. et al. The tissue distribution of the mRNA of ghrelin and subtypes of its receptor, GHS-R, in humans. *J. Clin. Endocrinol. Metab*. 2002; 87: 2988.
38. Knerr, I. et al. Leptin and ghrelin expression in adipose tissues and serum levels in gastric banding patients. *Eur. J. Clin. Invest*. 2006; 36: 389-94.
39. Zhu, X. et al. On the processing of proghrelin to ghrelin. *J. Biol. Chem*. 2006; 281: 38867-70.
40. Wells, T. Ghrelin - defender of fat. *Prog. Lipid Res*. 2009; 48: 257-74.
41. Rodriguez, A. et al. Acylated and desacyl ghrelin stimulate lipid accumulation in human visceral adipocytes. *Int. J. Obes.* 2009; 33(5): 541-52.
42. Delhanty, P. J. et al. Unacylated ghrelin rapidly modulates lipogenic and insulin signalling pathway gene expression in metabolically active tissues of GHSR deleted mice. *PLoS ONE*. 2010; 5: E11749.
43. Zhang, W. et al. Effect of des-acyl ghrelin on adiposity and glucose metabolism. *Endocrinology*. 2008; 149: 4710-16.
44. Thompson, N. M. et al. Ghrelin and des-octanoyl ghrelin promote adipogenesis directly in vivo by a mechanism independent of the type 1a growth hormone secretagogue receptor. *Endocrinology*. 2004; 145: 234-42.
45. Rodriguez, A. et al. Acylated and desacyl ghrelin stimulate lipid accumulation in human visceral adipocytes. *Int. J. Obes*. 2009; 33: 541-52.
46. Gurriarán-Rodríguez, U. et al. Obestatin as a regulator of adipocyte metabolism and adipogenesis. *J. Cell. Mol. Med.* 2011; 15: 1927–40.
47. Lodeiro, M. et al. c-Src regulates Akt signalling in response to ghrelin via beta-arrestin signalling-independent and -dependent mechanisms. *PLoS ONE*. 2009; 4: E4686.
48. Cho, H. et al. Akt1/PKBalpha is required for normal growth but dispensable for maintenance of glucose homeostasis in mice. *J. Biol. Chem.* 2001; 276: 38349-52.
49. Garofalo, R. S. et al. Severe diabetes, age-dependent loss of adipose tissue, and mild growth deficiency in mice lacking Akt2/PKB beta. *J. Clin. Invest*. 2003; 112: 197-208.
50. Xu, J. et al. Protein kinase B/Akt1 plays a pivotal role in insulin-like growth factor-1 receptor signalling induced 3T3-LI adipocyte differentiation. *J. Biol. Chem*. 2004; 279: 35914-22.
51. Manning, B. D. et al. Akt/PKB signalling: navigating downstream. *Cell*. 2007; 129: 1261-74.
52. Zhang, H. H. et al. Insulin stimulates adipogenesis through the Akt-TSC2- mTORC1 pathway. *PLoS ONE*. 2009; 4: E6189.
53. Berggreen, C. et al. Protein kinase B activity is required for the effects of insulin on lipid metabolism in adipocytes. *Am. J. Physiol. Endocrinol. Metab*. 2009; 296: E635-E646.

In agreement with our data obtained *in vitro*, where the expression of preproghrelin, PC1/3, and MBOAT4 was increased during adipogenesis, we found that, in both omental and subcutaneous fat of mice fed on HFD, the expression of these factors is higher than in the WAT of mice fed on SD. The only exception was the expression of preproghrelin in omental fat that remained unchanged between SD and HFD mice, indicating that preproghrelin is regulated in a fat depot-specific manner. Overall, our findings showing higher levels of preproghrelin-related factors in the WAT of animals where adipogenesis is stimulated suggest that preproghrelin, PC1/3, and MBOAT4 might play an important role in the accumulation of lipids during diet- induced obesity.

In summary, we have shown that insulin triggers the expression of preproghrelin, and have demonstrated that preproghrelin is a critical target for insulin-induced adipogenesis. The mechanisms of regulation of these targets by insulin await further investigation.

CHAPTER 3

We have shown that healthy skeletal muscle expresses obestatin and GPR39, and this expression strikingly increased upon muscle injury. *In vitro*, obestatin was preferentially expressed by L6E9 myotubes, whereas GPR39 was equally expressed in both myoblast and myotube cells. Expression of both obestatin and GPR39 was coordinately up-regulated during the early stages of myogenesis, and their levels remained sustained throughout terminal differentiation of L6E9 cells. Functionally, blocking obestatin during myogenesis induced a decrease in myogenic-associated markers (myogenin, MHC). Silencing of preproghrelin or GPR39 expression produced similar results. Obestatin stimulation of undifferentiated L6E9 cells promoted migration function and mitogenic activity of myoblasts. Furthermore, this peptide promoted myogenic differentiation, increasing the expression of myogenic markers. Additionally, these results were supported by *in vivo* testing of the gastrocnemius and soleus muscle obtained from male rats under continuous subcutaneous infusion of obestatin. The testing of this peptide showed an up-regulation of a set of transcription factors regulating myogenesis: (i) markers associated with satellite cell activation: Pax7 and Myf5; (ii) markers associated with early differentiation: MyoD, myogenin, and Myf6; and (iii) a marker associated with late differentiation: MHC. Altogether, these observations demonstrated that the obestatin/GPR39 system is involved in myogenesis and that obestatin is expressed by differentiating myogenic precursors to function in an autocrine manner.

After injury, SCs are activated and enter the cell cycle to proliferate, and eventually, they fuse to replace degenerated muscle fibers, preserving muscle structure and function. Several signals, derived both from damaged fibers and from infiltrating cells, are involved in SCs activation[54,55]. From the data presented thus far, obestatin should be incorporated into the list of myogenic regulatory factors derived from damaged fibers. Based on its overexpression in muscle injury, its up-regulation during myogenesis, and its promoter role on myogenic differentiation and fusion of L6E9 cells, it is possible to speculate that obestatin exerts an autocrine effect on the skeletal myogenic process. The fact that preproghrelin expression increased in the course of differentiation and remained sustained throughout terminal differentiation of L6E9 cells supports this hypothesis. Furthermore, preproghrelin knock-down experiments uncovered its contribution to myogenesis, although it would implicate both ghrelin and obestatin. The myogenic role of obestatin is supported by neutralization of this peptide with a specific antibody in L6E9 cells, which reduced its myogenic potential through myogenin and MHC down-regulation. Further support for a myogenic role for obestatin is demonstrated by the effect on the activation and proliferation of myoblasts, with the resulting growth arrest by contact and initiation of myogenesis, *e.g.* myogenesis activation of proliferating myoblasts in GM. The increased expression of myogenic regulator factors, Pax7, Myf5, MyoD, myogenin, Myf6, and MHC[56], associated with subcutaneous infusion of obestatin in rats reinforces this suggestion. Considering the myogenic characteristics of ghrelin and des-acyl ghrelin previously described[57], we hypothesized that preproghrelin-derived peptides mutually contribute to myogenesis as pro-myogenic factors, as corroborated by the mitogenic and myogenic roles for ghrelin and obestatin described in the present work. Although the myogenic characteristics of ghrelin found in this study are in agreement with previous works[58], the mitogenic action of ghrelin appears to be in contradiction with a previous study showing inhibition of C2C12 myoblast cells[59]. Even if the role of ghrelin and des-acyl ghrelin in mitogenesis remains unclear and varies depending on the nature of the study, the myogenic properties of preproghrelin-derived peptides reinforce our hypothesis.

Obestatin has multiple functional properties, and its capacity to stimulate myoblast migration, proliferation, and differentiation *in vitro* is particularly interesting. In L6E9 myoblasts, obestatin was shown to enhance ERK, Akt, and p38 activities. These pathways are activated by regeneration signals and demonstrate the ability of muscle progenitors to execute different stages of the regeneration program: (*a*) the ERK/MAPK pathway activates cell migration and proliferation[60,61]; (*b*) the Akt pathway promotes cell proliferation, survival, and differentiation[62]; and (*c*) the p38 pathway stimulates cell cycle arrest and terminal differentiation[63]. The convergence of these pathways at the chromatin level defines the mechanism for integration of mitogenic and myogenic signals to direct the transition from quiescence to terminal differentiation[64]. Thus, the range of obestatin functions, together with its expression in normal and regenerating

54. Chargé, S. B. et al. Cellular and molecular regulation of muscle regeneration. *Physiol. Rev*. 2004; 84: 209-38.
55. Ten Broek, et al. Regulatory factors and cell populations involved in skeletal muscle regeneration. *J. Cell. Physiol*. 2010; 224: 7-16.
56. Braun,T. et al. Transcriptional mechanisms regulating skeletal muscle differentiation, growth, and homeostasis. *Nat. Rev. Mol. Cell Biol*. 2011; 12: 349-61.
57. Filigheddu, N. et al. Ghrelin and des-acyl ghrelin promote differentiation and fusion of C2C12 skeletal muscle cells. *Mol. Biol. Cell*. 2007; 18: 986-94.
58. Filigheddu, N. et al. Ghrelin and des-acyl ghrelin promote differentiation and fusion of C2C12 skeletal muscle cells. *Mol. Biol. Cell*. 2007; 18: 986-94.
59. Filigheddu, N. et al. Ghrelin and des-acyl ghrelin promote differentiation and fusion of C2C12 skeletal muscle cells. *Mol. Biol. Cell*. 2007; 18: 986-94.
60. Mourkioti, F. et al. IGF-I, inflammation, and stem cells: interactions during muscle regeneration. *Trends Immu*nol. 2005; 26: 535-42.
61. Leloup, L. et al. Involvement of the ERK/MAP kinase signalling pathway in milli-calpain activation and myogenic cell migration. *Int. J. Biochem. Cell Biol*. 2007; 39: 1177-89.
62. Wu, M. et al. Akt/protein kinase B in skeletal muscle physiology and pathology. *J. Cell Physiol*. 2011; 226: 29-36.
63. Lluís, F. et al. Regulation of skeletal muscle gene expression by p38 MAP kinases. *Trends Cell Biol*. 2006; 16: 36-44.
64. Serra, C. et al. Functional interdependence at the chromatin level between the MKK6/p38 and IGF1/PI3K/Akt pathways during muscle differentiation. *Mol. Cell*. 2007; 28: 200-13.

skeletal muscle, is consistent with a role in regulating myofiber formation and homeostasis. In this regard, obestatin shows functional similarity with IGF-I and IGF-II, because both factors have the capacity to promote both proliferation and differentiation of muscle cells[65,66].

Silencing of GPR39 expression in L6E9 myoblast cells demonstrated that this G protein-coupled receptor is the extracellular target for obestatin action. Although there is ongoing controversy regarding GPR39[67,68], our findings on L6E9 myoblasts are consistent with the role of this receptor on obestatin signalling in preadipocyte 3T3-L1 cells[69,70] and in gastrointestinal and adipose tissues[71]. The expression of GPR39 in L6E9 cells and its changes during myogenesis further suggest a role for GPR39 in this process. Definitive evidence for the requirement of GPR39 in myogenesis came from the observation that its knock-down by siRNA significantly diminished the myogenic capacity of L6E9 cells. Furthermore, the preproghrelin expression up-regulation and, as a consequence, the increase of obestatin biosynthesis and secretion by myotubes, together with its faint expression in myoblasts, lead us to speculate that obestatin might exert a paracrine role on myoblasts via a GPR39-dependent mechanism. Similarly, the obestatin/GPR39 system exerts an autocrine/paracrine control on adipogenesis[72]. Combined, these all point to the role of obestatin/GPR39 signalling as a key component for proper skeletal and adipose tissue development. In fact, our results underscored a key role for pre-proghrelin-derived peptides on adipogenesis through an autocrine/paracrine mechanism as well[73].

Male rats under continuous subcutaneous infusion of obestatin showed a modified expression of transcription factors that regulate the progression through the myogenic lineage in soleus and gastrocnemius muscle tissue. Up-regulation of Pax7 expression might be indicative of a control on satellite cell activation to enhance myogenic specification and/or to induce self-renewal[74,75]. It is known that this transcription factor is maintained in satellite cells and proliferating myoblasts but is down-regulated before differentiation[76,77]. Furthermore, the expression of myogenic regulatory factors is coordinated by this factor. Indeed, up-regulation of MyoD and Myf5 was observed in obestatin-treated rats, denoting the conversion of satellite cells into myoblast[78], although it is not possible to rule out a role for this peptide in the replenishment of the satellite cell pool. MyoD and Myf5 are required for the expression of myogenic precursors and act upstream of Myf6 and myogenin. Accordingly, Myf6 and myogenin were up-regulated, denoting myoblast differentiation[79]. Moreover, MHC was observed to be up-regulated, as an indication of myogenic differentiation. Additionally, obestatin was shown to increase the expression of VEGF and VEGFR-2 in this tissue. Conversely, PEDF expression was down-regulated. The expression and role of VEGF as an autocrine myogenic factor in muscle was previously described. Furthermore, VEGFR2 was shown to be up-regulated during myogenic differentiation[80]. In addition to its myogenic action, it is important to note its known angiogenic role[81]. This latter effect is important in attracting distant vessels to the myoblast differentiation sites. This implies that VEGF, produced by differentiating myocytes, provides the needed vascularization of developing skeletal muscle. This is further supported by down-regulation of the anti-angiogenic factor PEDF[82]. All together, our data support the view that obestatin regulates the "hierarchy" of transcription factors involved in the control of the different stages of the myogenic program, including activation, proliferation, and differentiation, exerting a role in the expression of VEGF/ VEGFR2 for the potential regulation of the angiogenic process in skeletal muscle tissue.

In summary, we propose that the obestatin/GPR39 system signalling is involved in muscle regeneration, in which obestatin exerts an autocrine function to control the myogenic differentiation program, thereby implicating its potential for use as a therapeutic agent for the treatment of trauma-induced muscle injuries or skeletal muscle myopathies.

65. Mourkioti, F. et al. IGF-I, inflammation, and stem cells: interactions during muscle regeneration. *Trends Immunol*. 2005; 26: 535-42.
66. Matheny, R. W. et al. Minireview: Mechano-growth factor: a putative product of IGF-I gene expression involved in tissue repair and regeneration. *Endocrinology*. 2010; 151: 865-75.
67. Chartrel, N. et al. Comment on "Obestatin, a peptide encoded by the ghrelin gene, opposes ghrelin's effects on food intake". *Science*. 2007; 315: 766.
68. Holst, B. et al. GPR39 signalling is stimulated by zinc ions but not by obestatin. *Endocrinology*. 2007; 148: 13-20.
69. Gurriarán-Rodríguez, U. et al. Obestatin as a regulator of adipocyte metabolism and adipogenesis. *J. Cell. Mol. Med.* 2011; 15: 1927–40.
70. Gurriarán-Rodríguez, U. et al. Obestatin as a regulator of adipocyte metabolism and adipogenesis. *J. Cell. Mol. Med.* 2011; 15: 1927–40.
71. Zhang, J. V. et al. Obestatin induction of early-response gene expression in gastrointestinal and adipose tissues and the mediatory role of G protein-coupled receptor, GPR39. *Mol. Endocrinol*. 2008; 22: 1464-75.
72. Gurriarán-Rodríguez, U. et al. Obestatin as a regulator of adipocyte metabolism and adipogenesis. *J. Cell. Mol. Med.* 2011; 15: 1927–40.
73. Gurriarán-Rodríguez, U. et al. Obestatin as a regulator of adipocyte metabolism and adipogenesis. *J. Cell. Mol. Med.* 2011; 15: 1927–40.
74. Wang, Y. X. et al. Satellite cells, the engines of muscle repair. *Nat. Rev. Mol. Cell Biol*. 2012; 13: 127-33.
75. Olguin, H. C. et al. Pax7 up-regulation inhibits myogenesis and cell cycle progression in satellite cells: a potential mechanism for self-renewal. *Dev. Biol*. 2004; 275: 375-88.
76. Hu, P. et al. Codependent activators direct myoblast-specific MyoD transcription. *Dev. Cell*. 2008; 15: 534-46.
77. McKinnell, I. W. et al. Pax7 activates myogenic genes by recruitment of a histone methyltransferase complex. *Nat. Cell Biol*. 2008; 10: 77-84.
78. Bentzinger, C.F. et al. Building muscle: molecular regulation of myogenesis. *Cold Spring Harb. Perspect. Biol*. 2012; 4:1-16.
79. Tedesco, F. S. et al. Repairing skeletal muscle: regenerative potential of skeletal muscle stem cells. *J. Clin. Invest*. 2010; 120: 11-9.
80. Bryan, B. A. et al. Coordinated vascular endothelial growth factor expression and signalling during skeletal myogenic differentiation. *Mol. Biol. Cell*. 2008; 19: 994-1006.
81. Patel-Hett, S. et al. Signal transduction in vasculogenesis and developmental angiogenesis. *Int. J. Dev. Biol*. 2011; 55: 353-63.
82. Ek, E. T. et al. PEDF: a potential molecular therapeutic target with multiple anti-cancer activities. *Trends Mol. Med*. 2006; 12: 497-02.

CHAPTER 4

In this study, we described that obestatin controls the signalling pathway associated to glucose uptake in skeletal muscle. In L6E9 myotube cells, obestatin activated Akt phosphorylation and its downstream targets, GSK3α/β, S6K1 and inhibited AMPK activity. This fact was confirmed *in vivo* in gastrocnemius and soleus obtained from male rats under continuous *sc* infusion of obestatin. The significance of obestatin as regulator of myotubes metabolism was also supported by AS160 phosphorylation, GLUT4 translocation to plasma membrane and augment of glucose uptake *in vitro* in L6E9 myotube cells. This effect was further confirmed *ex vivo* in soleus and gastrocnemius muscles.

There are two major signalling pathways that participate in glucose transport in skeletal muscle. One is the Akt signalling pathway, and the other is the AMPK signalling pathway[83]. Whether crosstalk exists between these two signalling pathways is still unclear. In this study, we showed that obestatin-stimulated glucose uptake appears to be dependent on Akt activation hence obestatin triggered AMPK inactivation through dephosphorylation at Thr 172 from α subunit. Akt is known to stimulate glucose uptake by GLUT4 trafficking through GAP known as AS160[84]. Our results showed that obestatin increased AS160 phosphorylation on Thr 642, consistent with Akt mediating obestatin-induced phosphorylation. AS160 phosphorylation suppresses its GAP activity, shifting the equilibrium of its targets Rab(s) to an active GTP form, enabling it to mediate GLUT4 trafficking[85]. Certainly, an increase in GLUT4 membrane translocation and glucose transport was observed in L6E9 myotubes after obestatin treatment, although in smaller extension to that of insulin. By contrast, obestatin failed to regulate GLUT1 translocation in L6E9 myotubes, likely due to GLUT1 is more implicated in the control of glucose basal metabolism, and in overfeeding conditions is GLUT4 the transporter that mediates the glucose uptake[86]. Likewise, in the soleus and gastrocnemius muscles, there was an increased in muscle glucose uptake after obestatin treatment, the quantitative differences between both muscle types, may be due to the diverse type of fiber pattern, that is intimately correlated with the metabolism type[87]. In addition, obestatin showed to regulate mTORC1/S6K1 signalling, a critical element integrating cellular metabolism with growth factor signalling[88]. mTORC1 controls many aspects of cellular metabolism including skeletal muscle tissue metabolism[89]. One of the consequence of the increased glucose uptake in skeletal muscle mass is the cell mass increase which leads to hypertrophy in skeletal muscle fibers[90]. It has been described that *in vivo* muscle-specific overexpression of constitutively active Akt1 or Akt2 results in increased mTORC1/S61 activity, glycogen accumulation, and muscle fiber hypertrophy[91], as well as the opposite effect was reached after double-knockout of Akt1 and Akt2; these mice display severe skeletal muscle atrophy (50% decrease in muscle mass), mainly due to markedly decreased individual muscle fiber size[92].

In the cytoplasm, glucose is converted to glucose 6-phosphate that can be stored by conversion to glycogen or catabolized by glycolysis, both processes under the control of Akt signalling [93]. In this sense, obestatin inactivated GSK3α/β, an Akt substrate, through phosphorylation in L6E9 myotube cells. This inactivation leads to inactivation of GS, leading to glycogen synthesis and storage[94]. After obestatin treatment, L6E9 myotubes enhanced GSK3α/β phosphorylation, thereby stimulating glycogen synthesis. Parallel to Akt activation, AMPK inactivation was triggered by obestatin *in vivo* and *in vitro*. The decline in AMPK activation would be expected to lead to an increase in ACC activity. Indeed, it was found that ACC phosphorylation was decreased by obestatin. Based on it, decreased AMPK activity and increased ACC activity consequently leads to switch on anabolic pathways that consume ATP, such as synthesis of glycogen and protein, and to switch off catabolic pathways that generate ATP, such as lipid oxidation and glucose

83. Russell, R.R. et al. Translocation of myocardial GLUT-4 and increased glucose uptake through activation of AMPK by AICAR. *Am. J. Physiol.* 1999; 277(2): 643-9.
84. Eguez, L. et al. Full intracellular retention of GLUT4 requires AS160 Rab GTPase activating protein. *Cell Metab.* 2005; 2: 263-72.
85. Zaid H, et al. Insulin action on glucose transporters through molecular switches, tracks and tethers. *Biochem. J.* 2008; 413: 201-15.
86. Joost, H, et al. The extended GLUT-family of sugar/polyol transport facilitators: nomenclature, sequence characteristics, and potential function of its novel members. *Mol. Membr. Biol*. 2001; 18 (4): 247-56.
87. Henriksen, E.J. et al. Glucose transporter protein content and glucose transport capacity in rat skeletal muscles. *Am. J. Physiol.* 1990; 259(4): 593-8.
88. Um, S. H. et al. Nutrient overload, insulin resistance, and ribosomal protein S6 kinase 1, S6K1. *Cell Metab*. 2006; 3: 393-402.
89. Zoncu, R. et al. mTOR: from growth signal integration to cancer, diabetes and ageing. *Nat. Rev. Mol. Cell. Biol.* 2011 ;12(1):21-35.
90. Miaozong, W. et al. Akt/Protein Kinase B in skeletal muscle physiology and pathology. *J. Cell. Physiol.* 2010; 226: 29-36.
91. Cleasby, M. E. et al. Functional studies of Akt isoform specificity in skeletal muscle in vivo; maintained insulin sensitivity despite reduced insulin receptor substrate-1 expression. *Mol. Endocrinol.* 2007; 21: 215-28.
92. Peng, X. D. et al. Dwarfism, impaired skin development, skeletal muscle atrophy, delayed bone development, and impeded adipogenesis in mice lacking Akt1 and Akt2. *Genes Dev.* 2003; 17: 1352-65.
93. Manning, B. D. et al. Akt/PKB signalling: navigating downstream. *Cell*. 2007; 129: 1261-74.
94. Jørgen, F. P. et al. Invited Review: Effect of acute exercise on insulin signalling and action in humans. *J. Appl. Physiol*. 2002; 93: 384-92.

oxidation[95,96,97,98]. Therefore, Akt activation and AMPK inactivation seem to be inversely correlated during obestatin stimulation.

In summary, we described that obestatin is implicated in the regulation of glucose uptake in skeletal muscle. This role is supported by the activation of Akt signalling and the regulation of membrane translocation of GLUT4.

95. Zhang, B.B. et al. AMPK: an emerging drug target for diabetes and the metabolic syndrome. *Cell Metab*. 2009; 9(5): 407-16.
96. Long, Y.C. et al. AMP-activated protein kinase signalling in metabolic regulation. *J.Clin. Invest*. 2006;116(7):1776-83.
97. Hardie, D. G . et al. AMPK: a key regulator of energy balance in the single cell and the whole organism. *Int. J. Obes*. 2008; 32 (4): S7-12.
98. O´Neill, H. M. et al. AMPK regulation of fatty acid metabolism and mitochondrial biogenesis: Implications for obesity. *Mol. Cel. Endocrinology*. 2013; 366: 135-51.

CHAPTER 5

The obestatin/GPR39 system has been demonstrated to regulate the myogenic program. Such function is result of its autocrine role in the regulation of transcription factors involved in the control of the different stages of myogenesis. In this study, we further demonstrated that obestatin augments regeneration by stimulating SCs expansion as well as myofiber hypertrophy after muscle injury.

In response to obestatin the hierarchy of transcription factors regulating progression through the myogenic lineage was clearly increase. This is endorsed by the increased expression of myogenic regulator factors, Pax7, MyoD, myogenin, and MHC, demonstrating the myogenic potential for this peptide when it is administrated into injured muscle. SCs number increased on muscle sections as well as in myofibers obtained from obestatin-treated muscles 96 h after injury. The increased SCs proliferation was concomitant with enhanced tissue expression of Ki67, a proliferating cell marker, and cyclin D1, a well-known effector of the G1 to S cell cycle phase transition, 96 h after injury. In addition, Pax7 coordinates the expression of myogenic regulatory factors. Indeed, up-regulation of MyoD was observed in obestatin-treated mice, indicating the conversion into myoblasts. Furthermore, MyoD determines the expression of myogenic precursors acting upstream of myogenin. Accordingly, myogenin was up-regulated, implying myoblast differentiation. MyoD and myogenin act together to drive differentiation[99]. In this process, the expression of embryonic/developmental forms of MHC was observed to be enhanced denoting terminal myogenic differentiation. Further support was demonstrated by enhancement of the myogenic markers by *in vivo* overexpression of preproghrelin during muscle regeneration. However, it would implicate the mutual contribution of the known preproghrelin-derived peptides, ghrelin and obestatin[100,101,102]. Importantly, *in vivo* co-overexpression of GPR39 and preproghrelin during muscle regeneration resulted in an larger enhancement of the myogenic markers compared to that obtained from GPR39 or preproghrelin overexpression alone.

At the end of muscle regeneration, obestatin showed to increase the area of newly formed muscle fiber. However, muscle function is not only proportional to the muscle size but also depends on the myonuclei density in each myofiber, which is determined by SCs differentiation and fusion. In this sense, obestatin also promoted augment the number of myonuclei in agreement with the regulation of satellite cell activity. This duality might be interpreted as a result of elevated proliferation of satellite cell proliferation would provide an elevated potential for transcription and ultimately greater protein translation with little alteration in the kinetics of protein synthesis, leading to muscle hypertrophy. However, the role of SCs in the hypertrophy response is unclear[103]. In various experimental models, hypertrophy response was observed with no SCs incorporation[104,105]. On the other hand, several studies demonstrated the contribution of satellite cells to hypertrophy response in adult muscles[106,107]. In our particular case, the data obtained from obestatin stimulation 3 days after C2C12 differentiation or in AraC-treated cultures displayed similar enhancement of myofiber area and fusion. Furthermore, the protein expression of myogenin and MHC was not affect by AraC treatment. Therefore, the hypertrophic response to obestatin is not associated with and dependent on the addition of new myonuclei via proliferation and further fusion. The degree of muscle hypertrophy is strongly associated with the degree of Akt/mTOR/S6K1 activation[108,109], a pathway activated by obestatin during the distinct skeletal muscle regeneration processes or the differentiation program. This pathway controls mechanisms of protein synthesis at several stages (e.g., translation capacity, translation efficiency) through increases of translation of specific mRNAs, which terminate in myotube and fiber enlargement. Thus, we show that obestatin controls distinct stages from the myogenic program: proliferation, differentiation, myoblast fusion and hypertrophy response. These roles suggest different mechanisms of action in the processes associated to the skeletal muscle regeneration.

In addition to the myogenic action, obestatin showed to regulate the expression of factors that define the regenerative microenvironment responsible for stimulating and coordinating skeletal muscle repair. Obestatin showed to increase the expression of VEGF and its receptor isoform VEGF-R2 during muscle regeneration. In addition to its myogenic action[110], VEGF showed to stimulate muscle healing

99. Yin, H. et al. Satellite cells and the muscle stem cell niche. *Physiol. Rev.* 2013; 93(1):23-67.
100. Gurriarán-Rodríguez, U. et al. The obestatin/GPR39 system is up-regulated by muscle injury and functions as an autocrine regenerative system. *J. Biol. Chem.* 2012; 287(45): 38379-89.
101. Filigheddu, N. et al. Ghrelin and des-acyl ghrelin promote differentiation and fusion of C2C12 skeletal muscle cells. *Mol. Biol. Cell*. 2007; 18: 986–94.
102. Porporato, P.E. et al. Acylated and unacylated ghrelin impair skeletal muscle atrophy in mice. *J. Clin. Invest*. 2013;123(2):611-22.
103. O'Connor, R. S. et al. Last word on point: counterpoint: satellite cell addition is/is not obligatory for skeletal muscle hypertrophy *J. Appl. Physiol*. 2007;103:1107.
104. McCarthy, J. J. et al. Effective fiber hypertrophy in satellite cell-depleted skeletal muscle. *Development*. 2011; 138: 3657–66.
105. Wang, Q. et al. Myostatin inhibition induces muscle fibre hypertrophy prior to satellite cell activation *J. Physiol*. 2012; 590: 2151–65.
106. Guerci, A. et al. Srf-dependent paracrine signals produced by myofibers control satellite cell-mediated skeletal muscle hypertrophy. *Cell Metab*. 2012;15(1): 25-37.
107. Serrano, A. L. et al. Interleukin-6 is an essential regulator of satellite cell-mediated skeletal muscle hypertrophy. *Cell Metab*. 2008; 33-44.
108. Lee, C.H. et al. mTOR pathway as a target in tissue hypertrophy. *Annu. Rev. Pharmacol. Toxicol.* 2007; 47:443-67.
109. Glass, D. J. Skeletal muscle hypertrophy and atrophy signalling pathways. *Int. J. Biochem. Cell. Biol*. 2005; 37(10): 1974-84.
110. Bryan, B. A. et al. Coordinated vascular endothelial growth factor expression and signalling during skeletal myogenic differentiation. *Mol. Biol. Cell.* 2008; 19: 994 –1006.

by promoting angiogenesis[111,112,113]. In particular, VEGF produced by differentiating myocytes, provides the needed vascularization of developing skeletal muscle. Our results further indicated that obestatin-treated injured muscles increased capillary density being indicative of enhanced microvascularization. These new developed capillaries, sprout out from peripheral surviving capillaries, would help to provide the injured area with oxygen and substrates aiding in the regenerative process. Added to vascularization, obestatin treatment did not increase collagen deposition in regenerating muscle ruling out a fibrotic response. Thus, the enhancement of vascularization through the expression of the VEGF/VEGFR2 system and a normal accumulation of fibrous connective tissue contribute to the regenerative role of obestatin.

Obestatin reduced the expression of the endogenous muscle growth regulator myostatin. One mechanism by which myostatin regulates muscle growth appears to be direct inhibition of the proliferation and differentiation of SCs[114,115,116]. However, myostatin not only regulates the growth of myocytes but also directly regulates muscle fibrosis through stimulation of muscle fibroblasts and expression of extracellular matrix protein such as collagen[117]. Therefore, it is reasonable to expect that, in addition to its own myogenic effect, obestatin has the potential to increase muscle regeneration through a regulatory role on myostatin expression.

One of the most remarkable observations from this study was that obestatin has multiple functional properties associated to skeletal muscle regeneration, and its capacity to stimulate myoblast proliferation, differentiation, myoblast fusion and hypertrophy response is under regulation of a kinase hierarchy. In C2C12 differentiating myoblasts, obestatin showed to enhance ERK, Akt, CamkII and p38 activities. These pathways displayed the ability to execute different stages of the regeneration program. The ERK1/2 belongs to a well-defined pathway, which is critical for cellular proliferation and migration[118]. In the context of obestatin-induced activity, ERK does initially decrease with myoblast differentiation, which is necessary for differentiating myoblasts to overcome its inhibitory effect. In fact, ERK was showed to inhibit differentiation by preventing the nuclear accumulation of members of the myocyte enhancer factor-2 (MEF2)[119], and the expression of certain myogenic factors, including MyoD[120] and the CDK inhibitor p21[121]. CamkII signalling prevents formation of MEF2–HDAC complexes by phosphorylation of HDAC4/HDAC5, promoting nuclear export of these transcriptional repressors and rising MEF2 activity on muscle specific genes such as MyoD and myogenin[122]. In particular the faster activation of CamKII by obestatin (≥12 h), compared with that of control (≥144 h), is not consistent with an earlier expression response to obestatin of myogenin, compared with control. This reflects additional roles for CamKII in the obestatin-regulated signalling during differentiation. In this sense, it is possible to speculate about the role of this kinase in the regulation of cell cycle, and hence, controlling proliferative step during differentiation. This is based on role described on G2/M and the metaphase-anaphase transition[123]. The Akt pathway has emerged as a critical signalling node within myogenic program. Consequences of Akt activation include diverse responses, ranging from primarily metabolic functions such as glucose transport, glycolysis, glycogen synthesis and the suppression of gluconeogenesis to protein synthesis, increased cell size, cell-cycle progression and apoptosis suppression[124]. Obestatin showed to increase activated levels of Akt during myogenesis, from proliferating to differentiating cells. The wide range of cellular functions mediated by this kinase is related to the different Akt isoforms. Thus, Akt1 was described essential early in differentiation leading to cell cycle progression[125]. By contrast, Akt2 triggers myoblast cell cycle exit and drives differentiation determining myotube maturation[126]. Following commitment to differentiation, the hypertrophic muscle growth induced by obestatin might be under regulation of the downstream effectors of the Akt pathway, FoxO1 and FoxO3a[127]. Indeed, obestatin

111. Patel-Hett, S. et al. Signal transduction in vasculogenesis and developmental angiogenesis. *Int. J. Dev. Biol.* 2011; 55: 353-63.
112. Deasy, B.M. et al. Effect of VEGF on the regenerative capacity of muscle stem cells in dystrophic skeletal muscle. *Mol. Ther.* 2009 ;17(10):1788-98.
113. Messina, S. et al. VEGF overexpression via adeno-associated virus gene transfer promotes skeletal muscle regeneration and enhances muscle function in mdx mice. *FASEB J.* 2007;21(13):3737-46.
114. McCroskery, S. et al. Myostatin negatively regulates satellite cell activation and self-renewal. *J. Cell. Biol*. 2003;162(6):1135-47.
115. Wagner, K.R. et al. Muscle regeneration in the prolonged absence of myostatin. *Proc. Natl. Acad. Sci. U S A*. 2005; 102(7): 2519-24.
116. Schuelke, M. et al. Myostatin mutation associated with gross muscle hypertrophy in a child. *N. Engl. J. Med*. 2004; 350(26):2682-8.
117. Bo Li, Z. et al. Inhibition of myostatin reverses muscle fibrosis through apoptosis. *J. Cell Sci*. 2012; 125(17): 3957-65.
118. Leloup, L. et al. Involvement of the ERK/MAP kinase signalling pathway in milli-calpain activation and myogenic cell migration. *Int. J. Biochem. Cell Biol.* 2007; 39: 1177–89.
119. Winter, B. et al. Activated raf kinase inhibits muscle cell differentiation through a MEF2-dependent mechanism. *J. Cell. Sci.* 2000;113 (23):4211-20.
120. Gredinger, E. et al. Mitogen-activated protein kinase pathway is involved in the differentiation of muscle cells. *J. Biol. Chem*. 1998; 273(17): 10436-44.
121. Wu, Z. et al. p38 and extracellular signal-regulated kinases regulate the myogenic program at multiple steps. *Mol. Cell Biol*. 2000; 20(11): 3951-64.
122. Scicchitano, B. M. et al. Vasopressin-dependent myogenic cell differentiation is mediated by both Ca2+/calmodulin-dependent kinase and calcineurin pathways. *Mol. Biol. Cell.* 2005; 16(8): 3632-41.
123. Skelding, K. A. et al. Controlling the cell cycle: the role of calcium/calmodulin-stimulated protein kinases I and II. *Cell Cycle*. 2011; 10(4): 631-9.
124. Wu, M. et al. Akt/protein kinase B in skeletal muscle physiology and pathology. *J. Cell Physiol.* 2007; 226: 29 –36.
125. Rotwein, P. et al. Distinct actions of Akt1 and Akt2 in skeletal muscle differentiation. *J. Cell. Physiol*. 2009; 219(2): 503-11.
126. Héron-Milhavet, L. et al. Only Akt1 is required for proliferation, while Akt2 promotes cell cycle exit through p21 binding. *Mol. Cell. Biol*. 2006; 26(22): 8267-80.
127. Glass, D. J. et al. Skeletal muscle hypertrophy and atrophy signalling pathways. *Int. J. Biochem. Cell. Biol*. 2005;37(10):1974-84.

increased S6K1 activity, a key downstream signalling effector of Akt/mTOR for regulation of muscle cytoplasmic volume[128]. Other effectors of the Akt/mTOR, such as FoxO transcription factors might contribute to control obestatin-induced growth. The obestatin-induced inactivation of FoxO1 and FoxO3a by phosphorylation could justify such a function[129,130,131].The relative contribution of this pathway for the control of muscle cytoplasmic volume by obestatin remains lower than the contribution by S6K1. p38 kinase activity increased over the course of differentiation under obestatin treatment that fit well with the established role of this kinase in skeletal myogenesis. In fact, p38 stimulates cell cycle arrest and full myoblasts differentiation through the control of muscle-specific gene expression[132,133 ,134,135] . Our results further show that obestatin mediates cessation of the JNK/cJun proliferation-promoting pathway[136], which is a prerequisite for the commencement of the differentiation program. Interestingly, decreased activation of the JNK/cJun pathway was concomitant to p38 activation in differentiation-promoting conditions under obestatin treatment. The convergence of these pathways at the chromatin level defines the mechanism for integration of mitogenic and myogenic signals to direct the transition from quiescence to terminal differentiation[137]. Therefore, obestatin action is a highly coordinated process in which various signalling pathways integrate to activate a specific gene expression program associated to each stage of myofiber formation process.

Once obestatin activates GPR39, two routes are triggered in parallel: 1) a Gi-dependent, ERK1/2 activation; and ii) a β-arrestin 1-mediated signalling pathway causing Akt phosphorylation[138,139]. Akt activation is switched by cross-activation of receptor tyrosine kinases (RTKs), i.e. EGFR (REF). In skeletal muscle, obestatin showed to cross-activate IGFR, one of the main regulators of muscle mass by stimulating the Akt/mTOR pathway[140]. Under these conditions there was a substantial increase of the IRS-1 phosphorylation at S636/639, sites shown to inhibit PI3K binding to IRS-1[141] and thus the Akt/mTOR signalling associated to IGFR. At present, it is well documented that S6K1 is implicated in a negative feedback loop on IRS-1 S636/639 phosphorylation to suppress PI3K signalling[142,143]. Consistent with this finding, our results for obestatin showed that the increase of pS6K1(T389) levels paralleled to the enhance in pIRS-1(S636/639). Under these conditions, the S6K1 activation impaired IRS-1/PI3K signalling decreasing Akt associated signalling to IGFR. Thus, despite the cross-activation of IGFR by GPR39, the negative feedback loop from S6K1 to IRS-1 rules out the implication of IGFR/IRS-1 in the obestatin-induced Akt/mTOR signalling. Therefore, obestatin induces hypertrophy independent of IGFR/IRS-1 activity.

This study suggests that obestatin is an important therapeutic approach to stimulate muscle regeneration. The ability to increase muscle regeneration and hypertrophic muscle growth together with its role on vascularization and regulation of fibrosis, making obestatin a promising therapeutic candidate for treatment of trauma-induced muscle injuries or skeletal muscle myopathies.

128. Ohanna, M. et al. Atrophy of S6K1(-/-) skeletal muscle cells reveals distinct mTOR effectors for cell cycle and size control. *Nat. Cell Biol*. 2005; 7(3): 286-94.
129. Sandri, M. et al. Foxo transcription factors induce the atrophy-related ubiquitin ligase atrogin-1 and cause skeletal muscle atrophy. *Cell*. 2004; 117(3): 399-412.
130. Stitt, T. N. et al.The IGF-1/PI3K/Akt pathway prevents expression of muscle atrophy-induced ubiquitin ligases by inhibiting FOXO transcription factors. *Mol. Cell*. 2004; 14(3): 395-403.
131. Glass, D. J. et al. Skeletal muscle hypertrophy and atrophy signalling pathways. *Int. J. Biochem. Cell. Biol.* 2005; 37(10): 1974-84.
132. Keren, A. et al. The p38 MAPK signalling pathway: a major regulator of skeletal muscle development. *Mol.Cell. Endocrinol*. 2006; 252(1-2): 224-30.
133. Lluís, F. et al. Regulation of skeletal muscle gene expression by p38 MAP kinases. *Trends Cell. Biol.* 2006; 16(1): 36-44.
134. Perdiguero, E. et al. Genetic analysis of p38 MAP kinases in myogenesis: fundamental role of p38alpha in abrogating myoblast proliferation. *EMBO J.* 2007; 26(5): 1245-56.
135. Perdiguero, E. et al. Genetic deficiency of p38alpha reveals its critical role in myoblast cell cycle exit: the p38alpha-JNK connection. *Cell Cycle*. 2007; 6(11):1298-303.
136. Perdiguero, E. et al. Genetic deficiency of p38alpha reveals its critical role in myoblast cell cycle exit: the p38alpha-JNK connection. *Cell Cycle.* 2007; 6(11): 1298-303.
137. Serra, C. et al. Functional interdependence at the chromatin level between the MKK6/ p38 and IGF1/PI3K/AKT pathways during muscle differentiation. *Mol. Cell.* 2007; 28: 200 –13.
138. Alén, B. O. et al. The NMR structure of human obestatin in membrane-like environments: insights into the structure-bioactivity relationship of obestatin. *PLoS One*. 2012; 7 (10): E45434.
139. Alvarez, C. J. et al. Obestatin stimulates Akt signalling in gastric cancer cells through β-arrestin-mediated epidermal growth factor receptor transactivation. *Endocr. Relat. Cancer*. 2009; 16: 599-611.
140. Glass, D. J. et al. Skeletal muscle hypertrophy and atrophy signalling pathways. *Int. J. Biochem. Cell. Biol*. 2005;37(10): 1974-84.
141. Um, S. H. et al. Absence of S6K1 protects against age- and diet-induced obesity while enhancing insulin sensitivity. *Nature.* 2004; 431(7005): 200-5.
142. Um, S. H et al. Absence of S6K1 protects against age- and diet-induced obesity while enhancing insulin sensitivity. *Nature.* 2004; 431(7005): 200-5.
143. Zoncu, R. et al. mTOR: from growth signal integration to cancer, diabetes and ageing. *Nat. Rev. Mol. Cell. Biol*. 2011; 12(1): 21-35.

CHAPTER 6

Regulation of SCs division becomes one of the key steps in skeletal muscle regeneration to provide a sufficient number of cells to ensure the function of the newly formed muscle fibers[144]. However, it is now well established that SCs are limited in the their proliferative capacity, and this limitation determines the regenerative potential of the muscle[145]. Although the proliferative limit may not be crucial during the normal life span of an individual, it is vital in situations where cells are solicited to proliferate continually. This is the case for inherited disorders, such us the muscular dystrophies, characterized by muscle weakness and wasting, due to repetitive cycles of degeneration and regeneration. This puts a huge and permanent demand on the pool of satellite cells[146]. The development of therapeutic interventions depends on the knowledge of extrinsic and intrinsic regulatory signals that control the myogenic process. Previously, we identified a mechanism whereby the obestatin/GPR39 system is coordinately regulated as part of the myogenic program and operates as an autocrine signal regulating skeletal myogenesis. This was followed by an analysis of the potential use of obestatin as a therapeutic agent for treatment of trauma-induced muscle injuries. This study suggested that obestatin might be an important therapeutic approach to stimulate muscle regeneration based on its ability to increase muscle regeneration and hypertrophic muscle growth together with its role on vascularization and regulation of fibrosis. Based on these results, we decided to explore its role on SC activation taking into account its critical role for the development of therapeutic interventions. Data presented in the present Chapter showed no expression of obestatin in SCs residing on isolated myofibers whyle GPR39 expression was detected. However, obestatin treatment promoted apical-basal division *versus* planar division of SCs residing in its niche as shown in *ex vivo* fiber culture, favoring SC commitment state instated of quiescent state. This data was confirmed after analyzing Myf5 expression on TA along the regeneration process, where obestatin-treated muscles increased the number of SCs expressing Myf5/Pax7, as well as the number of SCs expressing solely Pax7 or Myf5. It was noteworthy the chemoattrant effect displayed by obestatin on SC-derived myoblasts.

The fact that obestatin was not expressed in SCs while GPR39 was expressed in SCs suggests that there is a paracrine effect on SCs. This is based on: (1) the expression of preproghrelin, and thus obestatin in healthy skeletal mucle; (2) the expression of obestatin is strikingly increased upon muscle injury; and, (3) silencing of GPR39 expression in L6E9 myoblast cells demonstrated that this G protein-coupled receptor is the extracellular target for obestatin action[147]. We propose that the obestatin/GPR39 system signalling is involved in SC activation, in which obestatin exerts a paracrine function to control the SC activation and an autocrine action on myoblast-derived SCs to drive myoblast migration and fusion to reach skeletal myotube formation. In this way, the autocrine/paracrine action of obestatin would operate as a signal regulating skeletal myogenesis under healthy or injuried-skeletal muscle.

SCs persist in muscle that is subjected to repeated cycles of degeneration and regeneration, suggesting that self-renewal or recruitment maintains the pool of these cells[148]. Recent advances have provided important insights into the role played by the microenvironment in regulating stem cell identity and the asymmetric generation of committed daughter cells. Stem cell polarity and spindle orientation relative to the basal lamina determines the fate of daughter cells[149,150]. Stem cell divisions in a planar orientation are mainly symmetric and generate identical daughter stem cells. By contrast, stem cell divisions in an apical-basal orientation are predominantly asymmetric and give rise to a stem cell at the basal surface and a committed daughter on the apical surface[151,152]. Obestatin enhanced apical-basal *versus* planar division under *ex vivo* conditions, thus favoring commitment against stemness. It remains unclear what intrinsic mechanism is responsible for the orientation of divisions and how subsequent events lead to commitment of the apical daughter cell. However, recent insights into extrinsic regulators proposed that inhibition of Notch signalling drives satellite stem cells to commitment and differentiation[153,154] similarly to embryonic $Pax7^+/Myf5^+$ cells in the dermomyotome.

The expression pattern of Pax7 and Myf5 in TA under obestatin treatment during the regeneration process fit well with SCs fate following division. During *in vivo* regeneration, SC division in the apical-basal orientation give rise to a committed $Myf5^+$ SC, which is pushed into the apical surface, and a daughter cell, which remains attached to basal lamina retaining the SC identity. By contrast, planar

144. Usas, A. et al. Skeletal muscle-derived stem cells: implications for cell-mediated therapies. *Medicina*. 2011; 47 (9): 469-479.
145. Decary, S. et al. Telomere length as a tool to monitor satellite cell amplification for cell mediated gene therapy. *Hum. Gene. Ther.* 1996; 7: 1347-50.
146. Renault, V. et al. Skeletal muscle regeneration and the mitotic clock. *Experimental Gerontology*. 2000; 35: 711-9.
147. Gurriarán-Rodríguez, U. et al. The obestatin/GPR39 system is up-regulated by muscle injury and functions as an autocrine regenerative system. *J. Biol. Chem*. 2012; 287(45):38379-89.
148. Seale, P. et al. A new look at the origin, function, and "stem-cell" status of muscle satellite cells. *Dev. Biol.* 2000; 218: 115-24.
149. Fuchs, E. et al. Socializing with the neighbors: stem cells and their niche. *Cell*. 2004; 116: 769-78.
150. Moore, K. A. et al. Stem cells and their niches. *Science*. 2006; 311: 1880-5.
151. Knoblich, J. A. The Drosophila nervous system as a model for asymmetric cell division. *Symp. Soc. Exp. Biol*. 2001; 53: 75-89.
152. Lechler, T. et al. Asymmetric cell divisions promote stratification and differentiation of mammalian skin. *Nature*. 2005; 437: 275-80.
153. Kuang, S. et al. Asymmetric self-renewal and commitment of satellite stem cells in muscle. *Cell*. 2007; 129: 999-1010.
154. Conboy, I. M. et al. The regulation of Notch signalling controls satellite cell activation and cell fate determination in postnatal myogenesis. *Dev. Cell.* 2002; 3: 397-409.

divisions of SCs occur along the host myofiber, after which both daughter cells remain in contact with the basal lamina, symmetrically expand, giving rise to two $Pax7^{+}/Myf5^{-}$ cells[155]. Our data showed in TA treated with obestatin a noteworthy increased in SCs only expressing Pax7, as well as the double stained population Pax7/Myf5, compared with non treated mice. Both populations are needed for fiber homeostasis, $Pax7^{+}$ cells repopulate SC niche, a self-renewal mechanism and $Pax7^{+}/Myf5^{+}$ give rise to commitment cells. It is also noteworthy that obestatin increased $Myf5^{+}$ cells, giving rise to a population of myoblasts triggered toward the differentiation process. These data supported the obestatin role as a dual effector on muscle recovery increasing the self-niche repopulation ($Pax7^{+}$) and, in the other hand, triggering myogenesis to promote muscle regeneration ($Pax7^{+}/Myf5^{+}$).

Molecular characterization of SCs is providing important insights into the molecular mechanisms regulating their function. Our identification of a role for the obestatin/GPR39 signal reveals a role in regulating the apical expansion of SCs. This finding represents a significant advance in understanding of satellite cell biology and muscle regeneration.

155. Wang, X. Y. et al. Satellite cells, the engines of muscle repair. *Nature Reviews.* 2012; 13: 127-33.

CONCLUSIONS

CHAPTER 1

1. Obestatin activated Akt and its downstream targets, GSK3α/β, mTOR and S6K1, in 3T3-L1 adipocyte cells. Simultaneously, obestatin inactivated AMPK in this cell model. In keeping with this, ACC phosphorylation was also decreased. This fact was confirmed *in vivo* in white adipose tissue (omental, subcutaneous and gonadal) obtained from male rats under continuous *sc* infusion of obestatin.

2. GPR39 siRNA reduced obestatin action involving this receptor as a extracellular target for obestatin.

3. The relevance of obestatin as regulator of adipocyte metabolism was supported by AS160 phosphorylation, GLUT4 translocation and augment of glucose uptake in 3T3-L1 adipocyte cells. In contrast, obestatin failed to modify translocation of fatty acid transporters, FATP1, FATP4 and FAT/CD36, to plasma membrane.

4. Obestatin treatment in combination with IBMX and DEX showed to regulate the expression of C/EBPα, C/EBPβ, C/EBPδ and PPARγ promoting adipogenesis.

5. Obestatin contributes to adipogenesis as an autocrine/paracrine factor.

CHAPTER 2

1. Insulin promoted the preproghrelin expression throughout adipogenesis identifying mTORC1 as a critical downstream substrate for this profile. The role of preproghrelin-derived peptides on the differentiation process was supported by preproghrelin knock-down experiments, which revealed its contribution to adipogenesis. Neutralization of endogenous O-acyl ghrelin (acylated ghrelin), unacylated ghrelin, and obestatin by specific antibodies supported their adipogenic potential. A parallel increase in the expression of ghrelin-associatedenzymatic machinery, prohormone convertase 1/3 (PC1/3) and membrane-bound O-acyltransferase 4 (MBOAT4), was dependent on the expression of preproghrelin in the course of insulin-induced adipogenesis.

2. The coexpression of preproghrelin system and their receptors, GHSR1a and GPR39, during adipogenesis supports an autocrine/paracrine role for these peptides.

3. The results underscore a key role for preproghrelin-derived peptides on adipogenesis through an autocrine/paracrine mechanism.

4. Preproghrelin, PC1/3, and MBOAT4 exhibited dissimilar expression depending on the white fat depot, revealing their regulation in a positive energy balance situation in mice.

CHAPTER 3

1. Obestatin and the GPR39 receptor are expressed in rat skeletal muscle and are up-regulated upon experimental injury.

2. In differentiating L6E9 cells, preproghrelin expression and correspondingly obestatin increased during myogenesis being sustained throughout terminal differentiation. Autocrine action was demonstrated by neutralization and knock-down experiments confirming the contribution of obestatin to the myogenic program.

3. GPR39 siRNA reduced obestatin action and myogenic differentiation.

4. Exogenous obestatin stimulation was also shown to regulate myoblast migration and proliferation.

5. The addition of obestatin to the differentiation medium increased myogenic differentiation of L6E9 cells. The relevance of the actions of obestatin was confirmed *in vivo* by the up-regulation of Pax7, MyoD, Myf5, Myf6, myogenin, and MHC in obestatin-infused rats when compared with saline-infused rats.

CHAPTER 4

1. Obestatin activated Akt and its downstream targets, GSK3α/β, and S6K1, in L6E9 myotube cells. Simultaneously, obestatin inactivated AMPK in this cell model. In keeping with this, ACC phosphorylation was also decreased. This fact was confirmed *in vivo* in rat skeletal muscle, gastrocnemius and soleus, obtained from male rats under continuous *sc* infusion of obestatin.

2. The relevance of obestatin as regulator of adipocyte metabolism was supported by AS160 phosphorylation, GLUT4 translocation and augment of glucose uptake L6E9 myotube cells. Furthermore, the effect of obestatin in glucose up-take was also observed in gastrocnemius and soleus muscle.

CHAPTER 5

1. The overexpression of the obestatin/GPR39 in skeletal muscle enhanced muscle regeneration after muscle injury

2. The intramuscular injection markedly enhances muscle regeneration, as evidenced by upregulation of the expression of the specific myogenic factors Pax7, MyoD, myogenin and eMHC, and, importantly, the significant increase of the myofiber size and the number of myonuclei per myofiber

3. The up-regulation of the specific satellite cells marker Pax7 associated to the increased number of activated satellite cell ($Pax7^{+}$) per myofiber demonstrated the actions of obestatin on satellite cells

4. The effective action was due to specific regulation of this peptide on different stages affecting myogenesis: proliferation, fusion and myofiber growth.

5. Added to the myogenic action, obestatin administration resulted in increased expression of VEGF/VEGFR2 and the consequent microvascularization, with no significant effect on collagen deposition in developing skeletal muscle

6. The potential inhibition of myostatin might contribute to the myogenic action improving muscle growth and regeneration.

7. The myogenic actions of obestatin were coordinated by a kinase hierarchy determined by the ERK1/2, CamkII, Akt and p38 axis.

CHAPTER 6

1. GPR39 was expressed in SCs while no expression was observed for obestatin.

2. Obestatin enhances SCs apical-basal division *versus* planar division on *ex vivo* myofibers.

3. Obestatin promotes *ex vivo* myoblast migration acting as chemoattrant molecule.

4. Obestatin enhances $Pax7^{+}$, $Pax7^{+}/Myf5^{+}$, $Myf5^{+}$ satellite cells populations during muscle *in vivo* regeneration, changing the ratio and the fate of the daughter cells, thus favoring commitment against stemness..

RESUMO

Dentro das diferentes capas xerminais, a capa mesodérmica, é a orixe común de varios tipos de tecidos, entre eles, o tecido adiposo e o muscular. Son as células mesenquimais (MSCs) provenientes do mesodermo, as que tras diversos procesos de diferenciación embrionaria dan lugar aos adipocitos e miotubos. Con todo, as MSCs non son a únicas implicadas no desenvolvemento embrionario e nos estadíos pre-natais, certos tecidos adultos manteñen pequenas cantidades de MSCs con potencial para dar lugar a todo tipo de células dos tecidos onde residen, de maneira que poden reparar ou substituír tecido, ou expandirse en resposta a un exceso enerxético crónico[1]. Este proceso está regulado por mecanismos moleculares complexos, aínda non coñecidos na súa totalidade. Numerosas publicacións demostraron o amplo potencial terapéutico das MSCs, debido á súa habilidade para diferenciarse en múltiples tipos celulares en condicións apropiadas despois do nacemento[2,3,4].

Durante a última década, os tecidos adiposo e muscular foron identificados como órganos secretores cunha función autócrina/parácrina[5,6]. De acordo con esta identificación, as citoquinas e outros péptidos liberados polo tecido muscular e adiposo deberían ser clasificados como mioquinas e adipoquinas, respectivamente. Este feito proporciona un novo paradigma conceptual, no cal os diferentes tecidos están intercomunicados con outros órganos e xogan un papel global no metabolismo enerxético. Certas hormonas actúan a nivel local como factores parácrinos; con todo, outras teñen un alcance máis amplo actuando a nivel do sistema central. Esta acción recíproca entre mioquinas e adipoquinas representa un balance de positividade e negatividade, especialmente en condicións patolóxicas, como a obesidade, onde os adipocitos secretan adipoquinas que contribúen a establecer un ambiente inflamatorio crónico que promove os procesos patolóxicos, tales como artereoesclerose e resistencia insulínica, así mesmo o músculo esquelético en condicións de exercicio é capaz de producir mioquinas que confiren beneficios saudables, tales como mioquinas que contrarrestan o efecto daniño das adipoquinas inflamatorias.

Polo tanto o estudo de factores secretados polos tecidos de orixe común como o muscular e adiposo, e a súa implicación autócrina/parácrina no proceso de diferenciación, son de gran utilidade para a identificación de dianas terapéuticas, contribuíndo ao coñecemento e tratamento das patoloxías relacionadas con anormalidades nos procesos de diferenciación celular.

Como punto de partida para as nosas investigacións tomamos o proceso de diferenciación adipoxénica, onde unha activación secuencial de factores de transcrición traducen información de sinais intra e extra-celulares indicativas das condicións acertadas para a diferenciación. Numerosas moléculas endócrinas, parácrinas e autócrinas están asociadas con cambios dinámicos no tecido adiposo. Recientemente, o péptido gástrico grelina suscitou especial atención polo seu papel como factor regulador da bioloxía adipocitaria. O xene da grelina está codificado por un polipéptido, prepropéptido, denominado preprogrelina, que sofre un procesamento posterior producindo dous péptidos: a obestatina e a grelina. A obestatina, un peptido de 23 aminoácidos, foi orixinalmente identificado e illado do estómago. Este péptido circulante mostra unha secreción pulsátil cunha ritmicidade ultradiana similar á grelina ou á hormona de crecemento. A acción da obestatina foi descrita inicialmente a través do receptor orfo GPR39, un receptor de sete dominios transmembrana pertencente á familia de receptores como o GHSR1a da grelina ou o da motilina. A pesar do entusiasmo inicial suscitado por devandita molécula, dado o potencial que posuía polos seus efectos antagónicos á grelina, numerosas observacións puxeron a súa efectividade en cuestión. Consecuentemente, o estado de coñecemento da obestatina sofre numerosas lagoas, especialmente pola falta de reproducibilidade da súa actividade a nivel central. Mantendo separadamente a controversia sobre o seu poder anorexixénico, existen varias publicacións que demostran a súa actividade en diferentes accións biolóxicas[7,8,9]. Neste sentido, propuxémosnos

1. Xiang, X. et al. mTOR and the differentiation of mesenchymal stem cells. *Acta Biochim. Biophys. Sin*. 2011; 43 (7): 501-10.
2. Malek, A. et al. Human placental stem cells: biomedical potential and clinical relevance. *J. Stem Cells*. 2011; 6 (2): 75-92.
3. Ball,S. G. et al. Mesenchymal stromal cells: Inhibiting PDGF receptors or depleting fibronectin induces mesodermal progenitors with endothelial potential. *Stem Cells*. 2013
4. Hughey, C. C. et al. Mesenchymal stem cell transplantation for the infarcted heart: therapeutic potential for insulin resistance beyond the heart. *Cardiovasc. Diabetol.* 2013;12(1):128.
5. Pedersen, B. K. et al. Muscle as a secretory organ. *Compr. Physiol*.2013;3(3):1337-62.
6. Trayhurn, P. et al. Secreted proteins from adipose tissue and skeletal muscle - adipokines, myokines and adipose/muscle cross-talk. *Arch. Physiol. Biochem*. 2011;117(2):47-56.
7. Pedersen, B. K. et al. Muscles, exercise and obesity: skeletal muscle as a secretory organ. *Nat. Rev. Endocrinol.* 2012; 8: 457-65.
8. Zhang, J. V. et al. Obestatin induction of early-response gene expression in gastrointestinal and adipose tissues and the mediatory role of G protein-coupled receptor, GPR39. *Mol. Endocrinol.* 2008; 22: 1464-75.
9. Sheng-Qiu, T. et al. Obestatin- Its physicochemical characteristics and physiological functions. *Peptides*. 2008; 29: 639-645

estudar a súa función nos procesos de diferenciación de orixe común, a adipoxénese e a mioxénese, así como a súa posible acción metabólica en ambas dianas tisulares.

A nosa investigación parte da estimación do papel da obestatina sobre o control do metabolismo de preadipocitos e adipocitos así como da adipoxenese. Para os ensaios *in vitro*, empregamos os preadipocitos 3T3-L1 baseándonos na regulación de nodos clave de señalización, Akt e AMPK e as súas dianas intracelulares. Para os ensaios *in vivo*, utilizamos tecido adiposo branco de ratas macho baixo a administración continuada de obestatina. Este péptido activou Akt e as súas dianas, GSK3α/β, mTOR e S6K1, en adipocitos 3T3-L1. Simultaneamente, a obestatina inactivou AMPK neste modelo celular. En relación con esta diana, a fosforilación de ACC foi tamén diminuída. Estes datos comprobáronse *in vivo* en tecido adiposo branco (omental, subcutaneo e gonadal) obtido de ratas macho baixo a administración *sc* de obestatina durante 24 e 72h. A relevancia da obestatina como regulador do metabolismo adipocitario está apoiado pola fosforilación de AS160, pola traslocación de GLUT4 á membrana plasmatica e o consecuente aumento da captación de glicosa polo adipocitos 3T3-L1. Pola contra, a obestatina non mostrou efecto significativo sobre a traslocación á membrana plasmática dos transportadores de acedos graxos FATP1, FATP4 e FAT/CD36. O tratamento con obestatina en combinación con IBMX e DEX regulou a expresión de C/EBPα, C/EBPβ, C/EBPσ e PPARγ promovendo a adipoxénese. De forma destacable, a expresión da preprogrelina, e polo tanto de obestatina, aumentou durante o proceso de adipoxénese sendo sostida durante a diferenciación terminal. A neutralización de obestatina endóxena secretada polas células 3T3-L1 mediante anticorpo anti-obestatina diminuíu a adipoxénese. Ademais, os ensaios de silenciado de preproghrelin mediante siRNA apoiaron os datos previos. En resumo, a obestatina promoveu a adipoxénese dun modo autócrino/parácrino, sendo un regulador do metabolismo adipocitario.

En base aos datos obtidos sobre a expresión da preprogrelina durante a adipoxénese, optamos por profundar no papel exercido polos péptidos derivados da grelina e a obestatina sobre o programa de diferenciación. A análise inmunocitoquímico de adipocitos 3T3-L1 mostrou un maior grao de expresión de preprogrelina en relación á súa expresión en preadipocitos. A insulina promoveu devandito patrón de expresión durante o desenvolvemento da adipoxénese identificando a mTORC1 como un nodo intracelular de señalización clave para esta acción. O papel dos péptidos derivados da preprogrelina sobre a adipoxénese confirmouse mediante ensaios de silenciado, os cales revelaron a súa contribución á diferenciación adipocitaria. A neutralización de O-acil grelina (grelina acilada), grelina desacilada e obestatina mediante a utilización de anticorpos específicos apoiaron os datos obtidos previamente. Ademais, constatouse que a expresion da maquinaria enzimática asociada ao procesado da grelina, PC1/3 e MBOAT4, foi dependente e paralela á expresión da preprogrelina na adipoxénese inducida por insulina. A co-expresión de GHSR1a e GPR39 durante a adipoxénese apoiou o papel autócrino/parácrino dos péptidos derivados da preprogrelina. MBOAT4, PC1/3 e preprogrelina mostraron diferentes graos de expresión en función do tipo de tecido adiposo branco analizado. Nós propoñemos un mecanismo polo cal a insulina activa a expresión de preprogrelina e a consecuente secreción dos péptidos derivados de preprogrelina, os cales intensifican o efecto da insulina na activación das cascadas implicadas en adipoxénese, tales como Akt e as súas dianas, dun xeito autócrino en preadipocitos.

Unha vez analizada a implicación autócrina da obestatina e os péptidos derivados da preprogrelina no metabolismo adipocitario, o noso seguinte obxectivo era estudar o papel autócrino da obestatina nun segundo proceso de diferenciación e de orixe común, a mioxénese. O mantemento e reparación do músculo esquelético é atribuíble a unha elaborada interacción entre sinais reguladoras extrínsecas e intrínsecas implicadas no proceso de mioxénese. Os nosos resultados mostraron que a obestatina e o receptor GPR39 están expresados no tecido muscular esquelético de rata e que a súa expresión vese aumentada logo da indución dun dano experimental no músculo esquelético. Para definir o papel do sistema obestatina/GPR39 na rexeneración muscular, utilizamos as células L6E9 para os ensaios *in vitro*. Para os ensaios *in vivo*, utilizouse tecido muscular esquelético obtido de ratas macho trala infusión continuada de obestatina. En células L6E9, a expresión de preprogrelina e obestatina aumentou durante o progreso da mioxénese sendo sostida na etapa tardía do mesmo. A acción autócrina demostrouse mediante ensaios de silenciado de preprogrelina utilizando siRNA durante o progreso da mioxénese. Estes datos, atribuíbles á obestatina, confirmáronse trala súa neutralización durante a mioxénese, empregando anticorpos específicos anti-obestatina. Ademais, o silenciado de GPR39 diminuíu a acción da obestatina así como o grao de progresión da mioxénese. A administración esóxena de obestatina mostrou regular tanto

a proliferación como a migración de mioblastos, así como un aumento da diferenciación mioxénica das células L6E9, cun poder hipertrófico. Estes datos foron ratificados *in vivo*, tras someter a ratas a unha infusión continua de obestatina; os resultados mostraron unha sobreexpresión de marcadores mioxénicos: Pax7, Myf5, MyoD, myogenin, Myf6 e MHC trala infusión de obestatina, así como de marcadores implicados na vascularización tales como VEGF e o seu receptor e PEDF. A análise do diámetro das fibras mostrou un poder hipertrófico que concordaba cos datos obtidos *in vitro*.

O conxunto de resultados obtidos demostrou o efecto autócrino do sistema obestatina/GPR39 sobre a mioxénese e o poder hipertrófico que esta exerce, así mesmo arroxaron a posibilidade de que o sistema obestatina/GPR39 tivese un potencial terapéutico no tratamento de traumas inducidos por un dano muscular ou o tratamento de miopatías

O aumento do diámetro das fibras, e os datos obtidos previamente en adipocitos que indicaban un incremento na captación de glicosa trala adición de obestatina, leváronnos a propoñer como hipótese que o maior diámetro da fibra podía ser debido a un aumento na captación de glicosa trala estimulación de obestatina.

A nivel de regulación do metabolismo do músculo esquelético, estudamos os nodos clave de señalización, Akt e AMPK e as súas dianas intracelulares de forma similar ao que realizamos no tecido adiposo. A obestatina activou Akt e as súas dianas, GSK3α/β, e S6K1, en miotubos L6E9. Simultáneamente, a obestatina inactivou AMPK neste modelo celular. En relación con esta diana, a fosforilación de ACC foi tamén diminuída. Estes datos comprobáronse *in vivo* en tecido muscular esquelético (sóleo e gastronemio) obtido de ratas macho baixo a administración *sc* de obestatina. A relevancia da obestatina como regulador do metabolismo muscular está apoiado pola fosforilación de AS160, e pola translocación de GLUT4 á membrana plasmática e consecuente aumento da captación de glicosa en miotubos L6E9. Este feito foi confirmado en tecido muscular esquelético. Estes datos demostraron que ademais da acción miogénica, previamente descrita, o sistema obestatina/GPR39 tamén mostra unha regulación sobre o metabolismo muscular a través da regulación da captación de glicosa.

A capacidade rexenerativa do músculo esquelético é crítica para o mantemento e cura de devandito tecido tanto en condicións normais como no caso das miopatías asociadas. Por iso, o desenvolvemento de intervencións terapéuticas depende en gran medida do coñecemento dos sinais intrínsecos e extrínsecos que regulan o proceso da mioxénese. En base aos resultados obtidos sobre o sistema obestatina/GPR39 sobre este proceso de diferenciación, é lóxico explorar o seu uso potencial como axente terapéutico para o tratamento do dano muscular inducido por dano. Para iso utilizamos un modelo animal de regeneración de músculo esquelético inducida por dano así como diferentes aproximación experimentais mediante o uso de células C2C12. Os resultados obtidos demostraron que a sobre-expresión do sistema obestatina/GPR39 no músculo esquelético previa á indución do dano muscular no TA aumentou a capacidade de rexeneración da zona afectada. Con todo, esta aproximación producía un dano consecuencia da metodoloxía aplicada, o que non nos permitiu diferenciar dunha forma clara a zona de rexeneración asociada ao dano por electroporación á zona de rexeneración asociada ao dano inducido. Con todo, a indución de dano en TA e posterior administración intramuscular local de obestatina demostrou de forma inequívoca un aumento significativo da capacidade rexenerativa do músculo. Iso púidose comprobar polo aumento da expresión de factores mioxénicos específicos como Pax7, MyoD, myogenin e eMHC. Este tratamento produciu ademais un aumento do tamaño das miofibras rexeneradas así como do número de mionúcleos asociados. A sobre-expresión do marcador Pax7, asociado ao aumento do número de células Pax7 por miofibra demostrou a acción da obestatina sobre a activación das células satélite (SCs). A acción pro-miogénica neste modelo de dano muscular está avalada pola regulación das diferentes etapas da mioxénese: proliferación, fusión e crecemento da miofibra (hipertrofia). Engadido á acción propia da obestatina sobre a mioxénese, este péptido mostrou inducir un aumento da expresión de VEGF/VEGFR2 e a consecuente microvascularización na zona de rexeneración, sen efecto significativo sobre a deposición de coláxeno na zona de rexeneración. A iso debemos engadir que a obestatina diminuíu a expresión do factor inhibidor do crecemento muscular, a miostatina, durante o proceso de regeneración. É importante sinalar que as accións mioxénicas da obestatina mostráronse reguladas por unha activación de tipo xerárquico de ERK1/2, CamkII, Akt e p38. Concluímos este capítulo demostrando que a obestatina regula o proceso multifactorial da regeneración muscular. O tratamento con obestatina aumenta a regeneración e a vascularización

necesaria para un bo restablecimiento da actividade muscular, sen incrementar por iso a fibrosis muscular.

Estudos realizados en miofibras illadas obtidas das zonas próximas ao dano muscular, durante a regeneración, demostraron que as SCs eran activas de forma significativa, mostrando unha alta porcentaxe de división tipo apical-basal; o que permite afirmar que ademais da xeración de células dirixidas á rexeneración ($Pax7^{+}$ /$Myf5^{+}$), a obestatina garante a repoboación da SCs en estado quiescente ($Pax7^{+}$ /$Myf5^{-}$). Engadido a este efecto, a obestatina mostrou ademais características de molécula quimiatraiente sobre os miobastos derivado das SCs o que xustifica a súa acción sobre a migración destas células á zona de dano. No seu conxunto, estes resultados demostraron que a obestatina regula positivamente a rexeneración muscular *in vivo*, mostra, ademais, características mioxénicas importantes como para considerala un potencial axente terapéutico a desenvolver para o tratamento de patologías asociadas á rexeneración do músculo esquelético incluíndo a sarcopenia, a caquexia e a distrofia muscular.

ACKNOWLEDGEMENTS

Por fin chegou o momento máis esperado deste periplo. Logo de sete anos de traballo, despois dun comezo difícil, chegamos á meta. Agora voto a vista atrás e penso en tódolos momentos que formaron parte desta carreira de fondo, na que moitas persoas contribuiron, en maior ou menor medida, para que este traballo collese forma pois o carácter de colaboración foi unha valor que caracterizou todo este proceso. Agardo non deixar ninguén no tinteiro, pois resulta difícil acordarse de todas e todos.

Quero mostrar o meu agradecemento ó Dr. Prof. Felipe Casanueva F. por darme a oportunidade de comezar este traballo de doutoramento. Ó Dr. Jesús P. Camiña, principal responsable para que este traballo chegase ó fin; para el un fondo agradecemento, por terme dirixido a tese con infinita dedicación.

Ó Dr. Rubén Nogueiras por estar sempre disposto a colaborar con nós e poñer á nosa disposición tódolos medios posibles, gracias tamén a todo o seu grupo. Á Dra. Rosalía Gallego por descubrirme o mundo da histoloxía, e pola atención que me adicou. Ó Dr. Manuel Martín Pastor da RIADIT por introducirme no complexo mundo do RMN. Ó Dr. Señarís do CHUS, por facilitarnos a colaboración clínica coa investigación básica. Ó inmunólogo do CHUS Juan Viñuela, por introducirme no mundo da citometría. Ó servicio de Anatomía Patolóxica do CHUS, por permitirnos o uso das súas instalacións.

Ó Prof. Jesús J. Barbero do CIB, gracias por darme a oportunidade de traballar no seu laboratorio. Ós meus compañeiros do CIB, en especial a Lidia Nieto. Je tiens à remercier au Prof. Vincent Mouly pour m'avoir offert l'opportunité de travailler au sein d'un laboratoire de myologie. Je tiens aussi à remercier les personnes avec lesquelles j'ai travaillé pendant mon stage Parisien. Al Prof. Sergio Adamo dell'Università di Roma "La Sapienza", per avermi dato l'opportunità di lavorare tre mesi nel suo laboratorio. Alla Dottssa. Viviana Moresi per la sua disponibilità durante il mio soggiorno a Roma.

Á Xunta de Galicia, Mutua Madrileña, CIBER, ISCIII, e en especial á FEBS polo seu financiamento.

Grazas ó Servizo de Normalización Lingüística da USC, a Claudia de Tórculo e a Follas Novas por contribuír á mellora desta tese.

Ós meus compañeiros do Laboratorio de Oncoloxía e ás rapazas do laboratorio 14 pola súa boa disposición. A María, Marga, Bea, Angel, Miguel, Marta "Confo" porque sempre estiveron ahí. A Dani, pola súa disposición a calquera hora. A Maribel, Sara, Begoña e a Lourdes por facer o día a día máis agradable e doado. A Turo pola amizade que me brindou e a súa colaboración informática. A Ceci por preocuparse por min. A Mery polos seus detalles. A Sisi e a María Pardo por axudarme tanto nos comezos. Ó meu querido compañeiro Omar, por darme ánimos desde hai tanto tempo.

A cousa vaise complicando… chegou o momento de agradecer o meu querido laboratorio Nº4. Nel atopei un sitio agradable e un bo ambiente de traballo, agarimo e apoio, especialmente neste último duro ano. A Jesús, por ser un exemplo a seguir como mentor, por ensinarme a traballar duro e profesionalmente, por facilitarme as cousas, pero sobre todo por amosar unha especial sensibilidade e condescendencia nos malos momentos persoais; estarei sempre en débeda con el. A Yola por axudarme tantas veces a discutir os datos difíciles, a conseguir o que sexa e onde sexa, por preocuparse máis aló do profesional demostrándome todo o seu agarimo. A Begoña por ser boa compañeira e estar sempre disposta a axudarme.
A Gus, pola súa bondade, alegría, creatividade e paciencia coas miñas tolerías informáticas. A Jess polas súas disposición para axudar sempre cun sorriso perenne. Ós novos fichaxes Lara, Saúl, Gabi, grazas por axudarme. Ó meu gran compañeiro Carlos, con el aprendín que traballar facendo grupo é o máis intelixente, grazas a unha das persoas que máis me fixo rir dentro e fóra do laboratorio, e por coidarme sempre que o precisei. Á miña prezada amiga Ici, mil grazas por estar aí sempre cando o pedín, por axudarme tanto pero sobretodo por ser a persoa que máis me apoiou o longo destes anos.

A Laura pola súa infinita axuda con esta tese. A toda a miña familia e ós meus amigos e amigas por estar sempre aí.

Os meus pais porque grazas as súas horas adicadas cheguei até aquí, por trasmitirme tantas cousas e darme tantas oportunidades. E o meu maior agradecemento para o meu compañeiro de viaxe, Álvaro, pola súa apoio incondicional.

Tamén quería facer unha lembranza especial a unha persoa que non coñecín, pero que foi para min un referente, o meu avó Gonzalo, que tivo que interromper a súa carreira científicia por mor da guerra civil e a ditadura franquista. Hoxe, ainda que vivimos nunha democracia, o periodo inicuo que estamos a vivir, vainos conducir a unha situación precaria. É necesario ter en conta o pasado para aprender dos erros, tal como xa pronunciara en 1954 o Premio Nobel de Medicina Bernardo Houssay: *"El desarrollo científico es condición de libertad, sin él se cae en el colonialismo político, económico y cultural; además se vive en la pobreza, ignorancia, enfermedad y atraso. Estamos en una era científica y la ciencia es cada vez más importante en la sociedad y rinde más y mejores frutos. Es indispensable su cultivo para que un país tenga bienestar, riqueza, poder y aun independencia"*.